厚生労働科学研究費補助金
難治性疾患等政策研究事業（難治性疾患政策研究事業）

ミトコンドリア病の調査研究

（H26-難治等（難）-一般-053）

平成 26-28 年度　総合研究報告書

研究代表者　　後　藤　雄　一

国立精神・神経医療研究センター

平成 29（2017）年 5 月

目　　次

厚生労働科学研究費補助金（難治性疾患等克服研究事業）
総合研究報告書

ミトコンドリア病に関する調査研究

研究代表者　　後藤　雄一　　国立精神・神経医療研究センター神経研究所

研究要旨　ミトコンドリア病の症状は多臓器に及び、心疾患、眼疾患、代謝性疾患としても重要な病気である。本研究班ではミトコンドリア病の正確な診断とそれに基づく適切な治療を目的として、グローバルな観点から診断基準・重症度スケールの策定、診療ガイドラインの策定、患者レジストリー構築を実施した。アウトリーチ活動については、市民公開講座を主催し、患者会勉強会に協力した。患者レジストリーについては、種々の要因で本格稼働には至っていないが、グローバルな活動との連携、新しい倫理ガイドラインへの準拠などを着実に行って、次年度に構築する予定である。診療ガイドラインの作成は、実用化研究班（村山班）と連携して行い、平成 28 年 12 月に、「診療マニュアル」を刊行した。

研究分担者
(1) 小坂　仁　自治医科大学小児科
(2) 大竹　明　埼玉医科大学小児科
(3) 北風政史　国立循環器病研究センター病院・研究開発基盤センター
(4) 古賀靖敏　久留米大学医学部小児科
(5) 小牧宏文　国立精神・神経医療研究センター
(6) 佐野　輝　鹿児島大学学術研究院医歯学系精神機能病学
(7) 末岡　浩　慶應義塾大学医学部産婦人科
(8) 田中雅嗣　東京都健康長寿医療センター
(9) 三牧正和　帝京大学医学部小児科
(10) 山岨達也　東京大学医学部耳鼻咽喉科
(11) 米田　誠　福井県立大学看護福祉学部

研究協力者
(1) 太田成男　日本医科大学大学院医学研究科
(2) 岡崎康司　埼玉医科大学・ｹﾞﾉﾑ医学研究ｾﾝﾀｰ
(3) 金田大太　東京都健康長寿医療センター
(4) 木村　円　国立精神・神経医療研究センター
(5) 砂田芳秀　川崎医科大学神経内科
(6) 須藤　章　楡の会こどもクリニック
(7) 竹下絵里　国立精神・神経医療研究センター
(8) 杉本立夏　国立精神・神経医療研究センター
(10) 中野和俊　東京女子医科大学病院小児科
(11) 西野一三　国立精神・神経医療研究センター
(12) 中川正法　京都府立医科大学付属北部医療センター
(13) 中村　誠　神戸大学大学院医学系研究科外科系講座眼科学
(14) 萩野谷和裕　拓桃医療療育センター
(15) 村山　圭　千葉県こども病院代謝科

A．目的

ミトコンドリアはすべての細胞内にあって、エネルギーを産生する小器官である。ミトコンドリアに異常があると、大量のエネルギーを必要とする神経・筋、循環器、代謝系、腎泌尿器系、血液系、視覚系、内分泌系、消化器系などに障害が起こる。なかでも、中枢神経や筋の症状を主体とするミトコンドリア病が代表的な疾患である。

国内においてミトコンドリア病の患者数の厳密な実態調査は行われていない。その理由は患者が多くの診療科に分散していること、診断基準が明確ではなかったことなどが挙げられるが、そのもっとも大きな要因は確定診断に必要な病理、生化学、遺伝子検査の専門性が高いことにある。平成 27 年 1 月にミトコンドリア病が指定難病に認定され認定基準を制定したが、本診断基準はミトコンドリア病を

包括的にとらえる事を目指したために、やや複雑な基準となっており、今後の診療・研究においては個別の病型の診断基準の作成が必要という状況になっている。

また英国では，ミトコンドリア病の一部の病型で、核移植を用いた生殖補助医療の適応が本格的に試みられようとしている（Nature 465: 82-85, 2010）。そのようなグローバルな研究や医療の流れに遅れないような本邦での調査研究が必要である。

本研究班では、ミトコンドリア病の検査手段（病理検査、生化学検査、DNA 検査）の標準化と集約的診断体制の確立、本疾患に関する情報提供手段の整備等を行い、臨床病型、重症度、合併症、主な治療の内容などの標準化をめざす。患者レジストリーを進め、具体的な治療に関する臨床研究や治験を進めるコーディネーター役を行うこと、また主に小児のミトコンドリア病を対象としている AMED 難治性疾患実用化研究事業の村山班と連携して診療ガイドラインを作成するとともに、市民公開講座や難病情報センター等を活用し、広報活動を行うことを目的とする。

B．方法

1）診断フローチャートの作成と検査標準化

ミトコンドリア病の診断に必要な 3 種類の検査方法（病理検査、生化学検査、遺伝子検査）の標準化と集約的な診断体制の構築を継続する。特に遺伝子検査の重要性が一段と増しており、臨床検査としての遺伝子検査実施体制の構築が行われる中に、ミトコンドリア病の遺伝子検査を位置づける。

① 遺伝子検査の実施と標準化

AMED 難治性疾患実用化研究事業の村山班と協力して、国立精神・神経医療研究センター、埼玉医科大学などを中心として、mtDNA 検査と核 DNA 上の原因遺伝子について、医療の中にどのように組み込むかを明確にする。また、先端的遺伝子検査（出生前診断）や適切な遺伝カウンセリングの提供体制を整備する。＜後藤、大竹、田中、末岡、杉本＞

② 病理検査の実施

ミトコンドリア異常を病理学的に捉えることは現在でも重要であり、国立精神・神経医療研究センターを中心に検査実施と標準化を行う。骨格筋以外の罹患臓器（心、肝など）の病理所見についても検討する。＜後藤、西野＞

③ 生化学検査の標準化

ミトコンドリア代謝系の異常を捉える生化学検査も確定診断に必要であり、特に小児期早期に発症する重症な代謝疾患を適切の診断できる体制を、国立精神・神経医療研究センター、埼玉医科大学等で拠点化して検査を実施し、標準化を行う。＜後藤、大竹、村山＞

2）認定基準の改定、重症度スケール、グローバルな診断基準作成に参加

新たな難病政策における指定難病として、診断基準と重症度分類を策定する。欧米で進んでいる新たな診断基準作成の動きに応じて、わが国の代表として参加する。この動きは、患者レジストリーにおける情報項目の共通化、将来の国際共同治験を推進するための基盤整備として行う。
＜後藤、古賀、大竹、小牧＞

3）診療ガイドラインの作成

ミトコンドリア病では、多くの臨床病型が知られている。ミトコンドリア病に比較的よく合併する臓器症状を診ている関連診療科（循環器科：北風、耳鼻科：山岨、精神神経科：佐野、など）の専門医も参加し、AMED 難治性疾患実用化研究事業の村山班と協力して、診療ガイドラインを作成する。＜全員＞

4）ミトコンドリア病に詳しい医師のネットワークと情報提供体制の整備とアウトリーチ活動

患者・家族や本疾患を診ている医療従事者に対して、本疾患の医療情報をホームページ等で提供する。また保健所等でのセミナーも積極的に行う。
＜小牧、三牧＞

5）実態調査を兼ねた患者レジストリーの構築

全国の主要な総合病院に対して、小児科、神経内科ばかりでなく、耳鼻咽喉科、眼科、精神科、

循環器内科、腎臓内科、糖尿病内科などにも、調査用紙を配布する実態調査を行う。AMED 難治性疾患実用化研究事業の村山班と連携して、日本におけるミトコンドリア病患者レジストリーを構築する。＜小牧、大竹、三牧＞

６）生殖補助医療の情報収集と見解のまとめ

ミトコンドリア病、特にミトコンドリア DNA 変異で発症するリー脳症においては、出生前診断や受精卵診断が欧米では行われている。日本においても、受精卵診断が慶應大学病院で 2 例行われている。しかし、受精卵診断では得られない発症リスクの低い受精卵を得るために「核移植治療」が検討されており、2015 年 2 月に英議会は、その臨床応用を認める判断を行った。この技術の有用性や倫理的問題について、本研究班で検討した。＜末岡、後藤＞

Ｃ．結果と考察

１）診断フローチャートの作成と検査標準化

ミトコンドリア病の確定診断には、病理検査、生化学検査、遺伝子検査を行い、総合的な評価が必要である。

① 病理検査

骨格筋の病理検査は国立精神・神経医療研究センター（以下 NCNP）が中心となって実施した。

② 生化学検査

検体は線維芽細胞もしくは各臓器を用いている。

NCNP と埼玉医科大学（千葉こども病院）で行われている。NCNP は神経症状を主体とする小児・成人例を、埼玉医科大学では主に代謝異常症状を中心とする乳児、小児例を中心に生化学検査を行った。＜後藤、大竹、村山＞

③ 遺伝子検査

（拠点形成、検査会社の関与、集約化について）

本疾患は、ミトコンドリア DNA 変異の場合は遺伝型と表現型が一対一に対応しない、核 DNA 上に 200 近くの原因遺伝子が報告されている、という特徴があるため、可能であれば解析可能な施設に集約すべきである。

ミトコンドリア DNA の全周シークエンスを行える施設として NCNP などのいくつかの施設、検査会社があるが、検査依頼に際しての基準、検査体制の整備、啓発が必要である。NCNP では、次世代シークエンサーを用いたミトコンドリア DNA 検査を確立した。

この方法は、ミトコンドリア DNA 全体を 1 セットのプライマーで増幅させ、核 DNA 上のミトコンドリア DNA 類似配列を除外した後に、MiSeq を用いてカバーレージを 1500～3000 程度までにあげることで、点変異の位置と種類、変異率が容易に計測できる。また、ミトコンドリア DNA の欠失は比較的頻度の高い変異であるが、その断点同定に時間がかかる作業であったが、この方法で断点周辺が簡単に見いだせることから作業の効率が格段に上昇した。

研究分担者の大竹らは、埼玉医科大学を中心に、千葉こども病院、自治医科大学、東京都健康長寿医療センターと協力して、特に乳児期発症の重症ミトコンドリア病に関して、酵素診断から網羅的な遺伝子検査にいたる系統的病因検索システムを構築した。＜大竹＞

2）診断基準、重症度スケールについて

2015 年 1 月の指定難病の認定に際して、新たな認定基準を作成した。本研究班の分担研究者の多くは、自らの患者における申請作業や各都道府県における認定作業に携わっており、概ね妥当なものと認識していた。

一方で、乳児期、小児期に発症するミトコンドリア病は重症例が多く、「代謝病」としての性格が前面にでる傾向がある。そのため、小児慢性特定疾患の認定基準は、そのような分類での認定方式を基本にしている。したがって、指定難病と小児慢性特定疾患の摺り合わせをどのようにするかが依然として問題になっている。さらに、本年度は、平成 29 年 4 月に追加してされる指定難病の中に、ミトコンドリア内酵素異常症が含まれており、その整合性について協議を行った。

さらに、本診断基準はできるだけ多くの患者を網羅できるようにと意図して作成しており、いわば「包括的診断基準」となっている。しかしながら、

新薬等の臨床試験等を考慮した場合には、個別の病型ごとに明確な診断基準を設定しておくことが望ましいという考え方がある。そこで、AMED 難治性疾患実用化研究班（村山班）と共同で、個々の病型の診断基準の作成に着手し、まずはMELAS と Leigh 脳症について確定させた。さらに、ミトコンドリア肝症やミトコンドリア心筋症の新たな診断基準の作成を試みた。

３）診療ガイドラインの作成

実用化研究班（村山班）と協力して、診療ガイドライン作成を行う予定であった。ミトコンドリア病は診断基準が確定されていないこともあって、エビデンスとして採用できる研究成果が少ない。したがって、Minds 方式のガイドライン作成は極めて困難な状況であり、「診療マニュアル」として平成 28 年 12 月に刊行した。

４）ミトコンドリア病に詳しい医師のネットワークと情報提供体制の整備とアウトリーチ活動

市民向けのセミナーとしては、平成 28 年 11 月 19 日に札幌で「市民公開講座：ミトコンドリア病を知る」を開催した。また、難病情報センターの HP の情報を更新した。患者会主催の勉強会でセミナーを行った（平成 28 年 7 月 2 日：大阪）。

「ミトコンドリア病に詳しい医師のネットワーク」を構築する計画については、当初予定していた全国を 7 つの地域に分け、それぞれの地域毎にミトコンドリア病をよく知る小児科、神経内科の専門医が担当し、医療情報の提供や実態調査の援助をする計画であったが、平成 28 年度にはその準備に止まった。

５）実態調査を兼ねた患者レジストリーの構築

実態調査については、平成 25 年度にミトコンドリア病の１病型である MELAS に関して、「ミトコンドリア脳筋症 MELAS の脳卒中用発作に対するタウリン療法の開発」研究班（研究代表者：砂田芳秀、川崎医科大学）で行った、日本小児神経学会及び日本神経学の会員に対するアンケート調査に協力した。しかし、他の臨床病型を含め、ミトコンドリア病全体の状況がつかめていないためので、平成 27 年 1 月に制定された新たな診断基準に基づく実態調査を行う計画であった、しかし、以下の述べるウェブを用いた患者レジストリー構築に手間取り、それに合わせて行う予定の実態調査はさらに遅れている。

患者レジストリーについては、AMED 難治性疾患実用化研究班（村山班）と連携して行うこととし、村山班では主に先天代謝異常症として小児（成人）患者レジストリーを、国立精神・神経医療研究センターでは、神経症状を中心とする成人（小児）患者レジストリーを行うこととした。

国立精神・神経医療研究センターにおけるミトコンドリア病患者レジストリーは、トランスレーショナル・メディカルセンターが実施している筋ジストロフィーの登録事業（Remudy）を敷衍する形態で作業を進めているが、費用等の面，新たな個人情報保護法施行に伴う倫理ガイドライン変更への対応、欧米での患者レジストリー事業との連携待ちの状況があり、平成 28 年度は明確な進展を得られず、平成 29 年以降に持ち越した。

一方、病気の原因や病態解析を進めて、新たな治療法、予防法を開発するには、患者の詳細は情報と患者由来の試料が不可欠である。こちらのレジストリーはバイオリソースとの連携で進めて行く必要があり、この点も欧米との連携を目指している。

６）生殖補助医療の情報収集と見解のまとめ

平成 28 年 10 月に、米国ニューヨークの不妊クリニックが、「核移植治療」で 8993 変異をもち、リー脳症の母から健常な子が産まれたと発表した。この方法では、父と母（核ゲノム）に加えて別の女性（ミトコンドリアゲノム）が関わっており、「3 人の親」がいる子となる。英国内でも、英国外でも倫理的問題があると議論されてきており、米国では禁止された行為であった。しかし、今回の米国にあるクリニックでは、この行為のほとんどをメキシコで行う事で法をすり抜けていた。

日本においては、核移植を行う技術は十分備わっていることから、実際に行うクリニック等が出現しないか懸念がある。したがって、日本においては、

臨床研究として情報公開をしながら施行することを認めることが必要ではないか、という意見が班会議において大勢を占めた。

D．結論

本研究班の活動はAMED難治性疾患実用化研究班（村山班）と連携しながら進め、「診療マニュアル」を刊行した。全国レベルの診断体制の整備、診断基準や重症度スケールの改定作業を進めた。アウトリーチ活動として、市民公開講座や患者会勉強会での講演を行い、生殖補助医療の情報収集と日本での実現可能性について議論した。患者レジストリーは、種々の要因で進んでいないが、グローバルな視点でバイオバンクとの連動を図りながら、着実に進めてゆく必要がある。

E．健康危険情報

なし

F．研究発表

１．論文発表

著書、総説

後藤雄一：ミトコンドリア病，831-833（小児の治療指針、小児科診療2014年増刊号、診断と治療社、東京）2014.4.2

後藤雄一：ミトコンドリア病，267-271（図説分子病態学　改訂第5版、中外医学社、東京）2014.5.10

後藤雄一:DNAポリメラーゼγ異常症，221-224（代謝性ミオパチー、診断と治療社、東京）2014.5.30

後藤雄一:ANT1などの遺伝子異常症，225-227（代謝性ミオパチー、診断と治療社、東京）2014.5.30

後藤雄一：ミトコンドリア病，817-822（神経症候群（第2版）、日本臨床別冊、日本臨床社、大阪）2014.6.20

後藤雄一：ミトコンドリア病，251-252（2015-2017神経疾患最新の治療、南江堂、東京）2015.1.30

後藤雄一：ミトコンドリアDNAの遺伝学，285-290（産婦人科医必読-臨床遺伝学の最新知識、産婦人科の実際増大号、金原出版、東京）2015.3.1

小坂　仁：大脳萎縮症　編集　水澤秀洋、新領域別症候群シリーズ No.29「神経症候群（第２版）IV、日本臨牀社，p.319-324. 2014

小坂　仁：小脳萎縮症　編集　水澤秀洋、新領域別症候群シリーズ No.29「神経症候群（第２版）IV、日本臨牀社、p.325-328. 2014（査読無）

竹下絵里、小牧宏文：ミトコンドリア病．別冊日本臨牀　神経症候群（第2版）．日本臨牀社，大阪，223-227，2014

竹下絵里、小牧宏文：MNGIE．代謝性ミオパチー．診断と治療社，東京，185-187頁，2014

三牧正和:ミトコンドリア異常症．小児科臨床ピクシス3 小児てんかんの最新医療改訂第2版．中山書店，東京，50-51，2014

山岨達也、越智　篤：聴覚に関わる社会医学的諸問題「加齢に伴う聴覚障害」．Audiology Japan 57(1)：52-62，2014

山岨達也．耳鼻咽喉科のアンチエイジング．老人性難聴の予防．Therapeutic Research 35:808-810,2014

山岨達也．難聴の基礎と臨床，Anti-aging medicine 10:916-924，2014

Arakawa K, Ikawa M, Tada H, Okazawa H, Yoneda M. Mitochondrial cardiomyopathy and usage of

L-arginine. Arginine in Clinical Nutrition. Ed. Victor R. Preedy. Springer, NY. USA, 2015 (in press)

井川正道, 米田誠. MERRF, 代謝性ミオパチー, 総編集　杉江秀夫,分担編集　福田冬季子,西野一三,古賀靖敏, 診断と治療社, 東京, 175-177, 2014

米田誠, 井川正道, 岡沢秀彦. パーキンソン病および関連神経変性疾患の PET 酸化ストレスイメージング.「脳内環境-恒常性維持機構の破綻と病気」. 編集　高橋良輔,渋谷真,山中宏二,樋口真人.MOOK 遺伝医学,メディカルドー社,大坂, 212-215, 2014

H. Okazawa, M. Ikawa, T. Tsujikawa, Y. Kiyono, M. Yoneda. Brain imaging for oxidative stress and mitochondrial dysfunction in neurodegenerative diseases. Q J Nucl Med Mol Imaging 58:387-397, 2014

井川正道, 米田誠. MERRF. 神経症候群Ⅳ, 日本臨床別冊, 345-348, 2014

荒川健一郎, 米田誠. ミトコンドリア心筋症に対する代謝治療. 細胞46, 21-24, 2014.

西野一三:ミトコンドリア脳筋症. 神経内科研修ノート. 診断と治療社, 東京, 522-526, 2015

西村洋昭,西野一三:組織化学染色(SDH と COX). 引いて調べる先天代謝異常症.診断と治療社, 東京, 114, 2014

後藤雄一:ミトコンドリア病, pp.313-316（小児科診療ガイドライン-最新の診療指針-（第3版)、総合医学社、東京）2016.3

後藤雄一：ミトコンドリア遺伝関連, pp.722-725（日常診療のための検査値のみかた、中外医学社、東京）2015.4.10

後藤雄一: ミトコンドリア脳筋症の治療, pp.230-231（小児神経科診断・治療マニュアル改訂第3版、診断と治療社、東京）2015.4.16

後藤雄一:MELAS（mitochondrial myopathy, encephalopathy, lactic acidosis and stroke-like episodes),pp.190-194(骨格筋症候群第2版(下)、日本臨床別冊、日本臨床社、大阪）2015.7.2

後藤雄一:MERRF（myoclonic epilepsy associated with ragged-red fibers), pp.195-197（骨格筋症候群第2版（下)、日本臨床別冊、日本臨床社、大阪）2015.7.20

後藤雄一:慢性進行性外眼筋麻痺症候群, Kearns-Sayre 症候群, pp.198-201（骨格筋症候群第2版（下)、日本臨床別冊、日本臨床社、大阪）2015.7.20

後藤雄一:Pearson 症候群, pp.202-204（骨格筋症候群第二版（下)、日本臨床別冊、日本臨床社、大阪）2015.7.20

後藤雄一:乳児致死型ミトコンドリア病, pp.214-216（骨格筋症候群第二版（下)、日本臨床別冊、日本臨床社、大阪）2015.7.20

後藤雄一:ミトコンドリアDNA検査,SRL宝函36(2):440-46, 2015

後藤雄一:ミトコンドリア脳筋症:遺伝子型と表現型, Heart View 20(2):42-47, 2015

後藤雄一:ミトコンドリア病, Equilibrium Research　75(1):1-4, 2016

大竹　明, 岡崎康司:「ミトコンドリア病の治療と予防」機能性アミノ酸5-アミノレブリン酸の科学と医学応用-

がんの診断・治療を中心に- ボルフィリン-ALA 学会編 *現代科学・増刊 45 東京化学同人(2015)*

Fujita Y, Taniguchi Y, Shinkai S, Tanaka M, Ito M: Secreted growth differentiation factor 15 as a potential biomarker for mitochondrial dysfunctions in aging and age-related disorders. *Geriatr Gerontol Int* 16 (Suppl. 1): *17-29, 2016*

三牧正和：Alpers 症候群. 別冊日本臨牀 新領域別症候群シリーズ No.33 骨格筋症候群（第 2 版)（下）pp. 217-221, 日本臨牀社, 大阪, 2015

三牧正和：Leigh 脳症. 別冊日本臨牀 新領域別症候群シリーズ No.33 骨格筋症候群（第 2 版）（下）pp. 222-228, 日本臨牀社, 大阪, 2015

三牧正和：良性乳児ミオパチー. 別冊日本臨牀 新領域別症候群シリーズ No.33 骨格筋症候群（第 2 版）（下）pp. 229-232, 日本臨牀社, 大阪, 2015

Yamasoba T. Interventions to prevent age-related hearing loss. Springer International Publishing VI: 335-349、2015

日本ミトコンドリア学会 編集 村山圭, 小坂仁, 米田誠 ： 「ミトコンドリア病診療マニュアル 2017」診断と治療社, 東京, pp.1-172 2016,

後藤雄一：Kearns-Sayre 症候群. 小児の症候群. 小児科診療 2016 年増刊号, 診断と治療社, 東京, pp.102, 2016

後藤雄一：ミトコンドリア病. 特集 慢性疾患児の一生を診る, 小児内科増刊号, 東京医学社, 東京, pp. 1527-1529, 2016

後藤雄一：ミトコンドリア病の病因研究の現状, 特集ミトコンドリア研究 UPDATE, 医学のあゆみ 260 (1): 63-66, 2017

後藤雄一：ミトコンドリア病に対する医療体制の現状と課題. 特集ミトコンドリア研究 UPDATE, 医学のあゆみ 260 (1): 123-127, 2017

三牧正和：MELAS 症候群. 小児科診療増刊号 小児の症候群 pp.108 頁, 診断と治療社, 東京, 2016

三牧正和：呼吸鎖複合体 I アセンブリー機構とミトコンドリア病. 医学のあゆみ 第 1 土曜特集 ミトコンドリア研究 UPDATE. Vol.260, No.1 pp.49-54, 医歯薬出版株式会社, 東京, 2017

Arakawa, K Ikawa M, Tada H, Okazawa H, Yoneda. M: Mitochondrial cardiomyopathy and usage of L-arginine. Arginine in Clinical Nutrition. Ed. Victor R. Preedy. Springer, NY. USA, pp.461-470, 2016.

井川正道, 米田誠：ミトコンドリア病の脳機能画像解析. 医学の歩み 260, 67-72, 2017.

井川正道, 岡沢秀彦, 米田誠：酸化ストレスイメージング. Annual Review 神経 2017, p87-93, 2017.

原著論文

Sakai C, Yamaguchi S, Sasaki M, Miyamoto Y, Matsushima Y, Goto Y.
ECHS1 mutations cause combined respiratory chain deficiency resulting in Leigh syndrome. Hum Mut 36: 232-239, 2015

Ohnuki Y, Takahashi K, Iijima E, Takahashi W, Suzuki S, Ozaki Y, Kitao R, Mihara M, Ishihara T, Nakamura M, Sawano Y, Goto Y, Izumi S, Kulski J-K, Shiina T, Takizawa S. Multiple deletions in mitochondrial DNA in a patient with progressive

external ophthaloplegia, leukoencephalopathy and
hypogonadism. Inter Med 53: 1365-1369, 2014

宮脇統子、古東秀介、石原広之、後藤雄一、西野一三、苅田典生、戸田達史. ミトコンドリア DNA8729G>A 変異を認めた neurogenic muscle weakness, ataxia, and retinitis pigmentosa (NARP) の1例. 臨床神経学 22:91-95, 2015

Imagawa E, Osaka H, Yamashita A, Shiina M, Takahashi E, Sugie H, Nakashima M, Tsurusaki Y, Saitsu H, Ogata K, Matsumoto N, Miyake N. A hemizygous GYG2 mutation and Leigh syndrome: a possible link? Hum Genet 133 : 225-234, 2014

Akiyama T, Osaka H, Shimbo H, Nakajiri T, Kobayashi K, Oka M, Endoh F, Yoshinaga H. A Japanese Adult Case of Guanidinoacetate Methyltransferase Deficiency. JIMD Rep. 12 : 65-69, 2014

van de Kamp J, Errami A, Howidi M, Anselm I, Winter S, Phalin-Roque J, Osaka H, van Dooren S, Mancini G, Steinberg S, Salomons G. Genotype-phenotype correlation of contiguous gene deletions of SLC6A8, BCAP31 and ABCD1. Clin Genet 2014 Mar 5. doi: 10.1111/cge.12355. [Epub ahead of print].

Kondo H, Tanda K, Tabata C, Hayashi K, Kihara M, Kizaki Z, Taniguchi-Ikeda M, Mori M, Murayama K, Ohtake A: Leigh syndrome with Fukuyama congenital muscular dystrophy: A case report. Brain Dev 36(8): 730-3, 2014.

Yamazaki T, Murayama K, Compton AG, Sugiana C, Harashima H, Amemiya S, Ajima M, Tsuruoka T, Fujinami A, Kawachi E, Kurashige Y, Matsushita K, Wakiguchi H, Mori M, Iwasa H, Okazaki Y, Thorburn DR, Ohtake A: Molecular diagnosis of mitochondrial respiratory chain disorders in Japan: Focusing on mitochondrial DNA depletion syndrome. Pediatr Int 56(2):180-187, 2014.

Ohtake A, Murayama, K, Mori M, Harashima H, Yamazaki T, Tamaru S, Yamashita Y, Kishita Y, Nakachi Y, Kohda M, Tokuzawa Y, Mizuno Y, Moriyama Y, Kato H, Okazaki Y: Diagnosis and molecular basis of mitochondrial respiratory chain disorders: exome sequencing for disease gene identification. Biochim Biophys Acta 1840(4):1355-1359, 2014.

Saitsu H, Tohyama J, Walsh T, Kato M, Kobayashi Y, Lee M, Tsurusaki Y, Miyake N, Goto Y, Nishino I, Ohtake A, King M-C, Matsumoto N: A girl with West syndrome and autistic features harboring a de novo TBL1XR1 mutation. J Hum Genet 59(10):581-3, 2014.

Fukao T, Akiba K, Goto M, Kuwayama N, Morita M, Hori T, Aoyama Y, Venkatesan R, Wierenga R, Moriyama Y, Hashimoto T, Usuda N, Murayama K, Ohtake A, Hasegawa Y, Shigematsu Y, Hasegawa Y: The first case in Asia of 2-methyl-3-hydroxybutyryl-CoA dehydrogenase deficiency (HSD10 disease) with atypical presentation. J Hum Genet 59(11): 609-14, 2014.

Uehara N, Mori M, Tokuzawa Y, Mizuno Y, Tamaru S, Kohda M, Moriyama Y, Nakachi Y, Matoba N, Sakai T, Yamazaki T, Harashima H, Murayama K, Hattori K, Hayashi J, Yamagata T, Fujita Y, Ito M, Tanaka M, Nibu K, Ohtake A, Okazaki Y: New *MT-ND6* and *NDUFA1* mutations in mitochondrial respiratory chain disorders. Ann Clin Transl Neurol 1(5):361-9, 2014.

Kopajtich R, Nicholls TJ, Rorbach J, Metodiev MD, Freisinger P, Mandel H, Vanlander A, Ghezzi D,

Carrozzo R, Taylor RW, Marquard K, Murayama K, Wieland T, Schwarzmayr T, Mayr JA, Pearce SF, Powell CA, Saada A, Ohtake A, Invernizzi F, Lamantea E, Sommerville EW, Pyle A, Chinnery PF, Crushell E, Okazaki Y, Kohda M, Kishita Y, Tokuzawa Y, Assouline Z, Rio M, Feillet F, de Camaret BM, Chretien D, Munnich A, Menten B, Sante T, Smet J, Régal L, Lorber A, Khoury A, Zeviani M, Strom TM, Meitinger T, Bertini ES, Van Coster R, Klopstock T, Rötig A, Haack TB, Minczuk M, Prokisch H: Mutations in *GTPBP3* cause a mitochondrial translation defect associated with hypertrophic cardiomyopathy, lactic acidosis and encephalopathy. Am J Hum Genet 95(6):708-20, 2014.

Montassir H, Maegaki Y, Murayama K, Yamazaki T, Kohda M, Ohtake A, Iwasa H, Yatsuka Y, Okazaki Y, Sugiura C, Nagata I, Toyoshima M, Saito Y, Itoh M, Nishino I, Ohno K: Myocerebrohepatopathy spectrum disorder due to *POLG* mutations: A clinicopathological report. Brain Dev. doi: 10.1016/j.braindev.2014.10.013. [Epub ahead of print]

Nozaki F, Kumada T, Kusunoki T, Fujii T, Murayama K, Ohtake A: Fever of Unknown Origin as the Initial Manifestation of Valproate-Induced Fanconi Syndrome. Pediatr Neurol 51(6): 846-849, 2014.

Brea-Calvo G, Tobias B Haack, Karall D, Ohtake A, Invernizzi F, Carrozzo R, Kremer L, Dusi S, Fauth C, Scholl-Bürgi S, Graf E, Ahting U, Resta N, Laforgia N, Verrigni D, Okazaki Y, Kohda M, Martinelli D, Freisinger P, Strom TM, Meitinger T, Lamperti C, Lacson A, Navas P, Mayr JA, Bertini E, Murayama K, Zeviani M, Prokisch H, Ghezzi D: COQ4 mutations cause a broad spectrum of mitochondrial disorders associated with CoQ10 deficiency. Am J Hum Genet 96: 309-317, 2015.

Haack T, Jackson C, Murayama K, Kremer L, Schaller A, Kotzaeridou U, de Vries M, Schottmann G, Santra S, Büchner B, Wieland T, Graf E, Freisinger P, Eggimann S, Ohtake A, Okazaki Y, Kohda M, Kishita Y, Tokuzawa Y, Sauer S, Memari Y, Kolb-Kokocinski A, Durbin R, Hasselmann O, Cremer K, Albrecht B, Wieczorek D, Engels H, Hahn D, Zink A, Alston C, Taylor R, Rodenburg R, Trollmann R, Sperl W, Strom T, Hoffmann G, Mayr J, Meitinger T, Bolognini R, Schuelke M, Nuoffer J-M, Kölker S, Prokisch H, Klopstock T: Deficiency of ECHS1 causes mitochondrial encephalopathy with cardiac involvement. Ann Clin Transl Neurol (in press)

Hayashi T, Asano Y, Shintani Y, Kioka H, Tsukamoto O, Higo S, Kato H, Hikita M, Shinzawa-Ito K, Yamazaki S, Takafuji K, Asanuma H, Asakura M, Minamino T, Goto Y, Kitakaze M, Komuro I, Sakata Y, Ogura T, Aoyama H, Tsukihara T, Yoshikawa S, Takashima S. Higd1a is a positive regulator of cytochrome c oxidase. Proc Natl Acad Sci U S A. 112(5):1553-1558, 2015

Tanisawa K, Ito T, Sun X, Ise R, Oshima S, Cao Z-B, Sakamoto S, Tanaka M, Higuchi M. High cardiorespiratory fitness can reduce glycated hemoglobin levels regardless of polygenic risk for type 2 diabetes mellitus in non-diabetic Japanese men. Physiological Genomics 46: 497-504, 2014

Kitazoe Y, Tanaka M. Evolution of mitochondrial power in vertebrate metazoans. PloS one 9(6): e98188, 2014

Fujii T, Nozaki F, Saito K, Hayashi A, Nishigaki Y, Murayama K, Tanaka M, Koga Y, Hiejima I, Kumada T. Efficacy of pyruvate therapy in patients with mitochondrial disease: A semi-quantitative clinical evaluation study. Mol Genet Metab 112(2): 133-138, 2014

Imasawa T, Tanaka M, Maruyama N, Kawaguchi T, Yamaguchi Y, Rossignol R, Kitamura H, Nishimura M. Pathological similarities between low birth weight-related nephropathy and nephropathy associated with mitochondrial cytopathy. Diagnostic Pathology 9:181, 2014

Imasawa T, Tanak M, Yamaguchi Y, Nakazato T, Kitamura H, Nishimura M. 7501 T > A mitochondrial DNA variant in a patient with glomerulosclerosis. Renal Failure 36(9): 1461-1465, 2014

Tanisawa K, Ito T, Sun X, Ise R, Oshima S, Cao Z-B, Sakamoto S, Tanaka M, Higuchi M. Strong influence of dietary intake and physical activity on body fatness in elderly Japanese men: age-associated loss of polygenic resistance against obesity. Genes & Nutrition 9: 5, 2014

長田治、岩崎章、西野一三、埜中征哉、後藤雄一. 高度のミトコンドリア DNAA3243G 変異率と臨床経過との関連が示唆された MELAS の一例. 神経内科 83(6) 520-524, 2016

Kim Y, Koide R, Isozaki E, Goto Y. Magnetic resonance imaging findings in Leigh syndrome with a novel compound heterozygous SURF1 gene mutation. Neurol Clin Neurosci 4:34-35, 2016

Suzuki T, Yamaguchi H, Kikusato M, Hashizume O, Nagatoishi S, Matsuo A, Sato T, Kudo T, Matsuhashi T, Murayama K, Ohba Y, Watanabe S, Kanno SI, Minaki D, Saigusa D, Shinbo H, Mori N, Yuri A, Yokoro M, Mishima E, Shima H, Akiyama Y, Takeuchi Y, Kikuchi K, Toyohara T, Suzuki C, Ichimura T, Anzai JI, Kohzuki M, Mano N, Kure S, Yanagisawa T, Tomioka Y, Tohyomizu M, Tsumoto K, Nakada K, Bonventre JV, Ito S, Osaka H, Hayashi KI, Abe T. Mitochonic acid 5 binds mitochondria and ameliorates renal tubular and cardiac myocyte damage. J Am Soc Nephrol. 2015 Nov 25. pii: ASN.2015060623. [Epub ahead of print]

Suzuki T, Yamaguchi H, Kikusato M, Matsuhashi T, Matsuo A, Sato T, Oba Y, Watanabe S, Minaki D, Saigusa D, Shimbo H, Mori N, Mishima E, Shima H, Akiyama Y, Takeuchi Y, Yuri A, Kikuchi K, Toyohara T, Suzuki C, Kohzuki M, Anzai J, Mano N, Kure S, Yanagisawa T, Tomioka Y, Toyomizu M, Ito S, Osaka H, Hayashi K, Abe T. Mitochonic acid 5 (MA-5), a derivative of the plant hormone indole-3-acetic acid, improves survival of fibroblasts from patients with mitochondrial diseases. Tohoku J Exp Med. 236(3): 225-232, 2015

Imai A, Fujita S, Kishita Y, Kohda M, Tokuzawa Y, Hirata T, Mizuno Y, Harashima H, Nakaya A, Sakata Y, Takeda A, Mori M, Murayama K, Ohtake A, Okazaki Y. Rapidly progressive infantile cardiomyopathy with mitochondrial respiratory chain complex V deficiency due to loss of ATPase 6 and 8 protein. *Int J Cardiol*. 207:203-205, 2016

Kohda M, Tokuzawa Y, Kishita Y (Equally first author), et al. A comprehensive genomic analysis reveals the genetic landscape of mitochondrial respiratory chain complex

deficiencies. *PLOS Genet.* 12(1):e1005679. doi:10.1371/journal.pgen.1005679. eCollection (2016)

Kishita Y, Pajak A, Bolar N-A, Marobbio C, Maffezzini C, Miniero D-V, Monne M, Kohda M, Stranneheim H, Murayama K, Naess K, Lesko N, Bruhn H, Mourier A, Wibom R, Nennesmo I, Jespers A, Govaert P, Ohtake A, Van Laer L, Loeys B-L, Freyer C, Palmieri F, Wredenberg A, Okazaki Y, Wedell A. Intra-mitochondrial Methylation Deficiency Due to Mutations in SLC25A26. Am J Hum Genet 97:1-8, 2015

Haack TB, Jackson CB, Murayama K, Kremer LS, Schaller A, Kotzaeridou U, de Vries MC, Schottmann G, Santra S, Büchner B, Wieland T, Graf E, Freisinger P, Eggimann S, Ohtake A, Okazaki Y, Kohda M, Kishita Y, Tokuzawa Y, Sauer S, Memari Y, Kolb-Kokocinski A, Durbin R, Hasselmann O, Cremer K, Albrecht B, Wieczorek D, Engels H, Hahn D, Zink AM, Alston CL, Taylor RW, Rodenburg RJ, Trollmann R, Sperl W, Strom TM, Hoffmann GF, Mayr JA, Meitinger T, Bolognini R, Schuelke M, Nuoffer JM, Kölker S, Prokisch H, Klopstock T. Deficiency of ECHS1 causes mitochondrial encephalopathy with cardiac involvement. *Ann. Clin. Transl. Neurol.* 2(5): 492-509, 2015

Haginoya K, Kaneta T, Togashi N , Hino-Fukuyo N, Kobayashi T, Uematsu M, Kitamura T, Inui T, Okubo Y, Takezawa Y, Anzai M, Endo W, Miyake N, Saitsu H, Matsumoto N, Kure S. FDG-PET study of patients with Leigh syndrome. J. Neurol Sci 362: 309-313, 2016

Yatsuga S, Fujita Y, Ishii A, Fukumoto Y, Arahata H, Kakuma T, Kojima T, Ito M, Tanaka M, Saiki R, Koga Y. Growth differentiation factor 15 as a useful biomarker for mitochondrial disorders. Ann Neurol. 78: 814-823, 2015

Formosa LE*, Mimaki M*, Frazier AE, McKenzie M, Stait TL, Thorburn DR, Stroud DA, Ryan MT: Characterization of mitochondrial FOXRED1 in the assembly of respiratory chain complex I. Hum Mol Genet. 24(10): 2952-2965, 2015
*These authors equally contributed.

Kamogashira T, Fujimoto C, Yamasoba T. Reactive Oxygen Species, Apoptosis, and Mitochondrial Dysfunction in Hearing Loss. BioMed Research International 617207: 1-7, 2015

Sakamoto T, Yamasoba T. Current Concepts of the Mechanisms in Age-Related Hearing Loss. J Clin Exp Pathol, 5: 1-2, 2015

Ikawa M, Okazawa H, Tsujikawa T, Matsunaga A, Yamamura O, Mori T, Hamano T, Kiyono Y, Nakamoto Y, Yoneda M. Increased oxidative stress is related to disease severity in the ALS motor cortex: A PET study. Neurology 84:2033-2039, 2015

Yokota M, Hatakeyama H, Ono Y, Kanazawa M, Goto Y: Mitochondrial respiratory dysfunction disturbs neuronal and cardiac lineage-commitment of human iPSCs. Cell Death Dis 8(1): e2551, 2017

Hatakeyama H, Goto Y: Respiratory chain complex disorganization impairs mitochondrial and cellular integrity: Phenotypic variation in cytochrome *c* oxidase deficiency. Am J Pathol 187(1): 110-121, 2017

Ling F, Niu R, Hatakeyama H, Goto Y, Shibata T, Yoshida M: Reactive oxygen species stimulate mitochondrial allele segregation toward homoplasmy in human cells. Mol Biol Cell 27(10):

1684-1693, 2016

Suzuki T, Yamaguchi H, Kikusato M, Hashizume O, Nagatoishi S, Matsuo A, Sato T, Kudo T, Matsuhashi T, Murayama K, Ohba Y, Watanabe S, Kanno SI, Minaki D, Saigusa D, Shinbo H, Mori N, Yuri A, Yokoro M, Mishima E, Shima H, Akiyama Y, Takeuchi Y, Kikuchi K, Toyohara T, Suzuki C, Ichimura T, Anzai JI, Kohzuki M, Mano N, Kure S, Yanagisawa T, Tomioka Y, Tohyomizu M, Tsumoto K, Nakada K, Bonventre JV, Ito S, Osaka H, Hayashi KI, Abe T: Mitochonic acid 5 binds mitochondria and ameliorates renal tubular and cardiac myocyte damage. Am J Soc Nephrol, 27(7): 1925-1932, 2016

Gorman GS, Chinnery PF, DiMauro S, Hirano M, Koga Y, McFarland R, Suomalainen A, Thorburn DR, Zeviani M, Turnbull DM. Mitochondrial diseases. Nature Reviews Disease Primers 2:16080, 2016

Yoshimuta H, Nakamura M, Kanda E, Fujita S, Takeuchi K, Fujimoto T, Nakabeppu Y, Akasaki Y, Sano A: The effects of olanzapine treatment on brain regional glucose metabolism in neuroleptic-naive first-episode schizophrenic patients. Hum Psychopharmacol 31, 419-426, 2016

Fujimoto C, Yamamoto Y, Kamogashira T, Kinoshita M, Egami N, Uemura Y, Togo F, Yamasoba T, Iwasaki S. Noisy galvanic vestibular stimulation induces a sustained improvement in body balance in elderly adults. Sci Rep. 6:37575, 2016

Kamogashira T, Hayashi K, Fujimoto C, Iwasaki S, Yamasoba T. Functionally and morphologically damaged mitochondria observed in auditory cells under senescence-inducing stress. npj Aging and Mechanisms of Disease 23: 2, 2017

２．学会発表

国際学会

Sakai C, Matsushima Y, Sasaki M, Miyamoto Y, Goto Y: Targeted exome sequencing identified a novel genetic disorder in mitochondrial fatty acid β-oxidation. Euromit 2014, Tampere, Finland, 6.16, 2014

Matsushima Y, Hatakeyama H, Takeshita E, Kitamura T, Kobayashi K, Yoshinaga H, Goto Y. Leigh-like syndrome associated with calcification of the bilateral basal ganglia caused by compound heterozygous mutations in mitochondrial poly(A) polymerase. Euromit 2014, Tampere, Finland, 6.16, 2014

Goto Y: Mitochondrial Disease. Asian & Oceanian Epilepsy Congress 2014.
Singapore, 8.7, 2014

Osaka H, Shimbo H, Murayama K, Ohtake A, Aida N. A rapid screening with direct sequencing from blood samples for the diagnosis of Leigh syndrome. Mitochondrial Medicine 2014: Pittsburgh, PA 6.4-6.7, 2014

Ohtake A, Murayama K, Yamazaki T, Harashima H, Tokuzawa Y, Kishita Y, Mizuno Y, Kohda M, Shimura M, Fushimi T, Taniguchi M , Ajima M, Takayanagi M, Yasushi Okazaki Y: 5-Aminolevulnic acid and Fe can bring a permanent cure for mitochondrial respiration chain disorders. The 4th Asian Congress for Inherited Metabolic Disease, Taipei, Taiwan, March 20, 2015

Kioka H, Kato H, Asano Y, Sakata Y, Kitakaze M, Takashima S. In Vivo Visualization of ATP

Dynamics under Hypoxia Reveals That G0/G1 switch gene 2 Provides Ischemic Tolerance through the Increase of ATP Production. AHA 2014 (2014/11/15-19, Chicago U.S.A.)

Tanaka M. GDF15 is a novel biomarker to evaluate efficacy of pyruvate therapy for mitochondrial diseases. 11th Conference of Asian Society of Mitochondrial Research and Medicine. November 14-15, 2014, Taiwan

Formosa LE, Mimaki M, Frazier AE, McKenzie M, Thorburn DR, Stroud DA, Ryan MT. Characterization of mitochondrial FOXRED1 in the assembly of respiratory chain complex I. AussieMit 2014, Perth, Australia, 12.1-3, 2014

Ikawa M, Okazawa H, Tsujikawa T, Muramatsu T, Kishitani T, Kamisawa T, Matsunaga A, Yamamura O, Mori T, Hamano T, Kiyono Y, Nakamoto Y, Yoneda M. Increased cerebral oxidative stress in amyotrophic lateral sclerosis: a 62Cu-ATSM PET study. 2014 AAN, Philadelphia, Apr 26 to May 3, 2014.

Arakawa K, Ikawa M, Tada H, Okazawa H, Yoneda M. The Impact of L-arginine administration on mitochondrial cardiomyopathy 5th World Congress on Targeting Mitochondria. Berlin, Germany, Oct. 29-31, 2014.

Yoneda M, Ikawa M, Tsujikawa T, Mori T, Hamano T, Nakamoto Y, Kiyono Y, Okazawa H. PET imaging of cerebral oxidative stress in neurodegenerative disorders. 5th World Congress on Targeting Mitochondria. Berlin, Germany, Oct. 29-31, 2014.

Miyazaki K, Ikawa M, Tsujikawa T, Mori T, Hamano T, Nakamoto Y, Kiyono Y, Okazawa H, Yoneda M. Increased cerebral oxidative stress in amyotrophic lateral sclerosis: a 62Cu-ATSM PET study. The 11th Conference of Asian Society for Mitochondrial Research and Medicine, Taipei, Taiwan, Nov. 14-15, 2014.

Fukuda H, Min K-D, Asanuma H, Ito S, Shindo K, Imazu M, Tomonaga T, Minamino N, Asakura M, Kitakaze M. Proteomic analysis of canine failing hearts induced by rapid pacing: evidence for the elevation of the protein levels related to either mitochondrial dysfunction or acute phase response signaling. ESC 2015(2015/8/29-9/2, London, UK)

Tanaka M, Fujita Y, Ito M, Kojima T, Yatsuga S, Koga Y. GDF15 is a novel biomarker to evaluate efficacy of pyruvate therapy for mitochondrial diseases. The 11th Mitochondrial Physiology Conference, Luční Bouda, Czech, 9.7-10, 2015

Fujita Y, Taniguchi Y, Shinkai S, Tanaka M, Ito M. GDF15 as a potential biomarker for mitochondrial dysfunction in aging and age-related disorders. 12th Conference of the Asian Society of Mitochondrial Research and Medicine, Hangzhou, China
11.14-15, 2015

Tanaka M, Fujita Y, Yatsuga S, Ishii A, Fukumoto Y, Arahata H, Kakuma T, Kojima T, Ito M, Reo Saiki R, Koga Y. GDF15 is a novel biomarker to evaluate efficacy of pyruvate therapy for mitochondrial disorders. International Symposium of Mitochondrial Biology and Medicine, Xian, China, 11.16-17, 2015

Yamasoba T, Kashio A, Yamada C, Kamogashira T,

Fujimoto C, Someya S. Prevention of cochlear damage due to GeO2-induced mitochondrial dysfunction by antioxidants. CORLAS annual meeting, San Francisco, USA, 8.23-26, 2015

Yamasoba T. The effect of mitochondrial damage on hearing loss. Gwangju Otology & Neurotology Symposium, Gwangju, Korea, 11.1, 2015

Okazawa H, Ikawa M, Tsujikawa T, Mori T, Makino A, Kiyono Y, Yoneda M. Evaluation of nigrostriatal oxidative stress intensity in patients with Parkinson’s disease using [Cu-62]ATSM PET and FP-CIT SPECT. European Association of Nuclear Medicine (EANM)’15, 10.10-14, Hamburg, Germany, 2015.

Goto Y : Overview - mtDNA medicine, The 13th Conference of Asian Society for Mitochondrial Research and Medicine (ASMRM), Tokyo, 10.31, 2016

Ling F, Niu R, Hatakeyama H, Goto Y, Shibata T, Yoshida M: An oxidative stress-stimulated mechanism for human mitochondrial alleles. The 13th Conference of Asian Society for Mitochondrial Research and Medicine, Tokyo, 10.30-11.1, 2016

国内学会

後藤雄一:ミトコンドリア病に関わる基礎研究の進展．企画セミナー１　ミトコンドリア病：A reappraisal. 第56回日本小児神経学会学術集会, 浜松, 5.30, 2014

後藤雄一：ミトコンドリア脳筋症：MELASの脳卒中発作に対するタウリン療法の開発.共同研究支援委員会主催セミナー. 第56回日本小児神経学会学術集会, 浜松, 5.30, 2014

水野葉子, 三牧正和, 太田さやか, 下田木の実, 高橋長久, 岩崎博之, 斉藤真木子, 岡明, 水口雅, 後藤雄一:ミトコンドリア呼吸鎖異常症の診断におけるBlue-Native電気泳動 (BN-PAGE). 第56回日本小児神経学会学術集会, 浜松, 5.30, 2014

坂井千香, 松島雄一, 山口清次, 佐々木征行, 宮本雄策, 後藤雄一：ECHS1の変異は呼吸鎖の活性低下を伴うLeigh脳症を引き起こす. 第14回日本ミトコンドリア学会年会, 福岡, 12.5, 2014

金田大太, 新宅雅幸, 窪田-坂下美恵, 加藤忠史, 後藤雄一：MELAS脳卒中発作におけるAQP4の発現低下.第14回日本ミトコンドリア学会年会,福岡, 12.5, 2014

Osaka H, Tsuyusaka Y, Iai M, Yamashita S, Shimozawa N, Eto Y, Saitsu H. Whole exome sequencing reveals molecular basis of childhood cerebellar atrophy. 第 56 回日本小児神経学会 2014.5.28-2014.5.30.　浜松

池田尚広, 山崎雅世, 鈴木　峻, 門田行史, 小坂仁, 杉江秀夫, 新保裕子, 山形崇倫. ミトコンドリア DNA m.3243A>T 変異を認めた mitochondrial encephalomyopathy, lactic acidosis and stroke-like episodesの1例. 第56回日本小児神経学会　2014.5.28-2014.5.30. 浜松

山岨達也. 加齢に伴う聴覚障害. 第59回日本聴覚医学会11.27-28, 2014. 下関

宮崎一徳, 井川正道, 辻川哲也, 中本安成, 岡沢秀彦, 米田誠. 62Cu-ATSM PETを用いた筋萎縮性側索硬化症 (ALS) における脳内酸化ストレスの検討. 第 14 回日本ミトコンドリア学会年会. 平成 26 年 12 月 3-5 日, 福岡.

後藤雄一：Incidental findings（偶発的所見）を考える － まとめと今後の課題. 日本人類遺伝学会第60回大会, 東京, 10.17, 2015

水野葉子、三牧正和、太田さやか、下田木の実、高橋長久、岩崎博之、岡明、片山菜穂子、生井良幸、水口雅、後藤雄一：Blue-Native PAGE（BN-PAGE）にて呼吸鎖複合体Ⅰ及びⅣ低下を求め、POLG 遺伝子異常が判明したミトコンドリア病の一例. 第57回日本小児神経学会学術集会, 大阪, 5.29, 2015

平出拓也、石山昭彦、瀬川和彦、竹下絵里、本橋裕子、小牧宏文、斎藤貴志、中川栄二、須貝研司、後藤雄一、佐々木征行：MELAS 患者における WPW 症候群の合併. 第57回日本小児神経学会学術集会, 大阪, 5.29, 2015

大竹 明, 村山 圭, 岡崎康司:ミトコンドリア呼吸鎖異常症とそれを引き起こす様々な遺伝子群 第 38 回日本分子生物学会年会・第88回日本生化学会大会 合同大会, 神戸, 12.2.2015

Fukuda H, Min K-D, Imazu M, Shindo K, Ito S, Tomonaga T, Minamino N, Asanuma H, Asakura M, Kitakaze M. イヌ心不全モデルのプロテオーム解析：LVEF とミトコンドリア機能異常との関連. 第19回日本心不全学会学術集会, 大阪, 10.25, 2015

田中雅嗣. ミトコンドリア病に対するピルビン酸ナトリウム療法の概念実証. 第56回日本神経学会学術総会 新潟, 5.19-22, 2015

田中雅嗣. ミトコンドリア病に対するピルビン酸ナトリウムによる治療法開発と GDF15 による体外診断薬の創出, 第15回日本ミトコンドリア学会年会, 福井, 11.19-20, 2015

米田誠. 大会長（学会主催）. 第15回日本ミトコンドリア学会年会, 福井, 11.19-20, 2015

米田誠. 神経疾患のミトコンドリア機能イメージング. 教育講演「分子病理画像と症候」. 第56回日本神経学会総会. 新潟, 5.20-23, 2015

米田誠. 神経疾患の酸化ストレス PET 脳イメージング. ワークショップ「ミトコンドリアが関与する神経障害」. 第68回 日本酸化ストレス学会, 鹿児島, 6.11-12, 2015

米田誠. Cu-ATSM PET による脳内酸化ストレスイメージング, オープニングセミナー７：「画像診断の進歩」. 第9回 パーキンソン病・運動障害疾患コングレス, 東京, 19.15-17, 2015

米田誠. オーバービュー（臨床医学）, シンポジウム「ミトコンドリアにおける臨床医学と基礎科学の融合」 . 第15回日本ミトコンドリア学会年会, 福井, 11.19-20, 2015

中村誠、三村治、若倉雅登、稲谷大、中澤徹、白神史雄. Leber 遺伝性視神経症認定基準. 日本眼科学会雑誌 119(5)：339-346, 2015

石山昭彦, 遠藤ゆかり, 斎藤義朗, 中川栄二, 小牧宏文, 須貝研司, 佐々木征行, 佐藤典子, 後藤雄一, 西野一三:鉄硫黄アッセンブリング調節因子である IBA57 遺伝子は progressive cavitating leukoencephalopathy をひきおこす. 第58回日本小児神経学会学術集会, 東京, 6.3, 2016

笠毛渓、中村雅之、大毛葉子、梅原ひろみ、佐野輝：精神症状を来し、 mtDNA 多重欠失を認めたミトコンドリア脳筋症の家系例. 第38回日本生物学的精神医学会総会, 福岡, 9.8, 2016

井川正道, 岡沢秀彦, 松永晶子, 山村修, 濱野忠則, 清野泰, 中本安成, 米田誠：抗 Evaluation of cerebral oxidative stress in patients with ALS using 62Cu-ATSM PET. 第57回日本神経学会総会, 神戸, 5.18-21, 2016

米田誠, 井川正道, 辻川哲也, 木村浩彦, 岡沢秀彦. 脳分子イメージングによる MELAS 脳卒中様発作の病態解明:第 34 回日本神経治療学会, 米子, 11.3-5, 2016

その他

後藤雄一:ミトコンドリア病患者家族の会―東京勉強会「ミトコンドリア病をとりまく医療と治療研究の現況」日本医科大学武蔵小杉病院、川崎、6.22, 2014

後藤雄一:ミトコンドリア病患者家族の会―大阪勉強会「ミトコンドリア病をとりまく医療と治療研究の現況」大阪市中央公会堂、大阪、10.11, 2014

大竹明：第 3 回先天代謝異常症患者会フォーラム 2014.11.9 TKP ガーデンシティ品川

大竹明：第 4 回有機酸・脂肪酸代謝異常症　医師と患者のシンポジウム　2014.12.6 TKP 品川カンファレンスルーム

山岨達也. 老人性難聴の予防と治療.　ラジオ日経「医学講座」　12.18, 2014

米田誠. ミトコンドリア機能異常と人の疾患. 国立遺伝研セミナー「オルガネラ研究会」. 平成 26 年 11 月 7 日, 三島.

米田誠. ミトコンドリア脳筋症の治療の現状. 第15回日本ミトコンドリア学会年会 市民公開講座「ミトコンドリアと病気」, 福井, 11.21, 2015

米田誠. 銅 ATSM-PET による神経難病患者の脳内酸化ストレスイメージング. 第 13 回 神経科学研究会, 東京, 10.10, 2015

上田香織、森實祐基、白神史雄、敷島敬悟、石川均、若倉雅登、中村誠. レーベル遺伝性視神経症の新規発症者数に関する疫学調査. 第 53 回日本神経眼科学会総会. 大宮、11.7, 2015

後藤雄一: ミトコンドリア病とはどんな病気？-難病研究班の活動と目標-, 市民公開講座-ミトコンドリア病を知る, 札幌, 11.19, 2016

後藤雄一: ミトコンドリア病, 第 7 回遺伝カウンセリング研修会, 札幌, 7.17, 2016

後藤雄一: ミトコンドリア病をとりまく医療と治療研究の現況, ミトコンドリア病患者家族の会 2016 年大阪勉強会, 大阪, 7.2, 2016

後藤雄一: エナジーメタボリズムとミトコンドリア病, ゲノム創薬・医療フォーラム第 5 回懇話会, 東京, 4.26, 2016

G．知的財産権の出願・登録状況（予定を含む）

１．　特許取得

1) ミトコンドリア病診断用バイオマーカーとしてのGDF15」PCT/JP2015/50833
(平成27年1月14日出願)
(研究分担者：田中雅嗣)

２．　実用新案登録

なし

３．　その他

なし

研究成果の刊行に関する一覧表

書籍・総説

著者氏名	論文タイトル名	書籍全体の編集者名	書　籍　名	出版社名	出版地	ページ	出版年
後藤雄一	ミトコンドリア病		小児の治療指針	診断と治療社	東京	831-833	2014
後藤雄一	ミトコンドリア病	一瀬泊帝、鈴木宏治	図説分子病態学	中外医学社	東京	267-271	2014
後藤雄一	DNAポリメラーゼγ異常症	杉江秀夫	代謝性ミオパチー	診断と治療社	東京	221-224	2014
後藤雄一	ANT1などの遺伝子異常症	杉江秀夫	代謝性ミオパチー	診断と治療社	東京	225-227	2014
後藤雄一	ミトコンドリア病	水澤英洋	新領域別症候群シリーズNo.29神経症候群（第2版）	日本臨床社	大阪	817-822	2014
後藤雄一	ミトコンドリア病	小林祥泰、水澤英洋、山口修平	2015-2017 神経疾患最新の治療	南江堂	東京	251-252	2014
後藤雄一	ミトコンドリアDNAの遺伝学	種元智洋、佐村修、岡本愛光	産婦人科医必読-臨床遺伝学の最新知識	金原出版	東京	285-290	2015
小坂　仁	大脳萎縮症	水澤英洋	新領域別症候群シリーズNo.29「神経症候群(第２版)Ⅳ」	日本臨床社	大阪	319-324	2014
小坂　仁	小脳萎縮症	水澤英洋	新領域別症候群シリーズNo.29「神経症候群(第２版)Ⅳ」	日本臨床社	大阪	325-328	2014
竹下絵里、小牧宏文	ミトコンドリア病	水澤英洋	新領域別症候群シリーズNo.29「　神経症候群（第２版）Ⅳ」	日本臨牀社	大阪	223-227	2014
竹下絵里、小牧宏文	MNGIE	杉江秀夫	代謝性ミオパチー	診断と治療社	東京	185-187	2014
三牧正和	ミトコンドリア異常症	五十嵐隆総編集，岡明専門編集	小児科臨床ピクシス 3 小児てんかんの最新医療	中山書店	東京	50-51	2014

米田誠, 井川正道, 岡沢秀彦	パーキンソン病および関連神経変性疾患のPET酸化ストレスイメージング.	高橋良輔, 渋谷真, 山中宏二, 樋口真人	脳内環境-恒常性維持機構の破綻と病気	メディカルドー社	大坂	212-215	2014
井川正道, 米田誠	MERRF	杉江秀夫, 福田冬季子, 西野一三, 古賀靖敏	代謝性ミオパチー	診断と治療社	東京	175-177	2014
西野一三	ミトコンドリア脳筋症.	総監修：永井良三, 責任編集：鈴木則宏, 編集：荒木信夫, 神田隆, 吉良潤一, 塩川芳昭, 西野一三, 水澤英洋	神経内科研修ノート	診断と治療社	東京	522-526	2015
西村洋昭, 西野一三	組織化学染色(SDHとCOX).	編集：遠藤文夫, 井田博幸, 山口清次, 高柳正樹, 深尾敏幸	引いて調べる先天代謝異常症	診断と治療社	東京	114	2014
後藤雄一	ミトコンドリア病	五十嵐隆	小児科診療ガイドライン-最新の診療指針-（第3版）	総合医学社	東京	313-316	2016
後藤雄一	ミトコンドリア遺伝関連	野村文夫、村上正巳、和田隆志、末岡栄三朗	日常診療のための検査値のみかた	中外医学社	東京	722-725	2015
後藤雄一	ミトコンドリア脳筋症の治療	佐々木征行、須貝研司、稲垣真澄	小児神経科診断・治療マニュアル改訂第3版	診断と治療社	東京	230-231	2015

後藤雄一	MELAS (mitochondrial myopathy, encephalopathy, lactic acidosis and stroke-like episodes)	埜中征哉	新領域別症候群シリーズ No.33、骨格筋症候群第2版（下）、日本臨床別冊	日本臨床社	大阪	190-194	2015
後藤雄一	MERRF (myoclonic epilepsy associated with ragged-red fibers)	埜中征哉	新領域別症候群シリーズ No.33、骨格筋症候群第2版（下）、日本臨床別冊	日本臨床社	大阪	195-197	2015
後藤雄一	慢性進行性外眼筋麻痺症候群, Kearns-Sayre 症候群	埜中征哉	新領域別症候群シリーズ No.33、骨格筋症候群第2版（下）、日本臨床別冊	日本臨床社	大阪	198-201	2015
後藤雄一	Pearson 症候群	埜中征哉	新領域別症候群シリーズ No.33、骨格筋症候群第2版（下）、日本臨床別冊	日本臨床社	大阪	202-204	2015
後藤雄一	乳児致死型ミトコンドリア病	埜中征哉	新領域別症候群シリーズ No.33、骨格筋症候群第2版（下）、日本臨床別冊	日本臨床社	大阪	214-216	2015
三牧正和	Alpers 症候群	埜中征哉	別冊日本臨牀新領域別症候群シリーズ No.33　骨格筋症候群（第2版）（下）	日本臨牀社	大阪	217-221	2015
三牧正和	Leigh 脳症	埜中征哉	別冊日本臨牀新領域別症候群シリーズ No.33　骨格筋症候群（第2版）（下）	日本臨牀社	大阪	222-228	2015

三牧正和	良性乳児ミオパチー	埜中征哉	別冊日本臨牀新領域別症候群シリーズ No.33　骨格筋症候群（第2版）（下）	日本臨牀社	大阪	229-232	2015
村山圭，小坂仁，米田誠ら、多数	ミトコンドリア病	ミトコンドリア学会、村山圭，小坂仁，米田誠	ミトコンドリア病診療マニュアル2017	診断と治療社	東京	1-172	2016
後藤雄一	ミトコンドリア病	賀藤均	特集　慢性疾患児の一生を診る（小児内科増刊号）	東京医学社	東京	1527-1529	2016
後藤雄一	Kearns-Sayre症候群	岡明	小児の症候群（小児科診療増刊号）	診断と治療社	東京	102	2016
三牧正和	MELAS症候群	岡明	小児の症候群（小児科診療増刊号）	診断と治療社	東京	108	2016
井川正道，岡沢秀彦，米田誠	酸化ストレスイメージング	鈴木 則宏，荒木 信夫，宇川 義一，桑原 聡，川原 信隆	Annual Review神経2017	中外医学社	東京	87-93	2017
Arakawa, K Ikawa M, Tada H, Okazawa H, Yoneda.	Mitochondrial cardiomyopathy and usage of L-arginine.	Victor R. Preedy	Arginine in Clinical Nutrition	Springer	USA	2016	461-470

原著論文

発表者氏名	論文タイトル名	発表誌名	巻号	ページ	出版年
長田治、岩崎章、西野一三、埜中征哉、後藤雄一	高度のミトコンドリアDNAA3243G変異率と臨床経過との関連が示唆されたMELASの一例.	神経内科	83(6)	520-524	2016
Kim Y, Koide R, Isozaki E, Goto Y	Magnetic resonance imaging findings in Leigh syndrome with a novel compound heterozygous SURF1 gene mutation.	Neurol Clin Neurosci	4	34-35	2016

Suzuki T, Yamaguchi H, Kikusato M, （中略 20 名）, Kure S, Yanagisawa T, Tomioka Y, Toyomizu M, Ito S, Osaka H, Hayashi K, Abe T.	Mitochonic acid 5 (MA-5), a derivative of the plant hormone indole-3-acetic acid, improves survival of fibroblasts from patients with mitochondrial diseases.	Tohoku J Exp Med.	236(3)	225-232	2015
Imai A, Fujita S, Kishita Y, Kohda M, Tokuzawa Y, Hirata T, Mizuno Y, Harashima H, Nakaya A, Sakata Y, Takeda A, Mori M, Murayama K, Ohtake A, Okazaki Y	Rapidly progressive infantile cardiomyopathy with mitochondrial respiratory chain complex V deficiency due to loss of ATPase 6 and 8 protein.	*Int J Cardiol.*	207	203-206	2016
Yatsuga S, Fujita Y, Ishii A, Fukumoto Y, Arahata H, Kakuma T, Kojima T, Ito M, Tanaka M, Saiki R, Koga Y.	Growth differentiation factor 15 as a useful biomarker for mitochondrial disorders.	Ann Neurol	78	814-823	2015
Formosa LE, Mimaki M, Frazier AE, McKenzie M, Stait TL, Thorburn DR, Stroud DA, Ryan MT	Characterization of mitochondrial FOXRED1 in the assembly of respiratory chain complex I.	Hum Mol Genet.	24(10)	2952-2965	2015
Kamogashira T, Fujimoto C, Yamasoba T	Reactive Oxygen Species, Apoptosis, and Mitochondrial Dysfunction in Hearing Loss.	BioMed research international	617207	1-7	2015
Sakamoto T, Yamasoba T	Current Concepts of the Mechanisms in Age-Related Hearing Loss.	J Clin Exp Pathol	5	1-2	2015
Yamasoba T	Interventions to Prevent Age-Related Hearing Loss.	Springer International Publishing	VI	335-349	2015
M. Ikawa, H. Okazawa, T. Tsujikawa, A. Matsunaga, O. Yamamura, T. Mori, T. Hamano, Y. Kiyono, Y. Nakamoto, M. Yoneda.	Increased oxidative stress is related to disease severity in the ALS motor cortex: A PET study1	Neurology	84	2033-2039	2015

中村誠、三村治、若倉雅登、稲谷大、中澤徹、白神史雄	Leber 遺伝性視神経症認定基準	*日本眼科学会雑誌*	119	339-346	2015
Haginoya K, Kaneta T, Togashi N, Hino-Fukuyo N, Kobayashi T, Uematsu M, Kitamura T, Inui T, Okubo Y, Takezawa Y, Anzai M, Endo W, Miyake N, Saitsu H, Matsumoto N, Kure S	FDG-PET study of patients with Leigh syndrome	Journal of the Neurological Sciences	362	309-313	2016
後藤雄一	ミトコンドリア病の病因研究の現状	医学のあゆみ	260(1)	63-66	2017
後藤雄一	ミトコンドリア病に対する医療体制の現状と課題	医学のあゆみ	260(1)	123-127	2017
三牧正和	呼吸鎖複合体Ｉアセンブリー機構とミトコンドリア病	医学のあゆみ	260(1)	49-54	2017
井川正道，米田誠	ミトコンドリア病の脳機能画像解析	医学のあゆみ	260(1)	67-72	2017
Yokota M, Hatakeyama H, Ono Y, Kanazawa M, Goto Y	Mitochondrial respiratory dysfunction disturbs neuronal and cardiac lineage-commitment of human iPSCs.	Cell Death Dis	8(1)	e2551	2017
Hatakeyama H, Goto Y.	Respiratory chain complex disorganization impairs mitochondrial and cellular integrity: Phenotypic variation in cytochrome *c* oxidase deficiency.	Am J Pathol.	187(1)	110-121	2017

RESEARCH ARTICLE

Human Mutation

OFFICIAL JOURNAL HGVS HUMAN GENOME VARIATION SOCIETY www.hgvs.org

ECHS1 Mutations Cause Combined Respiratory Chain Deficiency Resulting in Leigh Syndrome

Chika Sakai,[1] Seiji Yamaguchi,[2] Masayuki Sasaki,[3] Yusaku Miyamoto,[4] Yuichi Matsushima,[1,5]* and Yu-ichi Goto[1]*

[1]*Department of Mental Retardation and Birth Defect Research, National Institute of Neuroscience, National Center of Neurology and Psychiatry, Kodaira, Tokyo, Japan;* [2]*Department of Pediatrics, Shimane University, Izumo, Shimane, Japan;* [3]*Department of Child Neurology, National Center Hospital, National Center of Neurology and Psychiatry, Kodaira, Tokyo, Japan;* [4]*Department of Pediatrics, St. Marianna University School of Medicine, Kawasaki, Kanagawa, Japan;* [5]*Department of Clinical Chemistry and Laboratory Medicine, Graduate School of Medical Sciences, Kyushu University, Fukuoka, Japan*

Communicated by David Rosenblatt

Received 4 September 2014; accepted revised manuscript 5 November 2014.
Published online 13 November 2014 in Wiley Online Library (www.wiley.com/humanmutation). DOI: 10.1002/humu.22730

ABSTRACT: The human *ECHS1* gene encodes the short-chain enoyl coenzyme A hydratase, the enzyme that catalyzes the second step of β-oxidation of fatty acids in the mitochondrial matrix. We report on a boy with ECHS1 deficiency who was diagnosed with Leigh syndrome at 21 months of age. The patient presented with hypotonia, metabolic acidosis, and developmental delay. A combined respiratory chain deficiency was also observed. Targeted exome sequencing of 776 mitochondria-associated genes encoded by nuclear DNA identified compound heterozygous mutations in *ECHS1*. ECHS1 protein expression was severely depleted in the patient's skeletal muscle and patient-derived myoblasts; a marked decrease in enzyme activity was also evident in patient-derived myoblasts. Immortalized patient-derived myoblasts that expressed exogenous wild-type ECHS1 exhibited the recovery of the ECHS1 activity, indicating that the gene defect was pathogenic. Mitochondrial respiratory complex activity was also mostly restored in these cells, suggesting that there was an unidentified link between deficiency of ECHS1 and respiratory chain. Here, we describe the patient with ECHS1 deficiency; these findings will advance our understanding not only the pathology of mitochondrial fatty acid β-oxidation disorders, but also the regulation of mitochondrial metabolism.

Hum Mutat 36:232–239, 2015. © 2014 Wiley Periodicals, Inc.

KEY WORDS: combined respiratory chain deficiency; Leigh syndrome; ECHS1; fatty acid β-oxidation disorder

Introduction

Mitochondrial fatty acid β-oxidation provides carbon substrates for gluconeogenesis during the fasting state and contributes electrons to the respiratory chain for energy production. Once a fatty acid is activated to the acyl-coenzyme A (CoA) form and enters the mitochondrial fatty acid β-oxidation pathway, it undergoes the four following enzymatically catalyzed reaction steps during each β-oxidation cycle (Supp. Table S1): (1) dehydrogenation, (2) hydration, (3) a second dehydrogenation step, and finally (4) a thiolytic cleavage that generates one acetyl-CoA or, in certain cases, one propionyl-CoA and an acyl-CoA that is two carbons shorter than the acyl-CoA precursor. Each individual step involves specific enzymes encoded by different genes with different substrate preferences (Supp. Table S1). The first dehydrogenation reaction is catalyzed mainly by four enzymes—short-, medium-, long-, and very long chain acyl-CoA dehydrogenases (SCAD, MCAD, LCAD, and VLCAD)—with substrate optima of C4, C8, C12, and C16 acyl-CoA esters, respectively, still each dehydrogenase can utilize other suboptimal substrates [Ikeda et al., 1983, 1985a, 1985b; Ensenauer et al., 2005]. The short-chain enoyl-CoA hydratase (ECHS1) catalyzes the next step and has substrate optima of C4 2-trans-enoyl-CoA, also called crotonyl-CoA. Although ECHS1 also catalyzes hydration of medium chain substrates, longer acyl chains (e.g., C16-intermediates) are hydrated by mitochondrial trifunctional protein (MTP) [Uchida et al., 1992; Kamijo et al., 1993]. MTP consists of an alpha-subunit with long-chain enoyl-CoA hydratase and long-chain 3-hydroxyacyl-CoA dehydrogenase (LCHAD) activities and a beta-subunit with long-chain 3-ketothiolase activity.

Mitochondrial fatty acid β-oxidation disorders generally cause impaired energy production and accumulation of partially oxidized fatty acid metabolites. They are clinically characterized by hypoglycemic seizures, hypotonia, cardiomyopathy, metabolic acidosis, and liver dysfunction [Kompare and Rizzo, 2008]. The most common genetic defect in MTP is LCHAD deficiency [MIM #609016]; deficiency involving reduced activity of all three MTP enzymes [MIM #609015] is reported much less frequently and is often associated with infantile mortality secondary to severe cardiomyopathy [Spiekerkoetter et al., 2004]. Deficiency of SCAD [MIM #201470], which catalyzes the first dehydrogenation reaction and has similar substrate optima with regard to carbon chain as ECHS1, have been studied for years, and the range of associated phenotypes includes failure to thrive, metabolic acidosis, ketotic hypoglycemia, developmental delay, seizures, and neuromuscular symptoms such as myopathy and hypotonia [Jethva et al., 2008].

Additional Supporting Information may be found in the online version of this article.

*Correspondence to: Yu-ichi Goto. Department of Mental Retardation and Birth Defect Research, National Institute of Neuroscience, National Center of Neurology and Psychiatry, Kodaira, Tokyo, 187-8502, Japan. E-mail: goto@ncnp.go.jp; Yuichi Matsushima. Department of Clinical Chemistry and Laboratory Medicine, Graduate School of Medical Sciences, Kyushu University, Fukuoka, Fukuoka, 812-8582, Japan. E-mail: matsush5@cclm.med.kyushu-u.ac.jp

Contract grant sponsor(s): Grants-in-Aid for Research on Intractable Diseases (Mitochondrial Disease) from the Ministry of Health, Labor and welfare of Japan; Research Grant for Nervous and Mental Disorders from the National Center of Neurology and Psychiatry (21A-6, 24-8) and JSPS KAKENHI (25670275).

Here, we describe a patient with ECHS1 deficiency who presented with Leigh syndrome [MIM #256000] accompanied by hypotonia, metabolic acidosis, and developmental delay. Additionally, the patient presented with combined respiratory chain deficiency, which is not commonly described in most clinical reports of mitochondrial fatty acid β-oxidation disorders. Finally, we discuss the pathology of ECHS1 deficiency and possible interactions between mitochondrial fatty acid β-oxidation and the respiratory chain, which are two important pathways in mitochondrial energy metabolism.

Materials and Methods

This study was approved by the ethical committee of National Center of Neurology and Psychiatry. All the samples in this study were taken and used with informed consent from the family.

Whole-mtDNA Genome Sequence Analysis

Long and accurate PCR amplification of mtDNA followed by direct sequencing was performed according to the previous publication with a slight modification [Matsunaga et al., 2005].

Targeted Exome Sequencing

Almost all exonic regions of 776 nuclear genes (Supp. Table S2), in total 7,368 regions, were sequenced using the Target Enrichment System for next-generation sequencing (HaloPlex; Agilent Technologies, Santa Clara, California, USA) and MiSeq platform (Illumina, San Diego, California, USA). Sequence read alignment was performed with a Burrows–Wheeler Aligner (version 0.6.1) to the human reference genome (version hg19). Realignment and recalibration of base quality scores was performed with the Genome Analysis Toolkit (version 1.6.13). Variants were detected and annotated against dbSNP 135 and 1000 Genomes data (February 2012 release) by Quickannotator.

Sanger Sequencing

Sanger sequencing of candidate genes was performed with the BigDye Terminators v1.1 Cycle Sequencing kit (Thermo Fisher Scientific, Waltham, Massachusetts, USA) as per manufacturer's protocol. Details of primers and conditions are available upon request. DNA sequences from the patients were compared against the RefSeq sequence and the sequences of a healthy control or parents those were sequenced in parallel.

Cell Culture

The patient-derived primary myoblasts were established from the biopsy of patient's skeletal muscle and cultured in DMEM/F-12 (Thermo Fisher Scientific) supplemented with 20% (v/v) heat-inactivated fetal bovine serum (FBS, Thermo Fisher Scientific). DLD-1 (human colon carcinoma) cells were provided by Taiho pharmaceutical company (Tokyo, Japan) and cells were cultured in RPMI-1640 (Thermo Fisher Scientific) supplemented with 10% (v/v) heat-inactivated FBS (Thermo Fisher Scientific). All cells were cultured in 5% CO_2 at 37°C.

Preparation of Mitochondrial Fraction

Mitochondrial fractions from patient's skeletal muscle and patient-derived myoblasts were prepared according to the literature with a slight modification [Frezza et al., 2007].

Immunoblotting

Mitochondrial fraction and protein lysates were prepared from patient's skeletal muscle and patient-derived Myoblasts. Thirty micrograms of protein of mitochondrial fraction or 50 micrograms of protein lysate was separated on 4%–12% Bis-Tris gradient gels (Thermo Fisher Scientific) and transferred to polyvinylidene fluoride membranes. Primary antibodies used were against ECHS1 (Sigma-Aldrich, St. Louis, Missouri, USA), complex II 70 kDa subunit (Abcam, Cambridge, England), β-actin (Santa Cruz, Biotechnology, Dallas, Texas, USA), HA (Wako, Tokyo, Japan), and AcGFP (Thermo Fisher Scientific).

Enzyme Assays

Enzyme activities of mitochondrial respiratory complexes I–V and citrate synthase (CS) were measured in mitochondrial fraction prepared from patient's specimens. The assays for complexes I–IV and CS were performed as described previously [Shimazaki et al., 2012]. The assay for complex V was carried out following the method by Morava and his colleagues with modifications [Morava et al., 2006]. The enoyl-CoA hydratase activity was assayed by the hydration of crotonyl-CoA by a slight modification of the procedure described earlier [Steinman and Hill, 1975]. Five micrograms of protein of the mitochondrial fraction prepared from patient-derived myoblasts was added to 0.3 M Tris–HC1, pH 7.4, containing 5 mM EDTA (Ethylenediaminetetraacetic acid). The reaction was started by the addition of 200 μM crotonyl-CoA and the decrease in absorbance at 280 nm was monitored at 30°C.

Construction of the Immortalized Patient-Derived Myoblasts

The patient-derived myoblasts and control myoblasts were transfected with pEF321-T vector (A kind gift from Dr. Sumio Sugano, University of Tokyo) and the cells were cultured serially for more than ten population doublings until the morphological alteration was observed [Kim et al., 1990].

Expression Vector Preparation and Transfection

For construction of a mammalian expression vector, full-length *ECHS1* (GenBank accession number NM_004092.3) was amplified from a cDNA prepared from control subject using PrimeSTAR GXL DNA polymerase (TaKaRa, Tokyo, Japan). The PCR product was cloned into pEBMulti-Pur (Wako) and the clone was verified by Sanger sequencing. The empty expression vector or an ECHS1 expression vector was transfected into immortalized patient-derived myoblasts using Lipofectamine LTX Reagent (Thermo Fisher Scientific). Each of the two missense variants, c.2T>G; p.M1R and c.5C>T; p.A2V, was independently introduced into the clone by PCR-based site-directed mutagenesis. Each insert with C-terminal HA tag was cloned into pIRES2-AcGFP1 (Clontech Laboratories, Mountain View, California, USA) and the clones were verified by Sanger sequencing. WT and mutant ECHS1 expression vector were transfected into DLD-1 cells using Lipofectamine LTX Reagent (Thermo Fisher Scientific). Twenty-four hours later, the cell lysate was subjected to immunoblotting.

Results

The patient reported here was a boy born to unrelated, healthy parents after a 40-week pregnancy (weight 3,300 g, length 52 cm,

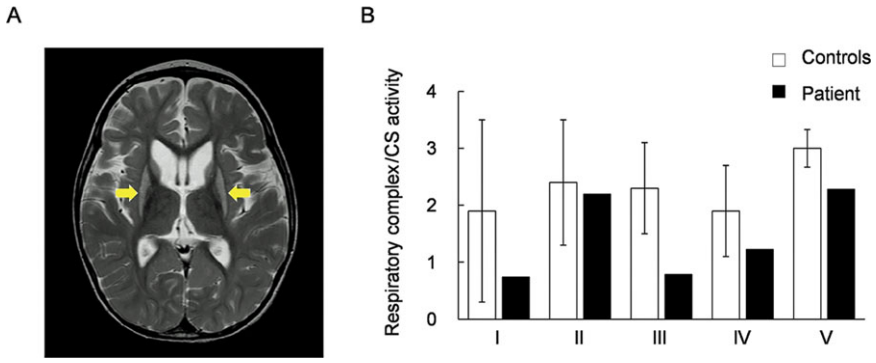

Figure 1. T2-weighted magnetic resonance scan image and enzyme activities of mitochondrial respiratory complexes. **A**: T2-weighted magnetic resonance scan image (MRI) shows bilaterally symmetrical hyperintensities in the putamen (arrows in the image); these are characteristic of Leigh syndrome. **B**: Enzymatic activities of five mitochondrial respiratory complexes (I, II, III, IV, and V) were measured in mitochondrial fractions prepared from the patient's skeletal muscle. Respiratory complexes activities were normalized to citrate synthase activity. Black bars show patient values and white bars show control values. Control values were mean values obtained from five healthy individuals. Patient activity values for complexes I, III, and IV were 39%, 34%, and 64% of the control values, respectively. Error bars represent standard deviations.

Table 1. Urinary Organic Acid Profiling

	Patient RPA (%)	Controls RPA (%)
TCA cycle intermediates		
α-Ketoglutarate	4.52	3.00–102.90
Aconitate	20.37	15.10–86.10
Isocitrate	8.98	8.30–29.00
Other metabolites		
Lactate	11.83[a]	<4.70
Pyruvate	3.18	<24.10
3-Hydroxyisobutyric acid	1.95	<9.00
Methylcitric acid	0.14[a]	Less than trace amount
p-Hydroxy-phenyllactic acid	40.05[a]	<7.00
Glyoxylate	37.71[a]	<6.10

[a] Values outside the normal range.
RPA(%), relative peak area to the area of internal standard (heptadecanoic acid, HDA).

occipitofrontal circumference (OFC) 34.5 cm). Auditory screening test at 2 months of age revealed hearing impairment, and he began to use a hearing aid at 6 months of age. Psychomotor developmental delay was noted at 5 months of age; he could not sit alone, or speak a meaningful word as of 4 years of age. Nystagmus was noted at 10 months of age. Muscle hypotonia, spasticity, and athetotic trunk movement became prominent after 1 year of age. His plasma (20.2 mg/dl) and a cerebrospinal fluid lactate were elevated (25.3 mg/dl, control below 15 mg/dl). Urinary organic acid profiling reveals significantly elevated excretion of glyoxylate (Table 1). Analysis of blood acylcarnitines showed no abnormalities. Brain magnetic resonance scan image showed bilateral T2 hyperintensity of the putamen, typical for Leigh syndrome (Fig. 1A). Because Leigh syndrome is generally caused by defects in the mitochondrial respiratory chain or the pyruvate dehydrogenase complex, we performed a muscle biopsy to measure enzyme activities of mitochondrial respiratory complexes in the patient. Mitochondrial fractions prepared from patient or control specimens were used for all activity measurements. Activity of each respiratory complex was normalized relative to CS activity; normalized values for complexes I, III, and IV activity were decreased to 39%, 34%, and 64% of control values, respectively (Fig. 1B). Moreover, we performed blue native PAGE (BN-PAGE) to examine if the assembly of respiratory complexes were altered in the patient. As a result, there were no clear difference between the patient and the control (Supp. Fig. S1).

Mitochondrial respiratory chain defects can be due to pathogenic mutations in mitochondrial DNA (mtDNA) or nuclear DNA (nDNA) coding for mitochondrial components. Initially, long and accurate PCR amplification of mtDNA followed by direct sequencing was performed and no mutations known to be associated with Leigh syndrome were identified, but previously reported polymorphisms were found (Supp. Table S3). Therefore, to identify the responsible mutations in nDNA, targeted exome sequencing was performed. Coverage was at least 10× for 86.2% of the target regions, and 30× or more for 73.4%. In all, 5,640 potential variants were identified; these included 811 splice-site or nonsynonymous variants. Among those 811 variants, 562 were on the mismapping reads that contained multiple apparent mismatches to the reference DNA sequence. Of the remaining 249 variants, nine that were on target regions with less than 10× coverage were eliminated because data reliability was low. Filtering against dbSNP 135 and 1000 Genomes data, this number was reduced to 13 including compound heterozygous variants in the *ECHS1* [MIM #602292] and 11 heterozygous variants in 11 separate genes (Supp. Table S4). Those variants have been submitted to dbSNP (http://www.ncbi.nlm.nih.gov/SNP/). Because most mitochondrial diseases caused by known nDNA mutations are inherited in an autosomal recessive manner, we focused on the compound heterozygous variants in *ECHS1*—c.2T>G; p.M1R and c.5C>T; p.A2V—as primary candidates.

To confirm the targeted exome sequencing results, we performed Sanger sequencing of genomic *ECHS1* DNA and *ECHS1* cDNA from the patient and his parents. We identified both variants, c.2T>G and c.5C>T, and the respective normal alleles in genomic DNA and cDNA from the patient (Fig. 2A and B) and no other *ECHS1* variants were detected except for common SNPs in the open reading frame. Analysis of genomic DNA from the patient's parents showed that patient's father was heterozygous for only one variant, c.2T>G, and the patient's mother for only the other variant, c.5C>T (Fig. 2A). These results indicated that the patient inherited each variant separately and that both mutant alleles were expressed in the patient (Fig. 2B). Each variant was nonsynonymous and in the region encoding the mitochondrial transit peptide (1–27 amino acids) of ECHS1 [Hochstrasser et al., 1992]; moreover, c.2T>G; p.M1R was a start codon variant (Fig. 2C).

Next, immunoblotting with primary antibodies against ECHS1 was performed to assess protein expression. Mitochondrial

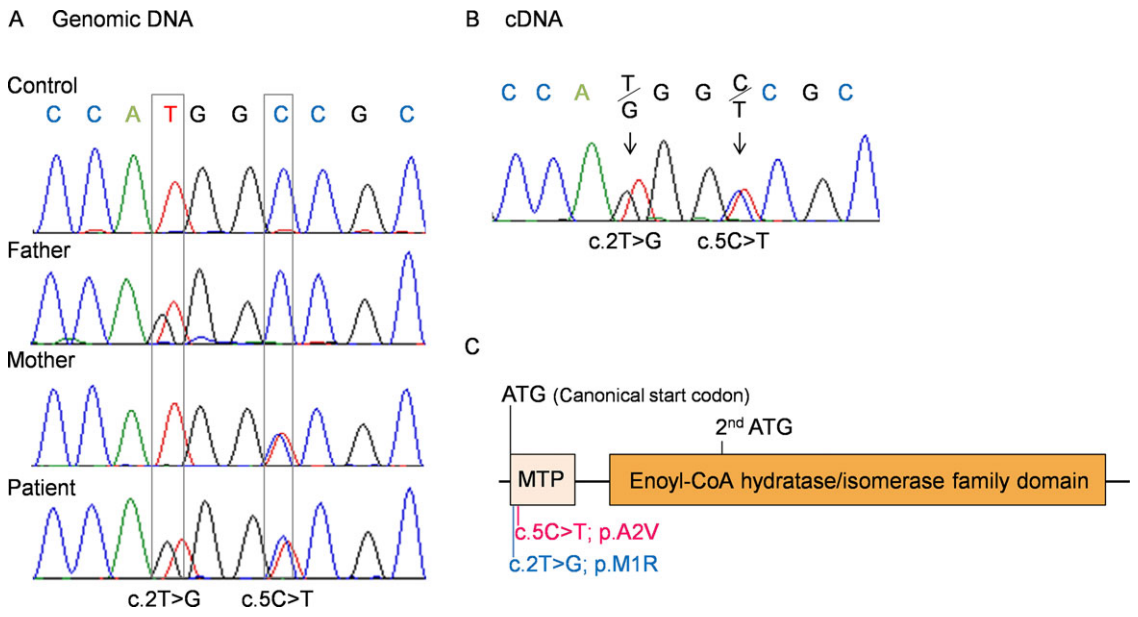

Figure 2. *ECHS1* Sanger sequencing analysis and ECHS1 functional domains. **A**: Sequence chromatograms from part of exon 1 of *ECHS1* were generated by Sanger sequencing of genomic DNA. Each parent had one wild-type allele; the patient's father also harbored a c.2T>G variant, and the patient's mother a c.5C>T variant. The patient inherited each variant allele and was a compound heterozygote. **B**: Sequence chromatograms from part of *ECHS1* exon 1 obtained by Sanger sequencing of cDNA prepared from patient mRNA. The same variants seen in genomic DNA were observed in the cDNA. **C**: A schematic diagram of the functional domains in ECHS1 and the locations of the mutations. MTP, mitochondrial transit peptide.

fractions prepared from patient and control skeletal muscle were used; whole-cell lysates or mitochondrial fractions prepared from patient-derived or control myoblasts were also used. All experiments using these specimens showed that the expression level of ECHS1 protein of the patient was too low to detect by immunoblotting even though the expression level of SDHA was almost the same as controls (Fig. 3A–C). These findings indicated that c.2T>G; p.M1R and c.5C>T; p.A2V mutations caused a remarkable reduction in ECHS1 protein expression. Notably, patient-derived and control myoblasts were similar with regard to *ECHS1* mRNA expression (Fig. 3D), indicating that the mutations apparently affected ECHS1 protein expression directly. Next, we measured ECHS1 enzyme activity in mitochondrial fractions prepared from patient-derived and control myoblasts. ECHS1 activity was normalized to CS activity, and activity in patient-derived myoblasts was 13% of that in control myoblasts (Fig. 3E). Therefore, the mutations caused a severe depletion of ECHS1 protein expression thereby decreasing ECHS1 enzyme activity.

To examine the stability of each mutated protein, we constructed three pIRES2-AcGFP1 expression plasmids, each expressed a different HA-tagged protein: wild-type, M1R-mutant, or A2V-mutant ECHS1. The expression of AcGFP was used as a transfection control. After the transfection into DLD-1 cells, immunoblotting of whole-cell lysate with anti-HA and GFP antibodies showed markedly higher expression of wild-type ECHS1 than of either mutant protein; all ECHS1 expression was normalized to AcGFP expression (Fig. 4, Supp. Fig. S2). This result indicated that ECHS1 protein expression was significantly reduced in the patient because of each mutation.

To confirm that the patient had ECHS1 deficiency, we performed a cellular complementation experiment. Patient-derived myoblasts had to be immortalized for these experiments because nonimmortalized cells exhibited poor growth and finite proliferation. The patient-derived myoblasts and control myoblasts were transfected with pEF321-T vector (a kind gift from Dr. Sumio Sugano, University of Tokyo). We then ascertained that ECHS1 protein expression and activity were lower in immortalized patient-derived myoblasts than in controls (Fig. 5A and B). We then transduced an empty expression vector, pEBMulti-Pur (Wako), or a pEBMulti-Pur construct containing a full-length, wild-type *ECHS1* cDNA into the immortalized patient-derived myoblasts; cells with the vector only or the ECHS1-expression construct are hereafter called vector-only and rescued myoblasts, respectively. ECHS1 protein expression level and enzyme activity were analyzed in mitochondrial fractions prepared from rescued myoblasts. Relative expression level of ECHS1 in rescued myoblasts was 11 times higher than that in vector-only myoblasts (Fig. 5A), and ECHS1 activity normalized to CS activity in rescued myoblasts was 49 times higher than that in vector-only myoblasts (Fig. 5B). From these cellular complementation experiments, we concluded the patient had ECHS1 deficiency.

Since the patient showed the combined mitochondrial respiratory chain deficiency in the skeletal muscle as mentioned above, we used a cellular complementation experiment to determine whether wild-type ECHS1 rescued the respiratory chain defect in patient-derived myoblasts. First, we measured enzyme activities of each mitochondrial respiratory complex in mitochondrial fractions prepared from immortalized patient-derived myoblasts. CS activity normalized values for complexes I, IV, and V activity in immortalized patient-derived myoblasts were decreased to 17%, 39%, and 43% of the mean values of immortalized control myoblasts (Fig. 5C). Then, we measured enzyme activity in mitochondrial fractions prepared from rescued myoblasts and found that each activity of complexes I, IV, and V was mostly restored relative to that in vector-only myoblasts. In rescued myoblasts, CS activity normalized values of complexes I, IV, and V were 3.5, 1.3, and 2.2 times higher than those in vector-only myoblasts (Fig. 5C). Mitochondrial respiratory complex activity was mostly restored in rescued myoblasts, suggesting that there was an unidentified link between deficiency of ECHS1 and respiratory chain.

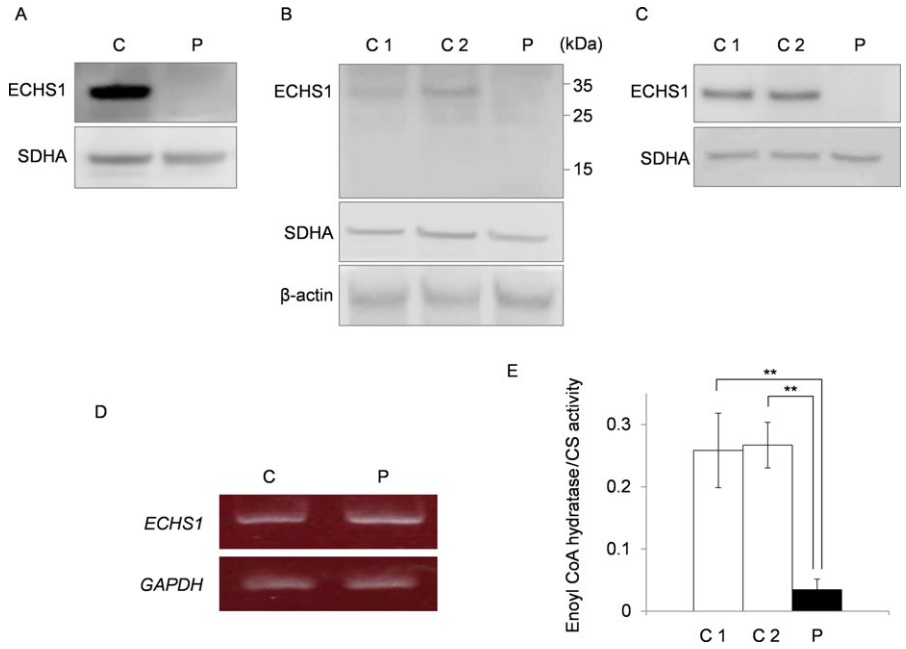

Figure 3. ECHS1 expression and enzyme activity. ECHS1 expression was analyzed by immunoblotting. C1/2, control; P, patient. Mitochondrial fraction prepared from patient's skeletal muscle (**A**) or whole-cell lysate (**B**) and mitochondrial fraction (**C**) prepared from the patient-derived myoblasts were analyzed via immunoblotting. All findings indicated that ECHS1 levels in patient samples were too low to detect by immunoblotting. **D**: RT-PCR was used to assess *ECHS1* mRNA levels in the patient. Notably, patient-derived myoblasts and control myoblasts did not differ with regard to *ECHS1* mRNA level. **E**: Mitochondrial fractions prepared from patient-derived myoblasts were used to estimate ECHS1 enzyme activity in the patient. All ECHS1 activity measurements were normalized to CS activity; ECHS1 activity in patient-derived samples was 13% of that in control samples. The experiments were performed in triplicate. Error bars represent standard deviations. (** $P < 0.005$ Student's *t*-test).

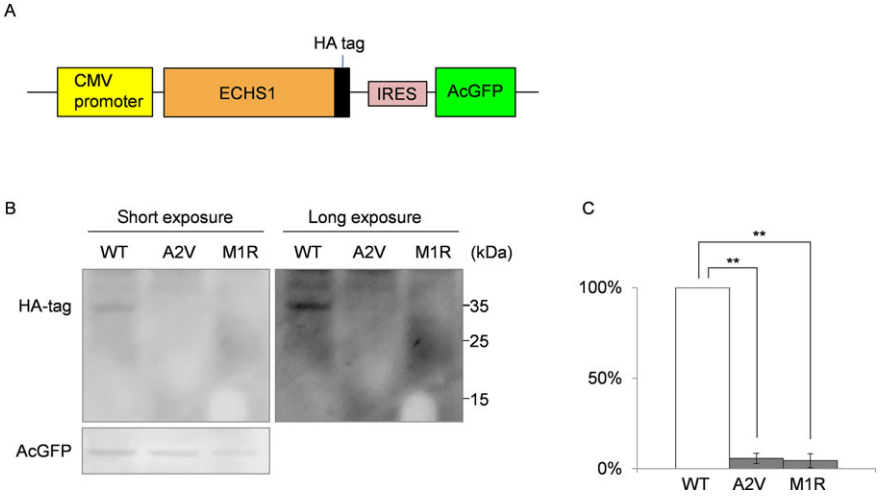

Figure 4. Exogenous expression of mutant ECHS1 protein in cancer cells. **A**: Schematic diagram of the pIRES mammalian expression vector. **B**: Representative image of an immunoblotting containing AcGFP, an internal control, and each HA-tagged ECHS1 protein; all proteins were isolated from DLD-1 cells that transiently overexpressed wild-type, A2V, or M1R HA-tagged ECHS1 from pIRES. The images obtained by short exposure (left) and long exposure (right). **C**: Overexpressed HA-tagged ECHS1 protein levels. Both mutant ECHS1 proteins showed dramatically decreased expression compared to wild-type ECHS1 protein, when ECHS1 was normalized relative to the internal control. Each experiment was performed in triplicate. Error bars represent standard deviations (** $P < 0.005$ Student's *t*-test).

Discussion

Here, we described a patient harboring compound heterozygous mutations in *ECHS1*. Immunoblotting analysis revealed that ECHS1 protein was undetectable in patient-derived myoblasts; moreover, these cells showed significantly lower ECHS1 enzyme activity than controls. Exogenous expression of two recombinant mutant proteins in DLD-1 cells showed c.2T>G; p.M1R and c.5C>T; p.A2V mutations affected ECHS1 protein expression. Cellular complementation experiment verified the patient had ECHS1 deficiency.

The c.2T>G; p.M1R mutation affected the start codon and therefore was predicted to impair the protein synthesis from canonical

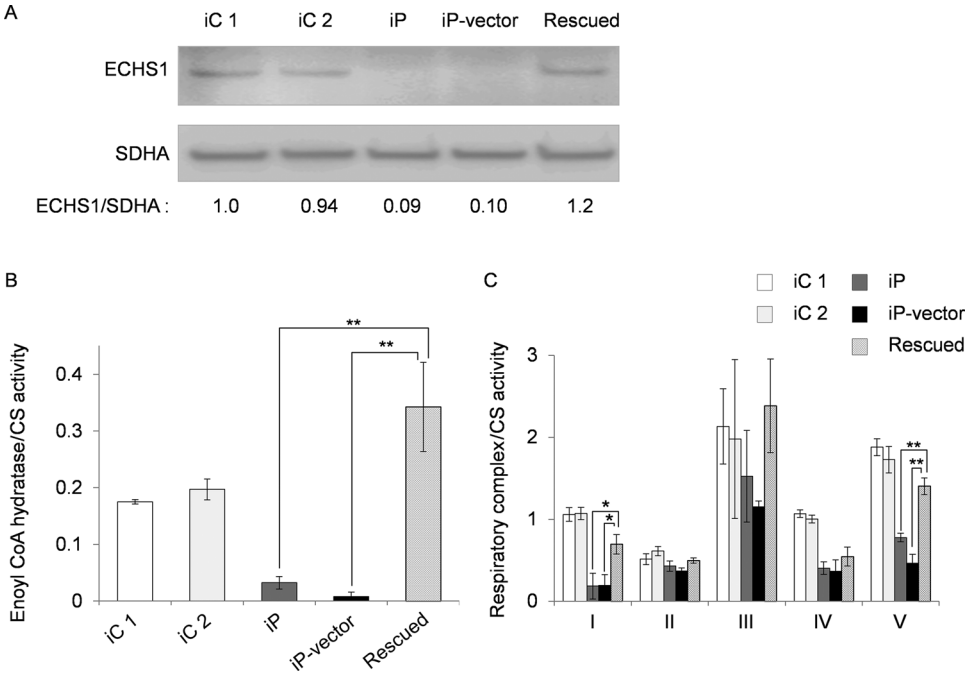

Figure 5. ECHS1 protein expression and enzyme activity in rescued myoblasts. An empty vector or a construct encoding wild-type ECHS1 was introduced into immortalized patient-derived myoblasts. iC1/2, immortalized control myoblasts; iP, immortalized patient-derived myoblasts; iP-vector, immortalized patient-derived myoblasts transfected with empty vector; Rescued, immortalized patient-derived myoblasts stably expressing wild-type ECHS1. **A**: ECHS1 levels were assessed on immunoblotting using mitochondrial fractions prepared from rescued myoblasts. ECHS1 level in "rescued" is 11 times higher than that in "iP-vector". **B**: Mitochondrial fractions prepared from rescued myoblasts were also used to measure ECHS1 enzyme activity. ECHS1 activity normalized to CS activity in "rescued" was 49 times higher than that in "iP-vector." Each experiment was performed in triplicate. Error bars represent standard deviations (** $P < 0.005$ Student's *t*-test). **C**: Mitochondrial fractions prepared from rescued myoblasts were used to measure enzyme activities of mitochondrial respiratory complexes. Activity values were normalized to CS activity. Activities of complexes I, IV, and V were mostly restored from "iP" and "iP-vector." In "rescued," the enzyme activities of complexes I, IV, and V were 3.5, 1.3, and 2.2 times higher, respectively, than the "iP-vector." Each experiment was performed in triplicate. Error bars represent standard deviations (** $P < 0.005$, * $P < 0.05$ Student's *t*-test).

initiation site. In the reference *ECHS1* sequence, the next in-frame start codon is located in amino acids 97 (Fig. 2C). Even if translation could occur from this second start codon, the resulting product would lack the whole transit peptide and part of the enoyl-CoA hydratase/isomerase family domain (Fig. 2C). The c.5C>T; p.A2V mutation was located in the mitochondrial transit peptide and the mutation may affect the mitochondrial translocation of ECHS1. Surprisingly, the MitoProt-predicted mitochondrial targeting scores for the wild-type and A2V-mutant proteins were 0.988 and 0.991, respectively [MitoProt II; http://ihg.gsf.de/ihg/mitoprot.html; Claros and Vincens, 1996] and not markedly different from each other. Nevertheless, mislocalized mutant protein may have been degraded outside of the mitochondria. Consistent with this speculation was the finding that immunoblotting of lysate from patient-derived myoblasts (Fig. 3B) or from transfected cells that overexpressed the recombinant p.A2V-mutant ECHS1 (Fig. 4B, Supp. Fig. S2) did not show upper shifted ECHS1 bands that indicated ECHS1 with the transit peptide. Another possible explanation is that the mutation affected the translation efficiency because it was very close to the canonical start codon. It can change secondary structure of ECHS1 mRNA or alter the recognition by the translation initiation factors. As stated above, even if there was a translation product from the second in-frame start codon, that product would probably not function.

This patient presented with symptoms that are indicative of fatty acid oxidation disorders (e.g., hypotonia and metabolic acidosis), but he also presented with neurologic manifestations, including developmental delay and Leigh syndrome, that are not normally associated with fatty acid β-oxidation disorders. Interestingly, developmental delay is also found in cases of SCAD deficiency [Jethva et al., 2008]. In the absence of SCAD, the byproducts of butyryl-CoA—including butyrylcarnitine, butyrylglycine, ethylmalonic acid (EMA), and methylsuccinic acid—accumulate in blood, urine, and cells. These byproducts may cause the neurological pathology associated with SCAD deficiency [Jethva et al., 2008]. EMA significantly inhibits creatine kinase activity in the cerebral cortex of Wistar rats but does not affect levels in skeletal or heart muscle [Corydon et al., 1996]. Elevated levels of butyric acid modulated gene expression because excess butyric acid can enhance histone deacetylase activity [Chen et al., 2003]. Moreover, the highly volatile nature of butyric acid as a free acid may also add to its neurotoxic effects [Jethva et al., 2008].

On the other hand, it is very rare for fatty acid β-oxidation disorders causing Leigh syndrome. Therefore, the most noteworthy manifestation in this patient was Leigh syndrome. Leigh syndrome is a neuropathological entity characterized by symmetrical necrotic lesions along the brainstem, diencephalon, and basal ganglion [Leigh, 1951]. It is caused by abnormalities of mitochondrial energy generation and exhibits considerable clinical and genetic heterogeneity [Chol et al., 2003]. Commonly, defects in the mitochondrial respiratory chain or the pyruvate dehydrogenase complex are responsible for this disease. This patient's skeletal muscle samples exhibited a combined respiratory chain deficiency, and this deficiency may be the reason that he presented with Leigh syndrome. Although it

remained unclear what caused the respiratory chain defect, cellular complementation experiments showed almost complete restoration, indicating there was an unidentified link between ECHS1 and respiratory chain. One of the possible causes of respiratory chain defect is the secondary effect of accumulation of toxic metabolites. For example, an elevated urine glyoxylate was observed in this patient. Although the mechanism of this abnormal accumulation is not clear at the moment, it was shown that glyoxylate inhibited oxidative phosphorylation or pyruvate dehydrogenase complex by in vitro systems [Whitehouse et al., 1974; Lucas and Pons, 1975]. Therefore, we speculate that in our patient, ECHS1 deficiency induced metabolism abnormality including glyoxylate accumulation, and glyoxylate played a role in decreased enzyme activities of respiratory chain complexes. Interestingly, a recent paper describing patients with Leigh syndrome and ECHS1 deficiency showed decreased activity of pyruvate dehydrogenase complex in fibroblasts [Peters et al., 2014], (Supp. Table S5). BN-PAGE showed the assembly of respiratory complex components in the patient was not clearly different from the control (Supp. Fig. S1). This result suggests that the respiratory chain defect in the patient is more likely because of the secondary effect of accumulation of toxic metabolites. On the other hand, many findings indicate interplays between mitochondrial fatty acid β-oxidation and the respiratory chain. For example, Enns et al. [2000] mentioned the possibility of the physical association between these two energy-generating pathways from overlapping clinical phenotypes in genetic deficiency states. More recently, Wang and his colleagues actually showed physical association between mitochondrial fatty acid β-oxidation enzymes and respiratory chain complexes (Wang et al., 2010). Similarly, Narayan et al. demonstrated interactions between short-chain 3-hydroxyacyl-CoA dehydrogenase (SCHAD) and several components of the respiratory chain complexes including the catalytic subunits of complexes I, II, III, and IV via pull-down assays involving several mouse tissues. Considering the role of SCHAD as a NADH-generating enzyme, this interaction was suggested to demonstrate the logical physical association with the regeneration of NAD through the respiratory chain [Narayan et al., 2012]. Still more recently, mitochondrial protein acetylation was found to be driven by acetyl-CoA produced from mitochondrial fatty acid β-oxidation [Pougovkina et al., 2014]. Because the activities of respiratory chain enzymes are regulated by protein acetylation [Zhang et al., 2012], this finding indicated that β-oxidation regulates the mitochondrial respiratory chain. Remarkably, acyl-CoA dehydrogenase 9 (ACAD9), which participates in the oxidation of unsaturated fatty acid, was recently identified as a factor involved in complex I biogenesis [Haack et al., 2010; Heide et al., 2012]. Cellular complementation experiments that involve overexpression of wild-type ACAD9 in patient-derived fibroblast cell lines showed restoration of complex I assembly and activity [Haack et al., 2010]. Accumulating evidence indicates that there are complex regulatory interactions between mitochondrial fatty acid β-oxidation and the respiratory chain.

ECHS1 has been shown to interact with several molecules outside the mitochondrial fatty acid β-oxidation pathway [Chang et al., 2013; Xiao et al., 2013] and the loss of this interaction can affect respiratory chain function in a patient. Further functional analysis of ECHS1 will advance our understanding of the complex regulation of mitochondrial metabolism.

Acknowledgments

We acknowledge the technical support of Dr. Ichizo Nishino, Dr. Ikuya Nonaka, Dr. Chikako Waga, Takao Uchiumi, Yoshie Sawano, and Michiyo Nakamura. We also thank Dr. Sumio Sugano (the University of Tokyo) for providing the pEF321-T plasmid.

Disclosure statement: The authors have no conflict of interest to declare.

References

Chang Y, Wang SX, Wang YB, Zhou J, Li WH, Wang N, Fang DF, Li HY, Li AL, Zhang XM, Zhang WN. 2013. ECHS1 interacts with STAT3 and negatively regulates STAT3 signaling. FEBS Lett 587:607–613.

Chen JS, Faller DV, Spanjaard RA. 2003. Short-chain fatty acid inhibitors of histone deacetylases: promising anticancer therapeutics? Curr Cancer Drug Targets 3:219–236.

Chol M, Lebon S, Bénit P, Chretien D, de Lonlay P, Goldenberg A, Odent S, Hertz-Pannier L, Vincent-Delorme C, Cormier-Daire V, Rustin P, Rötig A, et al. 2003. The mitochondrial DNA G13513A MELAS mutation in the NADH dehydrogenase 5 gene is a frequent cause of Leigh-like syndrome with isolated complex I deficiency. J Med Genet 40:188–191.

Claros MG, Vincens P. 1996. Computational method to predict mitochondrially imported proteins and their targeting sequences. Eur J Biochem 241:779–786.

Corydon MJ, Gregersen N, Lehnert W, Ribes A, Rinaldo P, Kmoch S, Christensen E, Kristensen TJ, Andresen BS, Bross P, Winter V, Martinez G, et al. 1996. Ethylmalonic aciduria is associated with an amino acid variant of short chain acyl-coenzyme A dehydrogenase. Pediatr Res 39:1059–1066.

Enns GM, Bennett MJ, Hoppel CL, Goodman SI, Weisiger K, Ohnstad C, Golabi M, Packman S. 2000. Mitochondrial respiratory chain complex I deficiency with clinical and biochemical features of long-chain 3-hydroxyacyl-coenzyme A dehydrogenase deficiency. J Pediatr 136:251–254.

Ensenauer R, He M, Willard JM, Goetzman ES, Corydon TJ, Vandahl BB, Mohsen A-W, Isaya G, Vockley J. 2005. Human acyl-CoA dehydrogenase-9 plays a novel role in the mitochondrial beta-oxidation of unsaturated fatty acids. J Biol Chem 280:32309–32016.

Frezza C, Cipolat S, Scorrano L. 2007. Organelle isolation: functional mitochondria from mouse liver, muscle and cultured filroblasts. Nat Protoc 2:287–295.

Haack TB, Danhauser K, Haberberger B, Hoser J, Strecker V, Boehm D, Uziel G, Lamantea E, Invernizzi F, Poulton J, Rolinski B, Iuso A, et al. 2010. Exome sequencing identifies ACAD9 mutations as a cause of complex I deficiency. Nat Genet 42:1131–1134.

Heide H, Bleier L, Steger M, Ackermann J, Dröse S, Schwamb B, Zörnig M, Reichert AS, Koch I, Wittig I, Brandt U. 2012. Complexome profiling identifies TMEM126B as a component of the mitochondrial complex I assembly complex. Cell Metab 6:538–549.

Hochstrasser DF, Frutiger S, Paquet N, Bairoch A, Ravier F, Pasquali C, Sanchez JC, Tissot JD, Bjellqvist B, Vargas R, Ron DA, Graham JH. 1992. Human liver protein map: a reference database established by microsequencing and gel comparison. Electrophoresis 13:992–1001.

Ikeda Y, Dabrowski C, Tanaka K. 1983. Separation and properties of five distinct acyl-CoA dehydrogenases from rat liver mitochondria. J Biol Chem 258:1066–1076.

Ikeda Y, Hine DG, Okamura-Ikeda K, Tanaka K. 1985a. Mechanism of action of short-chain, medium chain and long-chain acyl-CoA dehydrogenases: direct evidence for carbanion formation as an intermediate step using enzyme-catalyzed C-2 proton/deuteron exchange in the absence of C-3 exchange. J Biol Chem 260: 1326–1337.

Ikeda Y, Okamura-Ikeda K, Tanaka K. 1985b. Spectroscopic analysis of the interaction of rat liver short chain, medium chain and long chain acyl-CoA dehydrogenases with acyl-CoA substrates. Biochemistry 24:7192–7199.

Jethva R, Bennett MJ, Vockley J. 2008. Short-chain acyl-coenzyme A dehydrogenase deficiency. Mol Genet Metab 95:195–200.

Kamijo T, Aoyama T, Miyazaki J, Hashimoto T. 1993. Molecular cloning of the cDNAs for the subunits of rat mitochondrial fatty acid beta-oxidation multienzyme complex. Structural and functional relationships to other mitochondrial and peroxisomal beta-oxidation enzymes. J Biol Chem 268:26452–26460.

Kim DW, Uetsuki T, Kaziro Y, Yamaguchi N, Sugano S. 1990. Use of the human elongation factor 1 alpha promoter as a versatile and efficient expression system. Gene 91:217–223.

Kompare M, Rizzo WB. 2008. Mitochondrial fatty-acid oxidation disorders. Semin Pediatr Neurol 15:140–149.

Leigh D. 1951. Subacute necrotizing encephalomyelopathy in an infant. J Neurol Neurosurg Psychiatr 14:216–221.

Lucas M, Pons AM. 1975. Influence of glyoxylic acid on properties of isolated mitochondria. Biochimie 57:637–645.

Matsunaga T, Kumanomido H, Shiroma M, Goto Y, Usami S. 2005. Audiological features and mitochondrial DNA sequence in a large family carrying mitochondrial A1555G mutation without use of aminoglycoside. Ann Otol Rhinol Laryngol 114:153–160.

Morava E, Rodenburg RJ, Hol F, de Vries M, Janssen A, van den Heuvel L, Nijtmans L, Smeitink J. 2006. Clinical and biochemical characteristics in patients with a high mutant load of the mitochondrial T8993G/C mutations. Am J Med Genet A 140:863–868.

Narayan, SB, Master SR, Sirec AN, Bierl C, Stanley PE, Li C, Stanley CA, Bennett MJ. 2012. Short-chain 3-hydroxyacyl-coenzyme A dehydrogenase associates with a protein super-complex integrating multiple metabolic pathways. PLoS One 7: e35048.

Peters H, Buck N, Wanders R, Ruiter J, Waterham H, Koster J, Yaplito-Lee J, Ferdinandusse S, Pitt J. 2014. ECHS1 mutations in Leigh disease: a new inborn error of metabolism affecting valine metabolism. Brain 137: 2903–2908.

Pougovkina O, Te Brinke H, Ofman R, van Cruchten AG, Kulik W, Wanders RJ, Houten SM, de Boer VC. 2014. Mitochondrial protein acetylation is driven by acetyl-CoA from fatty acid oxidation. Hum Mol Genet 23:3513–3522.

Shimazaki H, Takiyama Y, Ishiura H, Sakai C, Matsushima Y, Hatakeyama H, Honda J, Sakoe K, Naoi T, Namekawa M, Fukuda Y, Takahashi Y, et al. 2012. A homozygous mutation of C12orf65 causes spastic paraplegia with optic atrophy and neuropathy (SPG55). J Med Genet 49:777–784.

Spiekerkoetter U, Khuchua Z, Yue Z, Bennett MJ, Strauss AW. 2004. General mitochondrial trifunctional protein (TFP) deficiency as a result of either alpha- or beta-subunit mutations exhibits similar phenotypes because mutations in either subunit alter TFP complex expression and subunit turnover. Pediatr Res 55:190–196.

Steinman HM, Hill RL. 1975. Bovine liver crotonase (enoyl coenzyme A hydratase). Methods Enzymol 35:136–151.

Uchida Y, Izai K, Orii T, Hashimoto T. 1992. Novel fatty acid beta-oxidation enzymes in rat liver mitochondria. II. Purification and properties of enoyl-coenzyme A (CoA) hydratase/3-hydroxyacyl-CoA dehydrogenase/3-ketoacyl-CoA thiolase trifunctional protein. J Biol Chem 267:1034–1041.

Wang Y, Mohsen AW, Mihalik SJ, Goetzman ES, Vockley J. 2010. Evidence for physical association of mitochondrial fatty acid oxidation and oxidative phosphorylation complexes. J Biol Chem 285:29834–29841.

Whitehouse S, Cooper RH, Randle PJ. 1974. Mechanism of activation of pyruvate dehydrogenase by dichloroacetate and other halogenated carboxylic acids. Biochem J 141:761–774.

Xiao CX, Yang XN, Huang QW, Zhang YQ, Lin BY, Liu JJ, Liu YP, Jazag A, Guleng B, Ren JL. 2013. ECHS1 acts as a novel HBsAg-binding protein enhancing apoptosis through the mitochondrial pathway in HepG2 cells. Cancer Lett 330:67–73.

Zhang J, Lin A, Powers J, Lam MP, Lotz C, Liem D, Lau E, Wang D, Deng N, Korge P, Zong, NC, Cai H, et al. 2012. Perspectives on: SGP symposium on mitochondrial physiology and medicine: mitochondrial proteome design: from molecular identity to pathophysiological regulation. J Gen Physiol 139:395–406.

Mitochondrion 20 (2015) 34–42

Contents lists available at ScienceDirect

Mitochondrion

journal homepage: www.elsevier.com/locate/mito

GDF15 is a novel biomarker to evaluate efficacy of pyruvate therapy for mitochondrial diseases

Yasunori Fujita [a], Masafumi Ito [a], Toshio Kojima [b], Shuichi Yatsuga [c], Yasutoshi Koga [c], Masashi Tanaka [d,*]

[a] Research Team for Mechanism of Aging, Tokyo Metropolitan Institute of Gerontology, 35-2 Sakae-cho, Itabashi, Tokyo 173-0015, Japan
[b] Health Support Center, Toyohashi University of Technology, 1-1 Hibarigaoka Tenpaku-cho, Toyohashi, Aichi 441-8580, Japan
[c] Department of Pediatrics and Child Health, Kurume University School of Medicine, 67 Asahi-machi, Kurume, Fukuoka 830-0011, Japan
[d] Department of Genomics for Longevity and Health, Tokyo Metropolitan Institute of Gerontology, 35-2 Sakae-cho, Itabashi, Tokyo 173-0015, Japan

ARTICLE INFO

Article history:
Received 20 May 2014
received in revised form 2 September 2014
accepted 29 October 2014
Available online 1 November 2014

Keywords:
GDF15
Pyruvate
Mitochondrial diseases
Cybrid
Microarray
Biomarker

ABSTRACT

Pyruvate therapy is a promising approach for the treatment of mitochondrial diseases. To identify novel biomarkers for diagnosis and to evaluate therapeutic efficacy, we performed microarray analysis of 2SD cybrid cells harboring a MELAS-causing mutation and control cells treated with either lactate or pyruvate. We found that expression and secretion of growth differentiation factor 15 (GDF15) were increased in 2SD cells treated with lactate and that serum GDF15 levels were significantly higher in patients with mitochondrial diseases than in those with other diseases, suggesting that GDF15 could be a useful marker for diagnosis and evaluating the therapeutic efficacy of pyruvate.

1. Introduction

Mitochondrial diseases are caused by mitochondrial or nuclear genome mutations that affect the functions of mitochondria. The symptoms are caused by impaired energy metabolism due to mitochondrial dysfunction and manifest mostly in tissues with a high energy demand such as brain, heart, and muscle. Mitochondrial myopathy, encephalopathy, lactic acidosis, and stroke-like episodes (MELAS) is one of the most common of the mitochondrial diseases (Pavlakis et al., 1984). The A-to-G transition at the 3243 position of the mitochondrial DNA (m.3243A > G) located in the mitochondrial $tRNA^{Leu\ (UUR)}$ gene is a MELAS-causing mutation, and it is detected in approximately 80% of patients with MELAS (Goto et al., 1990, 1992; Kirino et al., 2004; Yasukawa et al., 2000).

These pathogenic mutations typically result in defective ATP synthesis in mitochondria, and therefore ATP production depends on the glycolytic pathway. Since lactate production is aberrantly increased by the acceleration of glycolysis when energy demand is elevated, the lactate to pyruvate (L/P) ratio in serum is often increased in patients with mitochondrial diseases and has been clinically used for estimating the dysfunction of mitochondrial respiration. It is well known that the L/P ratio reflects the intracellular $NADH/NAD^+$ ratio. Since NAD^+ is indispensable for oxidation of glyceraldehyde 3-phosphate (GAP) to 1,3-bisphosphoglycerate (BPG) by glyceraldehyde 3-phosphate dehydrogenase (GAPDH) in the glycolytic pathway, a shortage of NAD^+ interrupts this reaction, resulting in decreased ATP biosynthesis. Tanaka et al. (2007) proposed that the addition of pyruvate would facilitate oxidation of NADH to NAD^+ via the lactate dehydrogenase reaction, which would restore ATP production by the glycolytic pathway even under defective respiratory conditions. Indeed, positive effects of sodium pyruvate on clinical manifestations of mitochondrial diseases have been reported (Koga et al., 2012; Saito et al., 2012). However, useful biomarkers for evaluating the therapeutic efficacy of pyruvate remain to be developed.

Cybrid cell lines established by the fusion of enucleated myoblast cells from a patient with a cultured cell line depleted of mtDNA have been used to elucidate the pathogenesis and underlying molecular mechanisms of mitochondrial diseases. We previously reported increased expression of amino acid starvation-responsive genes in cybrid cells with MELAS and NARP (neuropathy, ataxia, and retinitis pigmentosa) mutations (Fujita et al., 2007). In our earlier study (Kami et al., 2012), we found that exposure to excessive sodium lactate significantly increases the intracellular L/P and $NADH/NAD^+$ ratios in cybrid cells harboring the MELAS mutation (m.3243A > G), which implies worsening of lactic acidosis and NAD^+ shortage. On the other hand, we found that treatment with sodium pyruvate facilitates the ATP production and improves the energy status, as indicated by a decrease in the L/P ratio and retention of the $NADH/NAD^+$ ratio. Taken together, we considered that these experimental conditions would be ideal for identifying biomarker candidate genes, whose expression levels reflect

* Corresponding author. Tel.: +81 3 3964 3241; fax: +81 3 3579 4776.
E-mail address: mtanaka@tmig.or.jp (M. Tanaka).

http://dx.doi.org/10.1016/j.mito.2014.10.006
1567-7249/

the intracellular energy deficiency and the effect of pyruvate on energy metabolism.

In the present study, we performed a global gene expression analysis of cybrid cells with the MELAS mutation (m.3243A > G: 2SD cells) and control cybrid cells (2SA cells) treated or not with lactate or pyruvate. We identified several biomarker candidate genes, among which we focused on growth differentiation factor 15 (GDF15). The level of GDF15 in the conditioned medium was significantly higher in 2SD cells than in 2SA cells, which level was further increased by lactate but was not affected by pyruvate in 2SD cells. We also demonstrated that the concentration of GDF15 in the serum was markedly elevated in patients with mitochondrial diseases compared with that in those with other pediatric diseases. Thus, we identified GDF15 as a novel serum marker for the diagnosis of mitochondrial diseases and possibly for monitoring the disease status and progression and for evaluating the therapeutic efficacy of pyruvate.

2. Materials and methods

2.1. Cell culture

The 2SA and 2SD cybrid cell lines were previously established by Chomyn et al. (1992). Briefly, 14 cybrid clones were isolated after the fusion of enucleated myoblasts derived from a MELAS patient with mtDNA-deficient $\rho^0$206 cells generated from a human 143B osteosarcoma cell line. Among those clones, 10 clones had homoplasmic wild-type mtDNA, and 4 clones harbored strongly predominant mutant mtDNA. For our experiments, we chose two clones, 2SA and 2SD cybrid cell lines carrying 100% wild-type mtDNA and 94% m.3243A > G mutant mtDNA, respectively. The 2SD but not 2SA cybrid cells were shown to be defective in mitochondrial protein synthesis and respiratory capacity (Chomyn et al., 1992). Cells were cultured in high-glucose Dulbecco's modified Eagle's medium (DMEM) supplemented with 10% fetal bovine serum, 1 mM sodium pyruvate, and 0.4 mM uridine at 37 °C under a humidified atmosphere of 5% CO_2.

2.2. Microarray analysis

Total RNA was isolated from cells by using a miRNeasy mini kit (Qiagen, Venlo, Netherlands). One hundred nanograms of total RNA was labeled and amplified with a low input quick amp labeling kit (Agilent Technologies, Santa Clara, CA, USA) used according to the manufacturer's instructions. The labeled cRNA was hybridized to the Agilent SurePrint G3 Human GE 8x60K Microarray in a rotating hybridization oven at 10 rpm for 20 h at 65 °C. After hybridization, the microarrays were washed according to the manufacturer's instructions and scanned on an Agilent DNA Microarray Scanner with Scan Control software. The resulting images were processed, and raw data were collected by using Agilent Feature Extraction software. Expression data were analyzed by using GeneSpring GX 11 (Agilent Technologies). The signal intensity of each probe was normalized by a percentile shift, in which each value was divided by the 75th percentile of all values in its array. For pairwise comparison analysis, only the probes that had expression flags present under at least one condition were considered. The list was analyzed with Ingenuity Pathways Analysis software (Ingenuity Systems, Redwood, CA, USA)

2.3. Quantitative RT-PCR

Total RNA was reverse transcribed to cDNA with a High Capacity cDNA Reverse Transcription Kit (Life Technologies, Carlsbad, CA, USA) used according to the manufacturer's protocols. Real-time PCR was performed on the StepOnePlus Real-Time PCR System (Life Technologies) using Power SYBR Green PCR Master Mix. 18S rRNA gene was used as an internal control for normalization. The sequences of primers are listed in Supplementary Table 1.

2.4. Patients

A written informed consent was obtained from all patients or their legal guardians. Enrolled patients were diagnosed with mitochondrial diseases by medical doctors in Kurume University Hospital over the period of 2005–2013. Seventeen patients diagnosed at this hospital as having mitochondrial diseases were recruited for this study. As a control group, 13 patients diagnosed as having other pediatric diseases such as dwarfism were also recruited. The clinical information of the patients is listed in Supplementary Table 2. This study was approved by the Institutional Review Board (Kurume University #13099).

2.5. ELISA and multiplex suspension array

Cells were placed on 60-mm dishes 1 day before replacing the medium with fresh medium. Conditioned medium cultured for 24 h was collected, and the particulates were removed by centrifugation (at 500 ×*g* for 10 min, at 10,000 ×*g* for 30 min). The GDF15 and INHBE concentrations in the supernatants and in the sera of patients were determined in duplicate by using a Human GDF-15 Immunoassay (R&D Systems, Minneapolis, MN, USA) and enzyme-linked immunosorbent assay kit for Inhibin Beta E (Uscn Life Science, Wuhan, Hubei, PRC) according to the manufacturer's instructions. For measuring other cytokine concentrations, the sera were subjected to a multiplex suspension array, Bio-Plex Pro Human Cytokine Grp II Panel 21-Plex (Bio-Rad, Hercules, CA, USA). The cytokines measured by use of this array were the following: IL-1α, IL-2Rα, IL-3, IL-12 (p40), IL-16, IL-18, CTACK, GRO-α, HGF, IFN-α2, LIF, MCP-3, M-CSF, MIF, MIG, β-NGF, SCF, SCGF-β, SDF-1α, TNF-β, and TRAIL. We measured the FGF21 (BioVendor, Czech Republic) concentration in duplicate samples by ELISA. Unmeasurable high-concentration samples of FGF21 and GDF15 were diluted 10-fold prior to measurement. The value from each assay was determined by reference to the linear portion of the standard curves for FGF21 and GDF15. All assays were performed by a trained scientist or technical staff.

2.6. Statistical analysis

Statistical analyses were performed by using IBM SPSS statistics (IBM, Armonk, NY, USA). We used the nonparametric Mann–Whitney *U* test to validate differences in cytokine levels in serum between mitochondrial disease patients and controls. The correlation between GDF15 and FGF21 concentrations in serum was assessed by Spearman correlation analysis. We plotted the receiver operating characteristics (ROC) curve for GDF15, HGF, SCF, SCGF-β, and FGF21 and calculated the area under the curve (AUC). The data for the sensitivity and 100 minus the specificity were plotted on a continuous scale.

3. Results

3.1. Gene expression changes in response to intracellular energy deficiency in 2SD cells

We performed microarray analysis of 2SD cybrid cells harboring the MELAS mutation (m.3243A > G) and 2SA control cybrid cells treated with 10 mM lactate or 10 mM pyruvate for 0, 4 or 8 h (Fig. 1A). The numbers of gene probes whose signal intensities were altered by 2-fold for each comparison are given in Supplementary Tables 3–6. We found remarkable changes in gene expression in 2SD cells, but not in 2SA cells, treated with lactate for 8 h. As shown in Supplementary Fig. 1A, we then selected gene probes that were increased by lactate treatment for 8 h compared with those without treatment and concurrently up-regulated by lactate but not by pyruvate at 8 h after treatment and thereby identified 313 probes that were specifically up-regulated by lactate in 2SD cells at 8 h

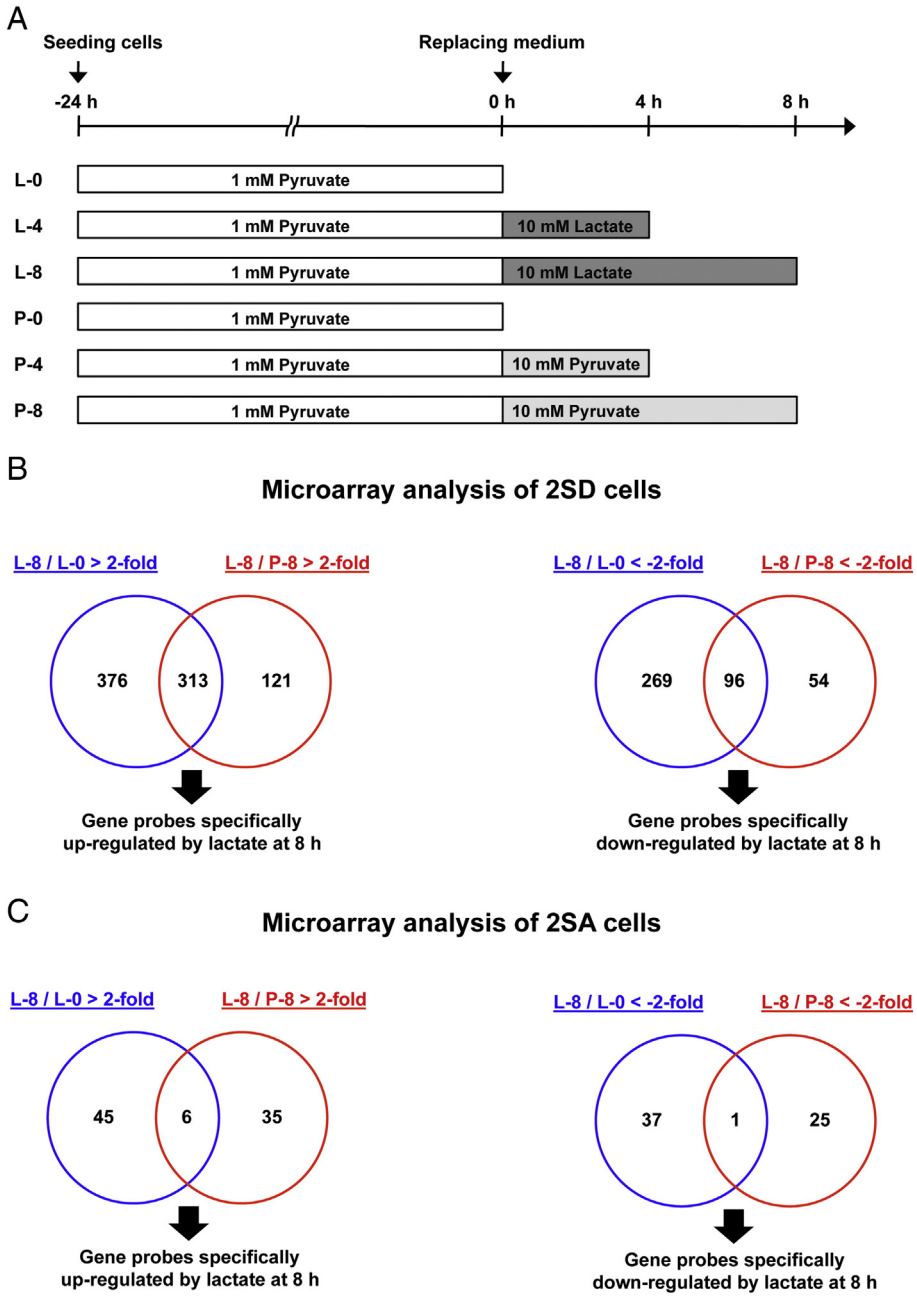

Fig. 1. Microarray analysis of 2SD and 2SA cells (A) Diagram of treatment protocols. Total RNA isolated from 2SD and 2SA cells treated with 10 mM lactate or 10 mM pyruvate for 0, 4, or 8 h were subjected to microarray analysis ($n = 2$). (B, C) Venn diagrams show the number of probes for genes in 2SD cells (B) or 2SA cells (C) that were increased (left panels) or decreased (right panels) in expression by lactate treatment for 8 h compared with their expression at 0 h and concurrently up-regulated by lactate but not by pyruvate after 8-h treatment. (For interpretation of the references to colour in this figure, the reader is referred to the web version of this article.)

(Fig. 1B). Using similar criteria (Supplementary Fig. 1B), we also identified 96 probes that were specifically down-regulated in 2SD cells by lactate treatment for 8 h (Fig. 1B). In 2SA cells, having normal mitochondrial function, the numbers of gene probes that responded to lactate treatment were limited (Fig. 1C). The clustering analysis of the 313 up-regulated (corresponding to 231 genes) and 96 down-regulated (corresponding to 75 genes) gene probes highlighted significant differences in gene expression patterns between 2SD and 2SA cells and also between lactate and pyruvate treatments (Fig. 2). These results suggest that a defective energy metabolism caused by exposure to a high dose of lactate resulted in significant changes in gene expression in 2SD cells.

3.2. Gene networks associated with intracellular energy deficiency in 2SD cells

In order to identify gene networks associated with a defective energy metabolism in the lactate-treated 2SD cells, a gene network analysis was performed on 231 up-regulated genes and 75 down-regulated ones. This analysis identified 11 and 5 gene networks for up- and down-regulated genes, respectively (Fig. 3 and Supplementary Figs. 2 and 3). The top-ranked gene network identified for the up-regulated genes contained those related to the amino-acid starvation response, such as ASNS, ATF3, NUPR1, DDIT3, CTH, TRIB3, STC2, and PCK2 (Fig. 3A). It is worth noting that GDF15, on which we focused in the

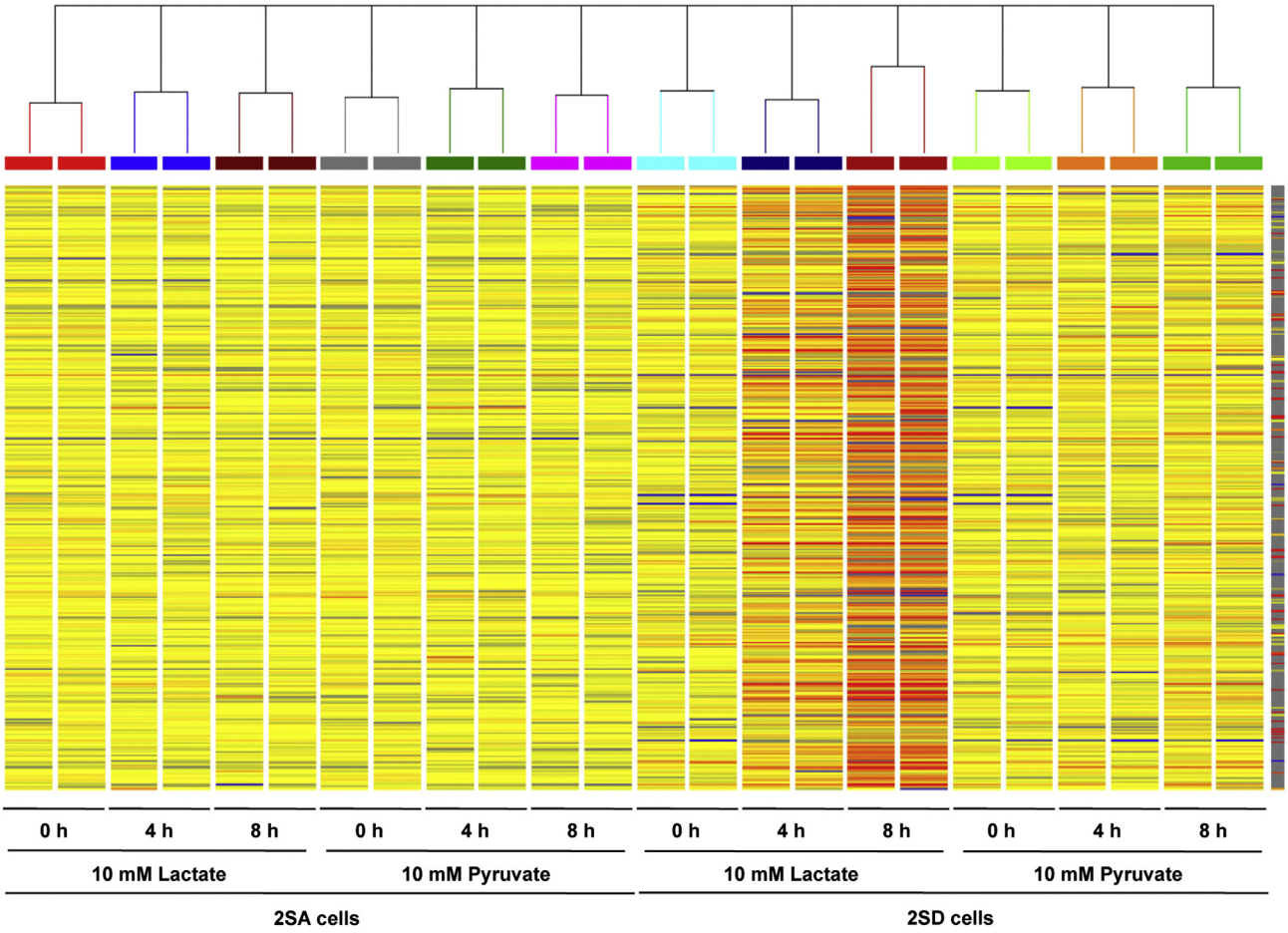

Fig. 2. Clustering analysis of the microarray data The gene probes up-regulated ($n = 313$) and down-regulated ($n = 96$) at 8 h after lactate treatment were subjected to clustering analysis. Part of the data are shown. (For interpretation of the references to colour in this figure, the reader is referred to the web version of this article.)

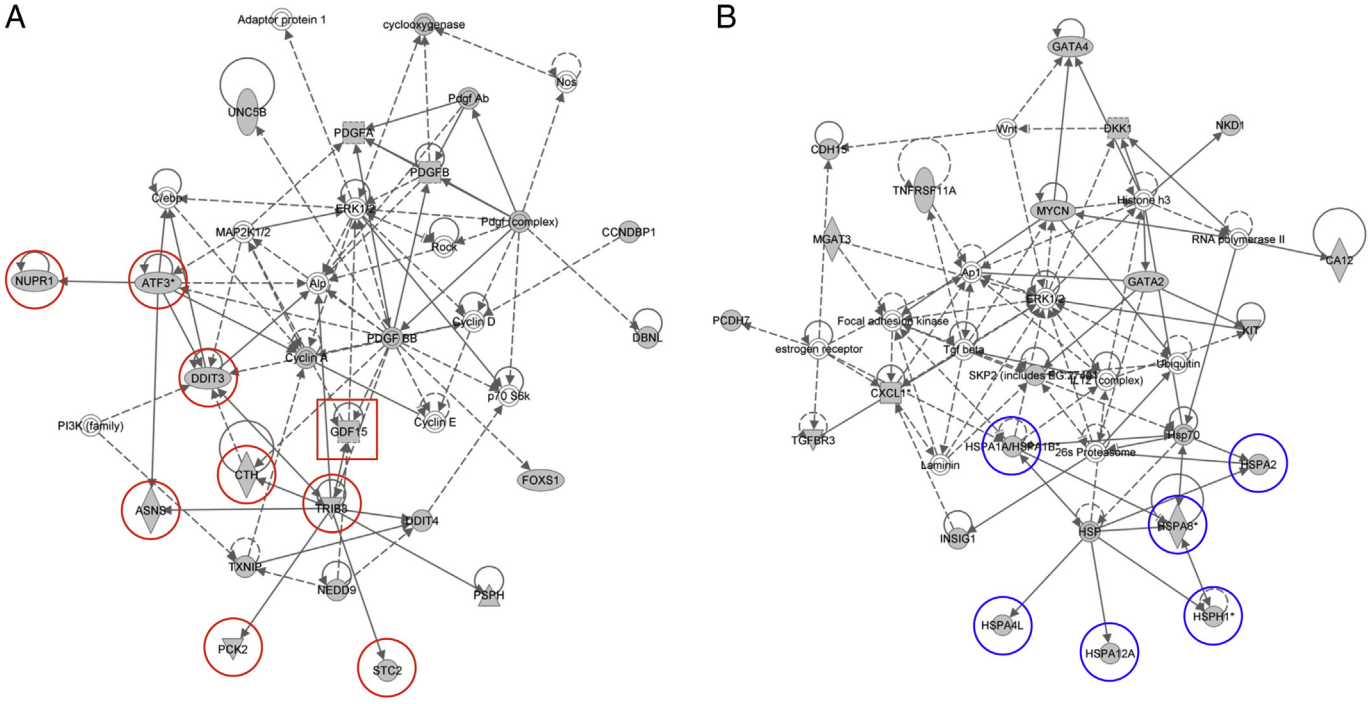

Fig. 3. Gene network analysis of the microarray data The genes specifically up-regulated ($n = 231$) and down-regulated ($n = 75$) at 8 h after lactate treatment were subjected to gene network analysis. The top-ranked gene networks in terms of the number of genes included are shown for up-regulated (A) and down-regulated (B) genes. Genes involved in the amino-acid starvation response (red circles) and heat-shock response (blue circles) as well as GDF15 (red square) are denoted. (For interpretation of the references to colour in this figure, the reader is referred to the web version of this article.)

present study, was included in this network. On the other hand, the gene network for down-regulated genes included those linked to the heat-shock protein response, such as HSPA1A, HSPA2, HSPA4L, HSPA8, HSPA12A, and HSPH1 (Fig. 3B).

3.3. GDF15 as a potential biomarker for diagnosis and evaluating the therapeutic efficacy of pyruvate

Proteins encoded by genes related to intracellular energy deficiency in 2SD cells and secreted into the medium could be potential biomarkers for mitochondrial diseases. Gene annotation analysis revealed the location of gene products that were specifically up- and down-regulated by lactate at 8 h (231 and 75 genes, respectively) (Table 1). Twenty-three up-regulated genes and 4 down-regulated genes were annotated to the extracellular space, each of which is listed in Tables 2 and 3. Among them, we focused on the top 2 ranked up-regulated genes, growth differentiation factor 15 (GDF15) and inhibin beta E (INHBE).

To validate the intracellular expression levels of these genes, we performed quantitative RT-PCR for GDF15 and INHBE. The expression levels of GDF15 (Fig. 4A) and INHBE (Fig. 4B) in the 2SD cells were increased by treatment with 10 mM lactate, but not with 10 mM pyruvate, for 4 or 8 h. Furthermore, GDF15 expression at 0 h was higher in 2SD cells than in 2SA cells. These results confirmed the reproducibility of our microarray data and identified GDF15 and INHBE as candidate biomarkers. To determine whether the secretion of GDF15 and INHBE proteins was increased in 2SD cells in response to lactate treatment, we measured their concentrations in medium from 2SA and 2SD cells cultured for 24 h in the presence of 1 mM pyruvate, 10 mM lactate, or 10 mM pyruvate. ELISA showed that the GDF15 levels were higher in the conditioned medium of 2SD cells than in that of 2SA cells under all of the culture conditions (Fig. 4C). Moreover, treatment with 10 mM lactate, but not with 10 mM pyruvate, promoted secretion of GDF15 in 2SD cells in comparison with treatment with 1 mM pyruvate, whereas 2SA cells did not respond to the high dose of lactate and pyruvate treatment. In contrast, INHBE protein was not detectable by ELISA in the conditioned medium of either 2SD or 2SA cells under any culture conditions (data not shown). These results indicate that GDF15 could be a potential biomarker for diagnosis and monitoring the disease status and progression as well as for assessing the therapeutic efficacy of pyruvate for the treatment of mitochondrial diseases.

3.4. GDF15 as a biomarker for diagnosis of mitochondrial diseases

In order to validate the feasibility of GDF15 as a serum biomarker, we measured its concentration in the serum of 17 patients with mitochondrial diseases as well as in that of 13 patients with other pediatric diseases as a control (Supplementary Table 2). ELISA showed that the average concentration of GDF15 in the serum of mitochondrial disease patients was 2632.9 pg/mL, whereas that for other pediatric disease patients was 285.2 pg/mL, suggesting that GDF15 levels were significantly increased in the serum of mitochondrial disease patients and could clearly distinguish mitochondrial disease patients from control patients (Fig. 5A).

Table 1
The location of probes (genes) up- and down-regulated in 2SD cells with lactate treatment for 8 h.

Location	Up-regulated		Down-regulated	
	Probe number	Gene number	Probe number	Gene number
Nucleus	39	35	14	14
Cytoplasm	51	47	25	19
Plasma membrane	37	33	16	16
Extracellular space	26	23	5	4
Unknown	160	93	36	22

Since fibroblast growth factor 21 (FGF21) was recently proposed as a diagnostic marker for mitochondrial diseases (Davis et al., 2013; Suomalainen et al., 2011), we also measured the FGF21 levels in the serum of the same mitochondrial disease patients and control patients (Fig. 5B). The serum FGF21 levels were higher in patients with mitochondrial diseases than in those with other diseases. Furthermore, there was a good correlation between the serum GDF15 and FGF21 levels (Fig. 5C).

In an attempt to find additional biomarkers, we determined the serum levels of 21 cytokines in the same patients by using the multiplex suspension array. As shown in Supplementary Fig. 4A, the serum concentrations of HGF and SCF were higher in patients with mitochondrial diseases than in control patients, whereas the serum levels of SCGF-β were lower in the former than in the latter.

Finally, we performed ROC curve analysis of GDF15, HGF, SCF, SCGF-β, and FGF21. As shown in Fig. 5D, the area under the curves (AUC) for GDF15 (0.986) was higher than that for FGF21 (0.787). The AUC for FGF21 was similar to those for HGF (0.747), SCF (0.729), and SCGF-β (0.837) (Supplementary Fig. 4B), indicating that GDF15 had the maximum sensitivity and specificity for diagnosis of mitochondrial diseases. These results suggest that GDF15 has the greatest potential as a novel diagnostic marker for MELAS and other mitochondrial diseases.

4. Discussion

Based on the global gene expression analysis of cybrid cells with mitochondrial dysfunction, we identified GDF15 as a potential biomarker whose expression and secretion reflected the intracellular energy deficiency and the effect of pyruvate therapy on the energy metabolism. We then determined the serum levels of GDF15 in patients with mitochondrial diseases and other diseases and identified GDF15 as a novel diagnostic marker for mitochondrial diseases. Although additional clinical studies are needed, the serum GDF15 concentration may be a useful biomarker not only for diagnosis of mitochondrial diseases but also for monitoring the disease status and progression as well as for determining the efficacy of pyruvate therapy.

GDF15 is a member of the transforming growth factor-β (TGF-β) superfamily and is widely expressed in mammalian tissues (Unsicker et al., 2013). GDF15 plays important roles in multiple pathologies including cardiovascular diseases, cancer, and inflammation. It has been shown that GDF15 is up-regulated by tumor suppressor p53 in response to high glucose or treatment with anti-cancer compounds (Baek et al., 2002; Li et al., 2013; Yang et al., 2003). The p53 protein is a transcription factor that responds to a variety of stresses such as DNA damage, oxidative stress, hypoxia, and metabolic stress, and it activates the expression of genes to induce cell cycle arrest, DNA repair, senescence, and cell death (Sermeus and Michiels, 2011; Sperka et al., 2012; Zhang et al., 2010). CDKN1A (p21), a potent cyclin-dependent kinase inhibitor, is a major downstream effector of p53, which induces cell-cycle arrest (Sperka et al., 2012). In our microarray data, the CDKN1A expression level was 3.5-fold increased by lactate treatment of 2SD cells (data not shown). Previous reports demonstrated increased expression of CDKN1A in the skeletal muscle of patients with mitochondrial diseases and a cell line depleted of mitochondrial DNA (Behan et al., 2005; Crimi et al., 2005). Besides CDKN1A, we found other p53 effector genes in the list of genes up-regulated in the lactate-treated 2SD cells, including GADD45A, EGR2, DDIT3, CHMP4C, SESN2, ULBP1, DDIT4, and NUPR1 (data not shown). These results suggest that p53 activation may have played an important role in the induction of GDF15 expression in 2SD cells treated with lactate. It has been also demonstrated that p53 activation caused by metabolic stress is mediated by AMP-activated protein kinase (AMPK; Zhang et al., 2010). Our previous metabolomic profiling revealed that the ATP level drops but that the ADP and AMP levels are increased in lactate-treated 2SD cells (Kami et al., 2012), implying that elevation of the AMP/ATP ratio may activate p53 through AMPK activation. Taken together, it is possible that p53 induced GDF15 expression in

Table 2
Genes annotated to the extracellular space among those specifically up-regulated by lactate treatment for 8 h.

Gene symbol	Accession number	Entrez gene name	Fold change	
			L-8/L-0[a]	L-8/P-8[b]
GDF15	NM_004864	Growth differentiation factor 15	27.4	14.8
INHBE	NM_031479	Inhibin, beta E	15.0	9.4
AREG	NM_001657	Amphiregulin	14.0	2.2
ECM2	NM_001393	Extracellular matrix protein 2, female organ and adipocyte specific	11.8	9.0
ADM2	NM_024866	Adrenomedullin 2	10.3	3.0
MMP3	NM_002422	Matrix metallopeptidase 3 (stromelysin 1, progelatinase)	9.8	4.2
IL1A	NM_000575	Interleukin 1, alpha	7.6	6.0
C12orf39	ENST00000256969	Chromosome 12 open reading frame 39	6.3	6.7
APOL6	NM_030641	Apolipoprotein L, 6	6.2	3.8
SCG5	NM_003020	Secretogranin V (7B2 protein)	5.2	3.0
SPOCK2	NM_014767	Sparc/osteonectin, cwcv and kazal-like domains proteoglycan (testican) 2	5.1	6.6
AMTN	NM_212557	Amelotin	5.0	3.9
IL23A	NM_016584	Interleukin 23, alpha subunit p19	4.4	2.8
ADAMTS17	NM_139057	ADAM metallopeptidase with thrombospondin type 1 motif, 17	3.5	2.2
VEGFA	NM_001025370	Vascular endothelial growth factor A	3.4	2.5
STC2	NM_003714	Stanniocalcin 2	3.4	2.6
PDGFB	NM_002608	Platelet-derived growth factor beta polypeptide	2.8	3.8
C1QTNF1	NM_198594	C1q and tumor necrosis factor related protein 1	2.6	2.9
HECW2	NM_020760	HECT, C2 and WW domain containing E3 ubiquitin protein ligase 2	2.4	2.1
IGFALS	NM_004970	Insulin-like growth factor binding protein, acid labile subunit	2.3	2.5
IGFBP1	NM_000596	Insulin-like growth factor binding protein 1	2.3	2.1
PDGFA	NM_002607	Platelet-derived growth factor alpha polypeptide	2.2	2.2
CLEC3B	NM_003278	C-type lectin domain family 3, member B	2.1	2.2

[a]Fold change between 8 h and 0 h after lactate treatment
[b]Fold change between lactate treatment and pyruvate treatment at 8 h

response to AMPK activation caused by the intracellular energy deficiency. However, it remains to be determined whether other stresses such as oxidative stress may also have participated in p53 activation and GDF15 induction in the lactate-treated 2SD cells.

Gene network analysis demonstrated that the top-ranked network contained not only genes associated with the amino-acid starvation response but also the GDF15 gene (Fig. 3A). In a mouse model of late-onset mitochondrial myopathy, the expression of amino-acid starvation-responsive genes was shown to be elevated (Tyynismaa et al., 2010). The asparagine synthetase (ASNS), which is a representative gene involved in the amino-acid starvation response, has been reported to be up-regulated in the skeletal muscle of patients with mitochondrial diseases and in cybrid cells established from a mitochondrial disease patient (Crimi et al., 2005; Fujita et al., 2007). Activating transcription factor 4 (ATF4) is a master regulator of integrated stress responses (ISR), in which a variety of stresses, including amino-acid starvation as well as glucose starvation, ER stress, hypoxia, and oxidative stress, induce phosphorylation of eIF2α followed by up-regulation of ATF4 to activate expression of stress-responsive genes (Harding et al., 2003; Jiang et al., 2004; Rouschop et al., 2010; Rzymski et al., 2010; Teske et al., 2011). It is noteworthy to point out that GDF15 has been shown to be up-regulated by ATF4 in mouse embryonic fibroblasts (Jousse et al., 2007). Taken together, such findings suggest that the ISR pathway may also contribute to the induction of GDF15 in response to defective energy metabolism and play a role in the pathogenesis of mitochondrial diseases.

In the present study, we validated the clinical usefulness of GDF15 as a diagnostic marker by determining the serum GDF15 levels in patients with mitochondrial diseases and in those with other pediatric diseases. The results showed that serum GDF15 levels were significantly elevated in patients with mitochondrial diseases, which finding is consistent with a recent report (Kalko et al., 2014). We also demonstrated that GDF15 had higher sensitivity and specificity than FGF21, which was recently identified as a sensitive and specific blood biomarker for muscle pathology in a wide range of mitochondrial diseases in adults and children (Suomalainen et al., 2011). Our small-scale study, however, may have underestimated the clinical usefulness of FGF21, because the AUC for FGF21 reported by 2 independent groups (0.95 and 0.91) was higher than that in the present study (0.787).

Using the multiplex suspension array, we also identified HGF, SCF, and SCGF-β as potential diagnostic markers for mitochondrial diseases. The ROC curve analysis, however, revealed that GDF15 had the maximum sensitivity and specificity for diagnosis of mitochondrial diseases compared with HGF, SCF, SCGF-β, or FGF21. Based on the microarray analysis, we also selected INHBE as the next best candidate gene (Table 2). INHBE is a member of the activin beta family, which has been reported to be primarily expressed in the liver and up-regulated by drug-induced ER stress, cysteine deprivation, and insulin treatment (Bruning et al., 2012; Dombroski et al., 2010; Hashimoto et al., 2009; Lee et al., 2008). Although secreted INHBE protein was not detectable in the conditioned medium from the cell cultures, we are currently investigating the clinical usefulness of INHBE as a biomarker for diagnosis and monitoring of the disease status and progression.

Table 3
Genes annotated to the extracellular space among those specifically down-regulated by lactate treatment for 8 h.

Gene symbol	Accession number	Entrez gene name	Fold change	
			L-8/L-0[a]	L-8/P-8[b]
CXCL1	NM_001511	Chemokine (C-X-C motif) ligand 1 (melanoma growth stimulating activity, alpha)	−3.4	−2.6
PDZRN3	NM_015009	PDZ domain containing ring finger 3	−2.4	−2.0
SLC39A10	NM_020342	Solute carrier family 39 (zinc transporter), member 10	−2.3	−2.9
DKK1	NM_012242	Dickkopf 1 homolog (Xenopus laevis)	−2.1	−2.3

[a]Fold change between 8 h and 0 h after lactate treatment
[b]Fold change between lactate treatment and pyruvate treatment at 8 h

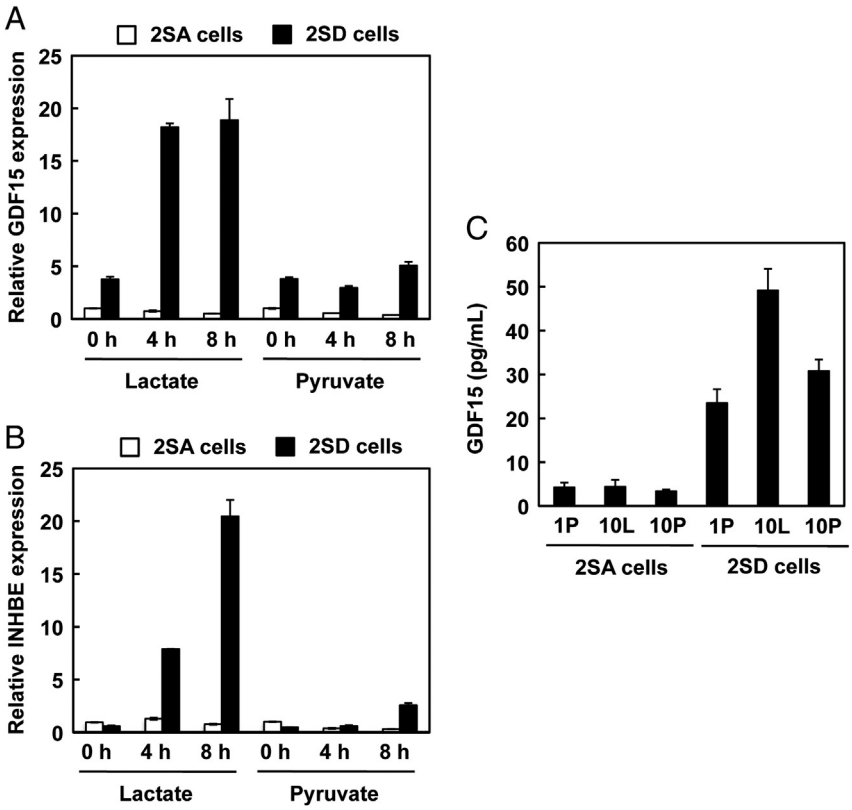

Fig. 4. Quantitative RT-PCR and ELISA for GDF15 and INHBE Total RNA isolated from 2SA and 2SD cells treated with 10 mM lactate or 10 mM pyruvate for 0, 4 or 8 h (n = 3) were subjected to quantitative RT-PCR for GDF15 (A) and INHBE (B). (C) The conditioned medium collected from 2SA and 2SD cell cultures treated with 10 mM lactate (10 L), 10 mM pyruvate (10P) or 1 mM pyruvate (1P) for 24 h was subjected to ELISA for GDF15 protein ($n = 3$).

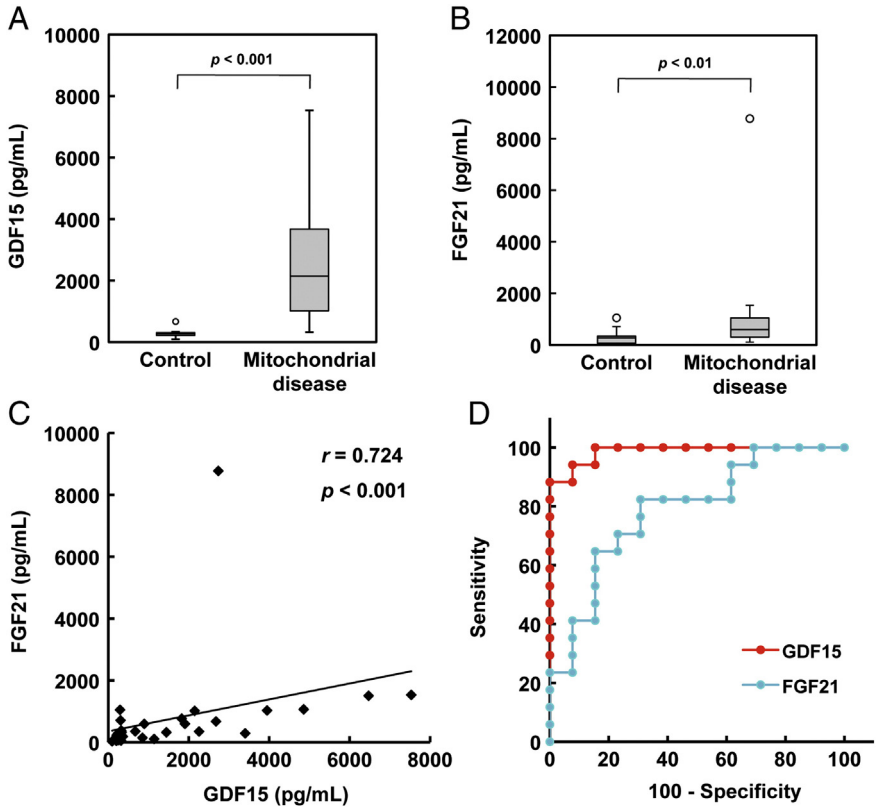

Fig. 5. Measurement of the GDF15 and FGF21 concentrations in the serum of patients. The serum GDF15 (A) and FGF21 (B) concentrations in 17 patients with mitochondrial diseases as well as those in 13 patients with other pediatric diseases were determined by ELISA. The outlier is shown with an open symbol. (C) A correlation analysis between the serum GDF15 and FGF21 levels was performed for the patients described above by use of IBM SPSS statistics. (D) The ROC curve analysis for GDF15 and FGF21 was performed. Areas under the curves (AUC) for GDF15 and FGF21 were 0.986 (95% CI 0.957-1.000) and 0.787 (95% CI 0.621-0.953), respectively.

It is well known that mitochondrial dysfunction is associated with the pathology of various diseases such as Parkinson's disease, Alzheimer's disease, diabetes, and aging (Exner et al., 2012; Lopez-Otin et al., 2013; Martin and McGee, 2014). GDF15, which may reflect mitochondria dysfunction, could be a useful marker for those diseases and the aging process. In support of this idea, the serum GDF15 level was reported to be elevated under various pathological conditions such as cancers, cardiovascular diseases, diabetes, and obesity (Dostalova et al., 2009; Kempf et al., 2007; Welsh et al., 2003); however, in most cases, it was not as high as that observed in mitochondrial diseases. Recent cohort studies also demonstrated that the serum GDF15 level is a novel predictor of all-cause mortality and is associated with cognitive performance and cognitive decline (Fuchs et al., 2013; Wiklund et al., 2010). We thus anticipate that GDF15 will attract more interest with respect to a variety of diseases and aging associated with mitochondrial dysfunction.

In conclusion, we identified GDF15 as a novel serum marker for the diagnosis of mitochondrial diseases and possibly both for monitoring the disease status and progression and for evaluating the therapeutic efficacy of pyruvate. Large-scale clinical trials including combined use of other markers such as FGF21 should confirm the clinical usefulness of GDF15.

Acknowledgments

This study was supported in part by the Ministry of Education, Culture, Sports, Science, and Technology of Japan; GMEXT/JSPS KAKENHI Grant Number: A-25242062, A-22240072, B-21390459, C-26670481, C-21590411, CER-24650414 (to M.T.), C-26350922 (to Y.F.), C-25461571 (to Y.K.), and YSB-25860891 (to S.Y.); the Ministry of Health, Labor, and Welfare of Japan; Grants-in-Aid for Research on Intractable Diseases (Mitochondrial Disorders): 23-Nanchi-Ippan-016, 23-Nanchi-Ippan-116, and 24-Nanchi-Ippan-005 (to M.T., and Y.K.); and the Takeda Science Foundation (to M.T.).

Appendix A. Supplementary data

Supplementary data to this article can be found online at http://dx.doi.org/10.1016/j.mito.2014.10.006.

References

Baek, S.J., Wilson, L.C., Eling, T.E., 2002. Resveratrol enhances the expression of non-steroidal anti-inflammatory drug-activated gene (NAG-1) by increasing the expression of p53. Carcinogenesis 23, 425–434.

Behan, A., Doyle, S., Farrell, M., 2005. Adaptive responses to mitochondrial dysfunction in the rho degrees Namalwa cell. Mitochondrion 5, 173–193.

Bruning, A., Matsingou, C., Brem, G.J., Rahmeh, M., Mylonas, I., 2012. Inhibin beta E is up-regulated by drug-induced endoplasmic reticulum stress as a transcriptional target gene of ATF4. Toxicol. Appl. Pharmacol. 264, 300–304.

Chomyn, A., Martinuzzi, A., Yoneda, M., Daga, A., Hurko, O., Johns, D., Lai, S.T., Nonaka, I., Angelini, C., Attardi, G., 1992. MELAS mutation in mtDNA binding site for transcription termination factor causes defects in protein synthesis and in respiration but no change in levels of upstream and downstream mature transcripts. Proc. Natl. Acad. Sci. U. S. A. 89, 4221–4225.

Crimi, M., Bordoni, A., Menozzi, G., Riva, L., Fortunato, F., Galbiati, S., Del Bo, R., Pozzoli, U., Bresolin, N., Comi, G.P., 2005. Skeletal muscle gene expression profiling in mitochondrial disorders. Faseb J. 19, 866–868.

Davis, R.L., Liang, C., Edema-Hildebrand, F., Riley, C., Needham, M., Sue, C.M., 2013. Fibroblast growth factor 21 is a sensitive biomarker of mitochondrial disease. Neurology 81, 1819–1826.

Dombroski, B.A., Nayak, R.R., Ewens, K.G., Ankener, W., Cheung, V.G., Spielman, R.S., 2010. Gene expression and genetic variation in response to endoplasmic reticulum stress in human cells. Am. J. Hum. Genet. 86, 719–729.

Dostalova, I., Roubicek, T., Bartlova, M., Mraz, M., Lacinova, Z., Haluzikova, D., Kavalkova, P., Matoulek, M., Kasalicky, M., Haluzik, M., 2009. Increased serum concentrations of macrophage inhibitory cytokine-1 in patients with obesity and type 2 diabetes mellitus: the influence of very low calorie diet. Eur. J. Endocrinol. 161, 397–404.

Exner, N., Lutz, A.K., Haass, C., Winklhofer, K.F., 2012. Mitochondrial dysfunction in Parkinson's disease: molecular mechanisms and pathophysiological consequences. EMBO J. 31, 3038–3062.

Fuchs, T., Trollor, J.N., Crawford, J., Brown, D.A., Baune, B.T., Samaras, K., Campbell, L., Breit, S.N., Brodaty, H., Sachdev, P., Smith, E., 2013. Macrophage inhibitory cytokine-1 is associated with cognitive impairment and predicts cognitive decline - the Sydney Memory and Aging Study. Aging Cell 12, 882–889.

Fujita, Y., Ito, M., Nozawa, Y., Yoneda, M., Oshida, Y., Tanaka, M., 2007. CHOP (C/EBP homologous protein) and ASNS (asparagine synthetase) induction in cybrid cells harboring MELAS and NARP mitochondrial DNA mutations. Mitochondrion 7, 80–88.

Goto, Y., Nonaka, I., Horai, S., 1990. A mutation in the tRNA(Leu)(UUR) gene associated with the MELAS subgroup of mitochondrial encephalomyopathies. Nature 348, 651–653.

Goto, Y., Horai, S., Matsuoka, T., Koga, Y., Nihei, K., Kobayashi, M., Nonaka, I., 1992. Mitochondrial myopathy, encephalopathy, lactic acidosis, and stroke-like episodes (MELAS): a correlative study of the clinical features and mitochondrial DNA mutation. Neurology 42, 545–550.

Harding, H.P., Zhang, Y., Zeng, H., Novoa, I., Lu, P.D., Calfon, M., Sadri, N., Yun, C., Popko, B., Paules, R., Stojdl, D.F., Bell, J.C., Hettmann, T., Leiden, J.M., Ron, D., 2003. An integrated stress response regulates amino acid metabolism and resistance to oxidative stress. Mol. Cell 11, 619–633.

Hashimoto, O., Sekiyama, K., Matsuo, T., Hasegawa, Y., 2009. Implication of activin E in glucose metabolism: transcriptional regulation of the inhibin/activin betaE subunit gene in the liver. Life Sci. 85, 534–540.

Jiang, H.Y., Wek, S.A., McGrath, B.C., Lu, D., Hai, T., Harding, H.P., Wang, X., Ron, D., Cavener, D.R., Wek, R.C., 2004. Activating transcription factor 3 is integral to the eukaryotic initiation factor 2 kinase stress response. Mol. Cell. Biol. 24, 1365–1377.

Jousse, C., Deval, C., Maurin, A.C., Parry, L., Cherasse, Y., Chaveroux, C., Lefloch, R., Lenormand, P., Bruhat, A., Fafournoux, P., 2007. TRB3 inhibits the transcriptional activation of stress-regulated genes by a negative feedback on the ATF4 pathway. J. Biol. Chem. 282, 15851–15861.

Kalko, S.G., Paco, S., Jou, C., Rodriguez, M.A., Meznaric, M., Rogac, M., Jekovec-Vrhovsek, M., Sciacco, M., Moggio, M., Fagiolari, G., De Paepe, B., De Meirleir, L., Ferrer, I., Roig-Quilis, M., Munell, F., Montoya, J., Lopez-Gallardo, E., Ruiz-Pesini, E., Artuch, R., Montero, R., Torner, F., Nascimento, A., Ortez, C., Colomer, J., Jimenez-Mallebrera, C., 2014. Transcriptomic profiling of TK2 deficient human skeletal muscle suggests a role for the p53 signalling pathway and identifies growth and differentiation factor-15 as a potential novel biomarker for mitochondrial myopathies. BMC Genomics 15, 91.

Kami, K., Fujita, Y., Igarashi, S., Koike, S., Sugawara, S., Ikeda, S., Sato, N., Ito, M., Tanaka, M., Tomita, M., Soga, T., 2012. Metabolomic profiling rationalized pyruvate efficacy in cybrid cells harboring MELAS mitochondrial DNA mutations. Mitochondrion 12, 644–653.

Kempf, T., Horn-Wichmann, R., Brabant, G., Peter, T., Allhoff, T., Klein, G., Drexler, H., Johnston, N., Wallentin, L., Wollert, K.C., 2007. Circulating concentrations of growth-differentiation factor 15 in apparently healthy elderly individuals and patients with chronic heart failure as assessed by a new immunoradiometric sandwich assay. Clin. Chem. 53, 284–291.

Kirino, Y., Yasukawa, T., Ohta, S., Akira, S., Ishihara, K., Watanabe, K., Suzuki, T., 2004. Codon-specific translational defect caused by a wobble modification deficiency in mutant tRNA from a human mitochondrial disease. Proc. Natl. Acad. Sci. U. S. A. 101, 15070–15075.

Koga, Y., Povalko, N., Katayama, K., Kakimoto, N., Matsuishi, T., Naito, E., Tanaka, M., 2012. Beneficial effect of pyruvate therapy on Leigh syndrome due to a novel mutation in PDH E1alpha gene. Brain Dev. 34, 87–91.

Lee, J.I., Dominy Jr., J.E., Sikalidis, A.K., Hirschberger, L.L., Wang, W., Stipanuk, M.H., 2008. HepG2/C3A cells respond to cysteine deprivation by induction of the amino acid deprivation/integrated stress response pathway. Physiol. Genomics 33, 218–229.

Li, J., Yang, L., Qin, W., Zhang, G., Yuan, J., Wang, F., 2013. Adaptive induction of growth differentiation factor 15 attenuates endothelial cell apoptosis in response to high glucose stimulus. PLoS One 8, e65549.

Lopez-Otin, C., Blasco, M.A., Partridge, L., Serrano, M., Kroemer, G., 2013. The hallmarks of aging. Cell 153, 1194–1217.

Martin, S.D., McGee, S.L., 2014. The role of mitochondria in the aetiology of insulin resistance and type 2 diabetes. Biochim. Biophys. Acta 1840, 1303–1312.

Pavlakis, S.G., Phillips, P.C., DiMauro, S., De Vivo, D.C., Rowland, L.P., 1984. Mitochondrial myopathy, encephalopathy, lactic acidosis, and strokelike episodes: a distinctive clinical syndrome. Ann. Neurol. 16, 481–488.

Rouschop, K.M., van den Beucken, T., Dubois, L., Niessen, H., Bussink, J., Savelkouls, K., Keulers, T., Mujcic, H., Landuyt, W., Voncken, J.W., Lambin, P., van der Kogel, A.J., Koritzinsky, M., Wouters, B.G., 2010. The unfolded protein response protects human tumor cells during hypoxia through regulation of the autophagy genes MAP1LC3B and ATG5. J. Clin. Invest. 120, 127–141.

Rzymski, T., Milani, M., Pike, L., Buffa, F., Mellor, H.R., Winchester, L., Pires, I., Hammond, E., Ragoussis, I., Harris, A.L., 2010. Regulation of autophagy by ATF4 in response to severe hypoxia. Oncogene 29, 4424–4435.

Saito, K., Kimura, N., Oda, N., Shimomura, H., Kumada, T., Miyajima, T., Murayama, K., Tanaka, M., Fujii, T., 2012. Pyruvate therapy for mitochondrial DNA depletion syndrome. Biochim. Biophys. Acta 1820, 632–636.

Sermeus, A., Michiels, C., 2011. Reciprocal influence of the p53 and the hypoxic pathways. Cell Death Dis. 2, e164.

Sperka, T., Wang, J., Rudolph, K.L., 2012. DNA damage checkpoints in stem cells, ageing and cancer. Nat. Rev. Mol. Cell Biol. 13, 579–590.

Suomalainen, A., Elo, J.M., Pietilainen, K.H., Hakonen, A.H., Sevastianova, K., Korpela, M., Isohanni, P., Marjavaara, S.K., Tyni, T., Kiuru-Enari, S., Pihko, H., Darin, N., Ounap, K., Kluijtmans, L.A., Paetau, A., Buzkova, J., Bindoff, L.A., Annunen-Rasila, J., Uusimaa, J., Rissanen, A., Yki-Jarvinen, H., Hirano, M., Tulinius, M., Smeitink, J., Tyynismaa, H., 2011. FGF-21 as a biomarker for muscle-manifesting mitochondrial respiratory chain deficiencies: a diagnostic study. Lancet Neurol. 10, 806–818.

Tanaka, M., Nishigaki, Y., Fuku, N., Ibi, T., Sahashi, K., Koga, Y., 2007. Therapeutic potential of pyruvate therapy for mitochondrial diseases. Mitochondrion 7, 399–401.

Teske, B.F., Wek, S.A., Bunpo, P., Cundiff, J.K., McClintick, J.N., Anthony, T.G., Wek, R.C., 2011. The eIF2 kinase PERK and the integrated stress response facilitate activation of ATF6 during endoplasmic reticulum stress. Mol. Biol. Cell 22, 4390–4405.

Tyynismaa, H., Carroll, C.J., Raimundo, N., Ahola-Erkkila, S., Wenz, T., Ruhanen, H., Guse, K., Hemminki, A., Peltola-Mjosund, K.E., Tulkki, V., Oresic, M., Moraes, C.T., Pietilainen, K., Hovatta, I., Suomalainen, A., 2010. Mitochondrial myopathy induces a starvation-like response. Hum. Mol. Genet. 19, 3948–3958.

Unsicker, K., Spittau, B., Krieglstein, K., 2013. The multiple facets of the TGF-beta family cytokine growth/differentiation factor-15/macrophage inhibitory cytokine-1. Cytokine Growth Factor Rev. 24, 373–384.

Welsh, J.B., Sapinoso, L.M., Kern, S.G., Brown, D.A., Liu, T., Bauskin, A.R., Ward, R.L., Hawkins, N.J., Quinn, D.I., Russell, P.J., Sutherland, R.L., Breit, S.N., Moskaluk, C.A., Frierson Jr., H.F., Hampton, G.M., 2003. Large-scale delineation of secreted protein biomarkers overexpressed in cancer tissue and serum. Proc. Natl. Acad. Sci. U. S. A. 100, 3410–3415.

Wiklund, F.E., Bennet, A.M., Magnusson, P.K., Eriksson, U.K., Lindmark, F., Wu, L., Yaghoutyfam, N., Marquis, C.P., Stattin, P., Pedersen, N.L., Adami, H.O., Gronberg, H., Breit, S.N., Brown, D.A., 2010. Macrophage inhibitory cytokine-1 (MIC-1/GDF15): a new marker of all-cause mortality. Aging Cell 9, 1057–1064.

Yang, H., Filipovic, Z., Brown, D., Breit, S.N., Vassilev, L.T., 2003. Macrophage inhibitory cytokine-1: a novel biomarker for p53 pathway activation. Mol. Cancer Ther. 2, 1023–1029.

Yasukawa, T., Suzuki, T., Ueda, T., Ohta, S., Watanabe, K., 2000. Modification defect at anticodon wobble nucleotide of mitochondrial tRNAs(Leu)(UUR) with pathogenic mutations of mitochondrial myopathy, encephalopathy, lactic acidosis, and stroke-like episodes. J. Biol. Chem. 275, 4251–4257.

Zhang, X.D., Qin, Z.H., Wang, J., 2010. The role of p53 in cell metabolism. Acta Pharmacol. Sin. 31, 1208–1212.

INTERNAL MEDICINE

□ CASE REPORT □

Multiple Deletions in Mitochondrial DNA in a Patient with Progressive External Ophthalmoplegia, Leukoencephalopathy and Hypogonadism

Yuko Ohnuki[1,2], Kazumi Takahashi[2,3], Eri Iijima[4], Wakoh Takahashi[4], Shingo Suzuki[1], Yuki Ozaki[1], Ruriko Kitao[5], Masatoshi Mihara[5], Tadayuki Ishihara[5], Michiyo Nakamura[6], Yoshie Sawano[6], Yu-ichi Goto[6], Shunichiro Izumi[2,3], Jerzy K. Kulski[1,7], Takashi Shiina[1] and Shunya Takizawa[4]

Abstract

Progressive external ophthalmoplegia (PEO) is one of a number of major types of mitochondrial disorders. Most sporadic PEO patients have a heteroplasmic large deletion of mitochondrial DNA (mtDNA) in the mitochondria in skeletal muscles. We herein analyzed mtDNA deletions using sub-cloning and Sanger sequencing of PCR products in a 31-year-old Japanese man with multiple symptoms, including PEO, muscle weakness, hearing loss, leukoencephalopathy and hypogonadism. A large number of multiple deletions was detected, as well as four kinds of deletion breakpoints identified in different locations, including m.3347_12322, m.5818_13964, m.5829_13964 and m.5837_13503.

Key words: mitochondrial DNA (mtDNA), multiple deletion, progressive external ophthalmoplegia (PEO), hypogonadism, leukoencephalopathy

(Intern Med 53: 1365-1369, 2014)
(DOI: 10.2169/internalmedicine.53.1320)

Introduction

Mitochondrial DNA (mtDNA) deletion syndromes comprise three major phenotypes: progressive external ophthalmoplegia (PEO), Kearns-Sayre syndrome (KSS) and Pearson syndrome. PEO is conventionally defined as progressive limitation of eye movements with normal pupils and ptosis of the eyelids. KSS is a multisystem disorder with the following symptoms: cardiac conduction block, pigmentary retinopathy and PEO. Pearson syndrome is characterized by sideroblastic anemia and exocrine pancreas dysfunction and is usually fatal in infancy. A few individuals with PEO have other manifestations of KSS but do not fulfill all of the clinical criteria for the diagnosis. This condition is called "PEO plus" in GeneReviews at the GeneTests Medical Genetics Information Resource (1). Most sporadic PEO patients have a heteroplasmic large deletion of mtDNA in the muscle. In patients with multiple mtDNA deletions, additional clinical features may be present, such as sensory axonal neuropathy, optic atrophy, ataxia, hypogonadism and parkinsonism (2, 3). Mutations in nuclear genes, such as *POLG1* and *POLG2* (DNA polymerase gamma) (4, 5), *PEO1* (the helicase Twinkle) (6) and *SLC25A4* (other alias: *ANT1*, the adenine nucleotide translocator) (7), have thus far been identified as driving multiple mtDNA deletion genes in PEO patients (2, 3). These proteins are involved in mtDNA replication and transcription, and their functional loss results in the

[1]Department of Molecular Life Science, Basic Medical Science and Molecular Medicine, Tokai University School of Medicine, Japan, [2]Department of Clinical Genetics, Tokai University Hospital, Japan, [3]Department of Obstetrics and Gynecology, Tokai University School of Medicine, Japan, [4]Department of Internal Medicine, Division of Neurology, Tokai University School of Medicine, Japan, [5]Department of Neurology, National Hakone Hospital, Japan, [6]Department of Mental Retardation and Birth Defect Research, National Center of Neurology and Psychiatry, Japan and [7]Centre for Forensic Science, The University of Western Australia, Australia
Received for publication July 8, 2013; Accepted for publication October 27, 2013
Correspondence to Dr. Yuko Ohnuki, yukom@is.icc.u-tokai.ac.jp

secondary accumulation of abnormal-sized mtDNA (3). In this report, we identified breakpoints of mtDNA deletions using sub-cloning and Sanger sequencing of polymerase chain reaction (PCR) products in a 31-year-old Japanese man with multiple symptoms, including PEO, muscle weakness, hearing loss, leukoencephalopathy and hypogonadism.

Case Report

The patient was initially diagnosed with IgA nephropathy, hypogonadism and hearing loss at 24 years of age. He noticed double vision and a gait disturbance; these symptoms gradually worsened at 30 years of age, and he was admitted to our hospital at 31 years of age. The patient's parents were not consanguineous. He had a younger sister who exhibited no symptoms. He had no family history of similar symptoms. He was 170 cm in height and 49 kg in weight. He had gynecomastia, bilateral ptosis and ophthalmoplegia with restriction of adduction. He also had mild muscle weakness in the limbs. Tendon reflexes were normal.

Laboratory examinations showed hypergonadotropic hypogonadism (testosterone: 0.13 ng/mL, LH: 14.8 mIU/mL, FSH: 6.14 mIU/mL). Although the serum lactate (12.6 mg/dL) and pyruvate (0.6 mg/dL) levels were normal, the lactate level was slightly elevated in the cerebral spinal fluid (18.2 mg/dL, compared to a normal level of <18.0 mg/dL). No aerobic exercise tests were performed. A chromosomal analysis showed that the patient's karyotype was 46,XY and that he did not have Klinefelter syndrome. An X-ray film of the chest showed a hilar shadow; however, there was not enough evidence of sarcoidosis. Fluid attenuated inversion recovery (FLAIR) brain magnetic resonance imaging (MRI) sequences (Fig. 1) showed diffuse leukoencephalopathy affecting both cerebral hemispheres, although the brain stem and cerebellum were spared. Needle electromyography (EMG) of the right first dorsal interosseous and right tibialis anterior muscles was normal. The patient's intelligence quotient (IQ) according to the Wechsler Adult Intelligence Scale III (WAIS-III) was estimated as follows: verbal IQ= 85, performance IQ= 78 and full-scale IQ= 80. Muscle biopsy specimens obtained from the left biceps showed brachii with many ragged-red fibers on a modified Gomori-trichrome stain (Fig. 2a, b). Succinate dehydrogenase (SDH) and cytochrome c oxidase (COX) staining were also examined and a COX deficiency was observed (Fig. 2c, d). Based on these findings, the patient was diagnosed with 'PEO plus;' therefore, we decided to analyze his mtDNA in detail in order to investigate and confirm the presence of multiple mtDNA deletions within the mitochondria.

DNA analysis and results

This study was approved by the ethics committee of Tokai University School of Medicine (11I-17). Informed consent was obtained from the patient and his mother to perform the genetic studies.

Genomic DNA was extracted directly from muscle tissue using the QIAamp DNA Investigator Kit (QIAGEN, Hilden, Germany). Whole mtDNA fragments, excluding the displacement loop (D-loop), were amplified via long-range PCR. A new set of mtDNA primers was designed for the conserved nucleotide sites provided by the GenBank database (www.ncbi.nlm.nih.gov) and to amplify sequences between the 12S rRNA gene and the Cytochrome b gene (amplified size: 14,457 bp on mtDNA sequence (GenBank/EMBL/DDBJ accession number: NC_012920) with the sense primer (mtDNA-F1: 5'-CAGCAATGCAGCTCAAAA CGCTTA-3') and the anti-sense primer (mtDNA-R2: 5'-GG CCTCGCCCGATGTGTAGGA-3'). The 20-μL amplification reaction volume contained 10 ng of genomic DNA, one unit of high-fidelity PrimeSTAR® GXL DNA Polymerase (TaKaRa BIO Inc., Otsu, Japan), 5×PCR buffer, 2.5 mM of each dNTP and 0.5 μM of each primer. The cycling parameters were as follows: 35 cycles of 98℃/10 sec, 60℃/20 sec and 68℃/15 min.

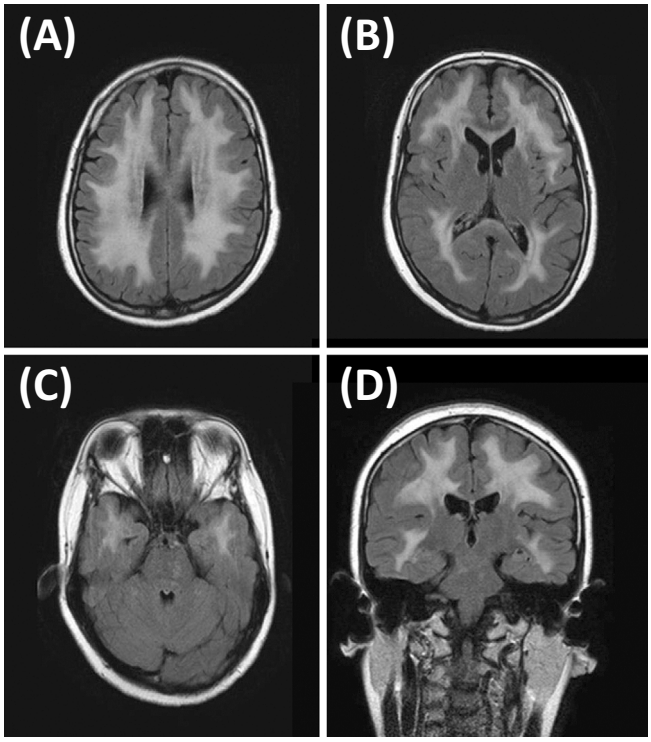

Figure 1. Brain MRI (FLAIR). (A-C) and (D) indicate MRI of axial and coronal sections, respectively. Symmetrical hyperintensity regions were observed in the bilateral cerebral white matter.

Based on our PCR analysis, we clearly detected evidence of PCR products from muscle DNA with multiple deletions within the mtDNAs in the electrophorese products. Namely, we observed the 15-kb wild-type mtDNA, 7-kb and 7.5-kb major deleted fragments and some minor deleted fragments ranging from 6 kb to 9 kb in the patient's genomic DNA (Fig. 3). These deletions were not observed in the patient's peripheral blood cells or the DNA obtained from the skeletal muscle and peripheral blood cells of control subjects.

In order to identify the breakpoints, we performed sub-

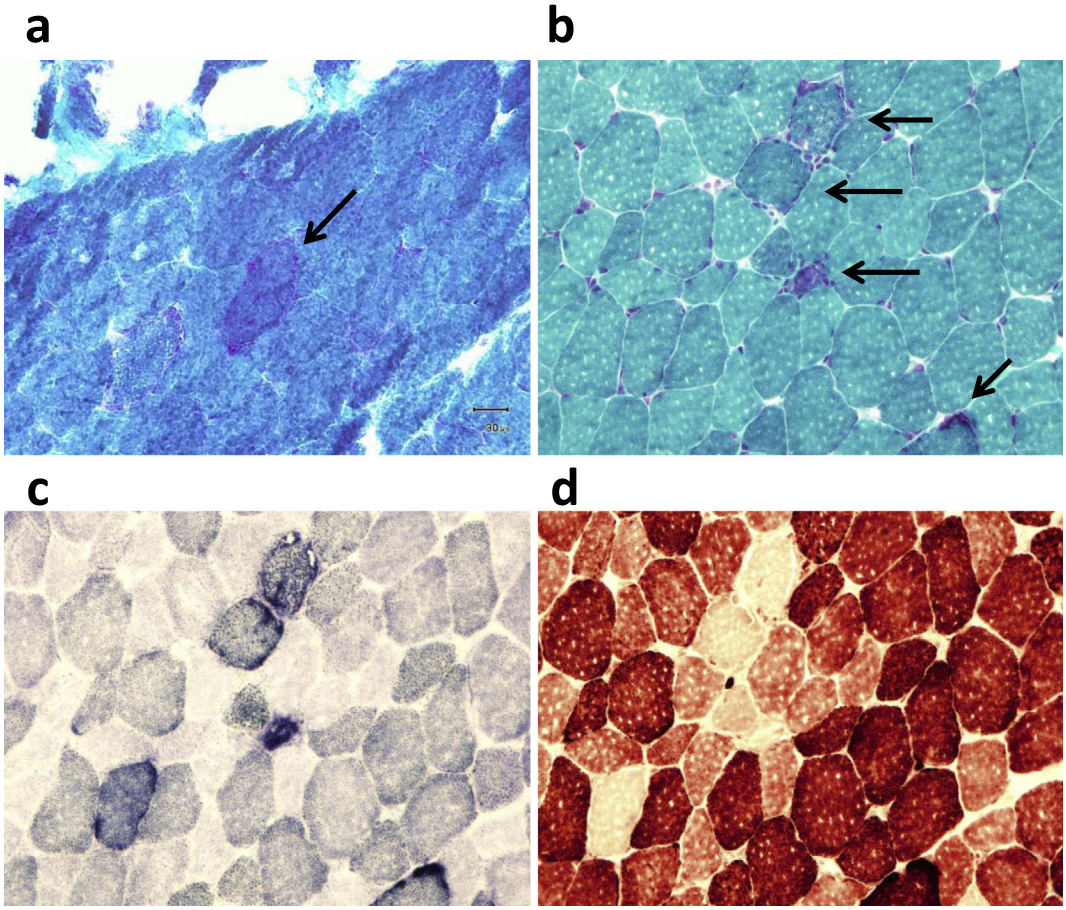

Figure 2. **Biopsy specimen of the brachial biceps muscle stained with modified Gomori-trichrome staining (a, b). The arrow indicates so-called "ragged-red fibers." (c) SDH (Succinate Dehydrogenase) staining (d) COX (Cytochrome Oxidase) staining; a COX deficiency is observed.**

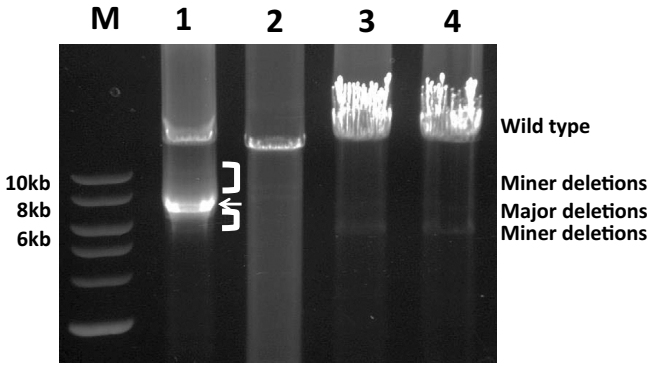

Figure 3. **A long-range PCR analysis of the patient's mtDNA. The 15-kb fragments from nucleotide positions 767 to 15050 were amplified via long-range PCR using total tissue DNA extracted from the skeletal muscle (Lane 1) and peripheral blood cells (Lane 3) of the patient. Lanes 2 and 4 show PCR fragments derived from control skeletal muscle and control peripheral blood cells, respectively. "M" indicates 1 kb in the DNA ladder.**

cloning and Sanger sequencing of the deleted DNA fragments. The targeted DNA fragments were isolated using a QIAquick gel extraction kit (QIAGEN). Sub-cloning and transformation of the fragments were performed according to the manufacturer's protocol for the TArget clone Kit (TOYOBO, Osaka, Japan) and DH5α-competent cells (TOYOBO). After sub-cloning, direct PCR was performed using the following parameters: 35 cycles of 98℃/10 sec, 65℃/20 sec and 68℃/7 min. The nucleotide sequences randomly selected nine subclones that were directly sequenced using an ABI3130 genetic analyzer (Life Technologies, Carlsbad, USA) in accordance with the protocol of the Big Dye terminator method. We used various primers to detect the sequence breakpoints of the deletions according to the primer walking method (Table). The sequence-generated chromatogram data were analyzed using the Sequencher ver. 4.10 DNA sequence assembly software program (Gene Code Co., Ann Arbor, USA).

Using this procedure, four kinds of deletion breakpoints were identified, including m.3347_12322 (1), m.5818_13964 (2), m.5829_13964 (3) and m.5837_13503 (4), which corresponded to 8,976-bp, 8,147-bp, 8,136-bp and 7,667-bp deletions, respectively (Fig. 4). Of the nine PCR sub-clones, six had m.3347_12322 (1), while the others had m.5818_13964 (2), m.5829_13964 (3) and m.5837_13503 (4). Hence, m.3347_12322 (1) was the most predominant deletion type in this case. The deletion breakpoints did not occur

Table. Primer List for Primer Walking Method of Sanger Direct-sequencing

Primer name	Location	Primer seqeunce (5' to 3')
mt-F1	mt.767_790	CAGCAATGCAGCTCAAAACGCTTA
mt-F2	mt.761_781	AGCACGCAGCAATGCAGCTCA
mt-F3	mt.858_881	CTATACTAACCCCAGGGTTGGTCA
mt-F4	mt.806_829	CACGGGAAACAGCAGTGATTAACC
mt-F5	mt.1345_1368	GAGGTGGCAAGAAATGGGCTACAT
mt-F6	mt.1764_1787	CCTGGCGCAATAGATATAGTACCG
mt-F7	mt.2250_2273	CACTCCTCACACCCAATTGGACCA
mt-F8	mt.2718_2741	CGAGAAGACCCTATGGAGCTTTAA
mt-F9	mt.3230_3253	GTTAAGATGGCAGAGCCCGGTAAT
mt-F10	mt.3649_3672	TCAATCCTCTGATCAGGGTGAGCA
mt-F11	mt.4179_4202	AAACTTCCTACCACTCACCCTAGC
mt-F12	mt.4526_4549	CACAGCGCTAAGCTCGCACTGATT
mt-R1	mt.15200_15223	GTCTGTCCCAATGTATGGGATGGC
mt-R2	mt.15030_15050	GGCCTCGCCCGATGTGTAGGA
mt-R3	mt.14978_15001	ATTGGCGTGAAGGTAGCGGATGAT
mt-R4	mt.14903_14926	TGAGGCGTCTGGTGAGTAGTGCAT
mt-R5	mt.14438_14461	AGCGATGGCTATTGAGGAGTATCC
mt-R6	mt.13985_14008	GTCAGGTTAGGTCTAGGAGGAGTA
mt-R7	mt.13538_13561	GGGCTCAGGCGTTTGTGTATGATA
mt-R8	mt.13069_13092	TATAGTGCTTGAGTGGAGTAGGGC
mt-R9	mt.12733_12756	CAGTTGGAATAGGTTGTTAGCGGT
mt-R10	mt.12345_12368	GTTAGGGTGGTTATAGTAGTGTGC
mt-R11	mt.12009_12032	TGTTAATGTGGTGGGTGAGTGAGC
mt-R12	mt.11633_11656	TGTTACTACGAGGGCTATGTGGCT

within the repeated sequences.

Discussion

Progressive external syndrome (PEO) is a mitochondrial myopathy associated with ptosis, ophthalmoplegia and variably proximal limb weakness. PEO is almost never inherited, suggesting that this disorder is caused by *de novo* mtDNA deletions that occur in the mother's oocytes during germline development or in the embryo during embryogenesis (1). Chen et al. (8) showed that the "common deletion" (m.8470_13446del4977) accounts for 0.01-0.1% of the approximately 150,000 copies of mtDNAs in the human oocyte (8). Even if mtDNA deletions were present in human oocytes, a small mitochondrial bottleneck would eventually effectively filter out these deletions. On rare occasions, a "deleted" mtDNA may slip through the ancestral line. On the other hand, many familial cases have been reported with multiple deletions of mtDNA. Most patients suffer from PEO and may have nuclear genetic defects, with the accumulation of mtDNA deletions (9). These nuclear genes are known to play important roles in controlling mtDNA synthesis and maintenance. However, no mutations were detected in *POLG* and *PEO1* that are known to be nuclear genes affecting mtDNA deletions (data not shown).

Multiple mtDNA deletions are associated with many clinical phenotypes (9), including cardiomyopathy, recurrent myoglobinuria, ataxia plus ketoacidotic coma, multiple symmetric lipomatosis, myoclonus epilepsy with ragged red fibers and myopathy with multisystemic features except

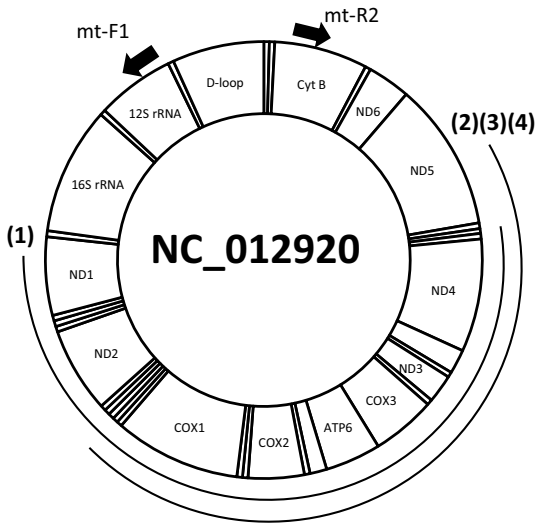

Figure 4. Locations of the mtDNA deletions. (1-4) indicate locations of four kinds of mtDNA deletions identified in this study such as m.3347_12322 (1), m.5818_13964 (2), m.5829_13964 (3), and m.5837_13503(4). Arrows indicate locations of long ranged PCR primers; mt-F1(mt.767_790) and mt-R2 (mt.15030_15050).

PEO (9). We herein described a patient suffering from PEO, muscle weakness, hearing loss, leukoencephalopathy and hypogonadism. There are few previous case reports of patients with hypogonadism associated with PEO.

Luoma et al. (3) reported four families that were diagnosed with PEO in addition to premature menopause and parkinsonism. The authors recorded mutations in *POLG* in all of the families. In one of the families, the affected men exhibited testicular atrophy (3). These facts point to a defect in steroidogenesis, in which mitochondria play a role in regulating the serum steroid hormone concentrations (3, 10). Melberg et al. (11) also reported a family with autosomal dominant PEO and hypogonadism.

In the present case history, we followed the patient's symptoms for almost six years to eventually diagnose him with hypogonadism preceded by ptosis and ophthalmoplegia. Therefore, clinicians should take into consideration hypogonadism as a symptom of mitochondrial disorders, including PEO. Furthermore, multiple symptoms associated with PEO may be caused by nuclear genetic defects stemming from multiple mtDNA deletions that may be transmitted via Mendelian inheritance, which must be explained to patients and their families.

The authors state that they have no Conflict of Interest (COI).

References

1. DiMauro S, Hirano M. Mitochondrial DNA Deletion Syndromes. In: GeneReviews® at GeneTests: Medical Genetics Infromation Resource (database online). Copyright. Pagon RA, Adam MP, Ardinger HH, Bird TD, Dolan CR, Fong CT, Smith RJH, Stephens K, Eds. University of Washington, Seattle, May 2011:

1993-2014. Available at http://www.genetests.org. Accessed June 11, 2013

2. Ronchi D, Garone C, Bordoni A, et al. Next-generation sequencing revieals DGUOK mutations in adult patients with mitochondrial DNA multiple deletions. Brain **135**: 3404-3415, 2012.

3. Luoma P, Melberg A, Rinne JO, et al. Parkinsonism, premature menopause, and mitochondrial DNA polymerase γ mutations: clinical and molecular genetic study. Lancet **364**: 875-882, 2004.

4. Van Goethem G, Dermaut B, Löfgren A, Martin JJ, Van Broeckhoven C. Mutation of POLG is associated with progressive external ophthalmoplegia characterized by mtDNA deletions. Nat Genet **28**: 211-212, 2001.

5. Longley MJ, Clark S, Yu Wai, et al. Mutant POLG2 disrupts DNA polymerase gamma subunits and causes progressive external ophthalmoplegia. Am J Hum Genet **78**: 1026-1034, 2006.

6. Spelbrink JN, Li FY, Tiranti V, et al. Human mitochondrial DNA deletions associated with mutations in the gene encoding Twinkle, a phage T7 gene 4-like protein localized in mitochondria. Nat Genet **28**: 223-231, 2001.

7. Kaukonen J, Juselius JK, Tiranti V, et al. Role of adenine nucleotide translocator 1 in mtDNA maintenance. Science **289**: 782-785, 2000.

8. Chen X, Prosser R, Simonetti S, Sadlock J, Jagiello G, Schon EA. Rearranged mitochondrial genomes are present in human oocytes. Am J Hum Genet **57**: 239-247, 1995.

9. Van Goethem G, Martin JJ, Van Broeckhoven C. Progressive external ophthalmoplegia characterized by multiple deletions of mitochondrial DNA: unraveling the pathogenesis of human mitochondrial DNA instability and the initiation of a genetic classification. Neuromolecular Med **3**: 129-146, 2003.

10. Bose H, Lingappa VR, Miller WL. Rapid regulation of steroidogenesis by mitochondrial protein import. Nature **417**: 87-91, 2002.

11. Melberg A, Arnell H, Dahl N, et al. Anticipation of autosomal dominant progressive external ophthalmoplegia with hypogonadism. Muscle Nerve **19**: 1561-1569, 1996.

神経内科，83(6)：520-524，2015

原著

高度のミトコンドリアDNA A3243G変異率と臨床経過との関連が示唆されたMELASの1例*

長田　治**　岩崎　章**　西野一三***
埜中征哉***　後藤雄一****

Key Words：MELAS, mtDNA, A3243G mutation, heteroplasmy level

はじめに

ミトコンドリア病は，細胞内小器官であるミトコンドリアの機能低下に起因する病気である．ミトコンドリアは体中の成熟赤血球以外のあらゆる細胞に存在していることから，いろいろな種類の細胞の機能が障害されたり，細胞が消失(細胞死)したりするため，その影響は多種多様な臨床症状として現れる[1]．Mitochondrial myopathy, encephalopathy, lactic acidosis and stroke-like episodes(MELAS)は，頭痛，てんかんおよび脳卒中様発作を特徴とするミトコンドリア病で最も多い病型である．報告されている遺伝子変異の中ではミトコンドリアDNA(mtDNA) A3243G変異が最も多く，80%を占める[2]．同じA3243G変異を有していても脳卒中様発作を発症することなく，糖尿病，感音性難聴，心筋症，消化器症状あるいは頭痛のみを呈する症例もあり，表現型の多様性が知られている．mtDNAに変異がある場合，その多くは変異したmtDNAと正常なmtDNAが細胞内に混在するheteroplasmyの状態で存在する．表現型の多様性は，罹患臓器や組織の変異mtDNAの割合(変異率)や閾値効果によって説明されている[3]．

高度のmtDNA A3243G変異率と臨床経過との関連が示唆されたMELASの1例を経験した．加齢や糖尿病罹病期間が長くなるにつれて変異率が増加し，新たな合併症状が加わっていった可能性と，変異率が92.7%と高度であるがゆえに新たな合併症が生じなくなった可能性が考えられた．文献的考察を加え報告する．

症　例

患者：38歳，女性．

主訴：呼吸苦．

既往歴・家族歴：母親と同胞全員(2人の兄，姉)が糖尿病である．

現病歴：1985年頃(12歳)から難聴，1991年頃(19歳)に糖尿病を発症した．インスリン依存状態の糖尿病でHbA1c 10%台とコントロール不良であった．2007年12月(35歳)，意識障害，左片麻痺が，2008年1月，不穏・拒薬などの精神症状が出現した．いずれも脳MRIで梗塞様病変が認められたが，エダラボン点滴投与後，いずれの

* MELAS supposed of relationship between high heteroplasmy level of the mitochondrial A3243G mutation and the clinical course. A case report.(Accepted October 13, 2015).

** Osamu OSADA, M.D. & Akira IWASAKI, M.D.: 深谷赤十字病院神経内科〔〒366-0052　埼玉県深谷市上柴町西5-8-1〕; Department of Neurology, Fukaya Red Cross Hospital, Fukaya, Saitama 366-0052, Japan.
*** Ichizo NISHINO, M.D., Ikuya NONAKA, M.D. & ****Yuichi GOTO, M.D.: 国立精神・神経医療研究センター疾病研究第1部，****疾病研究第2部; Departments of Neuromuscular Research and ****Mental Retardation and Birth Defect Research, National Center of Neurology and Psychiatry, Kodaira, Tokyo, Japan.

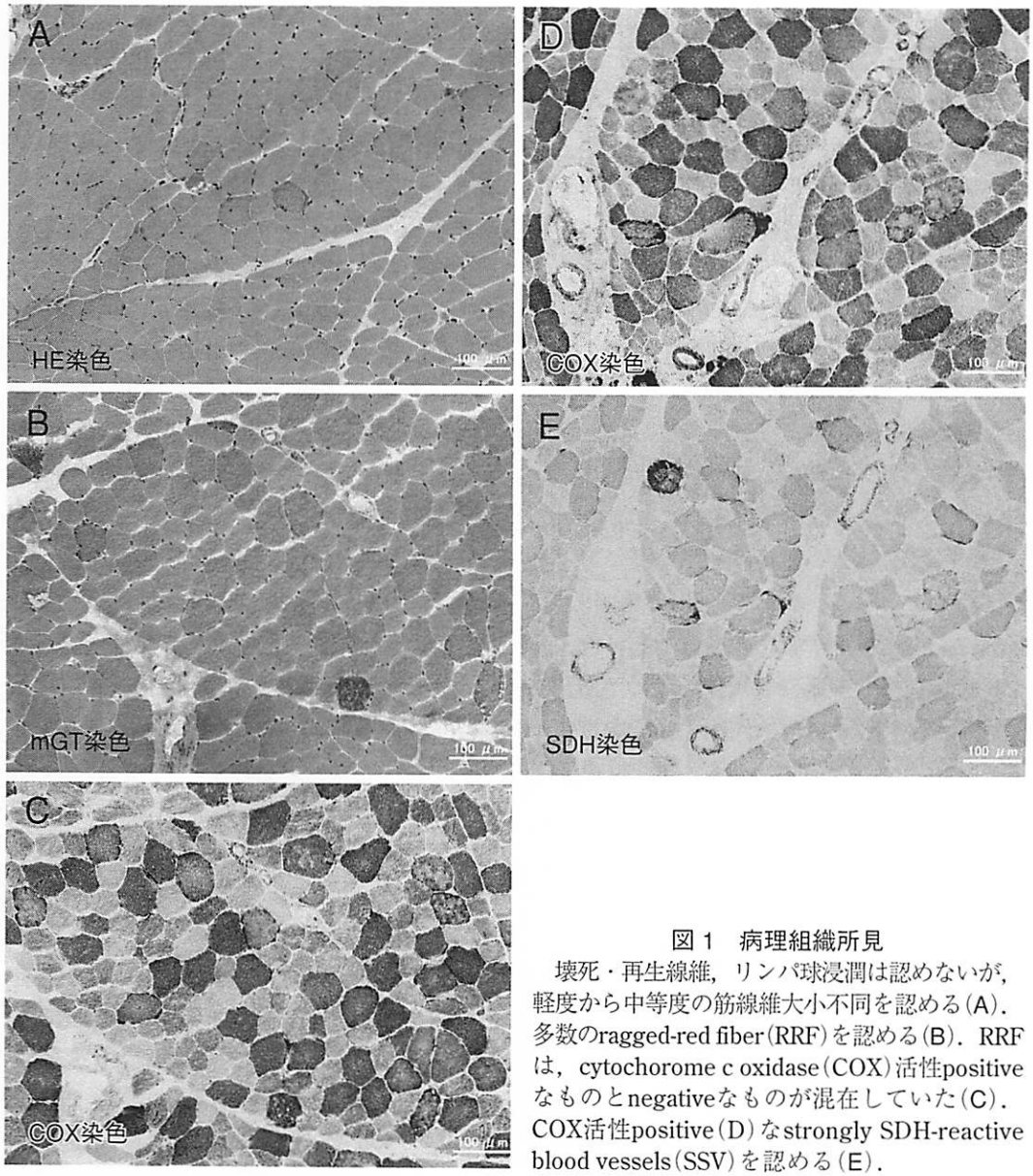

図1　病理組織所見
壊死・再生線維，リンパ球浸潤は認めないが，軽度から中等度の筋線維大小不同を認める(A)．多数のragged-red fiber(RRF)を認める(B)．RRFは，cytochorome c oxidase(COX)活性positiveなものとnegativeなものが混在していた(C)．COX活性positive(D)なstrongly SDH-reactive blood vessels(SSV)を認める(E)．

症状も改善した．2008年2月，両下腿の浮腫が出現し，心不全と診断され，フロセミドの内服で浮腫は改善した．精神退行が認められた．精査を拒否されたため，心不全の精査は行われなかった．その後は外来でインスリン注射指導と栄養指導が繰り返し行われ，HbA1cは6～8%に改善した．2011年3月初旬，呼吸苦が出現し当院内科を受診した．頭痛，嘔気あり．右胸水著明で入院した．胸水はフロセミド静注で消失した．冠動脈造影検査で有意な狭窄病変は認めなかった．多彩な症状を呈する疾患でミトコンドリア病が疑われ，当科に転科となった．

転科時所見：身長149 cm，体重40 kg．体温37.0℃，血圧121/88 mmHg，脈拍101回/分．SpO_2 94%(室内気)．ラ音なし，心雑音なし．四肢浮腫なし．神経学的には意識清明で，脳神経系では両側高度難聴を認めた．運動系は四肢近位筋でMMT 4レベルの筋力低下を認めた．四肢の筋萎縮は認めないが，四肢腱反射は減弱していた．病的足底反射は陰性であった．感覚系は，表在覚は顔面・四肢にいずれも異常を認めなかった．振動覚は両膝以下で軽度減弱していた．小脳性運動失調はなく，MMSEは24点であった．

検査所見：血液検査で血糖値は83 mg/dlでHbA1c 6.7%であった．乳酸値は1回目31.0 mg/dl，2回目36.9 mg/dl，ピルビン酸値は1回目1.01 mg/dl，2回目1.63 mg/dlといずれも繰り返し高値であった．髄液検査でも乳酸値46.0 mg/dl，ピ

表1　MELAS成人型の合併症状と本症例の対比

合併症状	頻度(%)	本症例	
		有無	概要
脳卒中様発作	84.2	○	35歳時，左片麻痺
けいれん・てんかん	68.4	×	
聴力障害	57.9	○	12歳時，難聴
視野異常/視力障害	57.9	×	
頭痛	57.9	○	
精神退行	47.4	○	
低身長	42.1	○	149 cm
意識障害	42.1	○	35歳時，意識障害
糖尿病	39.5	○	19歳時，糖尿病
歩行困難	36.8	○	
筋力低下	34.2	○	四肢近位筋 MMT 4
閃輝暗点	28.9	×	
心疾患	28.9	○	35歳時，心不全
認知症	23.7	×	MMSE 24点

ルビン酸値1.78 mg/dlといずれも高値であった．脳CTでは両側基底核と視床に石灰化を認め，MRIでは小脳萎縮と両側側頭葉から後頭葉にかけて梗塞様病変を認めた．経胸壁心臓超音波検査では心室中隔厚13.6 mm，左室後壁厚14.0 mmと左室肥大を認め，肥大型心筋症様の所見であった．三角筋，上腕二頭筋，大腿四頭筋で針筋電図検査を施行した．いずれの被検筋でも低振幅の短持続電位を認めた．筋原性変化の所見と考えた．標準純音聴力検査で両側78 dBと高度の感音性難聴を認めた．

転科後の経過：特定疾患認定基準で，ミトコンドリア病確実例と診断した．入院中にも発作性の頭痛や嘔気を認めたことと脳卒中様発作の既往があることからMELASが疑われ，左上腕二頭筋で筋生検を施行した．病理組織学的には，壊死・再生線維，リンパ球浸潤は認めないが，軽度から中等度の筋線維大小不同を認め(図1-A)，多数のragged-red fiber(RRF)を認めた(図1-B)．RRFは，cytochorome c oxidase(COX)活性positiveなものとnegativeなものが混在していた(図1-C)．COX活性positiveなstrongly SDH-reactive blood vessels(SSV)を認めた(図1-D, E)．遺伝子検査でmtDNA A3243G変異を認めた．定量PCR法で求めた筋での変異率は92.7%であった．厚生労働科学研究・古賀班診断基準からMELAS確実例と診断した．L-アルギニン0.4 g/kg/day，CoQ10 3 mg/kg/day，フロセミド40 mg/dayの内服を開始して同年4月中旬に退院した．2012年4月からは，本人希望でL-アルギニンの内服は中止した．その後，新たな症状の出現はなく，心筋症の進行，脳卒中様発作もみられない．

考　察

糖尿病の管理中にsick day時の糖欠乏によりMELASが誘発される機序が想定されている[4]．しかしながら本症例では，HbA1c 10%台と血糖値が高値で推移していた頃に，低血糖発作を起こしていないときにMELASを発症しており，sick dayとは別の機序で発症したものと考える．変異率が臨床症状に大きく影響することが示唆されたとの報告[5]や，変異率の高い症例ほど臨床症状が重い傾向があるとの報告がある[6]．以下，変異率と臨床経過との関連について考察した．

2002～2007年に行われた日本人のMELAS成人型(18歳以降に発症)38例の調査から得られたMELASの合併症状とそれぞれの頻度[3]を本症例と対比して示す(表1)．本症例では，10歳代で難聴，糖尿病を発症し，30歳代になってMELAS，心筋症を発症するなど，表1で合併症状として示したなかの多数の症状を認める．本症例と類似した経過を示した同じくA3243G変異を認めたMELASの症例報告がある．20歳代に難聴と糖尿病が出現し，その数年後に意識消失発作を認め，MELASと診断された症例である．著者らは，加齢とともに患者のmtDNA変異率は増加すると考えられていることから，ATP需要が多く機能不全をきたしやすい聴神経や膵B細胞では変異率が少ない時期から症状が明らかとなったのに対し，聴神経以外の中枢神経では徐々に変異率が増加して，ある閾値を越え，臨床症状を呈したと推定している[7]．

正常mtDNAと変異mtDNAが混在しているときには，変異mtDNAが増加する傾向が強いとされている[8]．高血糖状態は活性酸素種を生じ，変異mtDNAの増加を加速させる．糖尿病患者においては，糖尿病罹病期間が変異率の増加に最も関与すると推定されている[9]．本症例においては，加齢に加え，糖尿病罹病期間が長くなるにつれて変異率が増加し，組織それぞれの閾値を越えることで合併症状が加わっていった可能性が考

えられた．

本症例では，MELAS診断後，4年以上にわたり新たな合併症状の出現はみられない．変異率は組織により異なるが，筋で高値となり，最大で92％とされている[10]．本症例の筋での変異率92.7％は最大値に相当し，ほかの組織での変異率も同様に最大となっていると推定される．よって新たな合併症が生じないものと考えられた．

一般に心不全患者では心筋細胞内のCoQ10が欠乏していることにより，わが国では1974年から，うっ血性心不全の補助薬として30 mg/dayの用量で処方されている．しかし，この用量では効果が出にくいともされてきた．欧米を中心に30 mg/dayを超える用量での心不全患者に対する臨床研究が行われ，最近では有効との報告も出てきた[11]．

A3243G変異は主に呼吸鎖酵素複合体Ⅰの活性低下をひき起こし，ATP合成を低下させる[12]．とりわけエネルギー需要が高い心臓などで臓器障害が起こりやすいとされている[13]．CoQ10は呼吸鎖におけるATP合成に関与している電子伝達の担体であり[14]，CoQ10製剤は，虚血心筋内のATP含量を増大させ，細胞呼吸機能不全から組織を防御する作用があるとされる[7]．CoQ10製剤の投与により，MELASで心機能が回復した例の報告がある[15]．また，心不全で欠乏しているCoQ10が補充され，心筋症で合成の低下しているATPが増大すると考えられる．本症例では，内服開始後，4年以上にわたり，心筋症の進行がみられない．本症例のようにA3243G変異を有するミトコンドリア病の心筋症に由来する心不全では，CoQ10製剤の投与が心筋症の症状進行抑制に寄与している可能性が考えられる．引き続き経過を観察し検証していく．

結　語

高度のmtDNA A3243G変異率と臨床経過との関連が示唆されたMELASの1例を経験した．加齢や糖尿病罹病期間が長くなるにつれて変異率が増加し，新たな合併症状が加わっていった可能性と，変異率が92.7％と高度であるがゆえに新たな合併症が生じなくなった可能性が考えられた．

本論文の要旨は，第214回日本神経学会関東・甲信越地方会(2015年9月5日)において発表した．

文　献

1) 後藤雄一．ミトコンドリア病の臨床と診断．臨床症状と診断のしかた．Clin Neurosci 2012；30：997-9.
2) 飯塚高浩．代表的なミトコンドリア病．脳卒中様発作を伴うミトコンドリア脳筋症(MELAS)．Clin Neurosci 2012；30：1020-6.
3) 古賀靖敏．ミトコンドリア病の診断と治療―update review―．脳と発達 2010；42：124-9.
4) 鈴木　進，岡　芳知，門脇　孝，ほか．ミトコンドリアDNA異常による糖尿病調査報告．糖尿病 2004；47：481-7.
5) 三牧正和，竹下絵里，西野一三，ほか．ミトコンドリアDNA m.3243A>G変異を有する308例の検討[会]．脳と発達 2013；45 Suppl：S297.
6) 丹野芳範．ミトコンドリア脳筋症におけるヘテロプラスミー(heteroplasmy)と臨床症状，病理所見の関連性の研究．新潟医学会誌 2002；116：619-30.
7) 國府田尚子，長坂昌一郎，松本千明，ほか．糖尿病と感音性難聴が先行し，経過中MELASの症状を呈したミトコンドリア遺伝子異常の1例．糖尿病 1996；39：511-6.
8) 太田成男．ミトコンドリアDNAその特徴，遺伝，ヘテロプラズミー，閾値効果．臨床検査 2005；49：9-15.
9) Nomiyama T, Tanaka Y, Hattori N, et al. Accumulation of somatic mutation in mitochondrial DNA extracted from peripheral blood cells in diabetic patients. Diabetologia 2002 ; 45 : 1577-83.
10) Finsterer J. Genetic, pathogenetic, and phenotypic implications of the mitochondrial A3243G tRNALeu (UUR) mutation. Acta Neurol Scand 2007 ; 116 : 1-14.
11) 森下竜一．心不全とコエンザイムQ10に関する最近の話題．Anti-aging Science 2013；5：269-75.
12) 桐野陽平，鈴木　勉．MELASにおけるA3243G変異とtRNA修飾異常．臨床検査 2005；49：89-95.
13) 荒川健一郎，井川正道，米田　誠．ミトコンドリア心筋症と代謝治療．細胞 2014；46：320-3.

14) de Wit HM, Westeneng HJ, van Engelen BG, Mudde AH. MIDD or MELAS : that's not the question MIDD evolving into MELAS ; a severe phenotype of the m.3243A>G mutation due to paternal coinheritance of type 2 diabetes and a high heteroplasmy level. Neth J Med 2012 ; 70 : 460-2.
15) 寺井秀樹，猪原明子，麻薙美香，ほか．コエンザイムQ10投与により改善したミトコンドリア心筋症の1例[会]．第552回日本内科学会関東地方会 2008年3月．

<Abstract>

MELAS supposed of relationship between high heteroplasmy level of the mitochondrial A3243G mutation and the clinical course. A case report.

by

Osamu OSADA, M.D., Akira IWASAKI, M.D., *Ichizo NISHINO, M.D., *Ikuya NONAKA, M.D. & **Yuichi GOTO, M.D.

from

Department of Neurology, Fukaya Red Cross Hospital, Fukaya, Saitama 366-0052, Japan and Departments of *Neuromuscular Research and **Mental Retardation and Birth Defect Research, National Center of Neurology and Psychiatry, Kodaira, Tokyo, Japan.

We report a 38-year-old female patient with mitochondrial myopathy, encephalopathy, lactic acidosis and stroke-like episodes (MELAS). Around the age of 12, she developed hearing loss and around the age of 19, diabetes mellitus. She suffered from disturbance of consciousness and hemiplegia in December 2007, at the age of 35, and psychiatric symptoms in January 2008. Brain MRI revealed lesion suggesting acute infarction and edaravone infusion was successful for her symptoms. In February 2008, she noticed edema in the lower limbs. Cardiac dysfunction was pointed out and oral administration of furosemide was started. The symptom was improved. In March 2011 she was aware of dyspnea and was admitted to our hospital. Cardiac dysfunction was pointed out again. The echocardiogram showed hypertrophic cardiomyopathy. Laboratory tests revealed increased level of lactate and pyruvate acid both in blood plasma and the cerebrospinal fluid. We diagnosed her with mitochondrial disease (definite). Moreover, by biopsy of the left biceps brachii muscle, she was diagnosed as having MELAS associated with mitochondrial DNA A3243G mutation, of which heteroplasmy level (cellular content of the mitochondrial mutation) was 92.7% in the muscle. Since she was treated with coenzyme Q10, her condition has been stable for more than 4 years. We suppose that some symptoms, including stroke-like episodes and cardiac dysfunction, were manifested, as heteroplasmy level increased with age and duration of diabetes mellitus, and that no more symptoms were added after the highest heteroplasmy level.

* * *

ミトコンドリア病
診療マニュアル2017

編集

日本ミトコンドリア学会

作成

ミトコンドリア病診療マニュアル編集委員会

村山　圭　千葉県こども病院代謝科

小坂　仁　自治医科大学小児科学

米田　誠　福井県立大学看護福祉学部

診断と治療社

Chapter 36
Mitochondrial Cardiomyopathy and Usage of L-Arginine

Kenichiro Arakawa, Masamichi Ikawa, Hiroshi Tada, Hidehiko Okazawa, and Makoto Yoneda

Key Points

- Cardiomyopathy is present in 17–40 % of patients with mitochondrial disease and is one of the major causes of death in such patients.
- MELAS is a syndrome caused by an A-to-G transition at nucleotide position 3243 in tRNA-Leu of mtDNA and is the most common type of mitochondrial disease.
- In vivo functional imaging makes it possible to evaluate aspects of energy metabolism such as membrane potential and TCA cycle kinetics in MELAS patients noninvasively.
- L-Arg therapy is a promising approach for controlling the stroke-like episode of MELAS because of its vasodilative effect.
- L-Arg also has the potential to accelerate TCA cycle activity, irrespective of its vasodilative effect, and this can be used for treatment of mitochondrial cardiomyopathy.

Keywords Cardiomyopathy • MELAS • SPECT • PET • L-Arginine • TCA cycle

K. Arakawa, MD, PhD
Department of Cardiology, Jujinkai Medical Association Kimura Hospital,
4-4-9 Asahimachi Sabea City, Fukui 916-0025, Japan

Department of Cardiovascular Medicine, Faculty of Medical Sciences, University of Fukui,
23-3 Shimoaizuki, Matsuoka, Eiheiji, Fukui 910-1193, Japan
e-mail: ke.arakawa@jojinkai.or.jp

M. Ikawa, MD, PhD
Department of Neurology, Faculty of Medical Sciences, University of Fukui,
23-3 Shimoaizuki, Matsuoka, Eiheiji-Town, Fukui 910-1193, Japan

Molecular Imaging Branch, National Institute of Mental Health,
10 Center Drive, MSC-1026, Bldg. 10, Rm. B1D43, Bethesda, MD 20892-1026, USA
e-mail: iqw@u-fukui.ac.jp

H. Tada, MD, PhD
Department of Cardiovascular Medicine, Faculty of Medical Sciences, University of Fukui
23-3 Shimoaizuki, Matsuoka, Eiheiji, Fukui 910-1193, Japan
e-mail: htada@u-fukui.ac.jp

V.B. Patel et al. (eds.), *L-Arginine in Clinical Nutrition*, Nutrition and Health,
DOI 10.1007/978-3-319-26009-9_36

Abbreviations

MELAS	Mitochondrial myopathy, encephalopathy, lactic acidosis, and stroke-like episodes
mtDNA	Mitochondrial DNA
ATP	Adenosine triphosphate
LVH	Left ventricular hypertrophy
Arg	L-Arginine
NOx	Nitric oxide
SPECT	Single-photon emission computed tomography
^{99m}Tc-MIBI	Technetium 99 m methoxyisobutylisonitrile
^{123}I-BMIPP	Iodine-123-labeled 15-4-iodophenyl-3-(*R*,*S*)-methyl-pentadecanoic acid
PET	Positron emission tomography
TCA	Tricarboxylic acid
MBF	Myocardial blood flow

Introduction

It is well known that the most common morphology of cardiomyopathy is hypertrophy of the left ventricle. Practically, it is diagnosed as idiopathic hypertrophic cardiomyopathy, although occasionally it occurs secondary to systemic disease. The etiology of hypertrophic cardiomyopathy varies and can include ischemia, valve disease, inflammation, muscle dystrophy, toxemia, collagen disease, and metabolic diseases such as amyloidosis, Fabry's disease, and mitochondrial disease [1]. Accordingly, the treatment and prognosis of each individual disease differ, making a correct diagnosis important.

A recent epidemiological study has revealed that the prevalence or risk of developing mitochondrial DNA (mtDNA) disease is 12.48 per 100,000 individuals in the general population [2]. Moreover, pathogenic mtDNA mutations that can potentially cause disease are detected in at least one in 200 live births, indicating that mtDNA is not as rare a disease as once thought previously [3].

The human mitochondrial genome disorders discovered up to the present are cited in MITOMAP (URL: http://www.mitomap.org/), and more than 40 mutations of mtDNA or nuclear DNA associated with structural mitochondrial cardiomyopathy have been reported (Tables 36.1, 36.2, and 36.3). Mitochondrial myopathy, encephalopathy, lactic acidosis, and stroke-like episodes (MELAS) is the most common type of mitochondrial disease and is also related to familial cardiomyopathy, which is caused by an A-to-G transition at position 3243 (A3243G) in tRNA-Leu of the mtDNA [4, 5]. This mutation reduces the activity of NADH–ubiquinone oxidoreductase (complex I), leading to impairment of respiratory chain function with consequent reduction of adenosine triphosphate (ATP) production [6]. Furthermore, this mutant and wild-type mtDNA coexist in each individual cell (heteroplasmy), and the proportion of mutant mtDNA must exceed a certain fixed level in order to result

H. Okazawa, MD, PhD
Biomedical Imaging Research Center, University of Fukui
23-3 Shimoaizuki, Matsuoka, Eiheiji, Fukui 910-1193, Japan
e-mail: okazawa@u-fukui.ac.jp

M. Yoneda, MD, PhD (✉)
Faculty of Nursing and Social Welfare Sciences, Fukui Prefectural University,
4-1-1 Kenjojima, Matsuoka, Eiheiji, Fukui 910-1195, Japan
e-mail: myoneda@fpu.ac.jp

Table 36.1 mtDNA mutations in rRNA/tRNA regions causing cardiomyopathy

Position	Locus	Disease	Allele	RNA	Homoplasmy	Heteroplasmy
1391	MT-RNR1	HCM	T1391C	12S rRNA	+	–
1556	MT-RNR1	HCM	C1556T	12S rRNA	+	–
1644	MT-TV	HCM + MELAS	G1644A	tRNA Val	–	+
3242	MT-TL1	MM/HCM + renal tubular dysfunction	G3242A	tRNA-Leu (UUR)	+	+
3243	MT-TL1	DMDF/MIDD/SNHL/FSGS/ cardiac + multiorgan dysfunction	A3243G	tRNA-Leu (UUR)	–	+
3260	MT-TL1	MMC/MELAS	A3260G	tRNA-Leu (UUR)	–	+
3303	MT-TL1	MMC	C3303T	tRNA-Leu (UUR)	+	+
4269	MT-TI	FICP	A4269G	tRNA Ile	–	+
4295	MT-TI	MHCM/maternally inherited hypertension	A4295G	tRNA Ile	+	+
4316	MT-TI	HCM with hearing loss/poss. hypertension factor	A4316G	tRNA Ile	+	+
4317	MT-TI	FICP/poss. hypertension factor	A4317G	tRNA Ile	+	–
5545	MT-TW	HCM severe multisystem disorder	C5545T	tRNATrp	–	+
8296	MT-TK	DMDF/MERRF/HCM/epilepsy	A8296G	tRNA Lys	+	+
8348	MT-TK	Cardiomyopathy/SNHL/poss. hypertension factor	A8348G	tRNA Lys	+	+
8363	MT-TK	MICM+DEAF/MERRF/autism/ LS/ataxia + lipomas	G8363A	tRNA Lys	–	+
9997	MT-TG	MHCM	T9997C	tRNAGly	nd	+
12297	MT-TL2	Dilated cardiomyopathy/LS/ failure to thrive and LA	T12297C	tRNA-Leu (CUN)	+	+
12308	MT-TL2	CPEO/stroke/CM/breast and renal and prostate cancer risk/altered brain pH	A12308G	tRNA-Leu (CUN)	+	+
15923	MT-TT	Infantile CM	A15923G	tRNAThr	–	+
16032	MT-TP	Dilated cardiomyopathy	[a]	tRNA Pro	–	+

HCM hypertrophic cardiomyopathy, *MM* mitochondrial myopathy, *DMDF* diabetes mellitus + deafness, *MIDD* maternally inherited diabetes and deafness, *SNHL* sensorineural hearing loss, *FSGS* focal segmental glomerulosclerosis, *MMC* maternal myopathy and cardiomyopathy, *FICP* fatal infantile cardiomyopathy + a MELAS-associated cardiomyopathy, *MHCM* maternally inherited hypertrophic cardiomyopathy, *MERRF* myoclonic epilepsy and ragged-red muscle fibers, *MICM* maternally inherited cardiomyopathy, *DEAF* maternally inherited deafness or aminoglycoside-induced deafness, *LS* Leigh syndrome, *LA* lactic acidemia, *CPEO* chronic progressive external ophthalmoplegia, *CM* cardiomyopathy

[a]T16032TTCTCTGTTCTTTCAT (15 bp dup) (cited from MITOMAP and adapted to the text contents)

in clinically apparent respiratory chain failure [7, 8]. Thus, energy production differs from tissue to tissue and also among organs, markedly energy-dependent organs tending to be affected most significantly. The distinct clinical features of MELAS patients are systemic and include myopathy, lactic acidosis, stroke-like episodes, hearing loss, diabetes mellitus, gastrointestinal manifestations, renal failure, and cardiomyopathies [4, 7, 8].

Mitochondrial cardiomyopathy often results in concentric left ventricular hypertrophy (LVH), and the severity of the LVH correlates with the burden of mitochondrial disease (Fig. 36.1). The reasons for development of LVH have been investigated using knockout mice with a deficiency in the mitochondrial adenine nucleotide translocator [9]. Like MELAS patients, these experimental mice show

Table 36.2 mtDNA mutations in the coding/control genes causing cardiomyopathy

Position	Locus	Disease	Allele	Nucleotide change	Amino acid change	Homoplasmy	Heteroplasmy
3337	MT-ND1	Cardiomyopathy	G3337A	G-A	V-M	+	–
3395	MT-ND1	HCM with hearing loss	A3395G	A-G	Y-C	–	+
3397	MT-ND1	ADPD/possibly LVNC cardiomyopathy associated	A3397G	A-G	M-V	+	–
3407	MT-ND1	HCM/muscle involvement	G3407A	G-A	R-H	+	–
5001	MT-ND2	Developmental delay, seizure, cardiomyopathy, lactic acidosis	A5001AA	A-AA	Frameshift	–	+
8528	MT-ATP8/6	Infantile cardiomyopathy	T8528C	T-C	W-R (ATP); M(start)-T(ATP6)	+	+
8558	MT-ATP8/6	Possibly LVNC cardiomyopathy associated	C8558T	C-T	P-S(ATP8); A-V(ATP6)	+	–
9058	MT-ATP6	Possibly LVNC cardiomyopathy associated	A9058G	A-G	T-A	+	–
15498	MT-CYB	HCM/WPW, DEAF	G15498A	G-A	G-D	–	+
15693	MT-CYB	Possibly LVNC cardiomyopathy associated	T15693C	T-C	M-T	+	–

ADPD Alzheimer's disease and Parkinson's disease, *LVNC* left ventricular noncompaction, *WPW* Wolff–Parkinson–White syndrome (cited from MITOMAP and adapted to the text contents)

Table 36.3 Nuclear DNA mutations causing mitochondrial cardiomyopathy

Gene	Chromosome function	Chromosome	Inheritance	Clinical phenotype
Structural gene				
NDUFV2	FP fraction	18p11	AR	Cardiomyopathy, hypotonia, encephalopathy
Complex assembly				
NDUFAF1 (CIA30)	Assembly	15q13.3	AR	Cardioencephalopathy
SCO2	Copper transport	22q13	AR	Neonatal cardioencephalomyopathy
COX10	Heme A farnesyltransferase	17p12–p11.2	AR	Neonatal tubulopathy and encephalopathy, LS, cardiomyopathy
COX15	Heme A synthesis	10q24	AR	Early-onset hypertrophic cardiomyopathy
TMEM70	Assembly	8q21.11	AR	Neonatal encephalopathy, cardiomyopathy
Mitochondrial import				
DNAJC19	Protein import	3q26.3	AR	Cardiomyopathy, ataxia
Mt protein synthesis				
MRPS22	Mitochondrial translation	3q23	AR	Cardiomyopathy, tubulopathy
Iron homeostasis				
BOLA3	Iron–sulfur cluster biosynthesis	2p13.1	AR	Encephalomyopathy, cardiomyopathy
CoQ10 biosynthesis				
COQ9	CoQ10 deficiency	16q13	AR	Neonatal lactic acidosis, seizures, cardiomyopathy
Chaperon function				
G4.5 (tafazzin)	Cardiolipin defect	Xq28	X linked	Barth syndrome, X-linked dilated cardiomyopathy

FP flavin protein, *AR* autosomal recessive, *CoQ* coenzyme Q (cited from MITOMAP and adapted to the text contents)

Fig. 36.1 Representative photograph of hypertrophic cardiomyopathy of a patient with mitochondrial disease

ragged-red muscle fibers, lactic acidosis, and cardiac hypertrophy, suggesting that deficiency of ATP production plays an important role in these conditions. On the other hand, a rare form of dilated-type mitochondrial cardiomyopathy has also been reported [10, 11]. A subset of patients with LVH progress to the dilated phase, which resembles idiopathic hypertrophic cardiomyopathy [12], but in some cases dilated cardiomyopathy is already present in childhood [13]. This discrepancy has been explained using a transgenic mouse model of mtDNA mutations, in which increased production of mitochondrial reactive oxygen species during the aging process leads to initiation of apoptosis and plays a crucial role in the development of dilated cardiomyopathy [14].

The frequency of cardiomyopathy in patients with mitochondrial disease is reported to be 17–40 % and is one of the major causes of death in affected patients [15–17]. Unfortunately no effective therapies for cardiomyopathy have been found to date. Koga et al. reported that L-arginine (Arg) infusion during the acute phase of the stroke-like episodes in MELAS patients dramatically improved all of the stroke-like symptoms within 30 min [18]. Moreover, oral administration of L-Arg during the interictal phase significantly decreased the frequency and severity of stroke-like episodes in MELAS patients [19]. L-Arg therapy is therefore now a promising approach for controlling the stroke-like episode of MELAS. Here we further investigated the therapeutic effect of L-Arg infusion in patients with cardiomyopathy and the possible mechanisms responsible.

In Vivo Functional Imaging of Mitochondrial Cardiomyopathy

Although the histopathologic abnormalities of mitochondrial cardiomyopathy have been clearly revealed using autopsied and/or biopsied tissue samples, the pathogenesis of cardiomyopathy has been discussed largely on the basis of the experimental studies [9, 14, 20]. Here we evaluated energy states in the myocardium of patients with MELAS using in vivo functional imaging.

Evaluation of Mitochondrial Membrane Potential and the Anaerobic Pathway Using Single-Photon Emission Computed Tomography (SPECT)

Technetium 99 m methoxyisobutylisonitrile (^{99m}Tc-MIBI) is incorporated and retained in the mitochondria of myocardial cells, a process that depends on mitochondrial membrane potential [21]. This tracer is not retained in necrotic or irreversibly ischemic myocardium and therefore can be used for assessing myocardial perfusion and myocardial cell viability [22].

Iodine-123-labeled 15-4-iodophenyl-3-(*R*,*S*)-methyl-pentadecanoic acid (^{123}I-BMIPP) is converted to acyl-CoA, a common pathway of myocardial fatty acid metabolism, but is not metabolized via beta-oxidation, which reflects the enhanced triglyceride pool [23]. An increasing number of studies have reported that patients with idiopathic hypertrophic cardiomyopathy show reduced uptake of ^{123}I-BMIPP and that this is related to impairment of the plasma membrane of cardiac myocytes [24].

Using these two tracers, we recently reported that in MELAS patients, the ^{99m}Tc-MIBI washout rate (WOR) was increased, resulting in decreased uptake of ^{99m}Tc-MIBI (Fig. 36.2) [25]. In contrast, ^{123}I-BMIPP uptake increased according to the severity of left ventricular function (Fig. 36.2) [25]. These findings confirmed that respiratory chain failure leads to a continuous energy shift from the aerobic to the anaerobic (glycolytic) pathway, resulting in the lactic acidemia that is observed in MELAS patients. To ameliorate the over-reduction stress resulting from respiratory chain failure, reduction of dihydroxyacetone phosphate to glycerol-3-phosphate occurs in order to oxidize superfluous nicotinamide adenine dinucleotide [NADH] to [NAD$^+$], the excess glycerol-3-phosphate being utilized for synthesis of triglyceride. Accumulation of ^{123}I-BMIPP in MELAS patients was provoked by this enhanced triglyceride pool (Fig. 36.2) [25].

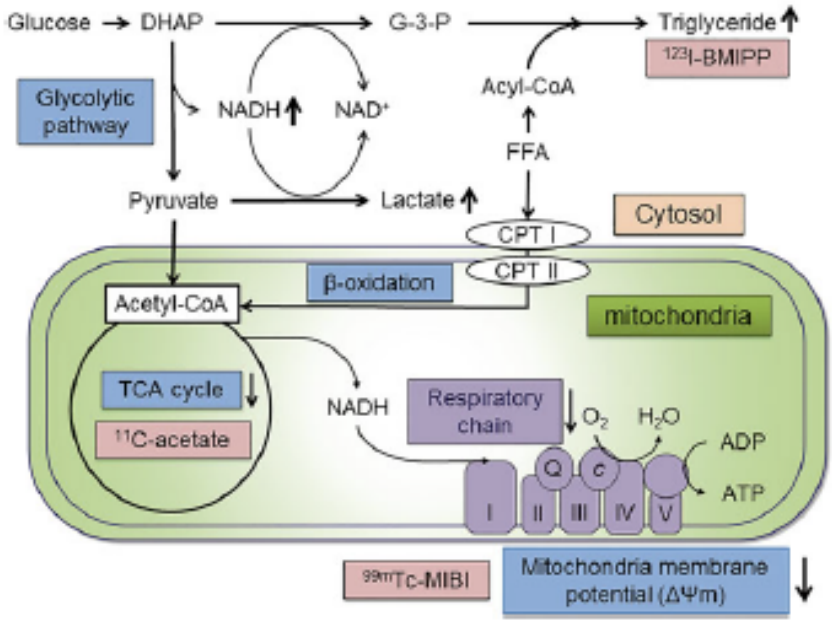

Fig. 36.2 Schematic illustration of energy production pathways in which functional imaging can be adapted. ^{99m}Tc-MIBI is incorporated and retained in the mitochondria depending on mitochondrial membrane potential created by the respiratory chain. ^{123}I-BMIPP is incorporated into the TG pool, associated with an excess of glycerol-3-phosphate (G-3-P), and is enhanced by increased glucose utilization. ^{11}C-acetate PET is responsible for the flux of TCA cycle. *CPT* carnitine palmitoyltransferase, *FFA* free fatty acid (cited from Ref. [25] with modifications)

Evaluation of TCA Cycle Kinetics Using Positron Emission Tomography (PET)

Radiolabeled ^{11}C-acetate kinetics demonstrated by PET are closely correlated with myocardial oxygen consumption [26, 27]. The acetate is known to be a substrate that can be utilized readily by the heart and is incorporated directly into the tricarboxylic acid (TCA) cycle after conversion to acetyl CoA. Therefore, ^{11}C-acetate can be used to measure the flux of the TCA cycle without being affected by conditions of energy production in the heart such as normoxemia, ischemia, and reperfusion, which advantages over other conventional tracers such as ^{18}F-deoxyglucose and ^{11}C-palmitate [28].

^{11}C-acetate PET also has the potential for detecting myocardial blood flow (MBF) using the early-phase (0–3 min after tracer injection) kinetics of ^{11}C-acetate [29]. Since the flux of the TCA cycle was measured using the delayed-phase (7–20 min after injection) kinetics of ^{11}C-acetate, these two parameters can be measured in exactly the same location in the heart.

Our SPECT study in MELAS patients with cardiomyopathy demonstrated a shift in energy production from the aerobic to the anaerobic pathway [25], although TCA cycle activity, which is of central importance in oxidative metabolism, was not fully evaluated. We therefore applied ^{11}C-acetate PET to MELAS patients and compared the findings with those in healthy controls [30]. The results revealed that TCA cycle activity tended to be lower in the patients than in the controls, thus confirming a shift of energy production to the anaerobic pathway according to impairment of electron transport and oxidative phosphorylation resulting from respiratory chain failure (Fig. 36.2) [25].

Effect of L-Arginine Administration on Mitochondrial Cardiomyopathy Evaluated by ^{11}C-Acetate PET

As described at the beginning of this chapter, L-Arg administration is now a promising therapy for the acute and interictal phase of the stroke-like episodes in MELAS patients [19]. One suggested mechanism is that L-Arg, which is a precursor of nitric oxide (NOx), may increase blood flow in the cerebral microcirculation and reduce ischemic damage to the brain. From the fact that the concentrations of L-Arg, citrulline, and NOx were low in the acute phase of the stroke-like episodes in MELAS patients, it seems plausible to supplement the amounts of these substances [19]. An improvement of endothelial function in MELAS patients was also observed after oral L-Arg supplementation, which would explain the long-term outcome [31]. As the impact of L-Arg administration on mitochondrial cardiomyopathy has not yet been reported, we recently evaluated the acute effect of L-Arg administration on cardiomyopathy using ^{11}C-acetate PET [30].

We performed ^{11}C-acetate PET before and after L-Arg infusion (0.5 g/kg, within 30 min) in six patients with clinically and genetically diagnosed MELAS. After L-Arg injection, TCA cycle activity (expressed as K_{mono}) of the entire heart did not increase significantly, although four of the six patients showed improvement after L-Arg administration. Due to heteroplasmy, mitochondrial dysfunction occurs in various tissues to varying degrees, a phenomenon known as "mosaicism of mitochondrial disease." Therefore, we further divided the heart into nine segments. TCA cycle activity was improved after L-Arg injection among six to eight segments in four responders, whereas it was five segments in two nonresponders. On the other hand, MBF increased in two patients, decreased in two patients, and remained the same in two patients after L-Arg infusion. To analyze the relationship between TCA cycle activity and MBF, we prepared a bull's-eye map of these two parameters before and after L-Arg injection. Figure 36.3 shows representative data for a MELAS patient who showed an increase of TCA cycle activity after L-Arg infusion. Surprisingly, the regions of improved TCA cycle activity did not correspond to the regions of increased MBF.

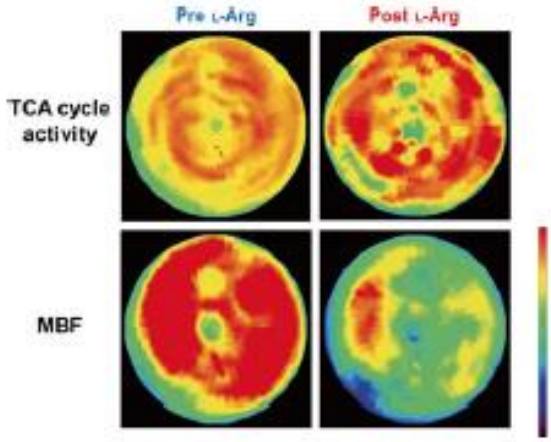

Fig. 36.3 Representative bull's-eye map of TCA cycle activity (*upper deck*) and myocardial blood flow (MBF; *lower deck*) before and after L-arginine administration in MELAS patients (cited from Ref. [30])

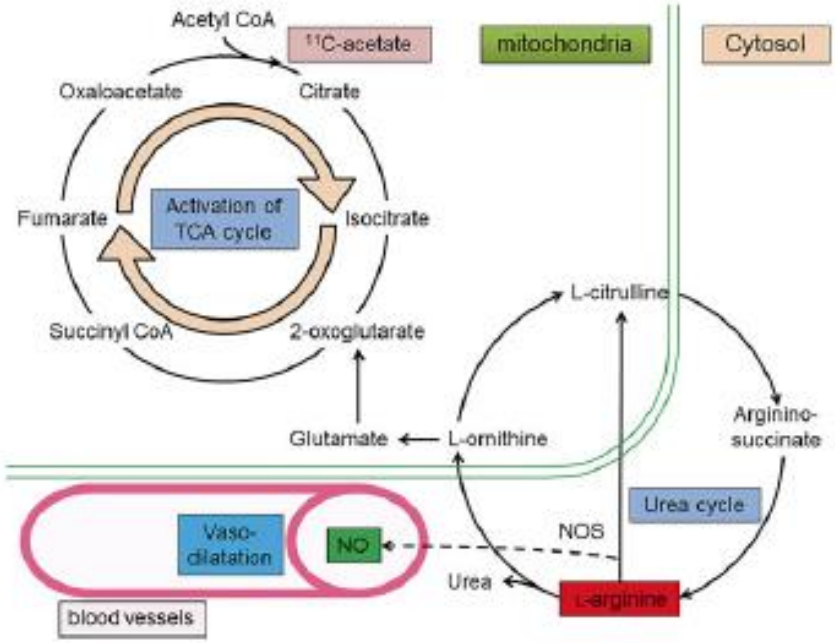

Fig. 36.4 Schematic illustration of L-Arg catabolism. Nitric oxide (NO) is synthesized from L-Arg catalyst of nitric oxide synthase (NOS). L-Arg has another potential to enter the TCA cycle by conversion to 2-oxoglutarate

L-Arg is a well-known precursor of NOx affected by endothelial nitric oxide synthase, a strong endogenous vasodilator [32, 33]. Accordingly, we expected that the regions of improved TCA cycle activity would match the regions of increased MBF, but no such relationship was observed. Although the reason for this remains obscure, Arg has a wide range of biological roles, such as a precursor for synthesis of urea, NOx, citrulline, ornithine, creatine, and agmatine. Furthermore, ornithine generates polyamine, proline, and particularly glutamate, which undergoes conversion to 2-oxoglutarate and enters the TCA cycle (Fig. 36.4). Therefore, an excess of 2-oxoglutarate in the TCA cycle induced by L-Arg injection could be responsible for acceleration of TCA cycle activity with little relevance to the coronary microcirculation.

The primary cause of the stroke-like episodes in MELAS patients remains uncertain but is thought to involve angiopathy, cytopathy, or both. Potential therapeutic effects of L-Arg for strokes are mainly thought to contribute to amelioration of angiopathy through its vasodilative effect and improvement of endothelial function. The logic of this approach is result from the loss of NOx in vascular endothelial and smooth muscle cells. However, the concentration of NOx was quite elevated in the interictal phase of stroke-like episodes [19]. Moreover, an in vitro experimental study has revealed that the synthesis of NOx was increased in cybrid cells carrying the A3243G mutation, which supports this condition [34]. Our study suggests that L-Arg enhances TCA cycle activity irrespective of vasodilation, which rescues the cytopathy (over-reduction stress) of MELAS patients. A recent study has also revealed that L-Arg improved the activity of complex I activity, a nonvascular system, in cybrid cells harboring A3243G mutation, thus strongly supporting our hypothesis regarding the metabolic effect of L-Arg [35].

Accordingly, our study has clearly demonstrated that L-Arg has dual pharmaceutical effects—vasodilatation (angiopathy) and acceleration of the TCA cycle (cytopathy)—which can be used as a treatment for patients with mitochondrial cardiomyopathy.

Conclusions

Mitochondrial cardiomyopathy is caused by respiratory chain failure due to mtDNA mutation, one of the key conditions that determine the prognosis of patients with mitochondrial disease. Functional imaging modalities such as SPECT and PET enable evaluation of in vivo energy production and the efficacy of treatment for patients with MELAS. It was clearly revealed that TCA cycle activity was markedly suppressed, resulting in a change in oxidative metabolism from an aerobic to an anaerobic state. L-Arg has the potential to enhance TCA cycle activity without being affected by any vasodilative effect, suggesting dual pharmaceutical effects that could be applied for treatment of mitochondrial cardiomyopathy.

Acknowledgments The research mentioned in this chapter was partially supported by Grants-in-Aid for Scientific Research on Innovative Areas from the Ministry of Education, Culture, Sports, Science and Technology of Japan to M.Y. (24111517); Grants-in-Aid for Research on Intractable Diseases (Mitochondrial Disorders) from the Ministry of Health, Labour and Welfare of Japan to M.Y.; and an intramural research fund (25-4-7) for cardiovascular diseases from the National Cerebral and Cardiovascular Center to H.T.

Conflict of Interest None.

References

1. Richardson P, Mckenna W, Bristow M, et al. Report of the 1995 World Health Organization/International society and federation of cardiology task force on the definition and classification of cardiomyopathies. Circulation. 1996;93:841–2.
2. Chinnery PF, Johnson MA, Wardell TM, et al. The epidemiology of pathogenic mitochondrial DNA mutations. Ann Neurol. 2000;48:188–93.
3. Elliott HR, Samuels DC, Eden JA, et al. Pathogenic mitochondrial DNA mutations are common in the general population. Am J Hum Genet. 2008;83:254–60.
4. Pavlakis SG, Phillips PC, DiMauro S, et al. Mitochondrial myopathy, encephalopathy, lactic acidosis, and stroke-like episodes: a distinctive clinical syndrome. Ann Neurol. 1984;16:481–8.
5. Förster C, Hübner G, Müller-Höcker J, et al. Mitochondrial angiopathy in a family with MELAS. Neuropediatrics. 1992;23:165–8.
6. Ichiki T, Tanaka M, Nishikimi M, et al. Deficiency of complex I and mitochondrial encephalomyopathy. Ann Neurol. 1988;23:287–94.

7. Holt IJ, Harding AE, Morgan-Hughes JA. Deletion of muscle mitochondrial DNA in patients with mitochondrial myopathies. Nature. 1988;331:717–9.
8. Schon EA, Bonilla E, DiMauro S. Mitochondrial DNA mutations and pathogenesis. J Bioenerg Biomembr. 1997;29:131–49.
9. Graham BH, Waymire KG, Cottrell B, et al. A mouse model for mitochondrial myopathy and cardiomyopathy resulting from a deficiency in the heart/muscle isoform of the adenine nucleotide translocator. Nat Genet. 1997;16:226–34.
10. Majamaa-Voltti K, Peuhkurinen K, Kortelainen ML, et al. Cardiac abnormalities in patients with mitochondrial DNA mutation 3243A>G. BMC Cardiovasc Disord. 2002;2:12.
11. Chinnery PF. Mitochondrial disorders overview. In: Pagon RA, Adam MP, Bird TD, et al., editors. GeneReviews™ [Internet]. Seattle, WA: University of Washington; 1993–2014
12. Ten Cate FJ, Roelandt J. Progression to left ventricular dilatation in patients with hypertrophic obstructive cardiomyopathy. Am Heart J. 1979;97:762–5.
13. Vilarinho L, Santorelli FM, Osas MJ, et al. The mitochondrial A3243G mutation presenting as severe cardiomyopathy. J Med Genet. 1997;34:607–9.
14. Wallace DC. Mitochondrial defects in cardiomyopathy and neuromuscular disease. Am Heart J. 2000;139:70–85.
15. Holmgren D, Wahlander H, Eriksson BO, et al. Cardiomyopathy in children with mitochondrial disease. Eur Heart J. 2003;24:280–8.
16. Scaglia F, Towbin JA, Craigen WJ, et al. Clinical spectrum, morbidity, and mortality in 113 pediatric patients with mitochondrial disease. Pediatrics. 2004;114:925–31.
17. Anan R, Nakagawa M, Miyata M, et al. Cardiac involvement in mitochondrial disease: a study on 17 patients with documented mitochondrial DNA defects. Circulation. 1995;91:955–61.
18. Koga Y, Akita Y, Nishioka J, et al. L-arginine improves the symptom of strokelike episodes in MELAS. Neurology. 2005;64:710–2.
19. Koga Y, Akita Y, Nishioka J, et al. MELAS and L-arginine therapy. Mitochondrion. 2007;7:133–9.
20. Ban S, Mori N, Saito K, et al. An autopsy case of mitochondrial encephalomyopathy (MELAS) with special reference to extra-neuromuscular abnormalities. Acta Pathol Jpn. 1992;42:818–25.
21. Carvalho PA, Chiu ML, Kronauge JF, et al. Subcellular distribution and analysis of technetium-99m-MIBI in isolated perfused rat hearts. J Nucl Med. 1992;33:1516–22.
22. Crane P, Laliberte R, Heminway S, et al. Effect of mitochondrial viability and metabolism on technetium-99m-sestamibi myocardial retention. Eur J Nucl Med. 1993;20:20–5.
23. Knapp Jr FF, Ambrose KR, Goodman MM. New radioiodinated methyl-branched fatty acids for cardiac studies. Eur Nucl Med. 1986;12:39–44.
24. Nakamura T, Suguhara H, Kinoshita N, et al. Serum carnitine concentrations in patients with idiopathic hypertrophic cardiomyopathy: relationship with impaired myocardial fatty acid metabolism. Clin Sci. 1999;97:493–501.
25. Ikawa M, Kawai Y, Arakawa K, et al. Evaluation of respiratory chain failure in mitochondrial cardiomyopathy by assessments of ^{99m}Tc-MIBI washout and ^{123}I-BMIPP/^{99m}Tc-MIBI mismatch. Mitochondrion. 2007;7:164–70.
26. Klein LJ, Visser FC, Knaapen P, et al. Carbon-11 acetate as a tracer of myocardial oxygen consumption. Eur J Nucl Med. 2001;28:651–68.
27. Buxton DB, Nienaber CA, Luxen A, et al. Noninvasive quantitation of regional myocardial oxygen consumption in vivo with [1-^{11}C]acetate and dynamic positron emission tomography. Circulation. 1989;79:134–42.
28. Brown M, Marshall DR, Sobel BE, et al. Delineation of myocardial oxygen utilization with carbon-11-labeled acetate. Circulation. 1987;76:687–96.
29. Kudo T, Hata T, Kagawa S, et al. Simple quantification of myocardial perfusion by pixel-by-pixel graphical analysis using carbon-11 acetate and nitrogen-13 ammonia. Nucl Med Commun. 2008;29:679–85.
30. Arakawa K, Kudo T, Ikawa M, et al. Abnormal myocardial energy-production state in mitochondrial cardiomyopathy and acute response to L-arginine infusion. Circ J. 2010;74:2702–11.
31. Koga Y, Akita Y, Junko N, et al. Endothelial dysfunction in MELAS improved by L-arginine supplementation. Neurology. 2006;6:1766–9.
32. Cooke JP, Andon NA, Girerd XJ, et al. L-Arginine restores cholinergic relaxation of hypercholesterolemic rabbit thoracic aorta. Circulation. 1991;83:1118–20.
33. Tsao PS, McEvoy LM, Drexler H, et al. Enhanced endothelial adhesiveness in hypercholesterolemia is attenuated by L-arginine. Circulation. 1994;89:2176–82.
34. Gamba J, Gamba LT, Rodrigues GS, et al. Nitric oxide synthesis is increased in cybrid cell with m.3243A>G mutation. Int J Mol Sci. 2013;14:394–410.
35. Desquiret-Dumas V, Gueguen N, Barth M, et al. Metabolically induced heteroplasmy shifting and L-arginine treatment reduce the energetic defect in a neuronal-like model of MELAS. Biochim Biophys Acta. 2012; 1822:1019–29.

ミトコンドリア病に対する医療体制の現状と課題

Current status of medical care system for mitochondrial diseases

Key Word　ミトコンドリア病，指定難病，診断システム

後藤雄一
Yu-ichi Goto
国立精神・神経医療研究センター メディカル・ゲノムセンター センター長

ミトコンドリア病の医療は正確な診断に基づいた特異的な治療を行うことが理想である．しかし，ミトコンドリア病は“多様性”という特徴があるがゆえに，正確な診断のためには疾患(検査)専門家の関与が必須であり，集約的な診断システムを構築して対応している．また，臨床症状が多臓器に及ぶため，担当医師団がチームとして活動することが多く，そのコーディネート役として小児科医と神経内科医の役割が重要である．最近は新しい薬剤の臨床試験がはじまっており，日頃患者をみる難病基幹病院とともに，疾患専門家のいる難病専門診断治療センターや臨床試験実施にかかわる病院ネットワークが重要になる．

ミトコンドリア病の特徴はミトコンドリア自体がもつ多機能が反映したものであり，それはDNA，ミトコンドリア，細胞，組織・臓器などの各解剖学的レベルの特徴と相まって，複雑な“多様性”を形づくっている．臨床的には，いかなる臨床症状，いかなる発症年齢，いかなる臨床経過，いかなる遺伝形式としても認められ，患者はどの診療科にもかかる可能性がある．中枢神経症状を呈することが多いので，子どもでは小児科，成人では神経内科を受診することが普通である．しかし，糖尿病，難聴，視力低下など，小児科・神経内科以外の診療科を訪れる患者もいる．ミトコンドリア病を担当医が認識していないために，長い間診断が定まらない患者がいることも事実であり，“隠れミトコンドリア病”患者が数多く存在している可能性がある．確定診断に至らない場合は原因不明の疾患として経過をみられており，対応可能な症状に対する加療(対症療法)がなされているのみと推測される．

適切な医療の出発点は正確に診断することである．その意味でミトコンドリア病を診断することはきわめて重要なことでありながら，その診断には専門的な検査技術と経験・知識を必要とする．その点を最初に論じたい．

ついで，確定診断がついた患者に対してどのように対応するかであるが，これには対症療法と根治治療があり，実はDNA，ミトコンドリア，細胞，組織・臓器などの各解剖学的レベルに応じた対応策の候補が出てきている．本特集の他稿で，ミトコンドリアターゲティング，薬物治療(臨床試験)，生殖補助医療などの解説がされている．本稿では，ミトコンドリア病に対する医療を実践するために，社会資源や難病政策全体の方向性との関係について述べる．

❖ミトコンドリア病の診断とその体制

ミトコンドリア病の診断にはミトコンドリアの変化を多次元でとらえる必要があり，遺伝子検査，病理検査，生化学検査の3つが必要である．それらはそれぞれ，①DNAレベル，②ミトコンドリア・細胞レベル，③細胞・組織レベルのミトコンドリア変化をとらえる手段であるからである(図1)．

遺伝子検査は病因を決定するにはもっとも決定的な所見を提供する．その遺伝子変異が実際に病気を発症させているかどうかを確かめることが確

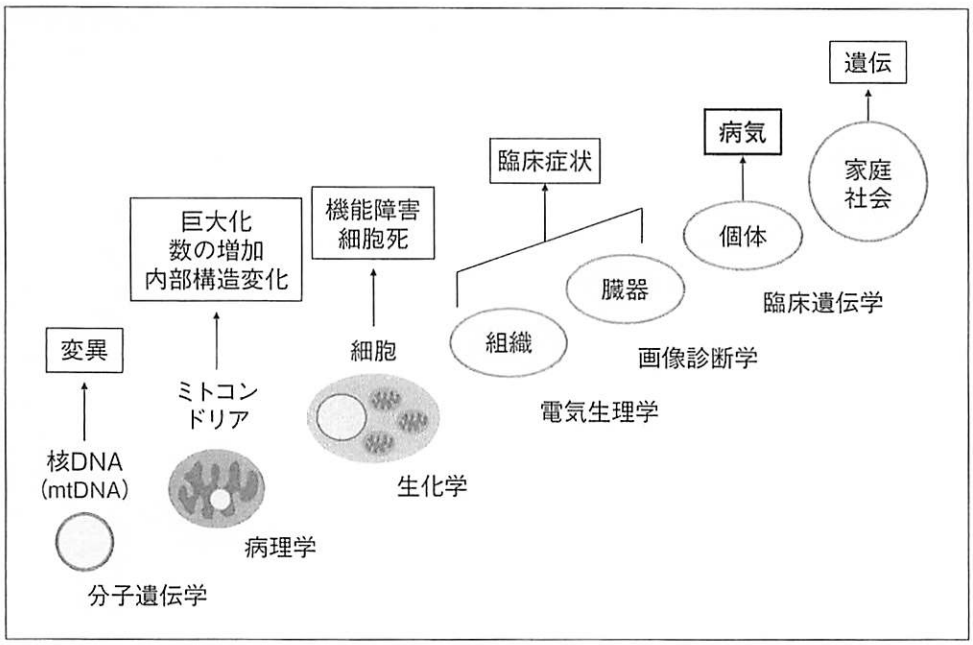

図 1　ミトコンドリア変化のレベルとアプローチ方法

ミトコンドリア変化はDNA，ミトコンドリア，細胞，組織，臟器，個体レベルで認められる．それぞれの解剖学的レベルに応じて，変化をとらえることができるが，そのためには種々のアプローチの方法を駆使することが必要になる．とくに細胞以下のレベルは確定診断に必須であり，分子遺伝学，病理学，生化学は検査の基本になる．

定診断であり，病理や生化学でのミトコンドリア変化の確認が診断の精度を高めることになる．

なぜ単独の検査で確定診断することを避けるべきかという点を解説しておきたい．たとえば，遺伝子検査で病因の候補となる変異が同定された場合，すでに病因として報告されていれば文献的にエビデンスがあるということになるが，その報告の内容が問題であり，当該遺伝子変異の機能解析がきちんとされていればよいが，曖昧な報告の場合はエビデンスとなりえないこともある．この点を考慮して，OMIM(Online Mendelian Inheritance in Man)やClinGen(Clinical Genome Resource)，MITOMAPなどの数多くの遺伝子変異データベースが公開されており，HGMD(Human Genome Mutation Database)のように市販されているものもある．ただし，それを参照したとしても病因と確定できないことは多々あり，その際には個々の遺伝子変異に対応した機能解析が必要になる．その機能解析は研究者の視点での取組みが必要であり，データベースを調べれば問題が解決することにはならないことを十分理解してデータベースを使用することが肝要である．不十分な証拠でミトコンドリア病と診断して不要なビタミン剤などを投与することは医療的に問題になる．

本特集・著者らの「ミトコンドリア病の病因研究の現状」の稿でも述べたように，ミトコンドリアDNA検査の特徴として，血液では変異を見出せずに，罹患している箇所(とくに骨格筋)で変異が同定できる場合や，別の要因で骨格筋病変が生じた結果，多種類のミトコンドリアDNA欠失が認められる場合(封入体筋炎など)がある．そもそもNGSを用いた遺伝子検査をしても，ミトコンドリアDNAや核DNA上に変異がきちんと同定できないことも多い．すなわち，遺伝子検査でも得られた結果が一次的か二次的かを判断する必要がある．

同様に，病理検査においてミトコンドリア変化の代表とされる赤色ぼろ線維(ragged-red fiber：RRF)やシトクローム酸化酵素欠損線維も小児皮膚筋炎や高齢者の筋では非特異的に出現することがある．さらに生化学検査では，もっとも頻度の高いシトクローム酸化酵素活性低下は寝たきりの患者や麻痺のある患者(不動症)でも認めることがある．すなわち，どのような状態で採取した試料でどのように検査したか，検査値に影響する要因

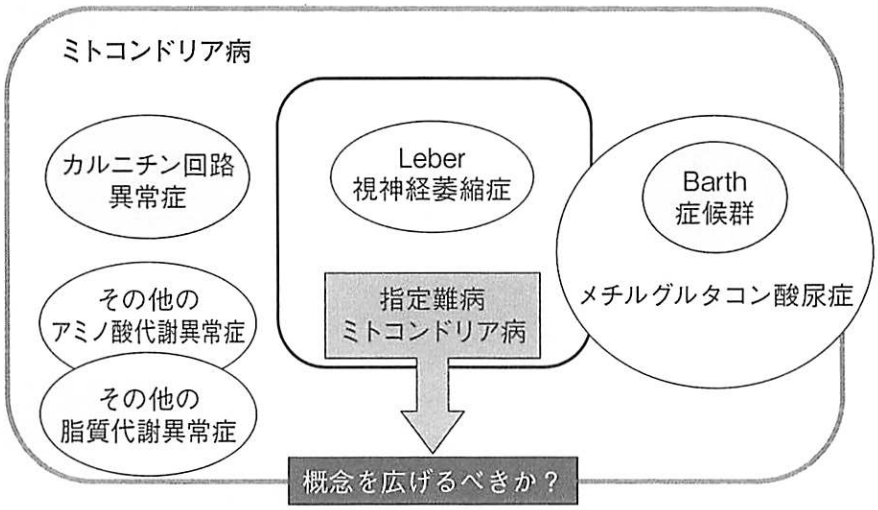

図 2　指定難病ミトコンドリア病の概念

中央に現行の指定難病ミトコンドリア病があるが，その中に別の指定難病であるLeber病が含まれている．また，平成29年度(2017)にカルニチン回路異常症やほかの謝酵素異常症があらたに指定難病に指定されようとしている．臨床病名と生化学的病名の合理的な共存が必要であるが，ただちにすっきりしたものになることは難しいであろう．

がないかを把握して，その結果の解釈を行うことが必要である．

したがって，遺伝子検査，病理検査，生化学検査のそれぞれに専門的な知識や経験が必須であり，さらに，得られた結果を検証できる(研究的)体制も必要である．その意味で希少疾患であればあるほど，検査を行う施設や人(専門家)を確保して集約化した診断体制を敷くべきである．ミトコンドリア病についてはミトコンドリア学会HPにそれらの検査を引き受ける施設が一覧表で示されている(http://j-mit.org/160330kensaihiran.pdf)．

❖指定難病としてのミトコンドリア病の診断

平成27年(2015)に制定された，通称“難病法”によって，それまで54疾患に絞られていた特定疾患が110疾患に拡大され，“指定難病”と名称が変わった．ミトコンドリア病はすでに特定疾患として認められていたが，指定難病になる時点でその診断基準を改定した(**表1**)．また，指定難病では重症度判定が必須であり，中等度以上の重症度の患者には医療費援助が行われることから，その分類表を作成した．

難病や指定難病の規定が明確化され，数千といわれる難病に対して指定難病にすべき疾患を慎重に検討しながら，厚労省は対象疾患を増加させている．平成28年(2016)現在は306疾患であるが，平成29年度(2017)からはさらに24疾患が追加される予定である．さきに述べたように，これら330疾患のひとつがミトコンドリア病であるが，ミトコンドリア病の一病型と考えられるレーベル遺伝性視神経症(Leber hereditary optic atrophy：LHON)が別の疾患として含まれたり，ミトコンドリア内の酵素欠損症であってミトコンドリア機能障害が本態である病気が今後含まれる予定であり，かならずしもすっきりした分類にはなっていない(**図2**)．

とはいうものの，患者やその家族のために正確な診断を得て医療費援助が受けられるように制度設計することがもっとも重要であり，日本ミトコンドリア学会などの研究者コミュニティーはその事業に積極的にかかわっている．また，小児慢性特定疾患事業と指定難病事業が連動し，小児患者が成人に達した際にシームレスに移行できる体制も必要になる．

❖ミトコンドリア病の治療体制と今後の方向性

ミトコンドリア病の特徴は臨床的多様性であり，患者はいろいろな診療科を初診するばかりでなく，多臓器の症状を有することから，同時に多くの診療科で診てもらうことが多い．その場合は

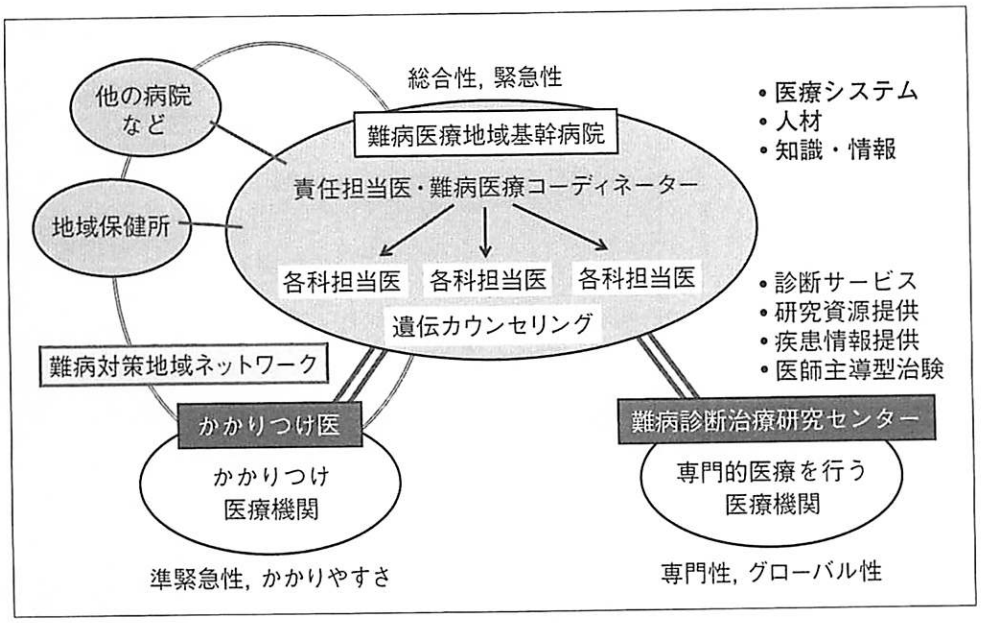

図 3　ミトコンドリア医療の全体像と将来

ミトコンドリア病は希少疾患であり，難病である．患者を診てゆくには，難病医療に共通する医療システムと人材，知識・情報共有が必要である．中央には，ミトコンドリア病患者を日頃診る難病医療地域基幹病院(総合病院)があり，多臓器に及ぶミトコンドリア病に対応する必要がある．同時に，家の近くのかかりつけ医や医療機関，一方であらたな治療法の開発に関係する専門性の高い難病診断治療研究センターが必要である．

多科が併設されている総合病院での診療が適している．また，臓器別診療の弊害がでないように全人的に診るコーディネーター機能が必要になる．その役割を担うのは多くの場合，小児患者ならば小児科医，成人患者ならば神経内科であろうと推察できるが，中枢神経症状のない成人ミトコンドリア病患者の場合は主要な症状を診ている担当医がその任にあたることが望ましい．

また，感冒などの軽症の合併症は家の近くで診てもらうこともあり，保健所機能を最大限活かす難病対策地域ネットワークが動くと有用であろう．また，最新の疾患情報を得たり，臨床試験を考慮したり，また通常の診療経過について定期的に疾患専門家からアドバイスを受ける機会を得るために，ミトコンドリア病の難病診断治療研究センター施設にかかることも必要である(**図 3**)．

とくに，疾患情報の取得や臨床試験をどのように進めていくかを考えると，専門性の高い病院群を用意する，あるいはネットワークを形成することが今後は必須であり，ミトコンドリア病研究班の大きな課題のひとつである．

URL

1) 難病情報センター：ミトコンドリア病．(http://www.nanbyou.or.jp/entry/194)
2) OMIM：http://www.omim.org
3) ClinGen：https://www.clinicalgenome.org
4) MITOMAP：http://www.mitomap.org/MITOMAP

*　　*　　*

ミトコンドリア病の病因研究の現状

Current status of research on etiology of mitochondrial diseases

Key Word　次世代シークエンサー(NGS)，データシェアリング，ミトコンドリアDNA変異

後藤雄一
Yu-ichi Goto
国立精神・神経医療研究センター メディカル・ゲノムセンター センター長

ミトコンドリア病の病因は多様であり，ミトコンドリアDNAと核DNA上の遺伝子群の変異がある．近年の次世代シークエンサー(NGS)の応用により網羅的な解析が格段と進んでおり，両者のDNA解析ともにNGSが主体になりつつある．一方で，複雑なミトコンドリア機能の解析には患者由来の組織や細胞が必要であり，それらを収集して基礎研究者とともに病因・病態研究を進めていくことが重要である．わが国のミトコンドリア病研究は臨床医と基礎研究者が連携して行う体制ができており，今後の成果が期待できる．

ミトコンドリア病はミトコンドリア機能が低下することによる病気の総称である．ミトコンドリアには1,500以上の分子が存在するので，その定義にすると膨大な数の疾患が含まれることになる．そのため，現在は便宜的に，ミトコンドリアのエネルギー代謝にかかわる機能障害によって起こる病気を総称することにしている．しかし，次世代シークエンサー(next generation sequencer：NGS)による解析の進展で，新しい原因遺伝子がつぎつぎと報告されている．

ミトコンドリアにおけるエネルギー産生に関連する分子は，エネルギー代謝経路に直接かかわる酵素群以外に，ミトコンドリア自体の生合成，オートファジー機構を含む形態維持に関する分子，ミトコンドリアDNAの複製や発現にかかわる分子，ミトコンドリアへの輸送にかかわる分子など，実にさまざまな機能分子の変化が病気の原因になりうる．したがって，ミトコンドリア病をエネルギー代謝にかかわる分子の変化に限定してみても，どこまでがエネルギー代謝かという点で明確な線が引きにくい．そういう意味で，最近の病因遺伝子発見のラッシュはミトコンドリア病の概念に少なからず影響を与えている．

ミトコンドリア病の原因となるのは，ミトコンドリアDNA変異と核DNA上の遺伝子群である(**図1**)．本稿では，近年精力的に行われているミトコンドリア病の病因解析の現況と動向を，ミトコンドリアDNAと核DNAに分けて解説する．

❖ミトコンドリアDNA検査の現状

ミトコンドリアDNAの特徴は，①細胞内に多数のコピーが存在すること(マルチコピー)，②核DNA上にミトコンドリアDNA類似の配列が多数存在していること，③細胞ごとに変異の有無や変異の比率が違うこと，など核DNAとは異なる性質がある点である．

現在一般的に行われているミトコンドリアDNA検査の流れを**図2**に示す．まず，核DNA上のミトコンドリアDNA類似配列を除外するために，ミトコンドリアDNAを一組あるいは二組のプライマーセットでPCR増幅をしている．核DNA上の配列を除外するという目的ではあるが，逆にこれを行うことで間違った塩基が取り込まれるリスクも一定の確率であることになる．したがって，核分画とミトコンドリア分画を最初に分けてからDNA分離を行う方法もあり，その点を考慮したDNA分離キットも市販されている．しかし，ミトコンドリアDNA欠乏(枯渇)を調べる

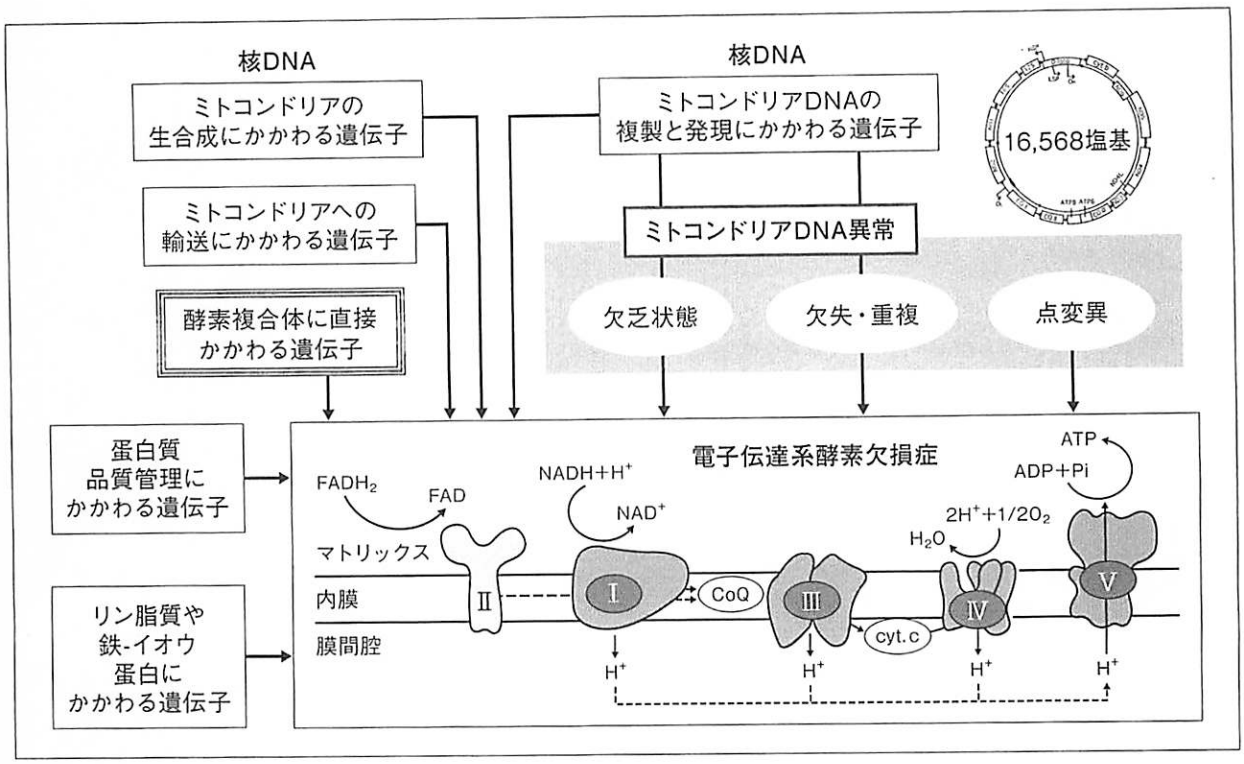

図 1　ミトコンドリア病の病因

ミトコンドリア病の病因は多彩である(表 1 も参照のこと)．核 DNA 上の原因遺伝子は優に 200 個を超えている．ミトコンドリア DNA の質的変化は欠失・重複などの構造変化と点変異であるが，マルチコピーであるミトコンドリア DNA は細胞内で，野生型と変異型が混在している場合(ヘテロプラスミー)，ほぼすべてが変異型の場合(ホモプラスミー)がある．単にミトコンドリア DNA コピー数が減少する欠乏(枯渇)状態でも病気になる．

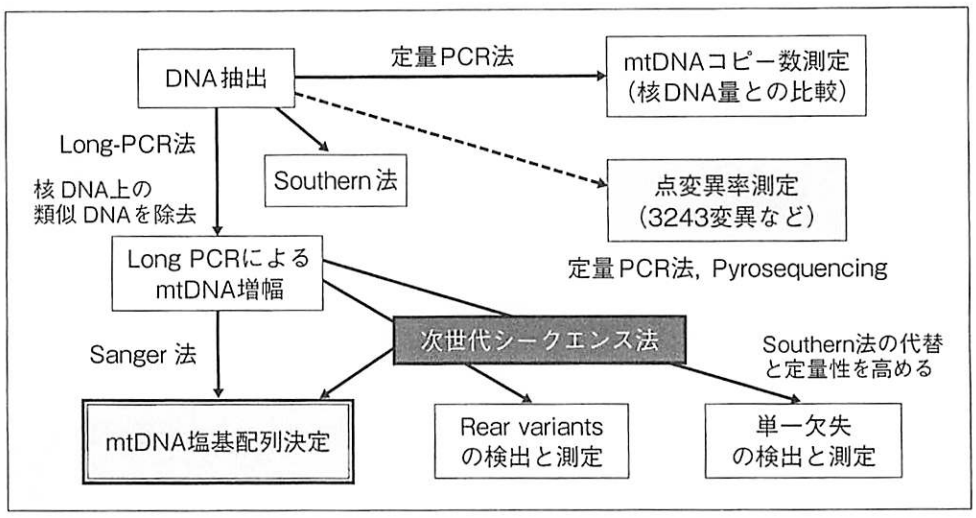

図 2　ミトコンドリアDNA解析の流れ

ミトコンドリア DNA は通常，核 DNA と一緒に抽出する(本文参照)．定量 PCR 法で核 DNA との相対比率でコピー数を推定する．頻度の高い変異は最初から定量 PCR やパイロシークエンスなどで変異の存在と変異率を計測する．通常の全周シークエンスは Sanger 法で行うが，解析前に核 DNA 上のミトコンドリア類似配列を除外するために long PCR を行う．次世代シークエンスは，まれなバリアントや単一欠失の検出とその比率を調べることができる点で優れている．

ためにはミトコンドリア DNA 量の検査が必要であり，その場合に核 DNA に対する相対的なミトコンドリア DNA 量を調べるために，核 DNA とミトコンドリア DNA を一緒に分離する方法が一般的である．

以前は病型に応じて頻度の高い点変異を調べる方法がよく行われてきたが，変異と病型との関係が緩く，病的点変異や欠失が存在すれば病型が一

表 1　核DNA上のおもな原因遺伝子とその機能[2)]

機能	原因遺伝子
1) リン脂質代謝	*AGK*, *SERAC1*, *TAZ*
2) 中毒分子の代謝	*HIBCH*, *ECHS1*, *ETHE1*, *MPV17*
3) 二硫化物代謝	*GFER*
4) 鉄-イオウ蛋白合成系	*ISCU*, *BOLA3*, *NFU1*, *IBA57*
5) 転移 RNA 修飾	*MTO1*, *GTP3BP*, *TRMU*, *PUS1*, *MTFMT*, *TRIT1*, *TRNT1*, *TRMT5*
6) アミノアシル転移 RNA 合成酵素	*AARS2*, *DARS2*, *EARS2*, *RARS2*, *YARS2*, *FARS2*, *HARS2*, *LARS2*, *VARS2*, *TARS2*, *IARS2*, *CARS2*, *PARS2*, *NARS2*, *KARS*, *GARS*, *SARS2*, *MARS2*
7) 転写調整因子	*C12orf65*
8) 転写伸長因子	*TUFM*, *TSFM*, *GFM1*
9) ミトコンドリアリボソーム蛋白	*MRPS16*, *MRPS22*, *MRPL3*, *MRP12*, *MRPL44*
10) mRNA プロセシング因子	*LRPPRC*, *TACO1*, *ELAC2*, *PNPT1*, *HSD17B10*, *MTPAP*, *PTCD1*
11) ミトコンドリア融合および分離因子	*OPA1*, *MFN2*
12) dNTP 合成系	*DGUOK*, *TK2*, *TYMP*, *MGME1*, *SUCLG1*, *SUCLA2*, *RNASEH1*, *C10orf2*, *POLG*, *POLG2*, *DNA2*, *RRM2B*
13) チアミンとリン酸の可溶性運搬体	*SLC19A3*, *SLC25A3*, *SLC25A19*
14) 呼吸鎖酵素系酵素サブユニット	・Complex Ⅰ：*NDUFS1*, *NDUFS2*, *NDUFS3*, *NDUFS4*, *NDUFS6*, *NDUFS7*, *NDUFS8*, *NDUFV1*, *NDUFV2*, *NDUFA1*, *NDUFA2*, *NDUFA9*, *NDUFA10*, *NDUFA11*, *NDUFA12*, *NDUFA13*, *NDUFAF2*, *NDUFAF6*, *NDUFB11* ・Complex Ⅱ：*SDHA*, *SDHB*, *SDHC*, *SDHD*, *SDHAF1* ・Complex Ⅲ：*UQCRB*, *BCS1L*, *UQCRQ*, *UQCRC2*, *CYC1*, *TTC19*, *LYRM7*, *UQCC2*, *UQCC3* ・Complex Ⅳ：*COA5*, *SURF1*, *COX10*, *COX14*, *COX15*, *COX20*, *COX6B1*, *FASTKD2*, *SCO1*, *SCO2*, *LRPPRC*, *TACO1*, *PET100* ・Complex Ⅴ：*ATPAF2*, *TMEM70*, *ATP5E*, *ATP5A1* ・Coenzyme Q10 deficiency：*PDSS1*, *PDSS2*, *COQ2*, *COQ4*, *COQ6*, *COQ8A*, *COQ8B*, *COQ9*(secondary defects：*ETFDH*, *APTX*)
15) 蛋白質品質管理システム	*FBXL4*, *AFG3L2*, *SPG7*
16) ATP, ADP 運搬体	*ANT1*

義的に定まるものではないため，ミトコンドリアDNA全体のシークエンスを行うことが一般的である．通常サンガー法で行っているが，変異率が低い(約10%)場合は同定が困難になる．正確な変異率を得るためには，定量PCRやパイロシークエンス法など他の方法を追加する必要がある．また，Sanger法は単一欠失例の欠失断点をとらえることもできる利点がある．欠失・重複についてはPCR法とともに，Southern法での量的評価が必要である．

上記のようなミトコンドリアDNA検査方法が，NGSを中核とする検査方法へと大きく変化してきているのが現状である．その理由は，①ミトコンドリアDNAの場合，点変異や欠失などの質的変化とともに量的変化，すなわちヘテロプラスミー(一細胞内に野生型と変異型が混在)の程度を，NGSのリード回数(デプス)を増加させることで推定できる，②単一欠失も，デプスが極端に低下する領域に欠失断点があることで欠失領域を推定できる，からである．

しかし，血液ではミトコンドリアDNA変異が同定できず，罹患臓器を用いて行うことが必要である．たとえば，ミトコンドリアDNAの多重欠失は血液では通常検出できず，罹患臓器である骨格筋でのみ確認できることが多い．また，筋生検時の不適切な検体処理や保存方法などによってミトコンドリアDNAが分断化し，正確な結果が得られない場合のあること，またわずかな量の欠失DNAは細胞の老化現象の結果として出現することもあり，その意義を解釈する際に病因的と確定

できないこともある．適切な試料採取・保存，適切な検査，適切な解釈が重要である．

ミトコンドリアDNA変異の情報については，MITOMAPが以前から共通データベースとして活用されている[1]．

❖核DNA上の原因遺伝子の解析

NGSを用いた解析が進展し，核DNA上に存在する原因遺伝子は増加の一途をたどっている．NGSを用いた遺伝子解析を行うとしても，①パネルを用いる方法．②エクソーム解析データのなかで興味ある遺伝子群の結果のみを解析する方法，が有力である．これらの方法では調べる遺伝子が限定されるので，別の疾患の原因遺伝子変異がみつかったりする二次的所見を生じることがない．しかし，NGSでみつかった変異は現在のところはSanger法で確認することが望ましく，NGSだけで検査が完結するわけではない．

みつかった遺伝子変異が病的意味のあるものかどうかの判定が，遺伝子解析のもっとも重要なステップである．得られたデータをほかの症例の遺伝子変異や多型データと比較検討することが有力な方法であり，そのためにできるだけ多くの症例データを共有する努力が必要である．欧米の同様な動きと歩調を合わせて，わが国でも大規模なデータ集積と共有化(データシェアリング)の研究事業が開始されることになっている．

核DNA上の原因遺伝子はすでに200種類以上になっている．それらの遺伝子の機能はエネルギー代謝に直接かかわるもの，ミトコンドリアDNAの複製と発現にかかわるものなど多彩である[2](**表1**)．細胞レベルのレスキュー実験などで病因としての役割は確定したもの，病態の詳細が明らかになっていない原因遺伝子も多数存在する．

また，ミトコンドリア病のなかで比較的均一の病型として定義されているLeigh脳症とその類縁疾患においては，関連する遺伝子は2016年に出版された論文で75種類以上とされた[3]．そのなかの10～20%はミトコンドリアDNAの変異であり，代表的なATPase6領域の変異を含む13個の変異がかかわっている．結果として，Leigh脳症とその類縁疾患患者の80～90%は核DNA上の遺伝子変異をもち，その種類は62種類以上になっており，さらに今後も増加していくことになるであろう．

❖今後の方向性

ミトコンドリアが関与する病態の広がりは想像以上に大きい．アメリカではじめられ，いまや日本を含め欧米各国がはじめている未診断患者のゲノム解析研究(undiagnosed disease program)によって，あらたに原因として明らかになる症例のなかにミトコンドリア関連の遺伝子がみつかることはよく知られている．従来のミトコンドリア病でみられた表現型とは異なる症例であっても，実はミトコンドリア機能異常がその本態であるということが見出される可能性がある．

ゲノム解析は血液が主体になることは避けられないとしても，得られたゲノム変異がもたらす機能変化はかならずしも血液では十分な検索対象にはならないことが多い．そのために，患者由来の組織がきわめて貴重であり，バイオリソースの重要性が理解できる．とくにミトコンドリア病ではあらゆる細胞・組織に影響を及ぼす可能性があることから，容易に取得できない脳や心臓の組織に近い性質をもつ研究材料が有用になる．患者培養細胞やそれに由来するiPS細胞は新規原因遺伝子の病因性確認とともに，病態を理解するには格好の材料になりうる．

しかし，病因性の最終確認は機能解析であり，ミトコンドリア機能に関しての多様な解析手段が必須になる．患者由来の細胞や組織，iPS細胞などの研究材料を得て多様な解析を行うことが重要である．その意味で，ミトコンドリアに関連する研究を行っている基礎研究者の関与が必須である．わが国では以前から“ミトコンドリア研究”は盛んであり，優れた基礎研究者が画期的な成果をあげており，その伝統と人脈を駆使してさらなるミトコンドリア病研究の進展が期待できる．

文献/URL

1) MITOMAP：http://www.mitomap.org/MITOMAP
2) Gorman, G. S. et al.：*Nat. Rev. Dis. Primers*, **2**：1-22, 2016.
3) Lake, N. J. et al.：*Ann. Neurol.*, **79**：190-203, 2016.

呼吸鎖複合体Ⅰアセンブリー機構とミトコンドリア病

Understanding mitochondrial complex I assembly in human mitochondrial disorders

Key Word　ミトコンドリア呼吸鎖複合体Ⅰ，ミトコンドリア病，アセンブリーファクター

三牧正和
Masakazu MIMAKI
帝京大学医学部小児科

ミトコンドリア呼吸鎖複合体Ⅰは，電子伝達系の最初の役割を担う，呼吸鎖のなかで最大の複合体である．哺乳類においては，ミトコンドリアDNAにコードされた7種のサブユニットと，37種にも及ぶ核にコードされたサブユニットから構成され，その分子量は980 kDaにも及ぶ．機能を発揮する成熟した複合体を形成するには44種類ものサブユニットを組み立てるための複雑なプロセス(アセンブリー機構)が必要となる．複合体Ⅰ欠損症はミトコンドリア病の原因としてもっとも多く，遺伝子診断に至っていない例も多いが，近年，アセンブリー機構の破綻を原因とする患者報告があいついでいる．また，これらの患者細胞の解析やプロテオミクスの応用などによりアセンブリー機構に必須の蛋白(アセンブリーファクター)が数多く見出されている．複合体Ⅰのアセンブリープロセスは複雑で解析が困難であるが，その解明がミトコンドリア呼吸鎖異常症の病因診断，そして分子病態に基づいた治療法開発をもたらすことを期待する．

ミトコンドリアにおいてエネルギー(ATP)を合成する機能の中核を担うのが蛋白の集合体である呼吸鎖複合体であり，その異常は，エネルギー産生低下，ひいては細胞機能障害に直結し，ヒトにおいてはさまざまな臓器障害を伴うミトコンドリア病の原因となる．

近年，呼吸鎖異常の原因として，その構成蛋白(サブユニット)の欠損のみならず，呼吸鎖の集合にかかわる因子の異常がつぎつぎに見出されている．

本稿では，ミトコンドリア病患者でもっとも多く異常が見出される呼吸鎖複合体Ⅰに焦点をあて，この巨大複合体の形成過程についてバイオジェネシスにかかわる因子に触れつつ解説する．

❖呼吸鎖複合体Ⅰの構造と機能

ミトコンドリア呼吸鎖はミトコンドリア内膜に存在する複合体Ⅰ(NADH-CoQ reductase)，複合体Ⅱ(succinate-CoQ reductase)，複合体Ⅲ(reduced CoQ-cytochrome *c* reductase)，複合体Ⅳ(cytochrome *c* oxidase)の電子伝達系を構成する4つの複合体と複合体Ⅴ(ATP synthase)の5つからなる．クエン酸回路や脂肪酸のβ酸化によって還元されたNADHやFADH2などの補酵素の還元電位エネルギーを用いて，ミトコンドリア内膜にプロトン濃度勾配を形成し，この電気勾配を用いて複合体ⅤがATPを合成する．

複合体Ⅰはこの呼吸鎖における電子伝達の最初の複合体であり，その分子量は約980 kDaに及び呼吸鎖複合体のなかで最大である．クエン酸回路の電子キャリアであるNADHから電子を受け取ってコエンザイムQ(ユビキノン)に渡し，ユビキノンが還元されユビキノールは膜の内部を自由に拡散し，複合体Ⅲに電子伝達を行う．電子を伝達する間に，複合体Ⅰはプロトンポンプ機構によってプロトンをミトコンドリアの内膜内(マトリックス)から外膜と内膜の間(膜間腔)に移動させ，プロトン濃度勾配をつくる．

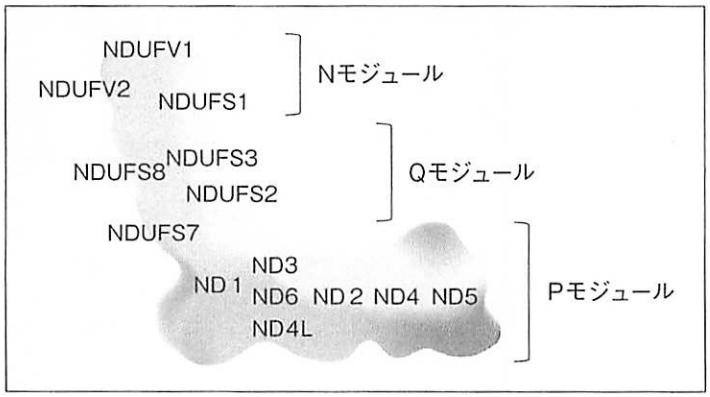

図 1　複合体Ⅰの模式図

3つの機能的モジュール(NADHを還元するNモジュール，電子をユビキノンに伝達するQモジュール，プロトンポンプ機能を果たすPモジュール)で構成されており，内膜に埋め込まれたmembrane armとマトリックス側に突出するmatrix armからなるL字型構造をとる．14個のコアサブユニットの位置を示す．

近年，哺乳類においても複合体Ⅰの構造が徐々に明らかとなっており，内膜に存在するmembrane armとマトリックス側に突出するmatrix armからなるL字型構造をとることがわかっている[1]．matrix armはNADHと結合して酸化するNモジュールと電子伝達を仲介するQモジュールからなり，membrane armはプロトンを膜間腔に汲み出すプロトンポンプの働きをもつPモジュールで構成される．それぞれのモジュールには種を超えて保存される14個の蛋白(コアサブユニット)が存在し，複合体Ⅰの機能の中核を担っている(**図1**)．コアサブユニットのうち，ミトコンドリアDNAにコードされているND1, ND2, ND3, ND4, ND4L, ND5, ND6の7つはmembrane armを，核DNAにコードされているNDUFV1, NDUFV2, NDUFS1, NDUFS2, NDUFS3, NDUFS7, NDUFS8の7つはmatrix armを構成する．哺乳類の複合体Ⅰはこれら14個のコアサブユニットに30種のsupernumerary subunitともよばれるアクセサリーサブユニットが加わり，合計44の蛋白サブユニットから構成されている．複合体Ⅰの機能の中核を担うコアサブユニットに対し，これらの“付加的な”アクセサリーサブユニットは，複合体Ⅰの安定化させたり活性酸素によるダメージから複合体Ⅰを防御したりしているといわれているが，その役割は十分には解明されていない．

❖呼吸鎖複合体Ⅰのアセンブリー

哺乳類の複合体Ⅰは多数の蛋白からなり，分子量が約1MDaにも及ぶ巨大な蛋白複合体であるがゆえに，その構造やサブユニットの集合，組立て(assembly：アセンブリー)機構の解析は困難である．さらに，核とミトコンドリアDNAの二重の遺伝子支配を受けているため，核にコードされた細胞質で生成された蛋白がミトコンドリア内に輸送され，ミトコンドリアDNAにコードされるサブユニットと共同して複合体Ⅰを形成する過程は非常に複雑で，いまだアセンブリー機構の全容を解明するには至っていない．

しかし，真菌モデルを用いた研究や，アセンブリー異常を有するミトコンドリア病患者の解析により，複合体Ⅰのアセンブリー機構は徐々に明らかになってきた．N. crassaの解析で，matrix armを構成するサブユニットの変異によってmatrix armの形成が完全に欠損した際に，membrane armが蓄積することが明らかにされ，2つのarmが別々に形成されていることが示された[2]．同様にヒトにおいても，membrane armを構成するmtDNAにコードされたサブユニットをすべて失っても，matrix armのアセンブリーが保たれることが示されている[3]．このころより，大分子蛋白複合体でもその構造を保ったままの解析が可能なBlue-Native電気泳動(BN-PAGE)が，複合体Ⅰの解析に盛んに応用され，membrane armと

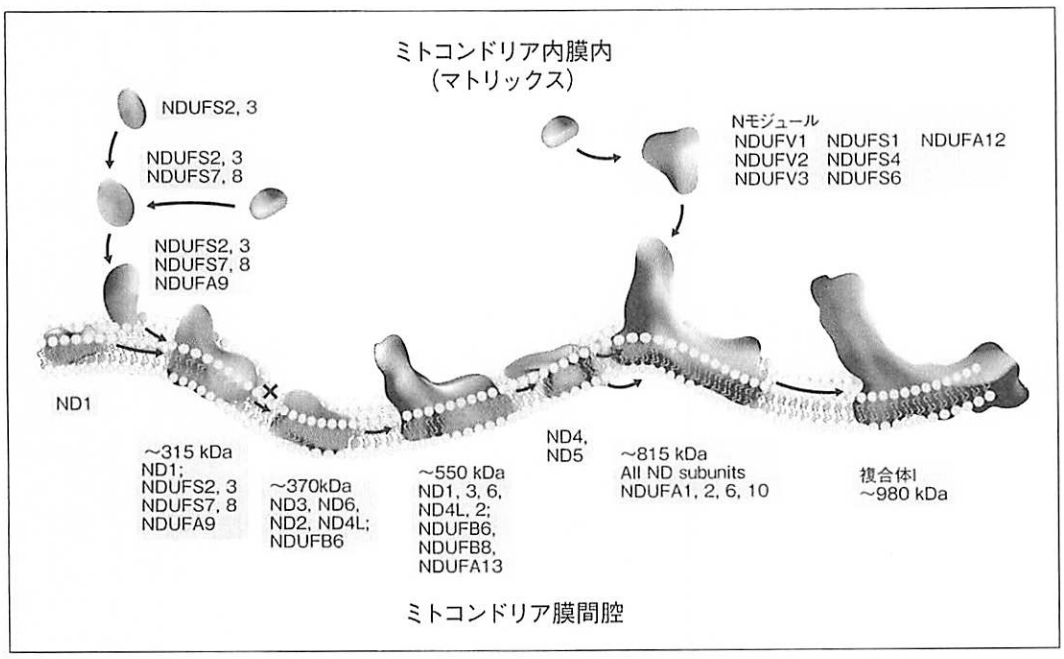

図 2　ミトコンドリア呼吸鎖複合体 I のアセンブリー過程のモデル(文献[7]より引用)

左から右へアセンブリーが進む過程で複合体が成熟し，約 980 kDa の巨大な複合体 I を形成していく．図中の蛋白名は複合体 I のサブユニットの一部を示しており，ND1, 2, 3, 4, 4L, 5, 6 はミトコンドリア DNA がコードする蛋白である．

アセンブリーの早期段階では，親水性のコアサブユニット(NDUFS2 と NDUFS3)がサブコンプレックスを形成し，続いてコアサブユニットの NDUFS7，NDUFS8，supernumerary subunit の NDUFA9 などと集合する．さらに，ミトコンドリア DNA にコードされた ND1 を含む membrane arm の一部と合わさり約 315 kDa 程度のサブコンプレックスを形成する．一方，内膜には，ND3，ND6，ND2，ND4L などからなる複合体も形成されており，両者が一緒になり約 550 kDa の中間複合体が形成され，これに ND4 や ND5 などが加わることでさらに成熟した約 815 kDa の複合体がつくられる．一方で親水性の N モジュールが NDUFV1，NDUFV2，NDUFS1 などからつくられ，最終段階に結合して成熟した複合体 I が完成すると考えられている．

matrix arm が別々に形成された後に，両者が集合して成熟した複合体 I をつくるというアセンブリー過程がしだいに明らかとなった[4,5]．

近年は，哺乳類を含む複合体 I の構造の解明や，質量分析をはじめとした蛋白解析法の進歩によりアセンブリー過程がつぎつぎとアップデートされている．最近提唱されているアセンブリーモデルの早期段階では，親水性のコアサブユニット(NDUFS2 と NDUFS3)が小さな複合体(サブコンプレックス)を形成し，続いて NDUFS7，NDUFS8 などと集合して Q モジュールがつくられると考えられている．そしてミトコンドリア DNA にコードされた ND1 を含む疎水性蛋白からなる membrane arm の一部と合わさり約 315 kDa 程度のサブコンプレックスを形成する．一方，ミトコンドリア DNA にコードされた ND2，ND3，ND6 などが membrane arm のもうひとつのサブコンプレックスを形成し，両者が集合して約 550 kDa のさらに大きなサブコンプレックスが形成される．membrane arm は最後に ND4 と ND5 などが加わることでさらに成熟し，約 815 kDa の複合体がつくられる．一方で親水性の N モジュールが NDUFV1，NDUFV2，NDUFS1 などからつくられ，最終段階で両者が集合して約 980 kDa の機能を有する成熟した複合体 I が完成すると考えられている(**図 2**)．さらに，最近の研究では約 815 kDa の複合体の段階で複合体Ⅲと複合体Ⅳが集合した後に複合体 I が完成し，複合体 I，Ⅲ とⅣによって構成されるスーパーコンプレックスが形成され，生理的な機能を発揮することがわかってきた[6]．

❖呼吸鎖複合体 I のアセンブリーファクター

この複雑なアセンブリー過程には複合体 I を構成するサブユニット以外に重要な因子が関与していることが明らかとなってきている．これらは一

表 1　複合体Ⅰのアセンブリーファクター

アセンブリーファクター	アセンブリープロセスにおいて機能が想定されるモジュール	報告されたおもなミトコンドリア病型	文献番号
ACAD9	P モジュール中間部(ND2 を含むモジュール)	脳筋症，心筋症	15)
ATP5SL	P モジュール遠位部(ND5 を含むモジュール)	ヒトでの疾患報告なし	18)
DMAC1	P モジュール遠位部(ND5 を含むモジュール)	ヒトでの疾患報告なし	18)
ECSIT	P モジュール中間部(ND2 を含むモジュール)	ヒトでの疾患報告なし	15)
FOXRED1	P モジュール遠位部(ND5 を含むモジュール)	Leigh 脳症	17)
NDUFAF1 (CIA30)	P モジュール中間部(ND2 を含むモジュール)	脳筋症，心筋症	15)
NDUFAF2 (NDUFA12L，B17.2L)	N モジュールと P モジュールの結合	脳筋症，Leigh 脳症	19)
NDUFAF3 (C3orf60)	Q モジュール，Q モジュールと P モジュールの結合	新生児/乳児ミトコンドリア病	8)
NDUFAF4 (C6orf66)	Q モジュール，Q モジュールと P モジュールの結合	新生児/乳児ミトコンドリア病	9)
NDUFAF5 (C20orf7)	P モジュール近位部(ND1 を含むモジュール)	新生児/乳児ミトコンドリア病，Leigh 脳症	11)
NDUFAF6 (C8orf 38)	P モジュール近位部(ND1 を含むモジュール)	Leigh 脳症	12)
NDUFAF7 (homolog of MIDA)	P モジュール近位部(ND1 を含むモジュール)	ヒトでの疾患報告なし	14)
NUBPL (Ind1)	N モジュール，Q モジュール	脳筋症(白質変性症)	10)
TIMMDC1 (C3orf 1)	P モジュール近位部(ND1 を含むモジュール)	ヒトでの疾患報告なし	13)
TMEM126B	P モジュール中間部(ND2 モジュール)	ミトコンドリア筋症	16)

時的にサブコンプレックスに結合することはあっても，最終産物である複合体Ⅰには存在せず，サブユニットとは区別してアセンブリーファクターとよばれている．ヒトにおいては現在までに10個以上のアセンブリーファクターの存在が明らかとなっており，その多くでミトコンドリア病の遺伝子異常が見出されている[7]（**表 1**）．すべてが核遺伝子にコードされており，細胞質でつくられてからミトコンドリア内に輸送され，サブコンプレックスの安定化や，サブコンプレックスどうしの集合に関与するシャペロン機能などを有すると考えられている．前述のように複合体Ⅰは，モジュールごとに形成され，それらが集合して成熟するが，このアセンブリー過程に沿って現在までに同定されている 15 個のアセンブリーファクターを紹介する．

1. Q モジュールのアセンブリー

matrix arm の近位部を形成する Q モジュールは，コアサブユニットの NDUFS2，NDUFS3，NDUFS7，NDUFS8 に加え，アクセサリーサブユニットの NDUFA5，NDUFA6，NDUFA9，NDUFAB1 と NDUFA7 からなるが，最初に NDUFS2，NDUFS3 と NDUFA5 が集合し，つぎの段階で NDUFS7 と NDUFS8 が加わると考えられている．その際アセンブリーファクターである NDUFAF3(NADH dehydrogenase 1alpha subcomplex assembly factor 3) と NDUFAF4 が作用して，Q モジュールの安定化や Q モジュールと P モジュールの結合にかかわっていると考えられている[8,9]．また，やはりアセンブリーファクターのひとつとされる NUBPL(Iron-sulfur protein required for NADH dehydrogenase：Ind1) は複合体Ⅰの鉄硫黄クラスターの取込みに関与していると考えられており，鉄硫黄クラスターをもつ Q モジュール内のコアサブユニット NDUFS7 と NDUFS8 の集合や機能に関与している可能性がある[10]．

2. P モジュールのアセンブリー

一方の membrane arm の主要部分については，ミトコンドリア DNA にコードされているコアサブユニットである ND1 を含むモジュールと，ND2 を含むモジュールが別々に形成された後に，両者が集合すると考えられている．

① P モジュール近位部

P モジュールの近位部には ND1 が位置しているが(**図 1**)，他にアクセサリーサブユニットの NDUFA8，NDUFA3，NDUFA13 や NDUFA1 が集合して“ND1 モジュール”がつくられ，前述の

ように形成されたmatrix armのQモジュールはこのモジュールと結合して約315 kDaのサブアセンブリーを形成する段階で内膜とつながると考えられている(**図2**). 次世代シーケンサーなどによる遺伝子解析によって発見された変異をもつ患者細胞の検討により, NDUFAF5とNDUFAF6がND1の生成や安定化にかかわる因子として報告されている[11,12]. さらに, 最近のプロテオーム解析技術を応用し, コアサブユニットやアセンブリーファクターとの相互作用を解析することにより内膜に存在する蛋白のTIMMDC1がND1モジュールの集合や安定化に必須の因子として見出されている[13]. また, Qモジュールを構成するNDUFS2と結合すると思われるNDUFAF7は, ND1と同じサブコンプレックスに存在し, ND1モジュールの安定化にも関与していると考えられている[14].

② Pモジュール中間部

Pモジュールの中間部にはND2が位置しているが, このコアサブユニットを含む部分"ND2モジュール"はアセンブリーの初期段階ではND1モジュールとは別々に形成されていることが以前から知られていた. ND2モジュールは, ミトコンドリアDNAにコードされるND3, ND6やND4Lと, おそらくはNDUFC1やNDUFC2といったアクセサリーサブユニットと約370 kDaの集合体を形成するが(**図2**), この際複数のアセンブリーファクター, すなわちNDUFAF1, ECSIT(Evolutionarily conserved signaling intermediate in Toll pathway), ACAD9(Acyl-CoA dehydrogenase family member 9)とTMEM126Bが結合して作用するとことがわかってきた[15,16]. これら4つの蛋白はたがいに結合してmitochondrial complex I assembly complex(MCIAコンプレックス)を形成し, ND2モジュールの安定化に寄与し, さらにTIMMDC1などと協働してND1モジュールとの集合に関与していると考えられる.

③ Pモジュール遠位部

Pモジュールの遠位部は, ミトコンドリアDNAにコードされたND4とND5に, NDUFB1～11とNDUFAB1から構成され, 複合体Iのmembrane armの集合の最終段階で付加されると考えられている. このプロセスで働いていると思われる因子としては, FOXRED1が報告されていたが[17], 最近になってあらたなアセンブリーファクターとしてDMAC1とATP5SLが報告された[18]. CRISPR/Cas-9などのゲノム編集技術を用いてさまざまなサブユニットをノックダウンし, アセンブリープロセスに異常をきたした細胞を定量プロテオミクスにより比較することにより, これらの2つの因子がND5とFOXRED1と相互作用をもち, Pモジュール遠位部が集合してmembrane armを形成する過程に寄与していることが示された.

3. Nモジュールのアセンブリー

matrix armのもっとも遠位部を構成するNモジュールは, NDUFV1, NDUFV2, NDUFS1, NDUFA2, NDUFS4と, おそらくNDUFV3からなり, NDUFS6とNDUFA12はQモジュールに面して位置していると考えられている. このモジュールは鉄硫黄クラスターをもつので, Qモジュール同様NUBPLがアセンブリーファクターとして機能していると思われる. 形成されたNモジュールは複合体Iの最終段階でNUDFAF2の作用のもと約815 kDaの中間複合体に付加されて成熟した複合体Iが完成し機能を発揮する[19].

❖おわりに

複合体Iのアセンブリー機構はサブユニットが徐々に大きくなる単純な過程ではなく, モジュールごとにサブユニットが集合してサブアセンブリーを形成し, それらが集合して成熟した巨大な複合体を組み立てる複雑なプロセスである. 種を超えて保存されているコアサブユニットに加え, これほどまでに多くのアクセサリーサブユニットが, さまざまなアセンブリーファクターの助けを借りて組み込まれる理由はよくわかっていないが, 生物の進化を考えるうえでたいへん興味深い.

一方, ミトコンドリア病患者のおよそ4割がいまだ遺伝子診断に至っていないといわれているが, なかでもミトコンドリア呼吸鎖複合体I欠損はミトコンドリア病患者の病因としてもっとも多く, 遺伝学的診断に至っていない症例も多い. そのため, この巨大な複合体のアセンブリー機構の理解は基礎研究のみならず臨床上も非常に重要で

ある．構造解析やプロテオミクスの進歩と，次世代シーケンサーをはじめとした最新の遺伝子解析技術を用いた患者解析は，複合体Ⅰのアセンブリー機構の理解に大きな進歩をもたらした．そして多くのアセンブリーファクターが見出されてミトコンドリア病の原因遺伝子として同定されてきたが(**表1**)，それぞれの遺伝子異常がどのような臨床病型をもたらすかははっきりせず，表現型と遺伝子異常の関連の解明にはさらなる症例の蓄積が必要である．また，あいついで発見されているアセンブリーファクターの作用機序もほとんどわかっておらず，アセンブリー機構の全容解明にはまだ時間を要する．しかし近年，蛋白どうしの相互作用の解析技術は長足の進歩を遂げており，さらなる未知のアセンブリーファクターの発見や複合体Ⅰの構造の解明がなされると思われる．アセンブリープロセスの解明が患者の病因診断と病態解析につながり，さらには分子病態に基づいた治療法開発をもたらすことを期待したい．

*　　*　　*

文献

1) Zhu, J. et al.：*Nature*, **536**：534-538, 2016.
2) Tuschen, G. et al.：*J. Mol. Biol.*, **213**：845-857, 1990.
3) Bourges, I. et al.：*Biochem. J.*, **383**：491-499, 2004.
4) Vogel, R. O. et al.：*Biochim. Biophys. Acta.*, **1767**：1215-1227, 2007.
5) Mckenzie, M and Ryan, M. T.：*IUBMB Life*, **62**：497-502, 2010.
6) Moreno-Lastres, D. et al.：*Cell Metab.*, **15**：324-335, 2012.
7) Mimaki, M. et al.：*Biocim Biophys. Acta.*, **1817**：851-862, 2012.
8) Saada, A. et al.：*Am. J. Hum. Genet.*, **84**：718-727, 2009.
9) Saada, A. et al.：*Am. J. Hum. Genet.*, **82**：32-38, 2008.
10) Scheftel, A. D. Et al.：*Mol. Cell. Biol.*, **29**：6059-6073, 2009.
11) Sugiana, C. et al.：*Am. J. Hum. Genet.*, **83**：468-478, 2008.
12) Mckenzie, M. et al.：*J. Mol. Biol.*, **414**：413-426, 2011.
13) Andrews, B. et al.：*Proc. Natl. Acad. Sci. USA*, **110**：18934-18939, 2013.
14) Zurita Rendon, L. et al.：*Hum. Mol. Genet.*, **23**：5159-5170, 2014.
15) Nouws, J. et al.：*Cell Metab.*, **12**：283-294, 2010.
16) Heide, H. et al.：*Cell Metab.*, **16**：538-549, 2012.
17) Formosa, L. E. et al.：*Hum. Mol. Genet.*, **24**：2952-2965, 2015.
18) Stroud, D. A. et al.：*Nature*, **538**：123-126, 2016.
19) Ogilvie, I. et al.：*J. Clin. Invest.*, **115**：2784-2792, 2005.

OPEN

Citation: Cell Death and Disease (2017) 8, e2551; doi:10.1038/cddis.2016.484
Official journal of the Cell Death Differentiation Association
www.nature.com/cddis

Mitochondrial respiratory dysfunction disturbs neuronal and cardiac lineage commitment of human iPSCs

Mutsumi Yokota[1,2], Hideyuki Hatakeyama*[,1,2], Yasuha Ono[1], Miyuki Kanazawa[3] and Yu-ichi Goto*[,1,2,3]

Mitochondrial diseases are genetically heterogeneous and present a broad clinical spectrum among patients; in most cases, genetic determinants of mitochondrial diseases are heteroplasmic mitochondrial DNA (mtDNA) mutations. However, it is uncertain whether and how heteroplasmic mtDNA mutations affect particular cellular fate-determination processes, which are closely associated with the cell-type-specific pathophysiology of mitochondrial diseases. In this study, we established two isogenic induced pluripotent stem cell (iPSC) lines each carrying different proportions of a heteroplasmic m.3243A > G mutation from the same patient; one exhibited apparently normal and the other showed most likely impaired mitochondrial respiratory function. Low proportions of m.3243A > G exhibited no apparent molecular pathogenic influence on directed differentiation into neurons and cardiomyocytes, whereas high proportions of m.3243A > G showed both induced neuronal cell death and inhibited cardiac lineage commitment. Such neuronal and cardiac maturation defects were also confirmed using another patient-derived iPSC line carrying quite high proportion of m.3243A > G. In conclusion, mitochondrial respiratory dysfunction strongly inhibits maturation and survival of iPSC-derived neurons and cardiomyocytes; our presenting data also suggest that appropriate mitochondrial maturation actually contributes to cellular fate-determination processes during development.
Cell Death and Disease (2017) **8,** e2551; doi:10.1038/cddis.2016.484; published online 12 January 2017

Mitochondria possess multiple copies of their own genome (mitochondrial DNA; mtDNA) and play some crucial roles in cellular energy metabolism. From the viewpoint of developmental biology, several recent studies have clearly indicated that mitochondria are functionally and morphologically reorganized for adaptation to an embryonic stem cell (ESC)-like intracellular environment during induced pluripotent stem cell (iPSC) generation.[1–6] Moreover, mtDNA haplogroups (i.e., genetic population groups that share a common ancestor), which are known to be associated with various phenotypes (e.g., disease susceptibility, environmental adaptation or aging), also affect their intrinsic gene expression signatures involved in pluripotency, differentiation, DNA methylation and mitochondrial energy metabolism.[7] Thus, appropriate mitochondrial rejuvenation or maturation may be one important step for *bona fide* cellular reprogramming or differentiation, as well as for epigenetic modification or resetting in nuclear DNA.

Most parts of pathogenic mutations in mtDNA-specific tRNA genes responsible for various types of mitochondrial diseases have been reported as heteroplasmy (i.e., wild-type mtDNA and mutant mtDNA coexist within a single cell), and induced mitochondrial dysfunction emerges only when mutation ratios of mtDNA exceed their intrinsic pathogenic thresholds at a cellular level.[8] Mitochondrial diseases caused by heteroplasmic mtDNA mutations present a wide variety of affected tissues and organs (e.g., central nervous system or cardiovascular system) among patients,[9,10] probably due to variations in mutant mtDNA proportions at each tissue and organ level. Therefore, disease-relevant iPSCs carrying heteroplasmic mtDNA mutations will greatly help us to open new avenues for studying the patient-specific definitive genotype–phenotype relationship of affected tissues and organs in mitochondrial diseases.[11] In fact, several groups and we have reported the generation and the application of patient-derived iPSCs carrying various heteroplasmic mtDNA mutations toward *in vitro* human mitochondrial disease modeling;[12–18] however, it remains uncertain whether and how such heteroplasmic mtDNA mutations affect particular cellular fate-determination processes during development. Recently, we also demonstrated that mitochondrial respiratory dysfunction caused by a heteroplasmic m.3243 A > G mutation in *MT-TL1* gene,[19] which is the most representative mutant mtDNA, strongly inhibits cellular reprogramming but does not affect maintenance of the pluripotent state.[20] Our findings may indicate that the degree of the molecular pathogenic influence of heteroplasmic mtDNA mutations actually changes during cellular lineage-commitment processes along with the degree of functional maturation in mitochondria.

In this study, we established two isogenic iPSC lines carrying different proportions of m.3243 A > G from the same patient; one exhibited apparently normal and the other showed

[1]Department of Mental Retardation and Birth Defect Research, National Institute of Neuroscience, National Center of Neurology and Psychiatry, Tokyo 187-8502, Japan; [2]AMED-CREST, Japan Agency for Medical Research and Development, Tokyo 100-0004, Japan and [3]Medical Genome Center, National Center of Neurology and Psychiatry, Tokyo 187-8551, Japan
*Corresponding author: H Hatakeyama or Y-i Goto, Department of Mental Retardation and Birth Defect Research, National Institute of Neuroscience, National Center of Neurology and Psychiatry (NCNP), 4-1-1 Ogawahigashi, Kodaira 187-8502, Tokyo, Japan. Tel: +81 42 346 1713; Fax: +81 42 346 1743; E-mail: hideyuki@ncnp.go.jp or goto@ncnp.go.jp
Received 02.9.16; revised 14.11.16; accepted 16.12.16; Edited by M Agostini

most likely impaired mitochondrial respiratory function. Using these isogenic iPSC lines, we demonstrated that induced mitochondrial respiratory dysfunction triggered by high proportions of m.3243 A > G strongly inhibits maturation and survival of iPSC-derived neurons and cardiomyocytes. Such *in vitro* neuronal and cardiac maturation defects were also confirmed by using another patient-derived iPSC line carrying quite high proportion of m.3243 A > G. Our presenting data therefore demonstrate that isogenic iPSC lines with different proportions of m.3243 A > G would make enormous contributions as *in vitro* human cellular disease models to greatly facilitate iPSC-based drug discovery and regenerative therapeutics in mitochondrial diseases.

Results

Generation of patient-derived isogenic iPSC lines carrying different proportions of m.3243A > G. First, we generated two isogenic iPSC lines from the same patient, each of which possessed different proportions of m.3243A > G (approximately 40 and 90% proportions of mutant mtDNA; denoted as P1-3243[40] and P1-3243[90], respectively). We also established two additional iPSC lines, each of which were derived from healthy control subject (denoted as Control) and from another patient carrying over 90% proportion of m.3243A > G (denoted as P2-3243[> 90]), respectively. We have previously reported that the molecular pathogenic threshold level of m.3243A > G with regard to mitochondrial respiratory function is ~90% in patient-derived clonal fibroblasts.[20] We confirmed that no marked difference was observed between all iPSC lines with regard to ESC-like pluripotent characteristics such as pluripotency markers expression and embryoid body (EB)-mediated *in vitro* spontaneous differentiation into three germ layers (Figures 1a and b), in addition to pluripotency genes expression and silenced transgenes expression (Supplementary Figures S1A and B). Genetic identity of these isogenic iPSC lines was also verified by analysis of short tandem repeat variations (Figure 1c). We measured the overall mitochondrial respiration profile of all iPSC lines by a flux analyzer. Although no statistical significance was observed between two isogenic iPSC lines (P1-3243[40] and P1-3243[90]), mitochondrial energy metabolic potentials (e.g., basal respiration and ATP production) of P1-3243[90] iPSC line were both lower than those of P1-3243 [40] iPSC line (Figure 1d). We further analyzed enzymatic activities of mitochondrial respiratory chain complexes in all iPSC lines. In fact, mitochondrial respiratory chain complex I activity was significantly suppressed by over 90% proportion of m.3243A > G (P2-3243[> 90] vs Control), whereas mitochondrial respiratory chain complex IV activity was apparently unaffected in all iPSC lines (Figure 1e). Although no statistical significance was observed between two isogenic iPSC lines (P1-3243[40] and P1-3243[90]), mitochondrial respiratory chain complex I activity of P1-3243[90] iPSC line was actually lower than that of P1-3243[40] iPSC line. We also randomly selected several iPSC colonies from each patient-derived iPSC line to determine m.3243A > G proportions at each single-iPSC-colony level and found no significant segregation in m.3243A > G proportions during self-renewal of iPSCs throughout this study (i.e., at least 5–10 passages in culture of each iPSC line) (Figure 1f). We therefore concluded that two isogenic iPSC lines with different proportions of m.3243 A > G from the same patient (P1-3243[40] and P1-3243[90]) were successfully established; one exhibited apparently normal and the other showed most likely impaired mitochondrial respiratory function.

Inhibited cardiac maturation triggered by exceeding the pathogenic threshold level of m.3243A > G. Next, we asked whether and how heteroplasmy levels of m.3243A > G affect cardiac maturation (Figure 2a). Using Control iPSC line, we confirmed the successful specification into cTNT-positive beating cardiomyocytes. P1-3243[90] iPSC line, which exhibited most likely impaired mitochondrial respiratory function, was also able to differentiate into beating cardiomyocytes expressing the representative cardiac lineage marker of cTNT similarly to those of isogenic P1-3243[40] iPSC line; in contrast, no beating cardiomyocytes were obtained from P2-3243[> 90] iPSC line, which exhibited impaired mitochondrial respiratory function (Figures 2b–d and Supplementary Movies S1–S3). Of note, no marked difference was observed during the time course of cardiac induction between these iPSC lines (see also Figure 2b). Interestingly, however, all cardiomyocytes derived from P1-3243[90] iPSC line possessed less than 90% proportions of m.3243 A > G (Figure 2e). To confirm the molecular pathogenic influence of m.3243A > G on cardiac lineage commitment, we measured mitochondrial respiratory function of iPSC-derived cardiomyocytes by a flux analyzer; as expected, cardiomyocytes derived from P1-3243[90] iPSC line, all of which exhibited below the molecular pathogenic threshold level of m.3243A > G, showed apparently normal mitochondrial respiration profile and mitochondrial energy metabolic potentials (e.g., basal respiration and ATP production) similarly to those derived from P1-3243[40] iPSC line (Figure 2f). In addition, we found that one out of five iPSC-derived cardiomyocytes showed a significant decrease in m.3243A > G heteroplasmy level (approximately 60% proportion of mutant mtDNA) when compared with the distributions of m.3243A > G heteroplasmy levels in the parental P1-3243 [90] iPSC line (77–92% proportions of mutant mtDNA) (see also Figure 2e). We also added mtDNA copy number analysis for iPSC-derived cardiomyocytes and their parental iPSCs. Cardiomyocytes derived from two isogenic iPSC lines (P1-3243[40] and P1-3243[90]) had more mtDNA copies per cell than those in the parental iPSCs; however, no significant difference in mtDNA copy number was observed between two isogenic iPSC lines (P1-3243[40] and P1-3243[90]), or among their iPSC-derived cardiomyocytes (Supplementary Figure S2). We therefore concluded that mitochondrial respiratory dysfunction caused by exceeding the pathogenic threshold level of m.3243A > G induced cardiac maturation defects.

Induced neuronal cell death triggered by exceeding the pathogenic threshold level of m.3243A > G. We then differentiated these iPSC lines into neurons using our stepwise induction method to clarify whether and how

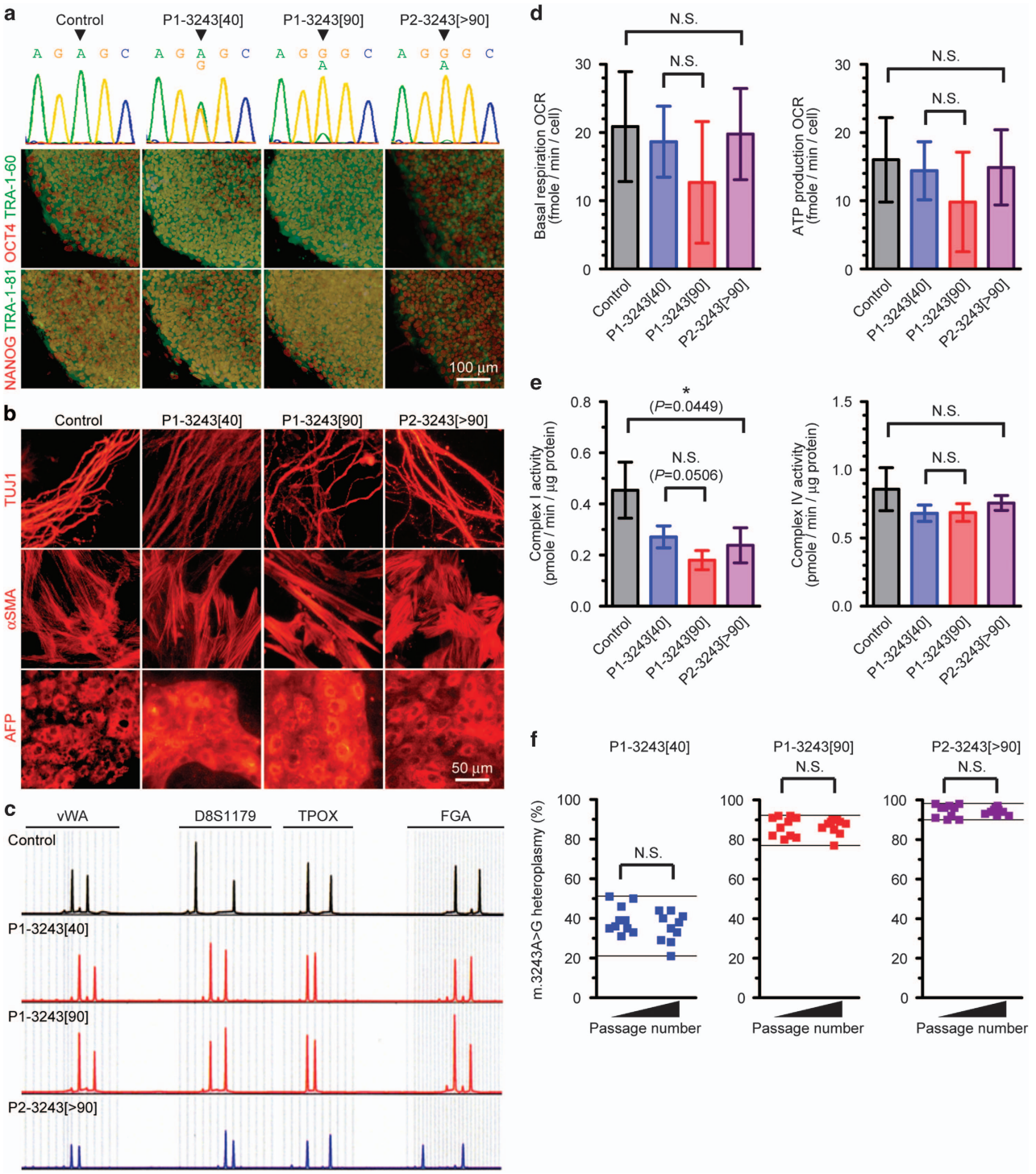

Figure 1 Generation of patient-derived isogenic iPSC lines carrying different proportions of m.3243A > G. (**a**) Representative images of the established iPSC lines; OCT4 (red), NANOG (red), TRA-1-60 (green) and TRA-1-81 (green). Electropherogram of heteroplasmic m.3243A > G mutation in each iPSC line was also shown. Arrowheads indicate m.3243A > G. (**b**) Representative images of the embryoid body (EB)-mediated *in vitro* spontaneous differentiation; TUJ1 (ectoderm, red), αSMA (mesoderm, red) and AFP (endoderm, red). (**c**) Representative images of STR variations (4 out of 16 genetic loci analyzed) demonstrated that isogenic iPSC lines carrying different proportions of m.3243A > G (P1-3243[40] and P1-3243[90]) shared the same nuclear DNA genetic background. (**d**) Mitochondrial respiratory function of patient-derived iPSC lines. Oxygen consumption rate (OCR) of each iPSC line was measured by a flux analyzer. Biological replicates of each iPSC line used were as follows: Control ($n = 5$), P1-3243[40] ($n = 3$), P1-3243[90] ($n = 5$), P2-3243[> 90] ($n = 4$). Statistical significance was evaluated by unpaired, two-tailed *t*-test. NS, not significant. (**e**) Mitochondrial respiratory chain complexes activity of patient-derived iPSC lines. Three biological replicates of each iPSC line were used for the measurements. Statistical significance was evaluated by unpaired, two-tailed *t*-test. $^*P < 0.05$, NS, not significant. (**f**) Time-dependent changes in the distributions of m.3243A > G proportions in patient-derived iPSC line at each single-iPSC-colony level. Statistical significance was evaluated by unpaired, two-tailed *t*-test. NS, not significant

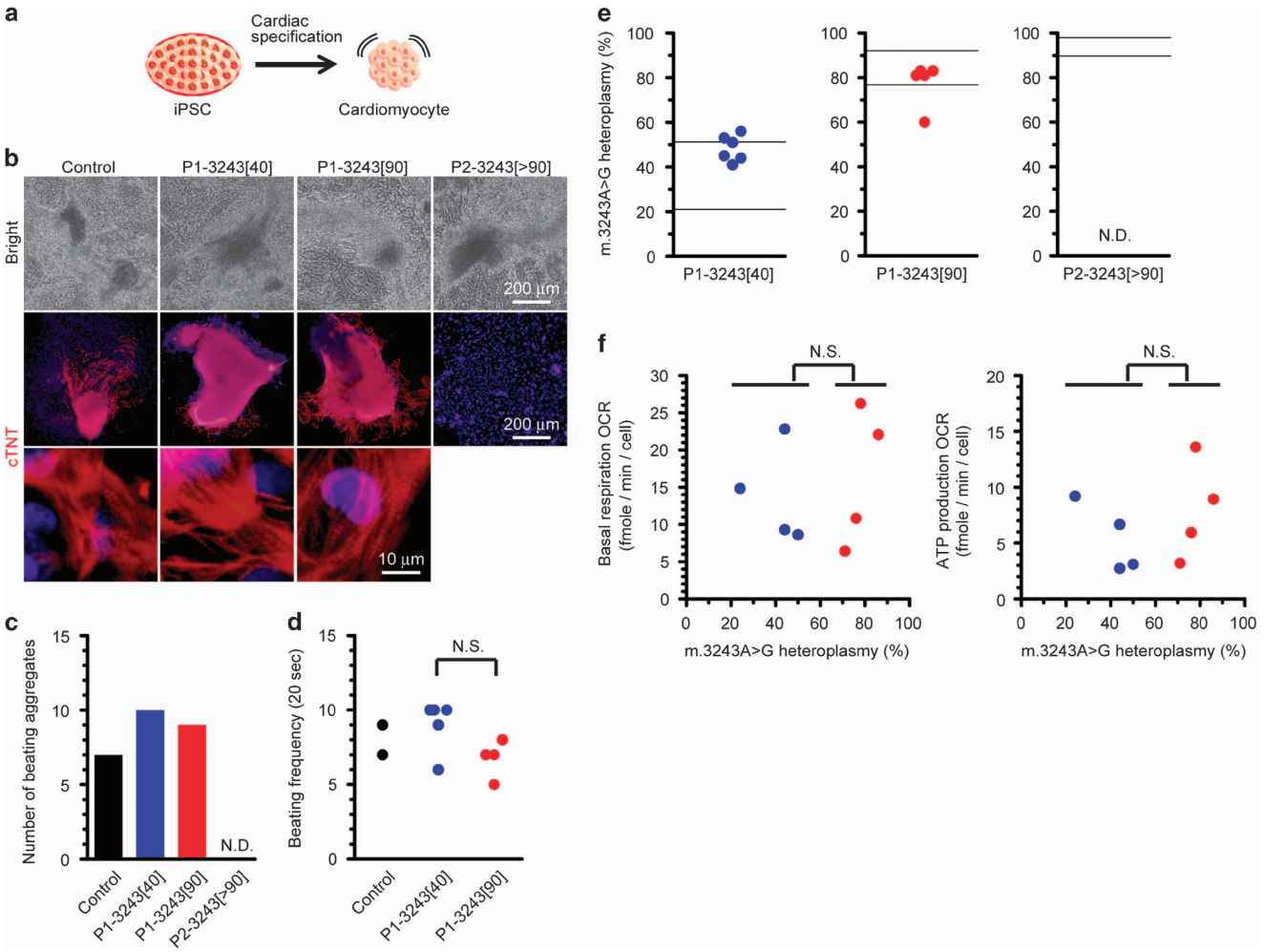

Figure 2 Induced cardiac maturation defects triggered by exceeding the pathogenic threshold level of m.3243A > G. (**a**) Experimental design used to identify the molecular pathogenic influence of m.3243A > G on cardiac differentiation. (**b**) Representative images of cardiomyocytes derived from each patient-derived iPSC line; cTNT (red). Cell nuclei were co-stained with Hoechst 33342 (blue). No cTNT-positive cardiomyocytes were observed in P2-3243[> 90] iPSC line. (**c**) Total number of beating aggregates after cardiac differentiation in each patient-derived iPSC line. Cardiac induction was independently performed three times, and data were gathered for graph preparation. ND, not detected. (**d**) Beating frequency of cardiomyocytes derived from each patient-derived iPSC line. Statistical significance was evaluated by unpaired, two-tailed *t*-test. NS, not significant. Representative movies of beating cardiomyocytes derived from each patient-derived iPSC line were also shown in Supplementary Movies S1–S3, respectively. (**e**) The distributions of m.3243A > G proportions in cardiomyocytes derived from patient-derived iPSC lines. Immunostained cells were collected for further mtDNA mutation analysis. ND, not detected. (**f**) Relationship between the distributions of m.3243A > G proportions and mitochondrial respiratory function in cardiomyocytes derived from patient-derived isogenic iPSC lines. Oxygen consumption rate (OCR) of beating cardiomyocytes was measured by a flux analyzer. The proportions of m.3243A > G in cardiomyocytes were determined after biochemical measurement. Biological replicates of beating cardiomyocytes used were as follows: P1-3243[40] ($n = 4$), P1-3243[90] ($n = 4$). Statistical significance was evaluated by unpaired, two-tailed *t*-test. NS, not significant

heteroplasmy levels of m.3243 A > G also affect neuronal maturation (Figure 3a). Using Control iPSC line, we confirmed that our neuronal induction protocol showed highly efficient neural stem cell (NSC) specification and neuronal differentiation (Figure 3b). Although P1-3243[40] iPSC line showed no apparent influence of m.3243 A > G on directed differentiation into TUJ1-positive neurons similarly to that of Control iPSC line, two other iPSC lines carrying high proportions of m.3243 A > G (P1-3243[90] and P2-3243 [> 90]) showed induced cell death during neuronal lineage commitment; in particular, poorly surviving neurons in P1-3243[90] iPSC line, which exhibited most likely impaired mitochondrial respiratory function, and no living neurons in P2-3243[> 90] iPSC line, which exhibited impaired mitochondrial respiratory function, were observed, respectively (Figures 3c and d). We also evaluated the completely detached and collapsed neurospheres in P2-3243[> 90] iPSC line as 'dead' in this experiment (see also Figure 3c). Of note, no cell death was observed during NSC specification and expansion in these iPSC lines, suggesting that m.3243 A > G has minimal molecular pathogenic influence on NSCs. Focusing on P1-3243[90] iPSC line, m.3243 A > G heteroplasmy levels were significantly higher in 'dead' neurospheres (86 ± 12% proportions of mutant mtDNA) than those in 'survival' neurons (73 ± 17% proportions of mutant mtDNA) with statistical significance (Figure 3e). To confirm

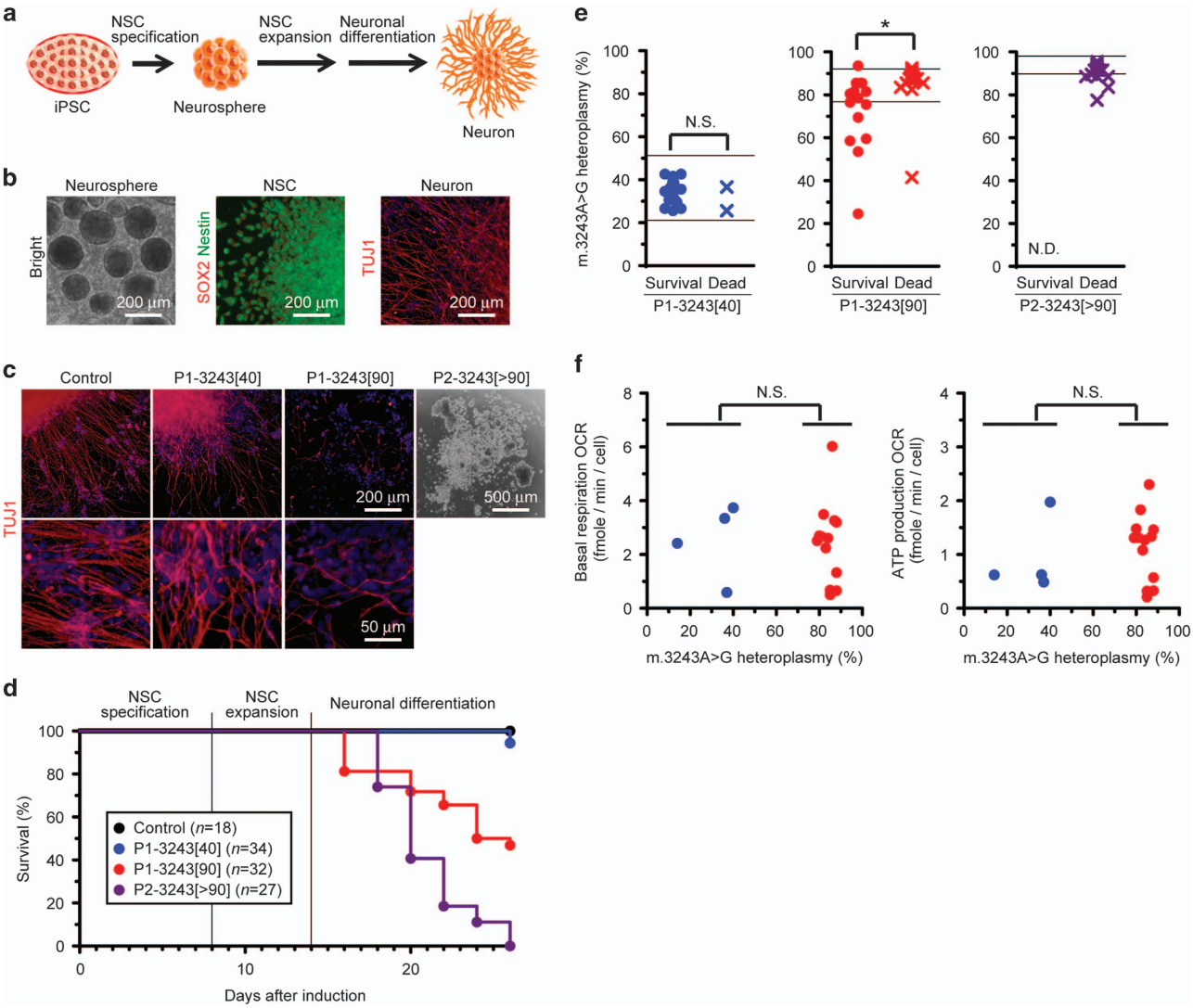

Figure 3 Induced neuronal cell death triggered by exceeding the pathogenic threshold level of m.3243A > G. (**a**) Experimental design used to identify the molecular pathogenic influence of m.3243A > G on neuronal differentiation. (**b**) Representative images of successive differentiation into neurons via neural stem cell (NSC) specification and expansion using Control iPSC line; SOX2 (red), Nestin (green), TUJ1 (red). Cell nuclei were co-stained with Hoechst 33342 (blue). (**c**) Representative images of neurons derived from each patient-derived iPSC line; TUJ1 (red). Cell nuclei were co-stained with Hoechst 33342 (blue). Representative image of induced neuronal cell death during neuronal differentiation in P2-3243[> 90] iPSC line was also shown. (**d**) Induced neuronal cell death, but stable NSC specification and expansion, in two patient-derived iPSC lines carrying high m.3243A > G proportions (P1-3243[90] and P2-3243[> 90]). Neuronal differentiation was independently performed three times, and data were gathered for graph preparation. (**e**) The distributions of m.3243A > G proportions in neurons derived from patient-derived iPSC lines. Immunostained 'survival' cells and spontaneously detached 'dead' neurospheres were collected for further mtDNA mutation analysis. Notably, 2 out of 34 neurospheres derived from P1-3243[40] iPSC line were detached from culture surfaces just before immunostaining (see also **d**). Therefore, we evaluated these detached neurospheres as 'dead' in this experiment. Statistical significance was evaluated by unpaired, two-tailed *t*-test. $^*P < 0.05$, NS, not significant; ND, not detected. (**f**) Relationship between the distributions of m.3243A > G proportions and mitochondrial respiratory function in neurons derived from patient-derived isogenic iPSC lines. Oxygen consumption rate (OCR) of neurons was measured by a flux analyzer. The proportions of m.3243A > G in neurons were determined after biochemical measurement. Biological replicates of neurons used were as follows: P1-3243[40] ($n = 4$), P1-3243[90] ($n = 13$). Statistical significance was evaluated by unpaired, two-tailed *t*-test. NS, not significant

the molecular pathogenic influence of m.3243 A > G on neuronal lineage commitment, we measured mitochondrial respiratory function of iPSC-derived 'survival' neurons by a flux analyzer; similarly to the case of iPSC-derived cardiomyocytes, 'survival' neurons derived from P1-3243[90] iPSC line, all of which possessed less than 90% proportions of m.3243 A > G, showed apparently normal mitochondrial respiration profile and mitochondrial energy metabolic potentials (e.g., basal respiration and ATP production) similarly to those derived from P1-3243[40] iPSC line (Figure 3f). More remarkable than the case of cardiac lineage commitment, some iPSC-derived 'survival' neurons also showed drastic decreases in m.3243 A > G heteroplasmy levels (i.e., 5 out of 15 neurons exhibited less than 70% proportions of mutant mtDNA) when compared with the distributions of m.3243 A > G heteroplasmy levels in the parental P1-3243 [90] iPSC line (77–92% proportions of mutant mtDNA) (see also Figure 3e), suggesting that mutant mtDNA segregation

may occur in some cell populations during neuronal maturation process in a stochastic manner. We further prepared other lines of iPSC-derived neurons from the parental P1-3243[90] iPSC line to experimentally reproduce such mutant mtDNA segregation behavior and to clarify the relationship between the segregation of m.3243 A > G heteroplasmy levels and the changes in mtDNA copy number. Unfortunately, however, no significant segregation of m.3243 A > G heteroplasmy levels was observed during the repetitive neuronal differentiation assays. In contrast to the case of iPSC-derived cardiomyocytes, 'survival' neurons derived from two isogenic iPSC lines (P1-3243[40] and P1-3243[90]) possessed less mtDNA copies per cell than those in the parental iPSCs; however, no significant difference in mtDNA copy number was observed between two isogenic iPSC lines (P1-3243[40] and P1-3243[90]), or among their iPSC-derived neurons (Supplementary Figure S3). We therefore concluded that mitochondrial respiratory dysfunction caused by exceeding the pathogenic threshold level of m.3243A > G also induced neuronal cell death; this phenomenon is similar to, but more pronounced than, that in cardiac lineage.

Neuronal maturation defect was also recapitulated by using mtDNA-depleted neuroblastoma cells. We further addressed whether severe mitochondrial respiratory dysfunction, which is triggered by mtDNA depletion, is also able to recapitulate neuronal maturation defect and even neuronal cell death during neuronal lineage commitment. We used SH-SY5Y neuroblastoma cell line (SH-SY5Y WT) to prepare its mtDNA-depleted cell line (SH-SY5Y ρ^0) and to differentiate both neuroblastoma cell lines into neurons (Figure 4a). We confirmed, in advance, that SH-SY5Y ρ^0 line showed severe mitochondrial respiratory dysfunction triggered by mtDNA depletion (Figure 4b). In fact, cytochemical staining of cytochrome *c* oxidase (COX), an indicator of mitochondrial respiration activity, also indicated that SH-SY5Y WT line showed strongly COX-positive, whereas SH-SY5Y ρ^0 line showed COX-negative (Figure 4d). As we expected, neuronal maturation was markedly suppressed by severe mitochondrial respiratory dysfunction triggered by mtDNA depletion, and in some cells, induced neuronal cell death was also observed in SH-SY5Y ρ^0 line during neuronal lineage commitment (Figure 4c and Supplementary Movies S4 and S5) with similar trend to iPSC-derived neurons carrying high proportions of m.3243 A > G. In this case, the remaining 'survival' neurons in SH-SY5Y ρ^0 line were COX-negative (Figure 4d). Although neuroblastoma cells have several distinct genetic, epigenetic and energy metabolic properties from iPSCs, we concluded that mitochondrial respiratory dysfunction caused by defective mtDNA with various mutation types actually induced neuronal maturation defect and even neuronal cell death *in vitro*.

Discussion

In this study, we generated two isogenic iPSC lines from the same patient; one exhibited apparently normal and the other showed most likely impaired mitochondrial respiratory function. Using these isogenic iPSC lines, our lineage-specific directed differentiation methods demonstrated that induced mitochondrial respiratory dysfunction triggered by high proportions of m.3243 A > G strongly inhibits maturation and survival of iPSC-derived neurons and cardiomyocytes. Such *in vitro* maturation defects in both neuronal and cardiac lineages were also confirmed using another patient-derived iPSC line carrying over 90% proportion of m.3243 A > G. In addition to our results, Hämäläinen *et al.*[15] reported the pathogenic influences of a heteroplasmic m.3243 A > G mutation on neuronal differentiation; briefly, their established patient-origin iPSC-derived neurons carrying approximately 80–85% proportions of m.3243 A > G exhibited specific down-regulation of mitochondrial respiratory chain complex I at both transcript and protein levels and showed accelerated mitophagy via the PARKIN–PINK1 pathway, probably due to clearance of damaged mitochondria for further neuronal differentiation and maturation. Taking these previous findings with our presenting data, we propose that appropriate mitochondrial rejuvenation or maturation must be required for *bona fide* cellular reprogramming or differentiation, and the degree of molecular pathogenic influence of mutant mtDNA actually determines the severity of the cell-type-specific disease phenotypes *in vitro*, including the differentiation efficiency into particular cell types (Figure 5).

As we noted above, severe mitochondrial respiratory dysfunction strongly induces neuronal cell death *in vitro*; however, most parts of mitochondrial disease patients carrying mutant mtDNA undergo normal brain development *in vivo* before symptomatic appearance. What is the crucial difference between iPSC-based *in vitro* cellular disease phenotypes and *in vivo* clinical symptoms? Some previous molecular neuropathological studies using postmortem brain of mitochondrial disease patients found that neuronal cells carrying higher proportions of mutant mtDNA frequently remained in some patients' cerebellar lesions (e.g., dentate nucleus neurons, olivary neurons and Purkinje cells).[21,22] These findings suggest that neuronal cell death does not always correlate with mutant mtDNA proportions, leading to the discrepancy between our iPSC-based *in vitro* recapitulation of neuronal development and *in vivo* brain pathology of mitochondrial disease patients. With regard to this discrepancy, it is hypothesized that physiological and physical interaction with other non-neuronal cell types in the brain (e.g., astrocytes) may strongly enhance maturation and long-term survival of neurons having damaged mitochondria. Astrocytes are known to play a role as an energy supplier to neurons through the release of lactate;[23] for example, a co-culture system with astrocytes is generally used for accelerated functional maturation and long-term survival of neurons *in vitro*. Moreover, the predominant energy metabolic system in astrocytes is glycolysis, while that in neurons is mitochondrial respiration,[23] suggesting no apparent influence of mitochondrial respiration defects on physiological function in astrocytes to support neurons. In fact, we displayed the successive observation of TUJ1-positive neurons derived from P2-3243[> 90] iPSC line through EB-mediated *in vitro* spontaneous differentiation, and even this iPSC line did not produce neurons using the directed neuronal differentiation method. On the other hand, aberrant early embryogenesis was reported using fertilized eggs derived from a female mito-mouse carrying 70% proportion of 4696-bp mtDNA

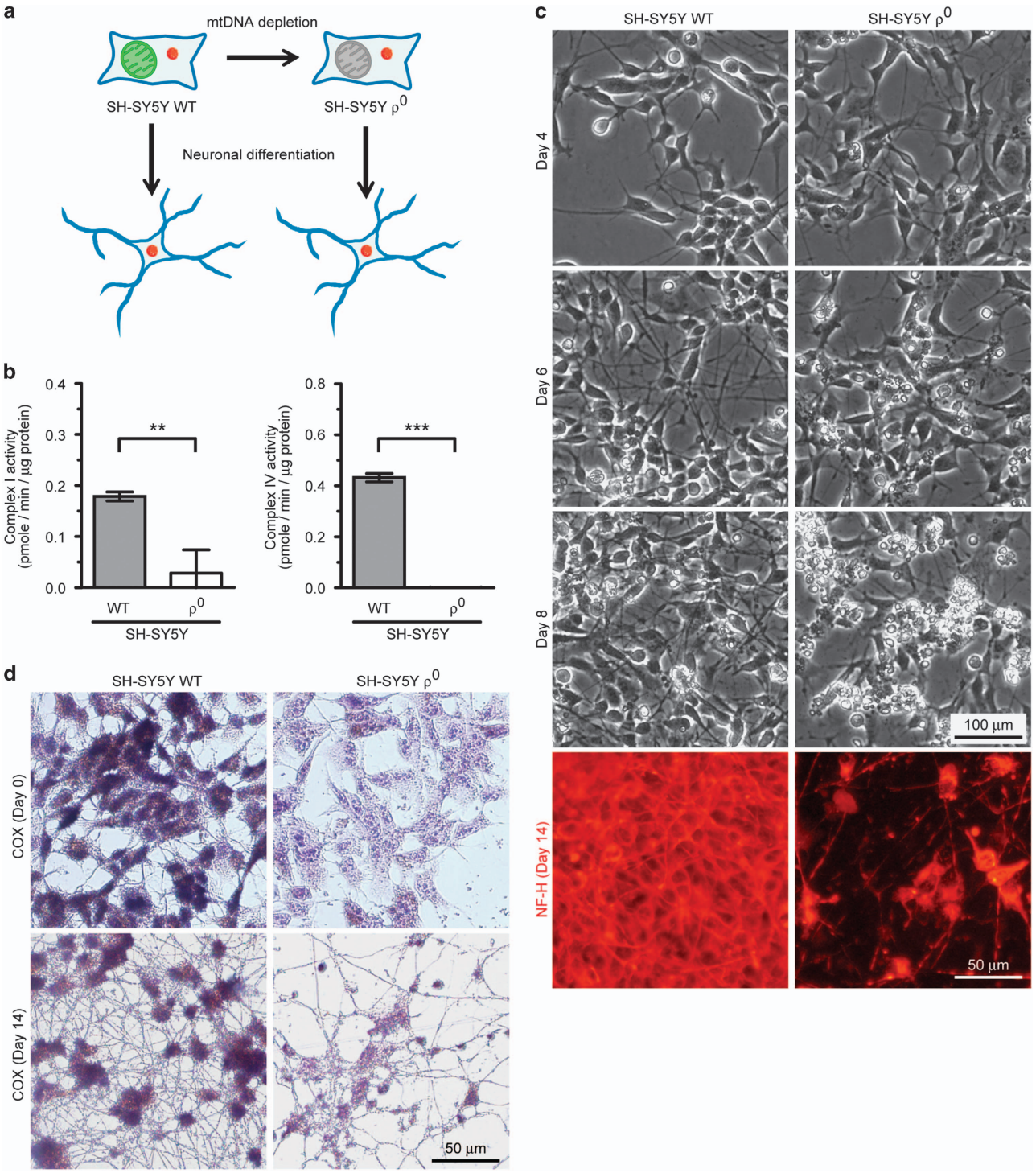

Figure 4 mtDNA-depleted neuroblastoma cells recapitulate neuronal maturation defect and even neuronal cell death during neuronal lineage commitment. (**a**) Experimental design used to identify whether mtDNA-depleted neuroblastoma cells recapitulate neuronal maturation defect and even neuronal cell death during neuronal lineage commitment. (**b**) Mitochondrial respiratory chain complexes activity of neuroblastoma cell lines. Three biological replicates of SH-SY5Y WT and SH-SY5Y ρ^0 were used for the measurements. Statistical significance was evaluated by unpaired, two-tailed *t*-test. $^{**}P<0.01$, $^{***}P<0.001$. (**c**) Representative images of neurons derived from SH-SY5Y WT and SH-SY5Y ρ^0; NF-H (red). Marked neuronal cell death in SH-SY5Y ρ^0 was also observed at day 8. Representative movies of differentiating neurons derived from SH-SY5Y WT and SH-SY5Y ρ^0 were also shown in Supplementary Movies S4 and S5, respectively. (**d**) Representative images of cytochemical COX staining for undifferentiated and differentiated SH-SY5Y WT and SH-SY5Y ρ^0; COX (brown). Cell nuclei were co-stained with hematoxylin (purple). Both samples of SH-SY5Y WT and SH-SY5Y ρ^0 were stained simultaneously for the same period

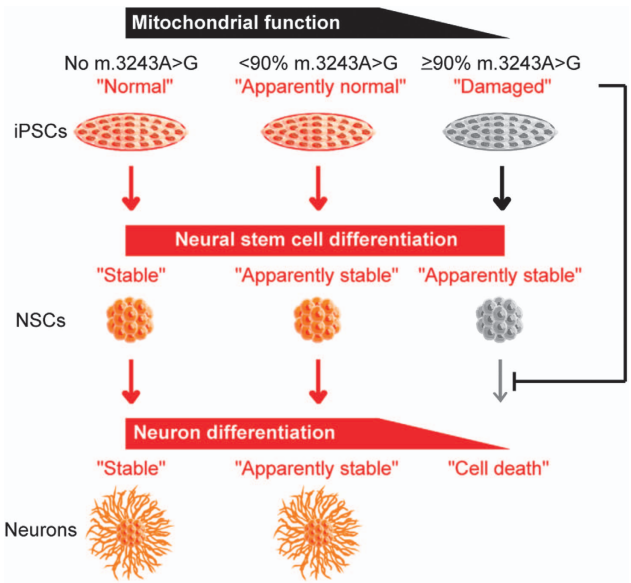

Figure 5 Graphical summary showing the relationship between mtDNA pathogenic threshold and inhibited neuronal differentiation. iPSC lines carrying over the pathogenic threshold level of m.3243A > G showed neuronal maturation defect and even neuronal cell death during neuronal lineage commitment; however, no cell death was observed during NSC specification and expansion in these iPSC lines, suggesting that m.3243A > G has minimal molecular pathogenic influence on NSCs

deletion;[24] this mouse mutant mtDNA exhibited the intrinsic pathogenic threshold level (60–80% proportions of mutant mtDNA) in relation to mitochondrial respiratory function, which was confirmed by *in vitro* biochemical analysis using trans-mitochondrial cellular systems and by *in vivo* phenotypic analysis using several lines of mito-mice.[25] Although there are some experimental differences between their findings and our presenting data (iPSC-based human model vs mouse model, mtDNA point mutation vs mtDNA partial deletion, etc.), the defective *in vitro* differentiation into particular cell types triggered by severely impaired mitochondrial respiration may be suggestive of such *in vivo* embryonic lethality.

Mitochondrial diseases present a broad clinical spectrum even among patients carrying the same heteroplasmic mtDNA mutations (e.g., variations in age of onset, in affected tissues and organs, or in disease progression and phenotypic severity), and vice versa, different mtDNA mutations share similar clinical features in mitochondrial diseases. Such clinical phenotypic diversity frequently makes us complicated to understand the overall pathology of mitochondrial diseases; therefore, curable treatments have yet to be established. Thus, our established isogenic iPSC lines from the same mitochondrial disease patient exhibiting either apparently normal or impaired mitochondrial respiratory function must be promising tools not only to recapitulate tissue- and organ-specific disease phenotypes but also to efficiently explore candidate chemical compounds (i) that ameliorate mitochondrial respiratory dysfunction or (ii) that induce reduced mutant mtDNA proportions. We believe that our presenting data display new insights not only into understanding how mitochondrial respiratory dysfunction triggered by heteroplasmic mtDNA mutations influences cellular fate-determining processes but also into facilitating the applications in future iPSC-based drug discovery and regenerative therapeutics in mitochondrial diseases.

Materials and Methods

Patients. This study was approved by NCNP Institutional Review Board and was stringently conducted in accordance with the ethical principles of the 'Declaration of Helsinki'. Patient biopsy was performed for diagnostic purposes only after we received written informed consent with permission to study patient-derived iPSCs.

Fibroblast culture. Primary fibroblasts were established from patient-derived skin biopsies via a standard protocol. Patient-derived fibroblasts were maintained in DMEM/F12 (Gibco, Waltham, MA, USA) supplemented with 10% FBS (Gibco), 100 units/ml penicillin (Gibco), 100 μg/ml streptomycin (Gibco) at 37 °C under humidified atmosphere of 5% CO_2. Culture medium was changed every 3 days. During establishment of primary fibroblasts, 0.5 μg/ml MC210 (DS Pharm, Osaka, Japan) as a mycoplasmacidal reagent and 2.5 μg/ml fungizone (Gibco) as a fungicidal reagent were also added to culture medium.

Generation of patient-derived iPSCs with episomal vector. Patient-derived iPSCs were generated using episomal vectors as described elsewhere[26] with modifications: briefly, each 1 μg of episomal plasmid vectors (Plasmid #27077, #27078, #27080; Addgene, Cambridge, MA, USA) were electroporated into patient-derived myoblasts (5×10^5 cells) with an electroporator (Neon; Invitrogen, Waltham, MA, USA). Transformed patient-derived myoblasts (1×10^5 cells) were reseeded onto mouse embryonic fibroblasts (MEF; ReproCELL, Yokohama, Japan) 4 days after electroporation. The next day, culture medium was replaced with primate ESC culture medium (ReproCELL) supplemented with 10 ng/ml bFGF (ReproCELL), 100 units/ml penicillin (Gibco), 100 μg/ml streptomycin (Gibco) and transformed patient-derived myoblasts were maintained at 37 °C under humidified atmosphere of 5% CO_2. Culture medium was changed every other day. Emergent colonies with ESC-like morphology were manually picked up to establish patient-derived iPSCs, and these iPSCs were expanded either on MEF-seeded dishes in primate ESC culture medium or on Geltrex (Gibco)-coated dishes in mTeSR1 medium (StemCell Technologies, Vancouver, BC, Canada) supplemented with 100 units/ml penicillin (Gibco) and 100 μg/ml streptomycin (Gibco) for long-term maintenance. Culture medium was changed daily.

To evaluate the distributions of m.3243 A > G proportions in each patient-derived iPSC line, we randomly picked up several iPSC colonies from each patient-derived iPSC line to extract DNA for determination of m.3243 A > G proportions at each single-iPSC-colony level.

Characterization of patient-derived iPSCs. Characterization of patient-derived iPSCs via detection of pluripotency markers was performed according to our previous report:[17] Briefly, cultured and harvested patient-derived iPSCs were transferred onto MEF-seeded multi-well culture plates and were maintained in primate ESC culture medium at 37 °C under humidified atmosphere of 5% CO_2. Culture medium was changed daily. After 3 days in culture, patient-derived iPSCs were characterized by standard immunocytochemical protocol. Fluorophore-conjugated primary antibodies used were as follows: Cy3-conjugated anti-OCT4 (1:100 dilution; Millipore, Billerica, MA, USA), Cy3-conjugated anti-NANOG (1:100 dilution; Millipore), AlexaFluor 488-conjugated anti-TRA-1-60 (1:100 dilution; Millipore), AlexaFluor 488-conjugated anti-TRA-1-81 (1:100 dilution; Millipore). Stained samples were observed under a fluorescent microscope (IX71 System; Olympus, Tokyo, Japan).

in vitro spontaneous differentiation of patient-derived iPSCs into EB-mediated three germ layers was also performed according to our previous report:[17] Briefly, cultured and harvested patient-derived iPSCs were transferred onto ultra-low-adherent culture dishes (HydroCell; CellSeed, Tokyo, Japan) and were maintained in primate ESC culture medium without bFGF at 37 °C under humidified atmosphere of 5% CO_2. Culture medium was changed every other day. After 7 days in floating culture, emergent EBs were transferred onto Geltrex (Gibco)-coated multi-well culture plates and were maintained in primate ESC culture medium without bFGF at 37 °C under humidified atmosphere of 5% CO_2. Culture medium was changed every other day. After 14 additional days in adherent culture, spontaneously differentiated cells were characterized by standard immunocytochemical protocol. Primary antibodies used were as follows: anti-TUJ1 (1:200 dilution; Abcam, Cambridge, UK), anti-αSMA

(1:40 dilution; Abcam), anti-AFP (1:200 dilution; Abcam). Secondary antibody used was AlexaFluor 568 (1:800 dilution; Molecular Probes, Waltham, MA, USA). Stained samples were observed under a fluorescent microscope (IX71 System; Olympus).

Short tandem repeat (STR) analysis was performed to confirm the genetic identity of the established isogenic iPSC lines: Briefly, extracted DNA as template (0.5 ng) was amplified using a thermal cycler (GeneAmp PCR System 9700; Applied Biosystems, Waltham, MA, USA) with a PowerPlex 16 HS System kit (Promega, Fitchburg, WI, USA) according to the manufacturer's instructions. The amplified DNA fragments were electrophoresed using a DNA analyzer (ABI PRISM 3130xl; Applied Biosystems). The obtained data were analyzed using GeneMapper Software (Ver. 5.0; Applied Biosystems).

Analysis of mtDNA mutation. Long PCR-based whole-mtDNA sequencing for the patient was performed as described elsewhere[27] with modifications to eliminate any adverse results arising from pseudo-sequences in nuclear DNA: Briefly, extracted DNA as a template (10 ng) was amplified via mtDNA-specific long-range PCR and the following mtDNA-specific nested PCR using a thermal cycler (GeneAmp PCR System 9700; Applied Biosystems). The amplified mtDNA fragments were sequenced using a DNA analyzer (ABI PRISM 3130xl; Applied Biosystems).

Pyrosequencing was performed to determine m.3243 A > G proportions: Briefly, extracted DNA as a template (10–20 ng) was amplified using a thermal cycler (GeneAmp PCR System 9700; Applied Biosystems). The amplified mtDNA fragments were sequenced using a pyrosequencing instrument (PyroMark Q24 Advanced; Qiagen, Venlo, Netherlands) with a PyroMark Q24 Advanced Reagents kit (Qiagen) according to the manufacturer's instructions. The obtained data were analyzed using PyroMark Q24 Advanced Software (Ver. 3.0.0; Qiagen). Primers used are listed in Supplementary Table S1.

Analysis of mtDNA copy number. mtDNA copy number analysis was performed according to our previous report:[20] Briefly, extracted DNA as a template (1 ng) was used for quantitative PCR with a SYBR Green I PCR Master Mix kit (Roche, Basel, Switzerland) according to the manufacturer's instructions. A real-time PCR system (LightCycler 480II; Roche) was used to measure mtDNA copy number per cell. Measurement for each sample was performed in triplicate. $\Delta\Delta C_T$-based relative quantification method was adopted for data analysis. Primers used are listed in Supplementary Table S1.

Analyses of pluripotency genes expression and transgenes silencing. Reverse transcription was performed with PrimeScript RT Master Mix kit (TaKaRa Bio, Shiga, Japan) according to the manufacturer's instructions. After reverse transcription of extracted total RNA, total cDNA as a template (10 ng) was used for quantitative PCR with a SYBR Green I PCR Master Mix kit (Roche) according to the manufacturer's instructions. A real-time PCR system (LightCycler 480II; Roche) was used to measure pluripotency genes expression and transgenes silencing. Measurement for each sample was performed in triplicate. $\Delta\Delta C_T$-based relative quantification method was adopted for data analysis. Primers used are listed in Supplementary Table S1.

Directed differentiation of iPSCs into cardiomyocytes. Directed differentiation of patient-derived iPSCs into cardiomyocytes was performed as described elsewhere[28] with modifications: Briefly, patient-derived iPSCs were cut into uniform-sized pieces of colonies using the STEMPRO EZ Passage (Invitrogen) to transfer onto Geltrex (Gibco)-coated culture dishes and were maintained in mTeSR1 medium (StemCell Technologies) at 37 °C under humidified atmosphere of 5% CO_2. Culture medium was changed daily. After 7 days in culture, culture medium was switched to Cardiac induction medium I (RPMI 1640 medium (Gibco) supplemented with 1 × B27 minus insulin (Gibco), 100 units/ml penicillin (Gibco), 100 μg/ml streptomycin (Gibco), 100 ng/ml Activin A (Peprotech, Rocky Hill, NJ, USA)) for first 1 day, Cardiac induction medium II (RPMI 1640 medium (Gibco) supplemented with 1 × B27 minus insulin (Gibco), 100 units/ml penicillin (Gibco), 100 μg/ml streptomycin (Gibco), 10 ng/ml BMP4 (Peprotech), 10 ng/ml bFGF (Peprotech)) for next 4 days, and Cardiac induction medium III (RPMI 1640 medium (Gibco) supplemented with 1 × B27 minus insulin (Gibco), 100 units/ml penicillin (Gibco), 100 μg/ml streptomycin (Gibco), 100 ng/ml DKK-1 (Peprotech)) for further 6 days, sequentially. Culture medium was changed every other day. Culture medium was finally switched to Cardiac maturation medium (RPMI 1640 medium (Gibco) supplemented with 1 × B27 minus insulin (Gibco), 100 units/ml penicillin (Gibco), 100 μg/ml streptomycin (Gibco)) and was changed every other day for terminal differentiation. The beating aggregates began to emerge at around 15 days of cardiac differentiation. At 26 or 27 days of cardiac differentiation in total, each beating cardiomyocyte-aggregate was transferred onto each well of Geltrex (Gibco)-coated multi-well culture plates and were used for further analyses.

Emergent cardiomyocytes were maintained in cardiac maturation medium and were characterized according to standard immunocytochemical protocol. Primary antibody used was as follows: anti-cTNT (1:200 dilution; ThermoFisher Scientific, Waltham, MA, USA). Secondary antibody used was as follows: AlexaFluor 568 (1:800 dilution; Molecular Probes). Stained samples were observed under a fluorescent microscope (IX71 System; Olympus).

Directed differentiation of iPSCs into neurons. Directed differentiation of patient-derived iPSCs into neurons was performed as follows: Briefly, cultured and harvested patient-derived iPSCs were transferred onto ultra-low-adherent culture dishes (HydroCell; CellSeed) and were maintained in NSC specification medium (Essential 6 medium (Gibco) supplemented with 100 units/ml penicillin (Gibco), 100 μg/ml streptomycin (Gibco), 10 μM SB431542 (Wako, Osaka, Japan), 100 nM LDN193189 (Wako)) for first 8 days at 37 °C under humidified atmosphere of 5% CO_2. Culture medium was changed every other day. After floating culture, each neurosphere was transferred onto each well of Geltrex (Gibco)-coated multi-well culture plates and were maintained in NSC expansion medium (1:1 mixture of DMEM/F12 (Gibco) and Neurobasal medium (Gibco) supplemented with 1 × N2 (Gibco), 1 × B27 minus vitamin A (Gibco), 1 × GlutaMAX (Gibco), 100 units/ml penicillin (Gibco), 100 μg/ml streptomycin (Gibco), 10 μM SB431542 (Wako), 100 nM LDN193189 (Wako), 20 ng/ml EGF (Peprotech), 20 ng/ml bFGF (Peprotech)) for next 6 days at 37 °C under humidified atmosphere of 5% CO_2. Culture medium was changed every other day. Culture medium was finally switched to Neuron induction medium (Neurobasal medium (Gibco) supplemented with 1 × N2 (Gibco), 1 × B27 minus vitamin A (Gibco), 1 × GlutaMAX (Gibco), 100 units/ml penicillin (Gibco), 100 μg/ml streptomycin (Gibco), 10 ng/ml BDNF (Peprotech), 10 ng/ml GDNF (Peprotech), 10 ng/ml NGF (Peprotech), 500 μM dbcAMP (Sigma), 200 μM ascorbic acid (Wako)) and was changed every other day for terminal differentiation. At 26 or 27 days of neuronal differentiation in total, neurons were used for further analyses.

Emergent NSCs were characterized according to the standard immunocytochemical protocol. Fluorophore-conjugated primary antibodies used were as follows: Cy3-conjugated anti-SOX2 (1:100 dilution; Millipore), AlexaFluor 488-conjugated anti-Nestin (1:100 dilution; Millipore). Stained samples were observed under a fluorescent microscope (IX71 System; Olympus).

Emergent neurons were characterized according to standard immunocytochemical protocol. Primary antibody used was anti-TUJ1 (1:200 dilution; Abcam). Secondary antibody used was AlexaFluor 568 (1:800 dilution; Molecular Probes). Stained samples were observed under a fluorescent microscope (IX71 System; Olympus).

Analysis of mitochondrial respiration. Analysis of mitochondrial respiratory potential was performed using a flux analyzer (Seahorse XF^e24 Extracellular Flux Analyzer; Seahorse Bioscience, North Billerica, MA, USA) with a Seahorse XF Cell Mito Stress Test Kit (Seahorse Bioscience) according to the manufacturer's instructions. Basal respiration and ATP production were calculated to evaluate mitochondrial respiratory function according to the manufacturer's instructions. After the measurement, cells were harvested to count the cell number, and each plotted value was normalized relative to the number of cells used. The detailed procedures are as follows:

For iPSCs, several pieces of iPSC colonies were transferred onto each well of Geltrex (Gibco)-coated XF^e24 cell culture plates (Seahorse Bioscience) and were maintained in primate ESC culture medium. After 3 days in culture, iPSCs were equilibrated in unbuffered XF^e assay medium (Seahorse Bioscience) supplemented with 10 mM glucose, 1 mM sodium pyruvate and transferred to a non-CO_2 incubator for 1 h before measurement. Oxygen consumption rate (OCR) was measured with sequential injections of 2 μM oligomycin, 1 μM FCCP and each 2 μM of rotenone/antimycin A.

For iPSC-cardiomyocytes, each beating cardiomyocyte-aggregate at 23 days of differentiation in total was transferred onto each well of Geltrex (Gibco)-coated XF^e24 cell culture plates (Seahorse Bioscience) and was maintained in Cardiac maturation medium. At 26 or 27 days of differentiation in total, beating cardiomyocytes were equilibrated in unbuffered XF^e assay medium (Seahorse Bioscience) supplemented with 10 mM glucose and 1 mM sodium pyruvate, and transferred to

a non-CO_2 incubator for 1 h before measurement. OCR was measured with sequential injections of 1 μM oligomycin, 0.5 μM FCCP and each 2 μM of rotenone/antimycin A.

For iPSC-neurons, each neurosphere at 8 days of differentiation in total was transferred onto each well of Geltrex (Gibco)-coated XF^{e}24 cell culture plates (Seahorse Bioscience) and was maintained in NSC expansion medium for next 6 days, followed by terminal differentiation in Neuron induction medium. At 26 or 27 days of differentiation in total, neurons were equilibrated in unbuffered XF^e assay medium (Seahorse Bioscience) supplemented with 10 mM glucose and 1 mM sodium pyruvate, and transferred to a non-CO_2 incubator for 1 h before measurement. OCR was measured with sequential injections of 2 μM oligomycin, 0.5 μM FCCP and each 2 μM of rotenone/antimycin A.

Analysis of mitochondrial respiratory chain complex activity. Analysis of mitochondrial respiratory chain complex activity was performed according to our previous report:[20] Briefly, mitochondrial respiratory complex activity was measured with Complex I Human Enzyme Activity Microplate Assay kit (Abcam) and with Complex IV Human Enzyme Activity Microplate Assay kit (Abcam) according to the manufacturer's instructions, respectively. Cell extracts (150 μg for complex I, 50 μg for complex IV) were used to measure time-dependent absorbance alterations on a multi-well plate reader (SPECTROstar Nano; BMG Labtech, Ortenberg, Germany).

Neuroblastoma cell culture and neuronal differentiation. SH-SY5Y neuroblastoma cell line was maintained in Neuroblastoma growth medium (DMEM (Gibco) supplemented with 4.5 mg/ml glucose, 110 μg/ml sodium pyruvate, 50 μg/ml uridine (Sigma, St. Louis, MO, USA), 10% FBS (Gibco), 100 units/ml penicillin (Gibco), 100 μg/ml streptomycin (Gibco)) at 37 °C under humidified atmosphere of 5% CO_2. Culture medium was changed every other day.

For the establishment of mtDNA-depleted cell line (SH-SY5Y ρ^0), sparsely plated SH-SY5Y cells were expanded in Neuroblastoma growth medium (DMEM (Gibco) supplemented with 4.5 mg/ml glucose, 110 μg/ml sodium pyruvate, 50 μg/ml uridine (Sigma), 10% FBS (Gibco), 100 units/ml penicillin (Gibco), 100 μg/ml streptomycin (Gibco)) with the addition of 5 μg/ml ethidium bromide to induce mtDNA depletion for at least 1 month in culture at 37 °C under humidified atmosphere of 5% CO_2. Culture medium was changed every other day.

For neuronal lineage commitment, SH-SY5Y WT and SH-SY5Y ρ^0 (1×10^5 cells, respectively) were transferred onto Geltrex (Gibco)-coated multi-well culture plates or culture dishes and were maintained in Neuroblastoma growth medium (DMEM (Gibco) supplemented with 4.5 mg/ml glucose, 110 μg/ml sodium pyruvate, 50 μg/ml uridine (Sigma), 10% FBS (Gibco), 100 units/ml penicillin (Gibco), 100 μg/ml streptomycin (Gibco)) at 37 °C under humidified atmosphere of 5% CO_2. The next day, culture medium was replaced with Neuron induction medium (Neurobasal medium (Gibco) supplemented with 1 × N2 (Gibco), 1 × B27 minus vitamin A (Gibco), 1 × GlutaMAX (Gibco), 100 units/ml penicillin (Gibco), 100 μg/ml streptomycin (Gibco), 10 ng/ml BDNF (Peprotech), 10 ng/ml GDNF (Peprotech), 10 ng/ml NGF (Peprotech), 500 μM dbcAMP (Sigma), 200 μM ascorbic acid (Wako)) with the addition of 50 μg/ml uridine (Sigma) and was changed every other day for terminal differentiation. At 14 days of neuronal differentiation, neurons were used for further analyses. Time-lapse images of neuronal lineage commitment from day 4 to day 8 were also obtained using a live cell imaging system (BioStudio; Nikon Engineering) at 30 min of interval.

Emergent neurons were characterized according to standard immunocytochemical protocol. Primary antibody used was as follows: anti-NF-H (1:200 dilution; Abcam). Secondary antibody used was as follows: AlexaFluor 568 (1:800 dilution; Molecular Probes). Stained samples were observed under a fluorescent microscope (IX71 System; Olympus).

Cytochemical COX staining. Cytochemical COX staining was performed as follows: Briefly, undifferentiated and differentiated SH-SY5Y WT and SH-SY5Y ρ^0 were stained with COX reaction buffer (pH 5.5; 100 mM sodium acetate, 0.1% $MnCl_2$, 0.001% H_2O_2, 10 mM diaminobenzidine) at 37 °C for 1 h, followed by subsequent incubation with 1% $CuSO_4$ at 37 °C for 5 min. Stained samples were observed under a microscope (IX71 System; Olympus).

Conflict of Interest

The authors declare no conflict of interest.

Acknowledgements. We are grateful to all patients and their families for participating in this study. We would also like to thank Junko Takei, Yumiko Ondo and Saki Okabe (NCNP, Japan) for their assistances. This study was financially supported in part by a Grant-in-Aid for Young Scientists (B) (Grant No. 25860732 to MY) from the Japan Society for the Promotion of Science; by a Grant-in-Aid for the Research on Intractable Diseases (Mitochondrial Disorders) from the Ministry of Health, Labour, and Welfare, Japan; and by an AMED-CREST from the Japan Agency for Medical Research and Development.

Author contributions

HH conceived the study. HH and YG supervised the study. MY and HH designed experiments. MY, YO and MK performed experiments. MY and HH analyzed and interpreted data. MY, HH and YG wrote the manuscript. All authors approved the final manuscript.

1. Armstrong L, Tilgner K, Saretzki G, Atkinson SP, Stojkovic M, Moreno R *et al.* Human induced pluripotent stem cell lines show stress defense mechanisms and mitochondrial regulation similar to those of human embryonic stem cells. *Stem Cells* 2010; **28**: 661–673.
2. Prigione A, Fauler B, Lurz R, Lehrach H, Adjaye J. The senescence-related mitochondrial/oxidative stress pathway is repressed in human induced pluripotent stem cells. *Stem Cells* 2010; **28**: 721–733.
3. Suhr ST, Chang EA, Tjong J, Alcasid N, Perkins GA, Goissis MD *et al.* Mitochondrial rejuvenation after induced pluripotency. *PLoS One* 2010; **5**: e14095.
4. Varum S, Rodrigues AS, Moura MB, Momcilovic O, Easley CA IV, Ramalho-Santos J *et al.* Energy metabolism in human pluripotent stem cells and their differentiated counterparts. *PLoS One* 2011; **6**: e20914.
5. Folmes CD, Nelson TJ, Martinez-Fernandez A, Arrell DK, Lindor JZ, Dzeja PP *et al.* Somatic oxidative bioenergetics transitions into pluripotency-dependent glycolysis to facilitate nuclear reprogramming. *Cell Metab* 2011; **14**: 264–271.
6. Folmes CD, Dzeja PP, Nelson TJ, Terzic A. Metabolic plasticity in stem cell homeostasis and differentiation. *Cell Stem Cell* 2012; **11**: 596–606.
7. Kelly RD, Rodda AE, Dickinson A, Mahmud A, Nefzger CM, Lee W *et al.* Mitochondrial DNA haplotypes define gene expression patterns in pluripotent and differentiating embryonic stem cells. *Stem Cells* 2013; **31**: 703–716.
8. Rossignol R, Faustin B, Rocher C, Malgat M, Mazat JP, Letellier T. Mitochondrial threshold effects. *Biochem J* 2003; **370**: 751–762.
9. Taylor RW, Turnbull DM. Mitochondrial DNA mutations in human disease. *Nat Rev Genet* 2005; **6**: 389–402.
10. Schon EA, DiMauro S, Hirano M. Human mitochondrial DNA: roles of inherited and somatic mutations. *Nat Rev Genet* 2012; **13**: 878–890.
11. Hatakeyama H, Goto Y. Heteroplasmic mitochondrial DNA mutations and mitochondrial diseases: toward iPSC-based disease modeling, drug discovery, and regenerative therapeutics. *Stem Cells* 2016; **34**: 801–808.
12. Fujikura J, Nakao K, Sone M, Noguchi M, Mori E, Naito M *et al.* Induced pluripotent stem cells generated from diabetic patients with mitochondrial DNA A3243G mutation. *Diabetologia* 2012; **55**: 1689–1698.
13. Cherry AB, Gagne KE, McLoughlin EM, Baccei A, Gorman B, Hartung O *et al.* Induced pluripotent stem cells with a mitochondrial DNA deletion. *Stem Cells* 2013; **31**: 1287–1297.
14. Folmes CD, Martinez-Fernandez A, Perales-Clemente E, Li X, McDonald A, Oglesbee D *et al.* Disease-causing mitochondrial heteroplasmy segregated within induced pluripotent stem cell clones derived from a patient with MELAS. *Stem Cells* 2013; **31**: 1298–1308.
15. Hämäläinen RH, Manninen T, Koivumäki H, Kislin M, Otonkoski T, Suomalainen A. Tissue- and cell-type-specific manifestations of heteroplasmic mtDNA 3243 A > G mutation in human induced pluripotent stem cell-derived disease model. *Proc Natl Acad Sci USA* 2013; **110**: E3622–E3630.
16. Kodaira M, Hatakeyama H, Yuasa S, Seki T, Egashira T, Tohyama S *et al.* Impaired respiratory function in MELAS-induced pluripotent stem cells with high heteroplasmy levels. *FEBS Open Bio* 2015; **5**: 219–225.
17. Hatakeyama H, Katayama A, Komaki H, Nishino I, Goto Y. Molecular pathomechanisms and cell-type-specific disease phenotypes of MELAS caused by mutant mitochondrial tRNA(Trp). *Acta Neuropathol Commun* 2015; **3**: 52.
18. Ma H, Folmes CD, Wu J, Morey R, Mora-Castilla S, Ocampo A *et al.* Metabolic rescue in pluripotent cells from patients with mtDNA disease. *Nature* 2015; **524**: 234–238.
19. Goto Y, Nonaka I, Horai S. A mutation in the tRNA(Leu)(UUR) gene associated with the MELAS subgroup of mitochondrial encephalomyopathies. *Nature* 1990; **348**: 651–653.
20. Yokota M, Hatakeyama H, Okabe S, Ono Y, Goto Y. Mitochondrial respiratory dysfunction caused by a heteroplasmic mitochondrial DNA mutation blocks cellular reprogramming. *Hum Mol Genet* 2015; **24**: 4698–4709.
21. Zhou L, Chomyn A, Attardi G, Miller CA. Myoclonic epilepsy and ragged red fibers (MERRF) syndrome: selective vulnerability of CNS neurons does not correlate with the level of

mitochondrial tRNA(lys) mutation in individual neuronal isolates. *J Neurosci* 1997; **17**: 7746–7753.
22. Lax NZ, Hepplewhite PD, Reeve AK, Nesbitt V, McFarland R, Jaros E *et al.* Cerebellar ataxia in patients with mitochondrial DNA disease: a molecular clinicopathological study. *J Neuropathol Exp Neurol* 2012; **71**: 148–161.
23. Petit JM, Magistretti PJ. Regulation of neuron-astrocyte metabolic coupling across the sleep-wake cycle. *Neuroscience* 2016; **323**: 135–156.
24. Ishikawa K, Kasahara A, Watanabe N, Nakada K, Sato A, Suda Y *et al.* Application of ES cells for generation of respiration-deficient mice carrying mtDNA with a large-scale deletion. *Biochem Biophys Res Commun* 2005; **333**: 590–595.
25. Inoue K, Nakada K, Ogura A, Isobe K, Goto Y, Nonaka I *et al.* Generation of mice with mitochondrial dysfunction by introducing mouse mtDNA carrying a deletion into zygotes. *Nat Genet* 2000; **26**: 176–181.
26. Okita K, Matsumura Y, Sato Y, Okada A, Morizane A, Okamoto S *et al.* A more efficient method to generate integration-free human iPS cells. *Nat Methods* 2011; **8**: 409–412.
27. Akanuma J, Muraki K, Komaki H, Nonaka I, Goto Y. Two pathogenic point mutations exist in the authentic mitochondrial genome, not in the nuclear pseudogene. *J Hum Genet* 2000; **45**: 337–341.
28. Masumoto H, Ikuno T, Takeda M, Fukushima H, Marui A, Katayama S *et al.* Human iPS cell-engineered cardiac tissue sheets with cardiomyocytes and vascular cells for cardiac regeneration. *Sci Rep* 2014; **4**: 6716.

Supplementary Information accompanies this paper on Cell Death and Disease website (http://www.nature.com/cddis)

The American Journal of Pathology, Vol. 187, No. 1, January 2017

ELSEVIER

The American Journal of
PATHOLOGY

ajp.amjpathol.org

CELL INJURY, REPAIR, AGING, AND APOPTOSIS

Respiratory Chain Complex Disorganization Impairs Mitochondrial and Cellular Integrity

Phenotypic Variation in Cytochrome c Oxidase Deficiency

Hideyuki Hatakeyama*† and Yu-ichi Goto*†‡

From the Department of Mental Retardation and Birth Defect Research, National Institute of Neuroscience, and the Medical Genome Center,‡ National Center of Neurology and Psychiatry, Tokyo; and AMED-CREST,† Japan Agency for Medical Research and Development, Tokyo, Japan*

Accepted for publication September 19, 2016.

Address correspondence to Hideyuki Hatakeyama, Ph.D., or Yu-ichi Goto, M.D., Ph.D., Department of Mental Retardation and Birth Defect Research, National Institute of Neuroscience, National Center of Neurology and Psychiatry, 4-1-1 Ogawahigashi, Kodaira, Tokyo 187-8502, Japan. E-mail: hideyuki@ncnp.go.jp or goto@ncnp.go.jp.

The relationships between the molecular abnormalities in mitochondrial respiratory chain complexes and their negative contributions to mitochondrial and cellular functions have been proved to be essential for better understandings in mitochondrial medicine. Herein, we established the method to identify disease phenotypic differences among patients with muscle histopathological cytochrome *c* oxidase (COX) deficiency, as one of the representative clinical features in mitochondrial diseases, by using patients' myoblasts that are derived from biopsied skeletal muscle tissues. We identified two obviously different severities in molecular diagnostic criteria of COX deficiency among patients: structurally stable, but functionally mild/moderate defect and severe functional defect with the disrupted COX holoenzyme structure. COX holoenzyme disorganization actually triggered several mitochondrial dysfunctions, including the decreased ATP level, the increased oxidative stress level, and the damaged membrane potential level, all of which lead to the deteriorated cellular growth, the accelerated cellular senescence, and the induced apoptotic cell death. Our cell-based *in vitro* diagnostic approaches would be widely applicable to understanding patient-specific pathomechanism in various types of mitochondrial diseases, including other respiratory chain complex deficiencies and other mitochondrial metabolic enzyme deficiencies. *(Am J Pathol 2017, 187: 110–121; http://dx.doi.org/10.1016/j.ajpath.2016.09.003)*

Cytochrome *c* oxidase [COX; alias complex IV (CIV)] is a terminal protein in the mitochondrial electron transport system with oxidative phosphorylation and comprises its 13 structural subunits. The three largest, most hydrophobic catalytic core subunits are encoded in mitochondrial DNA (mtDNA), and the others are encoded in nuclear DNA (nDNA). In addition, COX also requires several nDNA-encoded assembly factors for its holoenzyme organization and maintenance. COX deficiency is widely recognized as one of the representative clinical phenotypes in mitochondrial diseases and presents muscle histopathological diversity among patients (focally, diffusely, or completely deficient). Although disease-causative mutations in nDNA-encoded assembly factors are mostly inherited as autosomal recessive,[1] only a few detrimental mutations in nDNA-encoded COX structural subunits have been reported.[2,3] Other genetic defects in mtDNA-encoded COX structural subunits[4–10] or in several mitochondrial tRNA genes are also responsible for COX deficiency; moreover, infantile reversible COX deficiency (alias reversible infantile respiratory chain deficiency), which is caused by homoplasmic m.14674T>C or T>G mutations in *MT-TE* gene, has recently been identified as a new disease subtype with rare, distinct disease outcome.[11,12] To date, the relationships between pathogenic mutations in COX-

Supported in part by Japan Society for the Promotion of Science grant-in-aid for Young Researcher B 20790760 (H.H.); a Ministry of Health, Labour, and Welfare, Japan grant-in-aid of the Research on Intractable Diseases (Mitochondrial Disorder) (Y.G.); and Japan Agency for Medical Research and Development AMED-CREST.

Disclosures: None declared.

http://dx.doi.org/10.1016/j.ajpath.2016.09.003

associating components and the aberrant COX holoenzyme organization become evident at a molecular level. However, there still remains no reasonable explanation how such gene-specific defects actually affect widespread mitochondrial and cellular functions, resulting in the variation and the severity of disease phenotypes at tissue and organ levels.

To overcome this problem, the use of cells derived from the affected tissues and organs is advantageous, because such cells faithfully recapitulate cell type−specific pathophysiology in a patient-specific manner. Herein, we established the method to identify disease phenotypic differences in patients exhibiting mitochondrial diseases by using a comprehensive functional analysis at mitochondrion and cell levels. We demonstrated that severely disrupted COX holoenzyme integrity (its function and structure) actually triggered several mitochondrial dysfunctions, including the decreased ATP level, the increased oxidative stress level, and the damaged membrane potential level, followed by the injured cellular homeostasis like the deteriorated cellular growth, the accelerated cellular senescence, and the induced apoptotic cell death. Therefore, COX holoenzyme disorganization determines the variation and the severity in clinical phenotypes of patients exhibiting mitochondrial diseases with muscle histopathological COX deficiency, and our proposed molecular diagnostic criteria may also be suggestive for effectively exploring disease-causative genetic defects, which are responsible for patient-specific pathology.

Materials and Methods

Patients

This study was approved by the institutional review board of the National Center of Neurology and Psychiatry and was stringently conducted in accordance with the ethical principles of the Declaration of Helsinki. Patient skeletal muscle biopsy was performed for diagnostic purposes only after we received written informed consent. Note that 10 control subjects were also used in this study.

mtDNA Mutation Analysis

A long PCR-based whole mtDNA sequence in each patient was performed to eliminate any adverse results associating with pseudosequences in nDNA, as described elsewhere[13] with modifications: Extracted DNA from cultured patients' myoblasts (100 ng) was amplified by mtDNA-specific long-range PCR and the following mtDNA-specific nested PCR using a thermal cycler (GeneAmp PCR System 9700; Applied Biosystems, Waltham, MA). The amplified mtDNA fragments were sequenced using DNA analyzer (ABI PRISM 3130xl; Applied Biosystems). The obtained mtDNA sequence data in each patient were compared with the WEB databases of Human Mitochondrial Genome Database (MITOMAP) and Human Mitochondrial Genome Polymorphism (mtSNP)[14] to find any genetic variants.

RT-PCR

One-step RT-PCR was performed with the PrimeScript II High Fidelity RT-PCR kit (TaKaRa Bio, Shiga, Japan), according to the manufacturer's instructions. Extracted total RNA from cultured patients' myoblasts (100 ng) was applied for RT-PCR using a thermal cycler (GeneAmp PCR system 9700; Applied Biosystems). Amplified PCR products were electrophoresed, stained with ethidium bromide, and detected using UV transilluminator (GelDoc-It Imaging System; UVP, Upland, CA).

Primers used were as follows: *MT-CO1*, 5′-TTAGCTGACTCGCCACACTCC-3′ (forward) and 5′-AGTCAGGCCACCTACGGTGA-3′ (reverse); *MT-CO2*, 5′-CTCATGAGCTGTCCCCACATTAG-3′ (forward) and 5′-TTGACCGTAGTATACCCCCGG-3′ (reverse); *COX4*, 5′-CGGCAGAATGTTGGCTACCA-3′ (forward) and 5′-AGCGAAAAGTCTTCGCTCTTCAC-3′ (reverse); *COX5B*, 5′-TGGCATCTGGAGGTGGTGTT-3′ (forward) and 5′-TGCCTGAAGCTCCCTTTGG-3′ (reverse); and *GAPDH*, 5′-CAATGACCCCTTCATTGACCTC-3′ (forward) and 5′-CTCGCTCCTGGAAGATGGTG-3′ (reverse).

Cell Culture

Small portions of biopsied skeletal muscle tissues from the patients' biceps brachii were minced with surgical scissors and forceps, enzymatically digested with collagenase-trypsin solution [400 μg/mL collagenase (Wako, Osaka, Japan), 5× trypsin-EDTA (Gibco, Waltham, MA)] at 37°C for 1 hour, and centrifuged at 200 × *g* for 5 minutes to collect myoblasts. Cells were resuspended and seeded onto tissue culture dishes and were maintained at 37°C under humidified atmosphere of 5% CO_2. Myoblast culture medium used was as follows: Dulbecco's modified Eagle's medium with F12 nutrient mixture (Gibco) supplemented with 20% fetal bovine serum (Gibco), 100 U/mL penicillin (Gibco), and 100 μg/mL streptomycin (Gibco). During primary culture, 0.5 μg/mL MC210 (DS Pharm, Osaka, Japan) as a mycoplasmacidal reagent and 2.5 μg/mL fungizone (Gibco) as a fungicidal reagent were also added into myoblast culture medium.

For cellular proliferation experiment, patients' myoblasts (100 cells/mm^2) were seeded onto 96-well culture plates and were maintained at 37°C under humidified atmosphere of 5% CO_2. After 3 days in culture, cells were treated with bromodeoxyuridine chemiluminescence-based cell proliferation enzyme-linked immunosorbent assay kit (Roche, Basel, Switzerland), according to the manufacturer's instructions, and cellular proliferation potential was measured on chemiluminescent multiwell plate reader (Centro LB 960; Berthold Technologies, Bad Wildbad, Germany).

For cellular growth experiment, patients' myoblasts (50 cells/mm^2) were seeded onto 6-well culture plates and were maintained at 37°C under humidified atmosphere of 5% CO_2. Cells were observed under phase contrast microscope (IX71 System; Olympus, Tokyo, Japan) at

predetermined time intervals. Cell number per unit area was randomly counted and averaged in each sample. Cellular doubling time was also estimated at logarithmic proliferation stage.

For cellular senescence detection, patients' myoblasts (100 cells/mm^2) were seeded onto 4-well culture slides and were maintained at 37°C under humidified atmosphere of 5% CO_2. After 3 days in culture, cells were treated with senescence-associated β-galactosidase staining kit (Cell Signaling Technology, Danvers, MA), according to the manufacturer's instructions, and senescent cells were observed under optical microscope (BX50 System; Olympus).

For apoptotic cell death detection, patients' myoblasts (100 cells/mm^2) were seeded onto 6-well culture plates and were maintained at 37°C under humidified atmosphere of 5% CO_2. After 3 days in culture, cells were treated with caspase-3 detection kit (Biotium, Fremont, CA), according to the manufacturer's instructions, and apoptotic cell death was observed under fluorescent microscope (IX71 System; Olympus).

For terminal differentiation into myotubes, patients' myoblasts (200 cells/mm^2) were seeded onto 6-well culture plates and were maintained at 37°C under humidified atmosphere of 5% CO_2. After 3 days in culture, culture medium was switched to differentiation medium (Cell Applications, San Diego, CA) supplemented with 100 U/mL penicillin (Gibco) and 100 μg/mL streptomycin (Gibco), and cells were maintained for 2 weeks.

Cytochemistry

Patients' myoblasts (100 cells/mm^2) were seeded onto 4-well culture slides and were maintained at 37°C under humidified atmosphere of 5% CO_2. After 3 days in culture, cells were stained with COX reaction buffer (pH 5.5; 100 mmol/L sodium acetate, 0.1% $MnCl_2$, 0.001% H_2O_2, and 10 mmol/L diaminobenzidine) at 37°C for 1 hour and were incubated with 1% $CuSO_4$ at 37°C for 5 minutes. Cell nuclei were costained with hematoxylin. Stained cells were rinsed, fixed, and dehydrated according to standard histological protocol. Samples were sealed with cover glass and were observed under optical microscope (BX50 System; Olympus).

Immunocytochemistry

Cultured patients' myoblasts and differentiated myotubes were fixed, permeabilized, and blocked according to standard immunocytochemical protocol. Primary antibody probing was performed at room temperature for 90 minutes. Secondary antibody probing was performed with 2.5 μg/mL Alexa Fluor 568 (Molecular Probes, Waltham, MA) at room temperature for 45 minutes. Stained cells were observed under fluorescent microscope (IX71 System; Olympus).

Primary antibodies used were as follows: 2.5 μg/mL anti−MT-CO1 (Molecular Probes), 2.5 μg/mL anti-COX4 (Molecular Probes), 0.5 μg/mL anti-SDHA (Molecular Probes), 5 μg/mL anti-myogenin (Abcam, Cambridge, UK), and 5 μg/mL anti−actin, α 1, skeletal muscle (Abcam).

Mitochondrial Enzymatic Activity

Enzymatic activities for individual mitochondrial respiratory chain complexes were analyzed as described elsewhere[15] with modifications: Cultured and harvested patients' myoblasts (100,000 cells/assay) were permeabilized with 0.1% digitonin at room temperature for 1 minute with gentle pipetting and were used for the experiment. A spectrophotometer equipped with a thermostated unit (U-2010; Hitachi, Tokyo, Japan) was used, and a baseline calibration was done before each measurement.

For complex I activity measurement, permeabilized cells were added into reaction buffer (pH 7.4; 50 mmol/L Tris-HCl, 250 mmol/L sucrose, 1 mmol/L EDTA, 10 μmol/L decylubiquinone, 50 μmol/L NADH, 5 μg/mL antimycin A, and 2 mmol/L KCN) and were incubated in quartz cuvette at 37°C. Complex I activity was monitored by time-dependent absorbance alterations.

For complex II activity measurement, permeabilized cells were added into reaction buffer (pH 7.4; 50 mmol/L potassium phosphate, 20 mmol/L succinate, 50 μmol/L 2,6-dichlorophenolindophenol, 50 μmol/L decylubiquinone, 5 μg/mL rotenone, 5 μg/mL antimycin A, and 2 mmol/L KCN) and were incubated in quartz cuvette at 37°C. Complex II activity was monitored by time-dependent absorbance alterations.

For complex III activity measurement, permeabilized cells were added into reaction buffer [pH 7.4; 50 mmol/L Tris-HCl, 250 mmol/L sucrose, 1 mmol/L EDTA, 50 μmol/L cytochrome *c*, 50 μmol/L decylubiquinol (reduced form of decylubiquinone), and 2 mmol/L KCN] and were incubated in quartz cuvette at 37°C. Complex III activity was monitored by time-dependent absorbance alterations.

For complex IV activity measurement, permeabilized cells were added into reaction buffer [pH 7.4; 10 mmol/L potassium phosphate and 25 μmol/L ferrocytochrome *c* (reduced form of cytochrome *c*)] and were incubated in quartz cuvette at 37°C. Complex IV activity was monitored by time-dependent absorbance alterations.

For citrate synthase activity measurement, permeabilized cells were added into reaction buffer [pH 8.0; 125 mmol/L Tris-HCl, 300 μmol/L acetyl-CoA, 100 μmol/L 5,5′-dithiobis (2-nitrobenzoic acid), and 500 μmol/L oxaloacetate] and were incubated in quartz cuvette at 37°C. Citrate synthase activity was monitored by time-dependent absorbance alterations.

Electrophoretic Protein Separation

SDS-PAGE, blue native PAGE (BN-PAGE), and two-dimensional BN-PAGE/SDS-PAGE were performed as described elsewhere[16,17] with modifications, respectively: Cultured and harvested patients' myoblasts were resuspended

in isolation buffer (pH 7.4; 210 mmol/L mannitol, 70 mmol/L sucrose, 1 mmol/L EGTA, and 5 mmol/L HEPES) and were homogenated on ice. Cell lysates were centrifuged to isolate mitochondrial proteins. Obtained mitochondrial proteins were quantified by Bradford assay, and a calibration curve was generated using several known concentrations of bovine serum albumin.

For SDS-PAGE, isolated mitochondrial proteins (100 μg) were solubilized with 0.5% SDS containing 50 mmol/L dithiothreitol at 70°C for 10 minutes and were used for the experiment. Electrophoresis was performed on 4% to 12% NuPAGE polyacrylamide gel (Invitrogen, Waltham, MA) at room temperature under 200-V constant.

For BN-PAGE, isolated mitochondrial proteins (100 μg) were solubilized with either 0.5% *n*-dodecyl-β-D-maltoside (individual complexes detection) or 1% digitonin (supercomplexes detection) on ice for 30 minutes and were used for the experiment. Electrophoresis was performed on 3% to 12% NativePAGE polyacrylamide gel (Invitrogen) at 4°C under 150-V constant for 30 minutes, then resumed at 4°C under 250-V constant.

Western Blot for Immunodetection

Electrophoresed gels were blotted onto polyvinylidene difluoride membranes using iBlot transfer system (Invitrogen), according to the manufacturer's instructions. Blotted polyvinylidene difluoride membranes were blocked at room temperature for 30 minutes. Primary antibody probing was performed at room temperature for 90 minutes. Secondary antibody probing was performed with chromogenic antibody detection kit (WesternBreeze; Invitrogen), according to the manufacturer's instructions.

For SDS-PAGE and immunodetection, primary antibodies used were as follows: 0.5 μg/mL anti-SDHA (Molecular Probes), 2.5 μg/mL anti−MT-CO1 (Molecular Probes), 2.5 μg/mL anti−MT-CO2 (Molecular Probes), 2.5 μg/mL anti-COX4 (Molecular Probes), 2.5 μg/mL anti-COX5B (Molecular Probes), and 2.5 μg/mL anti-COX6B (Molecular Probes).

For BN-PAGE and immunodetection, primary antibodies used were as follows: 0.5 μg/mL anti-NDUFA9 (Molecular Probes), 0.5 μg/mL anti-SDHA (Molecular Probes), 0.5 μg/mL anti-UQCRC2 (Molecular Probes), 2.5 μg/mL anti−MT-CO1 (Molecular Probes), and 0.5 μg/mL anti-ATP5B (Molecular Probes).

Detection of Intracellular ATP

Cultured and harvested patients' myoblasts (100 cells/assay) were applied for the measurements. Cells were treated with rLuciferase/Luciferin chemiluminescence-based ATP detection kit (Promega, Fitchburg, WI), according to the manufacturer's instructions, and intracellular ATP amount was measured on chemiluminescent multiwell plate reader (Centro LB 960; Berthold Technologies). A calibration curve was generated using several known concentrations of ATP.

Detection of Mitochondrial Oxidative Stress and Mitochondrial Membrane Potential

Quantitative fluorometry was performed as follows: Patients' myoblasts (100 cells/mm^2) were seeded onto 96-well culture plates and were maintained at 37°C under humidified atmosphere of 5% CO_2. After 3 days in culture, cells were stained at 37°C for 1 hour. Stained cells were rinsed and measured on fluorescent multiwell plate reader (ARVO SX; Perkin Elmer, Waltham, MA), first at excitation/emission of 545/595 nm (red fluorescence) and then sequentially at excitation/emission of 485/535 nm (green fluorescence).

Fluorescent imaging was performed as follows: Patients' myoblasts (100 cells/mm^2) were seeded onto 6-well culture plates and were maintained at 37°C under humidified atmosphere of 5% CO_2. After 3 days in culture, cells were stained at 37°C for 1 hour. Stained cells were rinsed and observed under fluorescent microscope (IX71 System; Olympus).

Fluorescent dyes used were as follows: 0.25 μg/mL MitoTracker Green (Molecular Probes), 0.25 μg/mL MitoSOX Red (Molecular Probes), and 0.25 μg/mL JC-1 (Molecular Probes).

Results

Molecular Pathogenic Variation among Patients with COX Deficiency

We examined seven mitochondrial disease patients with muscle histopathological COX deficiency, all of whom carry no detrimental mutation on entire mtDNA sequence (Supplemental Tables S1−S7). In addition, no typical pathological abnormality was observed in all patient-derived skeletal muscle tissues other than COX deficiency (Supplemental Figure S1). On muscle histopathological COX staining, the numerical and distributional variation of COX-negative muscle fibers was observed among patients' tissues (Figure 1A); Patients 5 and 6 also exhibited completely deficient COX activity. On cytochemical COX staining, a wide variety of the decreased COX activity was also observed among patients' myoblasts (Figure 1A), showing a trend similar to muscle histopathological COX staining. BN-PAGE and immunodetection indicated that the apparently diminished band corresponding to COX holoenzyme was detected only in Patients 5 and 6, whereas the other patients showed stable COX holoenzyme organization (Figure 1B); Patients 5 and 6 also showed no COX-containing respiratory chain supramolecular architectures that were essential for efficient ATP production in the mitochondrial electron transport system (Figure 1C). The assembly of the other respiratory chain complexes was unaffected in all patients. We therefore defined Patients 5

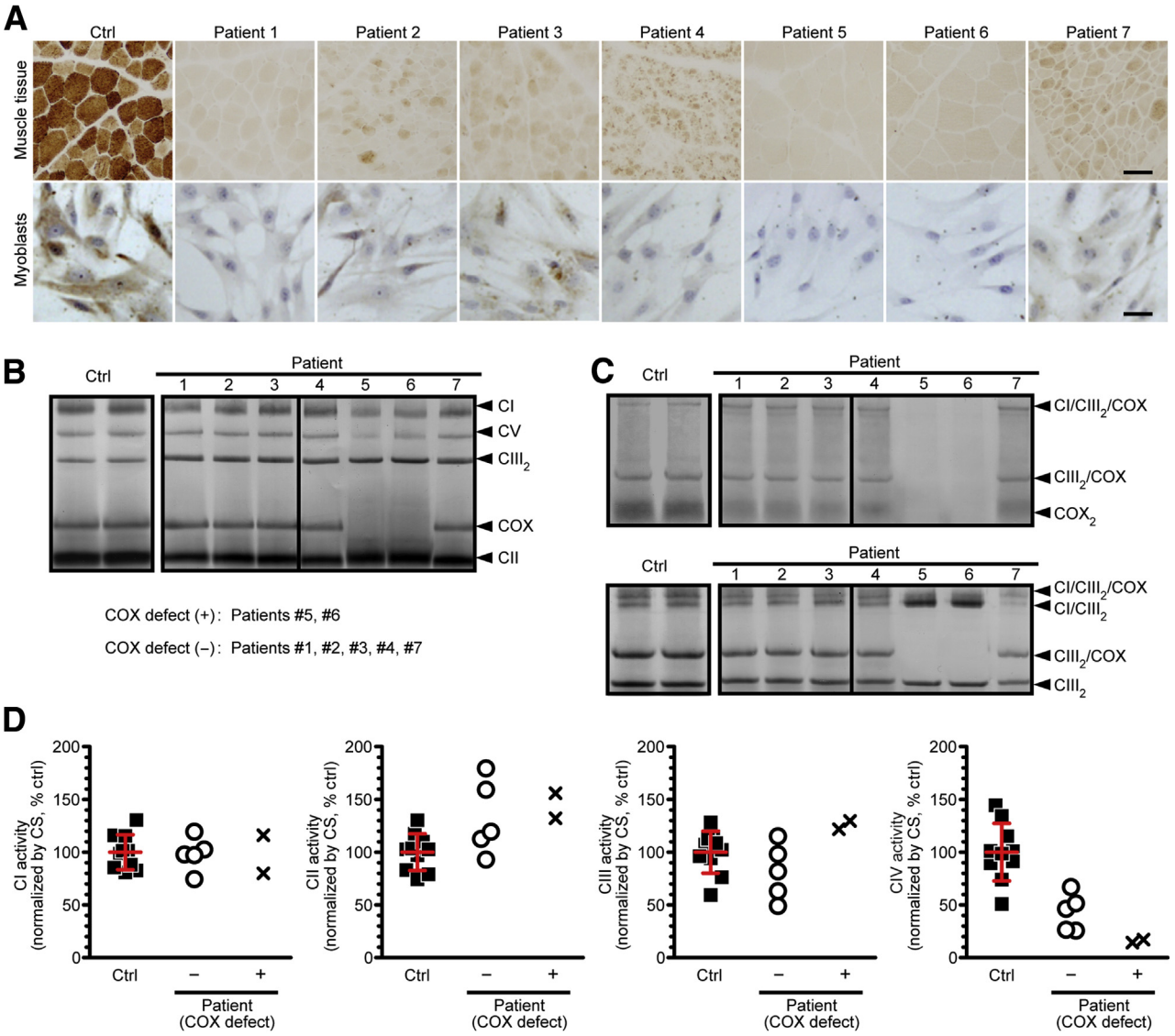

Figure 1 Molecular pathogenic variation among patients with COX deficiency. **A:** Representative images of COX staining for frozen section of skeletal muscle specimens (**top row**) and for cultured myoblasts (**bottom row**) of both controls (Ctrl) and patients. On cytochemical COX staining for cultured myoblasts, all samples were stained simultaneously with the same period. Cell nuclei were costained with hematoxylin. **B:** Immunodetection of individual respiratory chain complexes (CI, CII, CIII, COX, and CV) by BN-PAGE for the same amount of isolated mitochondrial proteins from both controls and patients. Primary antibodies used were as follows: anti-NDUFA9 (CI), anti-SDHA (CII), anti-UQCRC2 (CIII), anti—MT-CO1 (COX), and anti-ATP5B (CV). All samples were assayed at least in duplicate. **C:** Immunodetection of respiratory chain supercomplexes by BN-PAGE for the same amount of isolated mitochondrial proteins from both controls and patients. Primary antibodies used were as follows: anti—MT-CO1 (COX) (**top row**) and anti-UQCRC2 (CIII) (**bottom row**). All samples were assayed at least in duplicate. **D:** Enzymatic activities of individual mitochondrial respiratory chain complexes for cultured and harvested myoblasts of both controls and patients. Citrate synthase (CS) activity, as an internal marker in mitochondrial functions, was used for normalization in each sample. All samples were measured at least in duplicate and averaged. The **error bars** indicate means ± SD of controls (**D**). $n = 10$ (**D**, controls); $n = 5$ [**D**, COX defect (−)]; $n = 2$ [**D**, COX defect (+)]. Scale bars = 50 μm (**A**).

and 6 lacking COX holoenzyme as COX defect (+) and the other patients exhibiting stable COX holoenzyme as COX defect (−). Enzymatic activities of mitochondrial respiratory chain complexes revealed that COX activity in all patients was significantly decreased when compared with controls (Figure 1D); Patients 5 and 6 as COX defect (+) also displayed lower biochemical COX function. The other respiratory chain complex activities in all patients were almost within normal range, except for relatively higher complex II activity, probably because of functional compensation in mitochondrial oxidative phosphorylation. From molecular diagnostic aspects in mitochondrial respiratory chain complexes, we concluded that all patients used in this study must be isolated COX deficiency.

Two-dimensional BN-PAGE/SDS-PAGE implied that the apparent loss of COX holoenzyme found only in Patients 5 and 6 was because of drastically decreased amounts of all COX structural subunits when compared with other

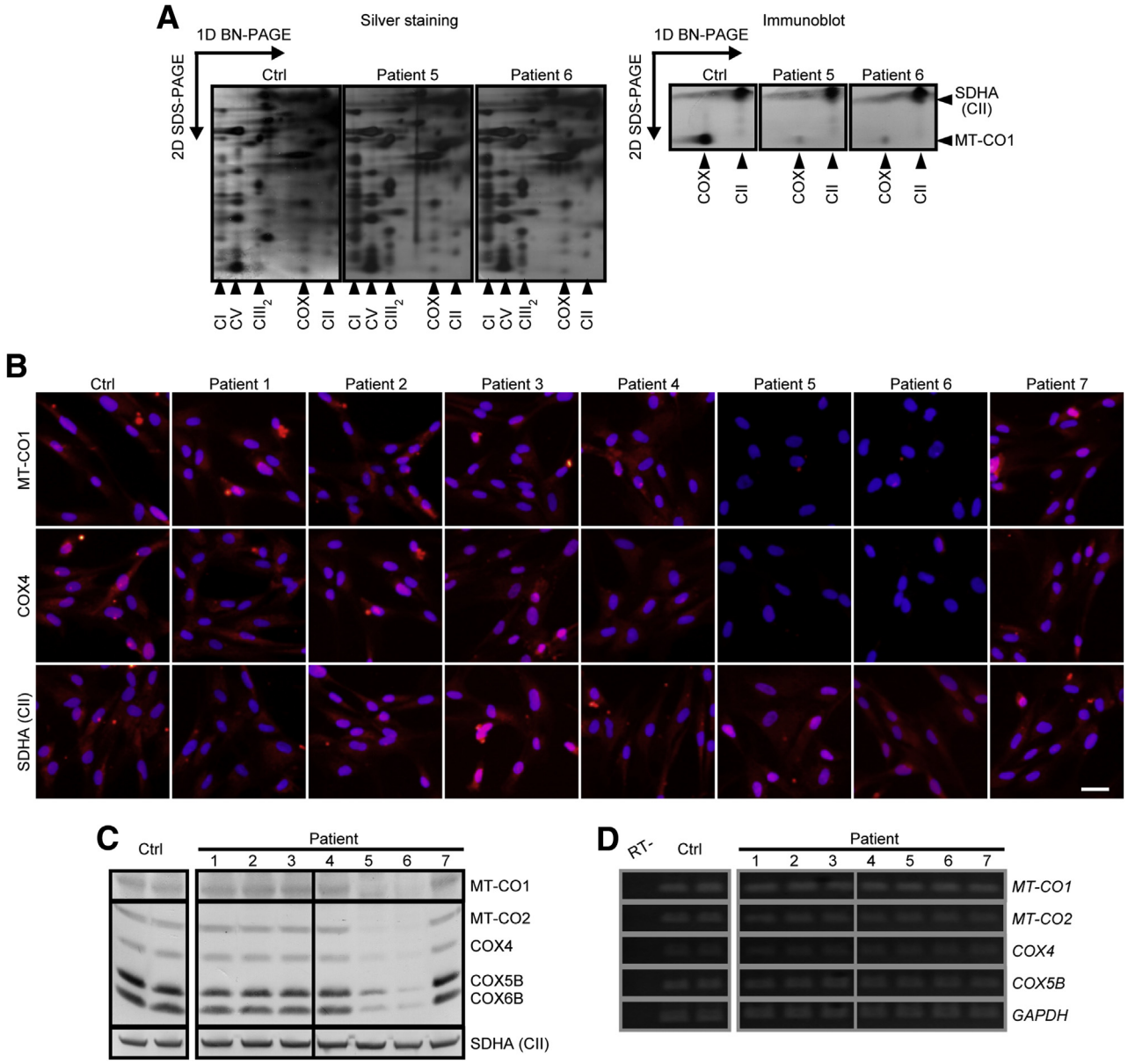

Figure 2 COX holoenzyme disorganization, found only in Patients 5 and 6, originates in the decreased protein levels, but not in mRNA levels, of each structural subunit. **A:** Visualization of all structural components in respiratory chain complexes by two-dimensional blue native PAGE (BN-PAGE)/SDS-PAGE and silver staining for the same amount of isolated mitochondrial proteins from both controls (Ctrl) and Patients 5 and 6 as COX defect (+). Immunodetection against MT-CO1 (COX) and SDHA (CII) was also shown. All samples were assayed at least in duplicate. **B:** Representative images of immunocytochemistry against MT-CO1 [COX, mitochondrial DNA (mtDNA) encoded], COX4 [COX, nuclear DNA (nDNA) encoded], and SDHA (CII) for cultured myoblasts of both controls and patients. Cell nuclei were costained with Hoechst 33342 (blue). **C:** Protein expression levels in COX structural subunits of MT-CO1 (mtDNA encoded), MT-CO2 (mtDNA encoded), COX4 (nDNA encoded), COX5B (nDNA encoded), and COX6B (nDNA encoded) by SDS-PAGE and immunodetection for the same amount of isolated mitochondrial proteins from both controls and patients. SDHA (CII) was used as an internal marker. All samples were assayed at least in duplicate. **D:** mRNA expression levels in COX structural subunits of *MT-CO1* (mtDNA encoded), *MT-CO2* (mtDNA encoded), *COX4* (nDNA encoded), *COX5B* (nDNA encoded) by RT-PCR for the same amount of extracted total RNA from both controls and patients. *GAPDH* was used as an internal marker. RT- indicates without the addition of reverse transcriptase in RT-PCR. All samples were assayed at least in duplicate. Scale bar = 50 μm (**B**).

respiratory chain complex components (Figure 2A); it was consistent with the results of immunocytochemistry against both COX structural subunits of mtDNA-encoded MT-CO1 and nDNA-encoded COX4 (Figure 2B). In fact, significantly lower protein expression levels of several COX structural subunits were confirmed only in Patients 5 and 6 when compared with controls and the other patients exhibiting stable COX holoenzyme organization (Figure 2C). However, no significant alteration in mRNA expression levels was observed in all patients when compared with controls (Figure 2D). These results suggest that COX holoenzyme disorganization, found only in Patients 5 and 6, originates in the decreased protein levels, but not in mRNA levels, of each COX structural subunit.

Severely Impaired COX Holoenzyme Integrity Triggers the Deteriorated Mitochondrial and Cellular Homeostasis, but Does Not Affect Skeletal Muscle Development

To further investigate the influences of severely impaired COX holoenzyme integrity on mitochondrial and cellular homeostasis, we added cell-based functional analysis in all patients. The decreased ATP level was observed only in Patients 5 and 6 as COX defect (+) when compared with controls and the other patients exhibiting stable COX holoenzyme organization (Figure 3A). Interestingly, the increased oxidative stress level (Figure 3, B and D) and the damaged membrane potential level (Figure 3, C and E) were both markedly detected only in Patients 5 and 6 as COX defect (+), whereas the other patients showed no significant alteration in mitochondrial functions when compared with those of controls. These results demonstrate that COX holoenzyme disorganization can strongly induce several mitochondrial dysfunctions.

Among patients' myoblast lines, Patients 5 and 6 as COX defect (+) exhibited significantly deteriorated proliferative potential in living cells (Figure 4A); it was consistent with the results of growth rate (Figure 4B) and doubling time (Figure 4B). Remarkably, some senescence-associated β-galactosidase−positive senescent cells (Figure 4C) and caspase 3−positive apoptotic cells (Figure 4D) were also detected only in Patients 5 and 6 as COX defect (+), even

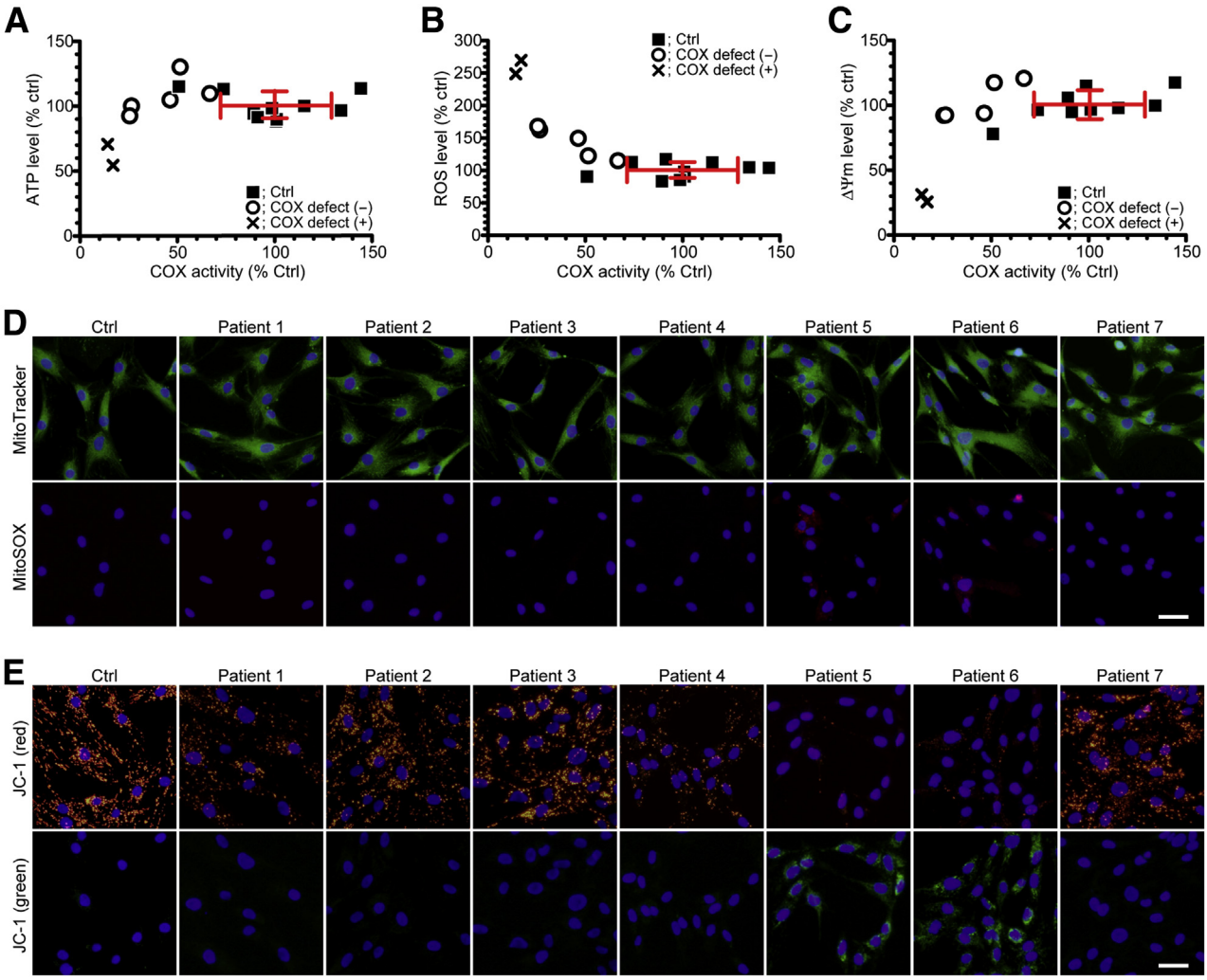

Figure 3 Severely impaired COX holoenzyme integrity triggers mitochondrial dysfunctions. **A:** Relationship between COX activity and ATP level for cultured and harvested myoblasts of both controls (Ctrl) and patients. All samples were measured at least in duplicate and averaged. **B:** Relationship between COX activity and oxidative stress [reactive oxygen species (ROS)] level for cultured myoblasts of both controls and patients. All samples were measured at least in duplicate and averaged. **C:** Relationship between COX activity and membrane potential (ΔΨm) level for cultured myoblasts of both controls and patients. All samples were measured at least in duplicate and averaged. **D:** Representative images of the intracellular localization of MitoTracker (green) or MitoSOX (red) for cultured myoblasts of both controls and patients. Cell nuclei were costained with Hoechst 33342 (blue). **E:** Representative images of the intracellular localization of JC-1 monomer (green) or aggregates (red) for cultured myoblasts of both controls and patients. Cell nuclei were costained with Hoechst 33342 (blue). The **error bars** indicate means ± SD of controls (**A**–**C**). $n = 10$ (**A**–**C**, controls); $n = 5$ [**A**–**C**, COX defect (−)]; $n = 2$ [**A**–**C**, COX defect (+)]. Scale bars = 50 μm (**D** and **E**).

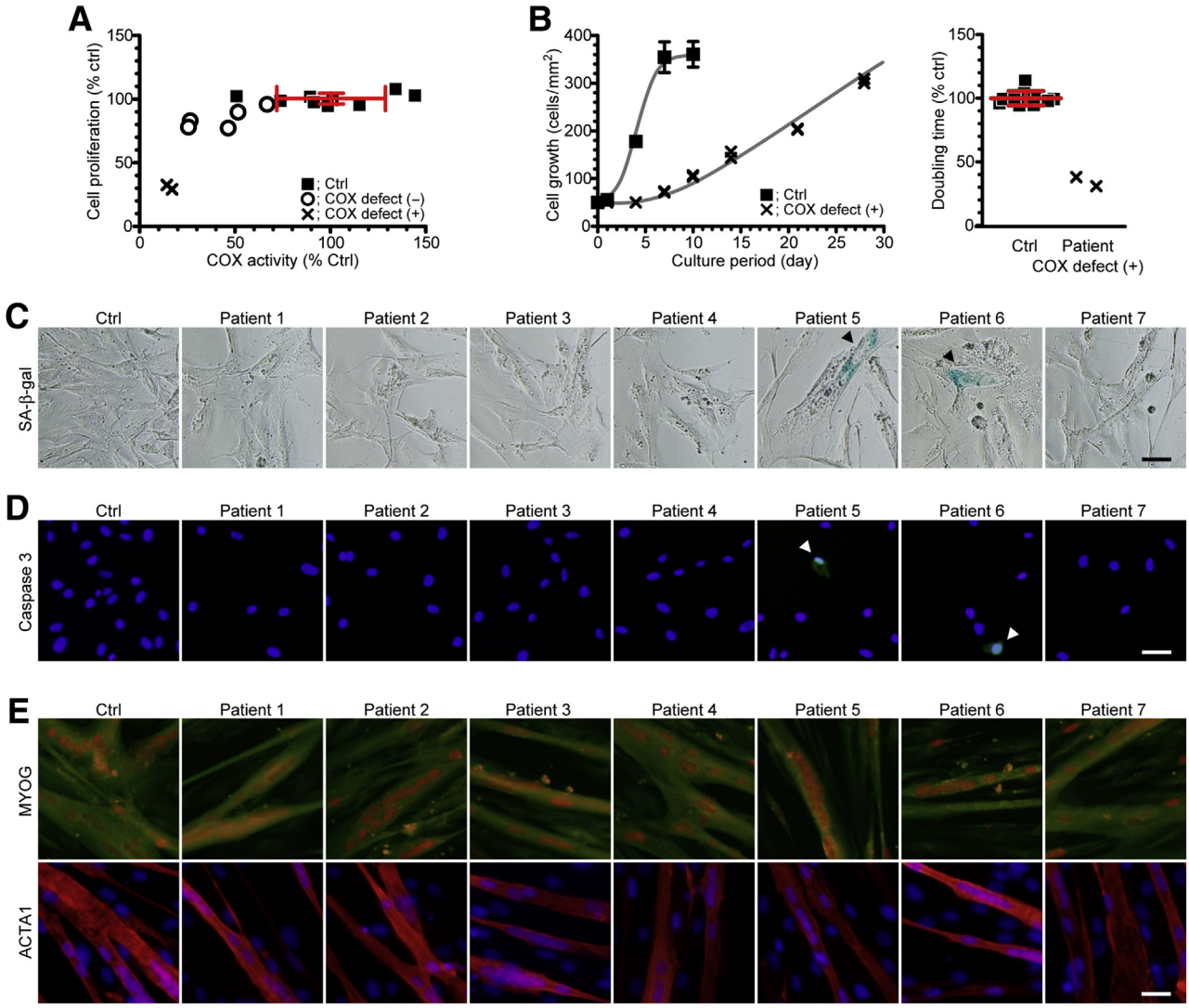

Figure 4 Severely impaired COX holoenzyme integrity also induces cellular dysfunctions, but does not affect skeletal muscle development. **A:** Relationship between COX activity and cellular proliferation potential (bromodeoxyuridine assay) for cultured myoblasts of both controls (Ctrl) and patients. All samples were measured at least in duplicate and averaged. **B:** Cellular growth rate for cultured myoblasts of both controls and Patients 5 and 6 as COX defect (+). The estimated doubling time in each sample was also shown. All samples were measured at least in duplicate and averaged. **C:** Representative images of cellular senescence for cultured myoblasts of both controls and patients. **Arrowheads** indicate senescence-associated β-galactosidase (SA-β-gal)—positive senescent cells. All samples were stained simultaneously with the same period. **D:** Representative images of apoptotic cell death for cultured myoblasts of both controls and patients. **Arrowheads** indicate caspase 3—positive apoptotic cells (green). Cell nuclei were costained with Hoechst 33342 (blue). **E:** Representative images of immunocytochemistry against skeletal muscle tissue—specific markers of myogenin (MYOG) and actin, α 1, skeletal muscle (ACTA1) for differentiated myotubes of both controls and patients. On MYOG immunostaining, mitochondria were costained with MitoTracker (green). On ACTA1 immunostaining, cell nuclei were costained with Hoechst 33342 (blue). The **error bars** indicate means ± SD of controls (**A** and **B**). $n = 10$ (**A** and **B**, controls); $n = 5$ [**A**, COX defect (−)]; $n = 2$ [**A** and **B**, COX defect (+)]. Scale bars = 50 μm (**C**–**E**).

under stable cell growth condition. Nevertheless, no apparent difference in *in vitro* differentiation propensity of myoblasts into myotubes was confirmed in all patients when compared with controls, which was determined by the results of immunocytochemistry against skeletal muscle tissue-specific markers of myogenin and actin, α 1, skeletal muscle (Figure 4E). These results demonstrate that mitochondrial dysfunctions triggered by COX holoenzyme disorganization can induce widespread cellular dysfunctions, but cannot affect skeletal muscle development in patients. The data presenting mitochondrial and cellular biochemical diagnosis in each patient are summarized in Table 1.

Discussion

In this study, we characterized disease phenotypic differences among patients exhibiting mitochondrial diseases with muscle histopathological COX deficiency by using a comprehensive functional analysis in mitochondria and cells. We demonstrated that widespread mitochondrial and cellular dysfunctions were actually dominated, at least in

Table 1 Mitochondrial and Cellular Biochemical Diagnosis in Each Patient with Muscle Histopathological COX Deficiency

Patient no.	COX function*	COX structure	ATP level*	ROS level*	ΔΨm level*	Cellular proliferation*	Cellular senescence	Cellular apoptosis	Cellular differentiation
10 Controls	100.0 ± 27.2	Normal	100.0 ± 10.3	100.0 ± 12.2	100.0 ± 11.2	100.0 ± 3.9	ND	ND	Normal
1	26.5	Normal	100.2	162.5	92.5	83.1	ND	ND	Normal
2	46.4	Normal	104.8	149.6	93.9	77.3	ND	ND	Normal
3	51.5	Normal	130.2	122.6	117.6	89.8	ND	ND	Normal
4	25.6	Normal	92.6	168.2	92.3	78.1	ND	ND	Normal
5	14.3	ND	70.7	248.9	31.1	32.5	Detected	Detected	Normal
6	17.1	ND	54.4	269.8	25.6	29.1	Detected	Detected	Normal
7	66.9	Normal	109.7	115.2	120.8	96.0	ND	ND	Normal

COX, cytochrome *c* oxidase; ND, not detected; ROS, reactive oxygen species; ΔΨm, membrane potential.
*Values are expressed as the percentage against the mean value of 10 controls.

part, by the aberrant COX holoenzyme organization, possibly underlying the variation and the severity in clinical phenotypes of patients. According to these results, we also think it reasonable to classify two obviously different severities in molecular diagnostic criteria of COX deficiency (Figure 5): structurally stable, but functionally mild/moderate defect and severe functional defect with the disrupted COX holoenzyme structure, followed by several mitochondrial and cellular dysfunctions. Patients 5 and 6 are categorized as histopathologically and biochemically severe COX deficiency because of COX holoenzyme disorganization, which must be caused by genetic defects in COX-associating genes. On the other hand, the other patients may be affected by functional abnormality of COX holoenzyme itself or by other unknown physiological abnormalities to apparently induce muscle histopathological COX deficiency as secondary clinical phenotypes. In these cases, it is speculated that disease-causative mutations of muscle

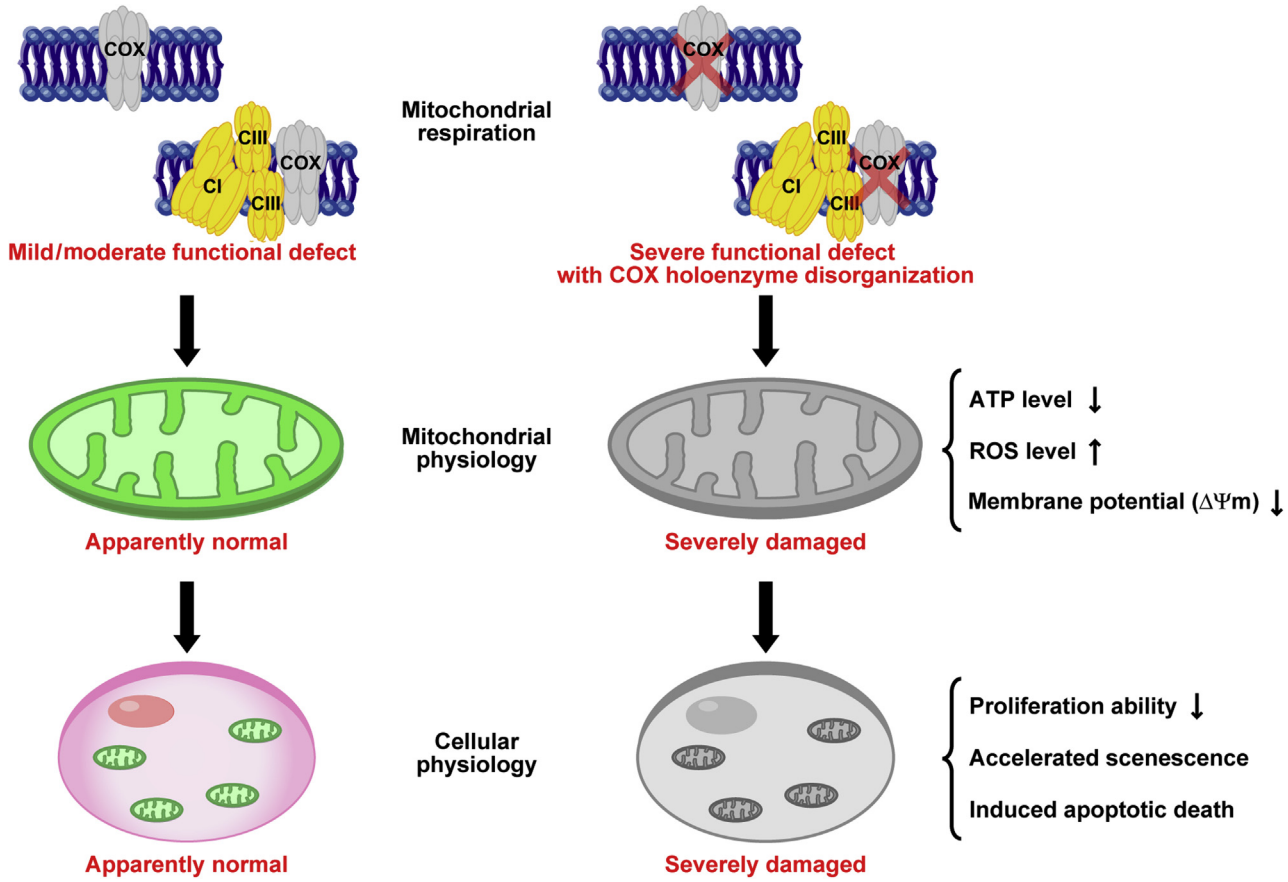

Figure 5 Mitochondrial and cellular phenotypic variation in COX deficiency: A graphical summary. Our *in vitro* diagnostic approaches successfully demonstrate two obviously different severities in molecular diagnostic criteria of COX deficiency: **left column**, structurally stable, but functionally mild/moderate defect; and **right column**, severe functional defect with the disrupted COX holoenzyme structure, followed by several mitochondrial and cellular dysfunctions.

histopathological COX deficiency patients exhibiting stable COX holoenzyme organization may be in non−COX-associating genes. Therefore, our proposed molecular diagnostic criteria would also be suggestive for effectively exploring the candidate genes, which are responsible for patient-specific pathology, by using next-generation sequencing technology.

The molecular pathomechanism of biochemically severe COX deficiency is summarized as follows: Genetic defects in any COX-associating genes can induce the aberrant COX holoenzyme organization,[1] and the synthesized but the unassembled COX structural subunits are gradually degraded by some mitochondrial metalloproteases to prevent their accumulation in mitochondrial inner membrane.[18] That is why lower protein expression levels of several COX structural subunits, despite their stable mRNA syntheses, were observed only in Patients 5 and 6 lacking COX holoenzyme. COX holoenzyme disorganization can induce not only its severe functional defect but also the diminished assembly to form COX-containing respiratory chain supramolecular architectures. In fact, the importance of COX holoenzyme in respiratory chain supercomplexes has been reported,[19] and the optimized protein ratio of each respiratory chain complex is critical for their supramolecular assembly formation, allowing much higher electron transfer rates in mitochondrial oxidative phosphorylation.[20] Thus, significant loss of COX holoenzyme induces drastically decreased activity in the production of ATP and thermal energy caused by an insufficient proton electrochemical gradient between mitochondrial matrix and intermembrane space. Mitochondrial respiratory chain complexes are also generally known to increase oxidative stress with their functional defects, and in this case, severely impaired COX holoenzyme integrity seems most likely to affect the increased oxidative stress level. To date, it still remains uncertain whether approximately 2.5-fold increase of oxidative stress level observed only in Patients 5 and 6 lacking COX holoenzyme is substantially harmful in *in vivo* mitochondrial physiology. However, the increased oxidative stress level may trigger the accumulated oxidative damages to other mitochondrial enzymes, substrates, lipids, and mtDNA, all of which lead to the depressed overall mitochondrial functions and induce premature senescence at a cell level. In addition, the damaged membrane potential level implies two major mitochondrial abnormalities: transport machinery defects of proteins and substrates essential for mitochondrial biogenesis and bioenergetics and the accelerated leak of freely mobile cytochrome *c* molecules, as a caspase activator, in mitochondrial electron transport system, followed by the induced apoptotic signaling. Therefore, widespread cellular dysfunctions, including the deteriorated cellular growth, the accelerated cellular senescence, and the induced apoptotic cell death, all of which were observed only in Patients 5 and 6, are clearly explained by primary COX holoenzyme disorganization and the following secondary mitochondrial dysfunctions.

The relationships between the molecular abnormalities in mitochondrial respiratory chain complexes and their negative contributions to mitochondrial and cellular functions have been proved to be essential for better understandings in mitochondrial medicine. In particular, most parts of mitochondrial diseases are caused by heteroplasmic mutations in mtDNA (wild-type mtDNA and mutant mtDNA coexist within a single cell) and present a wide variety of clinical spectrum among patients, probably because of variations in mutant mtDNA proportions at each tissue and organ level. To date, patients' fibroblasts are mainly used for biochemical analysis. However, such fibroblasts do not always exhibit mitochondrial respiratory defects, most likely because of relatively lower mutant mtDNA proportions than those in the affected tissues and organs of some patients. Although this study does not include mitochondrial disease patients with muscle histopathological COX deficiency, those carrying heteroplasmic mtDNA mutations, our *in vitro* diagnostic approaches by using patients' myoblasts may be more advantageous, because cells derived from the affected tissues and organs can faithfully recapitulate their cell type−specific pathophysiology in a patient-specific manner. We also believe the use of nonviral, integration-free cellular reprogramming technology[21,22] to generate disease-relevant induced pluripotent stem cells from patients' fibroblasts or peripheral blood cells can greatly help us to identify bona fide pathomechanism of complex, severe clinical phenotypes in mitochondrial diseases with multiple organ involvements. In fact, several groups and we have recently reported patient-specific induced pluripotent stem cells, those carrying various types of pathogenic mutant mtDNAs as *in vitro* human mitochondrial disease models,[23−29] toward possible applications in induced pluripotent stem cell−based drug discovery and regenerative therapeutics.[30]

Conclusions

Our cell-based *in vitro* diagnostic approaches documented herein would hold promise for enormous contributions to clinical research for future personalized medicine, which is based on the intrinsic molecular and cellular pathogenic features of each patient exhibiting various types of mitochondrial diseases, including other respiratory chain complex deficiencies and other mitochondrial metabolic enzyme deficiencies.

Acknowledgments

We thank all patients and their families for participating in this study; Mayuko Kato and Junko Takei (National Center of Neurology and Psychiatry, Tokyo, Japan) for helpful experimental assistance; and Dr. Ichizo Nishino (National Center of Neurology and Psychiatry, Tokyo, Japan) for providing clinical data of muscle histopathology in each patient.

H.H. conceived the study, designed and performed experiments, analyzed and interpreted data, and wrote the manuscript; and Y.G. analyzed and interpreted data and wrote the manuscript. All authors read and approved the final manuscript.

Supplemental Data

Supplemental material for this article can be found at *http://dx.doi.org/10.1016/j.ajpath.2016.09.003*.

References

1. Shoubridge EA: Cytochrome c oxidase deficiency. Am J Med Genet 2001, 106:46−52
2. Massa V, Fernandez-Vizarra E, Alshahwan S, Bakhsh E, Goffrini P, Ferrero I, Mereghetti P, D'Adamo P, Gasparini P, Zeviani M: Severe infantile encephalomyopathy caused by a mutation in COX6B1, a nucleus-encoded subunit of cytochrome c oxidase. Am J Hum Genet 2008, 82:1281−1289
3. Indrieri A, van Rahden VA, Tiranti V, Morleo M, Iaconis D, Tammaro R, D'Amato I, Conte I, Maystadt I, Demuth S, Zvulunov A, Kutsche K, Zeviani M, Franco B: Mutations in COX7B cause microphthalmia with linear skin lesions, an unconventional mitochondrial disease. Am J Hum Genet 2012, 91:942−949
4. Keightley JA, Hoffbuhr KC, Burton MD, Salas VM, Johnston WS, Penn AM, Buist NR, Kennaway NG: A microdeletion in cytochrome c oxidase (COX) subunit III associated with COX deficiency and recurrent myoglobinuria. Nat Genet 1996, 12:410−416
5. Comi GP, Bordoni A, Salani S, Franceschina L, Sciacco M, Prelle A, Fortunato F, Zeviani M, Napoli L, Bresolin N, Moggio M, Ausenda CD, Taanman JW, Scarlato G: Cytochrome c oxidase subunit I microdeletion in a patient with motor neuron disease. Ann Neurol 1998, 43:110−116
6. Hanna MG, Nelson IP, Rahman S, Lane RJ, Land J, Heales S, Cooper MJ, Schapira AH, Morgan-Hughes JA, Wood NW: Cytochrome c oxidase deficiency associated with the first stop-codon point mutation in human mtDNA. Am J Hum Genet 1998, 63:29−36
7. Bruno C, Martinuzzi A, Tang Y, Andreu AL, Pallotti F, Bonilla E, Shanske S, Fu J, Sue CM, Angelini C, DiMauro S, Manfredi G: A stop-codon mutation in the human mtDNA cytochrome c oxidase I gene disrupts the functional structure of complex IV. Am J Hum Genet 1999, 65:611−620
8. Clark KM, Taylor RW, Johnson MA, Chinnery PF, Chrzanowska-Lightowlers ZM, Andrews RM, Nelson IP, Wood NW, Lamont PJ, Hanna MG, Lightowlers RN, Turnbull DM: An mtDNA mutation in the initiation codon of the cytochrome c oxidase subunit II gene results in lower levels of the protein and a mitochondrial encephalomyopathy. Am J Hum Genet 1999, 64:1330−1339
9. Rahman S, Taanman JW, Cooper JM, Nelson I, Hargreaves I, Meunier B, Hanna MG, García JJ, Capaldi RA, Lake BD, Leonard JV, Schapira AH: A missense mutation of cytochrome oxidase subunit II causes defective assembly and myopathy. Am J Hum Genet 1999, 65:1030−1039
10. Tiranti V, Corona P, Greco M, Taanman JW, Carrara F, Lamantea E, Nijtmans L, Uziel G, Zeviani M: A novel frameshift mutation of the mtDNA COIII gene leads to impaired assembly of cytochrome c oxidase in a patient affected by Leigh-like syndrome. Hum Mol Genet 2000, 9:2733−2742
11. Horvath R, Kemp JP, Tuppen HA, Hudson G, Oldfors A, Marie SK, Moslemi AR, Servidei S, Holme E, Shanske S, Kollberg G, Jayakar P, Pyle A, Marks HM, Holinski-Feder E, Scavina M, Walter MC, Coku J, Günther-Scholz A, Smith PM, McFarland R, Chrzanowska-Lightowlers ZM, Lightowlers RN, Hirano M, Lochmüller H, Taylor RW, Chinnery PF, Tulinius M, DiMauro S: Molecular basis of infantile reversible cytochrome c oxidase deficiency myopathy. Brain 2009, 132:3165−3174
12. Mimaki M, Hatakeyama H, Komaki H, Yokoyama M, Arai H, Kirino Y, Suzuki T, Nishino I, Nonaka I, Goto Y: Reversible infantile respiratory chain deficiency: a clinical and molecular study. Ann Neurol 2010, 68:845−854
13. Akanuma J, Muraki K, Komaki H, Nonaka I, Goto Y: Two pathogenic point mutations exist in the authentic mitochondrial genome, not in the nuclear pseudogene. J Hum Genet 2000, 45:337−341
14. Tanaka M, Takeyasu T, Fuku N, Li-Jun G, Kurata M: Mitochondrial genome single nucleotide polymorphisms and their phenotypes in the Japanese. Ann N Y Acad Sci 2004, 1011:7−20
15. Trounce IA, Kim YL, Jun AS, Wallace DC: Assessment of mitochondrial oxidative phosphorylation in patient muscle biopsies, lymphoblasts, and transmitochondrial cell lines. Methods Enzymol 1996, 264:484−509
16. Schägger H: Tricine-SDS-PAGE. Nat Protoc 2006, 1:16−22
17. Wittig I, Braun HP, Schägger H: Blue native PAGE. Nat Protoc 2006, 1:418−428
18. Arnold I, Langer T: Membrane protein degradation by AAA proteases in mitochondria. Biochim Biophys Acta 2002, 1592:89−96
19. Schafer E, Seelert H, Reifschneider NH, Krause F, Dencher NA, Vonck J: Architecture of active mammalian respiratory chain supercomplexes. J Biol Chem 2006, 281:15370−15375
20. Schägger H, Pfeiffer K: Supercomplexes in the respiratory chains of yeast and mammalian mitochondria. EMBO J 2000, 19:1777−1783
21. Okita K, Matsumura Y, Sato Y, Okada A, Morizane A, Okamoto S, Hong H, Nakagawa M, Tanabe K, Tezuka K, Shibata T, Kunisada T, Takahashi M, Takahashi J, Saji H, Yamanaka S: A more efficient method to generate integration-free human iPS cells. Nat Methods 2011, 8:409−412
22. Okita K, Yamakawa T, Matsumura Y, Sato Y, Amano N, Watanabe A, Goshima N, Yamanaka S: An efficient nonviral method to generate integration-free human-induced pluripotent stem cells from cord blood and peripheral blood cells. Stem Cells 2013, 31:458−466
23. Fujikura J, Nakao K, Sone M, Noguchi M, Mori E, Naito M, Taura D, Harada-Shiba M, Kishimoto I, Watanabe A, Asaka I, Hosoda K, Nakao K: Induced pluripotent stem cells generated from diabetic patients with mitochondrial DNA A3243G mutation. Diabetologia 2012, 55:1689−1698
24. Cherry AB, Gagne KE, McLoughlin EM, Baccei A, Gorman B, Hartung O, Miller JD, Zhang J, Zon RL, Ince TA, Neufeld EJ, Lerou PH, Fleming MD, Daley GQ, Agarwal S: Induced pluripotent stem cells with a mitochondrial DNA deletion. Stem Cells 2013, 31:1287−1297
25. Folmes CD, Martinez-Fernandez A, Perales-Clemente E, Li X, McDonald A, Oglesbee D, Hrstka SC, Perez-Terzic C, Terzic A, Nelson TJ: Disease-causing mitochondrial heteroplasmy segregated within induced pluripotent stem cell clones derived from a patient with MELAS. Stem Cells 2013, 31:1298−1308
26. Hämäläinen RH, Manninen T, Koivumäki H, Kislin M, Otonkoski T, Suomalainen A: Tissue- and cell-type-specific manifestations of heteroplasmic mtDNA 3243A>G mutation in human induced pluripotent stem cell-derived disease model. Proc Natl Acad Sci U S A 2013, 110:E3622−E3630
27. Kodaira M, Hatakeyama H, Yuasa S, Seki T, Egashira T, Tohyama S, Kuroda Y, Tanaka A, Okata S, Hashimoto H, Kusumoto D, Kunitomi A, Takei M, Kashimura S, Suzuki T, Yozu G, Shimojima M, Motoda C, Hayashiji N, Saito Y, Goto Y, Fukuda K: Impaired respiratory function in MELAS-induced pluripotent stem cells with high heteroplasmy levels. FEBS Open Bio 2015, 5:219−225
28. Hatakeyama H, Katayama A, Komaki H, Nishino I, Goto Y: Molecular pathomechanisms and cell-type-specific disease phenotypes of

MELAS caused by mutant mitochondrial tRNA(Trp). Acta Neuropathol Commun 2015, 3:52

29. Ma H, Folmes CD, Wu J, Morey R, Mora-Castilla S, Ocampo A, Ma L, Poulton J, Wang X, Ahmed R, Kang E, Lee Y, Hayama T, Li Y, Van Dyken C, Gutierrez NM, Tippner-Hedges R, Koski A, Mitalipov N, Amato P, Wolf DP, Huang T, Terzic A, Laurent LC, Izpisua Belmonte JC, Mitalipov S: Metabolic rescue in pluripotent cells from patients with mtDNA disease. Nature 2015, 524:234−238

30. Hatakeyama H, Goto Y: Heteroplasmic mitochondrial DNA mutations and mitochondrial diseases: toward iPSC-based disease modeling, drug discovery, and regenerative therapeutics. Stem Cells 2016, 34: 801−808